Collective oscillations of a trapped atomic gas in low dimensions and thermodynamics of one–dimensional Bose gas

Giulia De Rosi

Prof. Sandro Stringari
PhD Supervisor

Members of the Committee :

Prof. Stefano Giorgini
Università degli Studi di Trento
President of the Committee

Prof. Anna Minguzzi
CNRS, LPMMC, Grenoble
Referee

Prof. Roberta Citro
Università degli Studi di Salerno
Referee

Collective oscillations of a trapped atomic gas in low dimensions and thermodynamics of one-dimensional Bose gas

Giulia De Rosi

PhD Thesis submitted to the

Dipartimento di Fisica
Università degli Studi di Trento

In fulfilment of the requirements for the Degree of

Philosophiæ Doctor in Physics

Under the Supervision of
Prof. Sandro Stringari

PhD Supervisor:

 Prof. Sandro Stringari

Members of the Committee:

 Prof. Stefano Giorgini - Università degli Studi di Trento

 Prof. Anna Minguzzi - CNRS, LPMMC, Grenoble

 Prof. Roberta Citro - Università degli Studi di Salerno

Ai miei nipoti, Diego, Eva & Matilde

"...Toujours rechercher la difficulté. Non pas le danger.
Aller de l'avant, tenter, oser.
Dans l'audace il y a l'enchantement..."

- Street Art in Chamonix (France) -

"Ho imparato questo, almeno, dal mio esperimento; che se uno avanza fiducioso nella direzione dei suoi sogni, e si sforza di vivere la vita che ha immaginato, incontrerà un successo inatteso nei momenti più comuni. Si porrà qualcosa alle spalle, supererà un confine invisibile; leggi nuove, universali e più liberali cominceranno ad affermarsi intorno e dentro di lui; oppure le vecchie leggi si espanderanno, e saranno interpretate a suo favore in un senso più liberale, e vivrà con la licenza di un superiore ordine di esseri. Nella misura in cui semplificherà la sua vita, le leggi dell'universo appariranno meno complesse, e la solitudine non sarà solitudine, né la povertà povertà o la debolezza debolezza. Se avete costruito castelli in aria, il vostro lavoro non deve andare perduto; è lì che devono stare. Ora metteteci sotto delle fondamenta."

- Henry David Thoreau, "*Walden; or, Life in the Woods*" -

Ringraziamenti
Acknowledgements
Remerciements

Il Dottorato di Ricerca è molto importante nella vita di una persona, sia scientificamente che umanamente. Alcuni lo definiscono come un vero e proprio trauma, altri come il momento più bello della propria vita e forse (e purtroppo!) anche l'unico periodo in cui si apprezza veramente la Ricerca: quella fatta con calma, con il tempo necessario per sviluppare le idee, in controtendenza rispetto ai tempi frenetici e consumistici dell'attuale avanzamento della conoscenza mondiale. Il mio PhD è stato orgogliosamente entrambe le cose: un "trauma bello", insomma. 3 anni e mezzo di picchi altissimi e bassissimi, con il mio umore che seguiva ossequiosamente l'andamento degli eventi. E' stato un momento molto formativo, che mi ha cambiato tantissimo e di cui non ho rimpianti particolari. Probabilmente, rivivrei il "trauma bello". In tutte le sue sfumature. Sono certa che, quando sarò più grande, mi mancherà anche la parte traumatica del Dottorato.

Vorrei ringraziare tutte le infinite persone che oggi non mi permettono di avere rimpianti alla fine di questo percorso. Alcune sono state la fonte del "bello". Nessuna solo del "trauma". Tutte però, nessuno escluso, mi hanno permesso di arrivare alla fine e, cosa meno banale, di insegnarmi qualcosa.

La prima persona che vorrei ringraziare è il mio Supervisor, il Prof. Sandro Stringari. Lui ha avuto un ruolo centrale in tutto il mio percorso. Esattamente 3 anni e mezzo fa, mi vedevo come un astroparticellare e, in effetti, avevo studiato per quello, ma la vita aveva in serbo per me qualcosa di più grande. Il mio Supervisor è stato, di fatto, un'ottima motivazione per intraprendere l'avventura dei gas ultrafreddi, cosa minimamente pianificata. Questo perché è un eccellente Ricercatore, con una rara chiarezza mentale. Pochi scienziati di oggi sono così bravi. Inoltre, ha l'idea giusta della Ricerca che richiede tempo, impegno, tenacia, motivazione, idee, passione e onestà intellettuale, cose che si stanno un po' perdendo oggi. Infine, rasenta anche l'impossibile, perché, nonostante i suoi milioni di impegni, trova sempre il tempo di insegnare. Questo perché vuole sempre trasmettere il suo meglio ai suoi studenti. Lo ringrazio anche per l'ottimo corso di gas quantistici e superfluidità, grazie al quale tutte le nozioni che vagavano random nella mia testa, hanno finalmente trovato un nesso. E' riuscito a insegnarmi qualcosa anche attraverso i traumi e le discussioni da elmetto in testa... In questo triennio di lotte varie, ho capito che la Fisica Teorica (e la vita!) richiede una strenua difesa delle proprie opinioni, con una logica ferrea e una genuina fiducia in se stessi, cose forse anche più difficili della Fisica stessa. Il mio Supervisor non mi ha permesso di avere rimpianti nei confronti del mio cambio di rotta inaspettato. Sono molto contenta di aver scoperto un nuovo campo di Ricerca e ho imparato una quantità spropositata di cose. E quindi Grazie!

Un grazie speciale va anche al Prof. Gregory Astrakharchik. L'ultima parte del mio lavoro è stata supervisionata anche da lui. Lo ringrazio per avermi ospitato nel suo gruppo di Ricerca a Barcelona per due settimane, dove mi sono sentita subito a casa. Ho apprezzato di cuore la sua filosofia zen del lavorare slow, che ha contrastato la mia ansia perenne. Lui è un fisico teorico computazionale eccezionale. Nel tempo che io prendo in mano un foglio di carta e la mia penna, lui ha già risolto il problema con il computer. Durante la mia visita scientifica a Barcelona, ho cominciato seriamente a vedere il computer sotto una luce del tutto diversa: da macchina oscura e randomica a strumento potentissimo. Grazie anche per i pranzi ogni giorno in posti diversi con i suoi amici. Anche se il posto migliore resta "la terrazza di Shakira" nel quartiere più chic della città! Grazie anche per i dolcetti e i té russi: mi hanno rincuorato quando i miei conti erano sbagliati!

Grazie alle Prof.sse Anna Minguzzi e Roberta Citro per aver accettato di essere le mie Referee. Non solo faranno parte della commissione del mio esame, ma, soprattutto, hanno letto e controllato il manoscritto della mia Tesi. Grazie anche al Prof. Stefano Giorgini per essere il Presidente della mia commissione. Lo ringrazio anche per l'ottimo corso di Meccanica Statistica e per avermi insegnato a pensare come un computazionale, oltre che per la squisita gentilezza e pazienza che ha sempre avuto nei miei confronti.

Un sentito e affettuoso grazie al Prof. Omar Benhar. Anche se lui è stato il mio relatore della Tesi magistrale, ha avuto un ruolo di rilievo anche durante il mio PhD. In questi ultimi anni ci siamo rivisti nei posti più disparati: dall'isola d'Elba (durante la festa a sorpresa per i suoi 60 anni), a Trento, a Roma e a Barcelona (per puro caso)! Lui è stata la prima persona che mi ha insegnato quanto sia bello e importante cambiare campo di Ricerca. Inoltre, mi ha convinto a intraprendere lo studio dei gas ultrafreddi, pur facendomi sentire parte della comunità di *"many-body"* (se gli dici che fa Fisica nucleare si arrabbia, se gli dici che fa stelle di neutroni si arrabbia, se gli dici che studia i gas pure... perché lui è orgogliosamente many-bodista!). Poi il motto "Roma non s'è costruita in un giorno" è entrato talmente tanto nel mio essere che è diventato uno dei miei post-it motivazionali attaccati sullo schermo in ufficio. Causandomi anche botte assurde di nostalgia di quanto mi manca Roma e "La Sapienza" in generale. Un altro posto di cui non ho rimpianti! Grazie anche perché alla fine del mio Dottorato, i risultati della mia Tesi magistrale sono stati presentati in una conferenza a Trento (che includeva le comunità many-body e gas ultrafreddi e mi sentivo orgogliosamente parte di entrambe!) e saranno pubblicati poco dopo la mia PhD defence. E' stato bello! Grazie anche per la gentilezza, l'importanza di dissentire, una fiducia enorme nel futuro e il fatto di difendere sempre i propri studenti. Lui ha un imprinting enorme sulla persona che sono diventata.

Un grazie veramente speciale al Prof. Alessio Recati. Lui è il mio "Mentoruccio". Lui è quello che mi ha difeso, sopportato, supportato, aiutato e dato sempre degli ottimi consigli. Quasi tutto il mio primo anno di PhD è stato supervisionato da lui. Poi mi ha "abbandonato" per Monaco. In effetti, l'unico rimpianto che potrei avere è stato quello di aver trascorso buona parte del mio PhD senza la sua presenza a Trento. Probabilmente sarebbe stato molto diverso. Tuttavia, il suo non è stato un vero e proprio abbandono, perché ogni volta che avevo bisogno di lui c'è sempre stato. Dalle serate passate col vino a discutere della vita complicata dei Ricercatori, ai consigli per i PostDocs, al semplice fatto che è una persona sensibile e empatica che ascolta e comprende. Mi ha anche trasmesso l'intolleranza verso i nerd e i sociopatici presenti nel mondo della Fisica, oltre che l'esempio giusto del buon Ricercatore: colui che lavora tanto ma che ha anche una vita là fuori e che non se la lascia sfuggire. La vera definizione di persona smart, insomma.

Un grande grazie anche al Prof. Iacopo Carusotto. Per il suo bel corso di Quantum Optics e perché è stato presente in alcuni dei momenti più difficili del mio PhD. La sua storia del "facevo un sacco di conti ma non funzionavano mai con i gas e poi li ho fatti con la luce ed è nato un nuovo campo della Fisica" è troppo bella. E soprattutto, insegna a

guardare i periodi brutti con occhi diversi. Grazie!

I would like to thank Prof. Lev Pitaevskii. His patience, kindness and expertise were a continuous source of inspiration for me. Thank you a lot for all the insightful discussions!!!

Ringrazio anche il Prof. Franco Dalfovo perché è sempre sorridente, per la sua calma sempiterna e perché condividiamo la passione per i Radiohead.

Ringrazio di cuore anche la Prof.ssa Chiara Menotti. Se ora uso Matlab, lo devo a lei. La ringrazio anche perché, oltre ad essere un'ottima ricercatrice, è anche una persona dolcissima e sensibile oltre che una mamma. E' un buon esempio per tutte le giovani scienziate che transitano da Trento.

Grazie anche al Prof. Giacomo Lamporesi. Lui è il "Mentoruccio 2". Il suo essere mentore implicava insegnarmi ad andare sullo snowboard. Dopo il primo tentativo traumatico ho lasciato perdere. Però è rimasto mentore per tutte le volte che l'ho incontrato per caso in giro la sera per locali, consolidando in me l'idea che non esiste buona Ricerca senza una vita là fuori. Grazie anche per le milioni di chiacchierate nei corridoi.

Ringrazio anche il Prof. Gabriele Ferrari. Lui mi ha permesso di entrare nel suo laboratorio per osservare come venivano eseguite le misure dei modi collettivi, spiegandomi un sacco di cose. In quei 2 giorni ho davvero imparato molto.

Grazie anche a Giuseppe Froner per il supporto tecnico e informatico. Lui ha risolto gli innumerevoli e incredibili problemi che ho avuto con la tecnologia, tra i quali "il mio computer si è aperto come un panino!".

Grazie di cuore anche alle fantastiche segretarie che ho incontrato a Trento. Tutte loro mi hanno fatto ricredere che il personale amministrativo può essere gentile. Grazie a Beatrice Ricci con cui condivido la passione per la musica e i concerti. Grazie a Rachele Zanchetta perché mi ha sempre sostenuto e aiutato nei vari incubi amministrativi, dalle missioni ai timesheets. Grazie a Micaela Paoli e Lucia Appoloni perché, oltre all'infinito supporto per la scuola di Dottorato, sono sempre state molto disponibili nel sostenere ogni mia idea per rivoluzionare il PhD Workshop, anche se ciò ha comportato infiniti problemi burocratici e ore di lavoro in più.

Un sentito grazie anche al Prof. Renzo Leonardi, il mio dirimpettaio di ufficio. Grazie per gli auguri in varie festività e per la sua squisita cortesia. Spero che si rimetta presto dal suo infortunio.

Je profite également de ces remerciements pour exprimer ma sympathie et mes amitiés à tous les chercheurs de Paris qui m'ont accueillie, pendant ma visite. Je remercie chaleureusement le Laboratoire de Physique Théorique et Modèles Statistiques, le Laboratoire de Physique Théorique de la Matière Condensée, le Prof. Christophe Mora du Laboratoire Pierre Aigrain de l'École Normale Supérieure et le Prof. Michael Urban de l'Institute de Physique Nucléaire. Merci pour toutes les discussions enrichissantes que nous avons eues ensemble. J'ai appris beaucoup de choses et j'espère vous avoir un peu apporté de mon côté.

Thank everyone that I met during my visit in Barcelona. I deeply owe it to all scientists of Computer Simulation in Condensed Matter Research Group of Universitat Politécnica de Catalunya who have allowed me to work there for almost two weeks. Thanks a lot to Prof. Artur Polls of Universitat de Barcelona who attended my seminar very carefully. He dragged also all members of his group to my talk. I learned a lot on that occasion. It is always a pleasure to meet him! Thank a lot also to the whole Quantum Atom Optics group of Prof. Verònica Ahufinger and Jordi Mompart of Universitat Autònoma de Barcelona. I really felt like at home there. I hope also find some time to work together...
I have not forgotten you!

Un grazie davvero speciale va alla Prof.ssa Giovanna Morigi, per avermi invitato nel suo gruppo di Ricerca a Saarbrücken. Grazie per i due giorni fantastici che ho passato lì. Grazie per gli infiniti té per tenermi sveglia (2 notti precedenti la mia partenza per la

Germania, ho consegnato questa Tesi). Grazie per le milioni domande durante il mio talk, per avermi apprezzato e grazie anche per essere un buon esempio come persona. Da grande vorrei essere "flippata" esattamente come lei! A special thank goes to all other young and cool members of the Theoretical Quantum Physics group in Saarbrücken. Thanks a lot for the endless and insightful discussions we had together. I have really appreciated that you work all together like a big family!

A huge thank to all young present, former and visiting members of the INO-CNR BEC Center of Trento. Most of them are some of my best friends now.

Thank a lot to Russell and Tomoki who have read some parts of my PhD Thesis. Thank Russell because he gave me a new perspective from the other side of the world (!) and thank Tomoki because he is my "Little Mentor". He supervised me during my first PhD year. Thank also for Topological lectures and because he is always zen and full of good pieces of advice!

Grazie di cuore a Marco per essere uno dei miei migliori amici. Lui è uno di quelli che mi hanno sostenuto durante il mio Dottorato. In particolare, mi ha anche sopportato durante gli ultimissimi mesi che sono stati i più complicati, soprattutto quando ero in preda al panico ed ero veramente insopportabile! Grazie per il cibo cucinato da lui, per avermi accompagnato alle partite del Trentino volley e per esserci sempre stato.

Ringrazio affettuosamente anche Grazia per una serie di motivi. Il primo è che ci siamo sostenute a vicenda e questo rafforza in me l'idea che in ogni gruppo di Ricerca ci devono essere almeno 2 ragazze. Se poi si raggiunge il 50% è anche meglio. Grazie per le infinite discussioni, le uscite notturne, i dolci fatti in casa nel week-end e per l'aiuto ricevuto in un migliaio di occasioni almeno. Grazie anche per avermi gentilmente passato il template della sua Tesi (faticosamente creato da lei!) che io ho solo leggermente modificato. La mia Tesi non sarebbe mai stata così bella senza il suo aiuto!

Grazie a José. La nostra amicizia ha avuto degli alti e bassi e delle evoluzioni assurde. Durante il primo anno, eravamo sempre assieme e ci raccontavamo tutto tutto. Abbiamo fatto un viaggio a Ponza che verrà ricordato per secoli (soprattutto la parte in cui abbiamo rischiato la vita tra i serpenti) e ci siamo sostenuti a vicenda. Lui mi ha aiutato a esprimere il lato più ironico e goliardico di me. Condivido con lui una quantità enorme di ricordi belli. Poi abbiamo capito che due persone che panicano facilmente e si stressano con poco non possono passare troppo tempo assieme, altrimenti impazziscono. Ora siamo cresciuti, perlomeno proviamo a essere più razionali e a panicare di meno!

Un grazie speciale va a Giacomo. Con lui ho condiviso ben l'esperienza di due scuole, tra cui quella di Les Houches che ci ha obbligati a vivere un viaggio di 12 h assieme. Penso che sia proprio in quel momento che siamo diventati ottimi amici, raccontandoci un sacco di cose, anche quelle che facevano più male!

Merci à Tom aussi. Si je n'ai encore perdu mon français, c'est parce-que je le force à le parler avec moi! Merci pour avoir partagé tes soins sur le futur de la Recherche avec moi. C'est vraiment difficile en ce moment de penser de suivre ses propres rêves dans le monde de la Science. Selon moi, on doit être fier du chemin fait quel que soit le résultat final. On a fait ce que nous voulions plus, avec tous les efforts possibles et ça c'est déjà vraiment beaucoup.

Grazie anche a Eleonora. Ho condiviso anche con lei l'esperienza di Les Houches. Ringrazio anche Simone S. per avermi sopportato mentre eravamo entrambi rappresentanti dei dottorandi. E' stato quasi impossibile soprattutto durante l'organizzazione del PhD Workshop! Grazie anche per aver vissuto con me la scuola di Varenna. Grazie a Carmelo per le serate assieme, thank Hannah for her endless enthusiasm and the Topological lectures. Grazie a tutti i nuovi arrivati/ Thanks to all newcomers. Grazie a Chunlei, Fabrizio L., Luca, Matteo, Elena, Miki e Elia.

J'aimerais d'autre part témoigner ma reconnaissance à Pilou pour un ensemble innombrable des choses. Merci pour la visite de Paris pendant la nuit, pour m'avoir soutenue pendant ma Recherche de PostDocs et pour avoir été présent à Orsay le jour de mon séminaire. Merci pour Cippi, pour le français, pour les Radiohead, pour les photons (notre bébé), pour m'avoir soutenue toujours chaque fois que j'étais triste, pour avoir réveillé mon côté rebelle et pour m'avoir convaincue que chaque personne est le fabricant de son propre destin. Maintenant je le sais. Il a plus révolutionné ma personne, ma vision de choses et mon Univérs pendant mon Doctorat. Donc Merci. Tous simplement pour être important pour moi.

Un grazie di cuore anche a Luis. Lui è una persona estremamente curiosa, sensibile e buona. Grazie per aver condiviso con me alcuni traumi e la passione per i Radiohead. Condividiamo esattamente la stessa visione della Ricerca e sono certa che é uno di quelli che vuole lottare per cambiare le cose in meglio, più che essere vittima del sistema.

Grazie a Giovanni che mi ha portato alla scoperta di un quartiere parigino. Grazie anche per il tempo passato assieme come dirimpettai nell'open-space e di aver permesso alla mia pianta di fagiolo di valicare sfacciatamente il confine e di invadere beata la sua scrivania. Grazie anche per aver condiviso con me la scuola di Varenna. L'ultima volta che l'ho visto mi ha augurato che la vita mi porti quello che è meglio per me sul lungo termine. Lo auguro di cuore anche a lui.

Grazie a Marta A. per il fantastico giro turistico a Barcelona. Sono certa che sarà un'ottima insegnante.

Ringrazio anche Marek che ha condiviso con me e José l'avventura di Ponza!

Grazie a Giulio per les Houches, lo "sfinciunello" e le serate passate assieme con tutti gli altri "meridionali" smarriti per Trento.

Un grazie di cuore a Mathias. Lui è l'unica persona con la quale parlo tre lingue che, a volte, vengono cambiate anche all'interno della stessa discussione. Grazie per le serate nei bar trentini, per le jam sessions, per i concerti e per l'amore sfegatato per Thom.

Ringrazio anche Fabrizio M. che ha fatto uno stage a Trento un sacco di tempo fa. Grazie per i tour turistici per la regione, per la scoperta enogastronomica del territorio e, soprattutto, grazie per le milioni di discussioni erudite. Ha una cultura vastissima che va ben oltre la Fisica!

Grazie anche a Andrei e Francesco R. per le chiacchierate durante i loro stage trentini. Grazie a Francesco anche per averlo ritrovato a Saarbrücken e per le colazioni/cene tedesche assieme.

Un grazie speciale anche alle fantastiche ragazze del ciclo 29-esimo della scuola di Dottorato in Fisica. Ringrazio in particolare Roby, Mary e Giovanna per il mio primo anno passato in open-space e Loredana che ogni tanto incontro in giro per il Dipartimento. Siamo ufficialmente il ciclo più rosa della storia! Grazie anche per tutte le discussioni, soprattutto quelle in fase di scrittura Tesi, che cominciavano sempre con "Ma ti pare normale che..." e a seguire lista enorme di problemi!

Grazie anche a Claude e Marco alias Amur Tet. Il primo, dopo la sua partenza per Monaco, è diventato l'omino di Telegram con il quale discuto quotidianamente su qualsiasi cosa (a volte in modo molto nichilista). Il secondo, invece, nel suo ufficio del sole con la porta a vetri, sta scrivendo la sua Tesi magistrale con una calma pazzesca che invidio tantissimo! Grazie anche per il concerto a Calcatronica!

Ringrazio di cuore il mio ufficio, dopo l'upgrade dall'open-space. L'ufficio 305. Un grazie speciale va a Sergio (il mio cdb!), Lorenzo, Fabrizio e Francesco. Ecco, loro sono le prime vittime. Se gli altri mi hanno sopportato di tanto in tanto, loro hanno vissuto tutti gli sbalzi d'umore della sottoscritta, dalle ansie al panico, dalla gioia all'esultanza. E poi non potevano neanche scappare, visto che quello era anche il loro ufficio! Grazie per aver reso quella stanza la più "umana" di tutto il piano con le merendine, il té, la cioccolata,

la macchina del caffé espresso, la poltrona rossa, la musica sparata a palla e le feste di compleanno a sorpresa. Chiaramente anche il mio fagiolo ha avuto un ruolo di rilievo in questo senso. Grazie anche per avermi insegnato a usare il computer. Non è detto che abbia ancora imparato, ma, sicuramente, sto a buon punto rispetto a prima.

Grazie a Guido e Marta e a casa disagio. Là dentro ho passato il periodo più assurdo e divertente di tutta la mia vita! Grazie per la feste al MUSE, le cene a base di birra e Milka quando non avevamo una cucina, la prima cena calda quando la cucina era stata costruita ma faceva comunque schifo, per aver condiviso con me tutti i traumi con la casa e con i coinquilini inquietanti che sono passati da quell'abitazione. Grazie infinite per le innumerevoli feste là dentro e per l'esperienza del SotAlaZopa. E' stato davvero bello!

Un grazie speciale anche a tutti i miei amici trentini. Grazie a Riccardo che è un po' come se fosse il mio fratellone maggiore. Grazie anche per l'eterna lotta per chi è romano puro sangue! Quando sento il suo accento mi sento proprio a casa. Grazie alle mie "amichette" Marzia e Nadia. Dopo una serie sconfinata di fisici, molti dei quali uomini, loro occupano un posto di rilievo! Grazie a Marzia per avermi insegnato che le persone forti sono quelle che si sforzano di essere felici e di stare bene! Grazie a Nadia che mi è stata molto vicino: soprattutto negli ultimi mesi terrificanti, mi scriveva molto spesso per accertarsi della mia salute (anche mentale!).

Grazie anche a Matteo per le serate passate assieme. Lui ha una ragazza fantastica (vedi pag. viii)!

Ringrazio affettuosamente chi mi ha aiutato a rendere questa Tesi migliore (pur comprendendo poco). Grazie infinite a Sarah e Elena. Hanno fatto uno sforzo enorme! Grazie anche per il viaggio a Lampedusa assieme (che in effetti, è stato abbastanza sfigato). Grazie a Elena anche per le serate parigine e, soprattutto, per avermi praticamente portato all'aereoporto e essere stata l'artefice del mio rientro in Italia. Io sarei rimasta molto volentieri lì!

Ringrazio Allegra che, da quando ci siamo laureate, non l'ho più vista, ma l'ho ritrovata a Parigi. Abbiamo colmato in una serata quello che ci dovevamo raccontare e che è accaduto negli ultimi 4 anni! Per lo stesso motivo ringrazio anche Noemi (questa volta il posto prescelto è stato l'ufficio 305) e Angela che mi ha fatto compagnia a Barcelona.

Grazie di cuore anche alle mie amiche a Viterbo. Grazie a Virginia e Roberta. Loro sanno il perché e da anni sono un pilastro del mio Universo.

Ringrazio Laura perché è la mia perfetta compagna di viaggio che condivide con me la filosofia del "non esiste riposo, né sonno in viaggio. Si deve visitare tutto!". Barcelona e Siviglia sono state fantastiche! Grazie perché è presente per me da 23 anni.

Grazie alla mia famiglia, in particolare alla mia mamma, al mio papà e a mia sorella Tata. In realtà, casa mi è mancata tantissimo in questi anni, come non avrei mai immaginato. Loro sono i miei primi sostenitori e le persone che sono più orgogliose di me. Anche quando non avevo più la forza per andare avanti, loro hanno sempre saputo che ce l'avrei fatta. Anche questa volta.

I ringraziamenti a cui tengo di più li lascio alla fine. Sono quelli più importanti.

La Ricerca ha come fine ultimo il progresso per le future generazioni, sia tecnologico che epistemologico. Idealmente, anche questa Tesi fa parte di tutto questo. Perciò dedico questo manoscritto ai miei nipoti Diego, Eva e Matilde. Tutto ciò che mi ha permesso di arrivare fino a questo punto e tutto ciò che questa Tesi rappresenta è il frutto delle cose che reputo le più importanti e che non baratterei con nulla. Auguro loro di avere la libertà di fare tutto quello che più desiderano della loro vita. E nel caso questa libertà venga meno o non ci siano le condizioni adatte, di lottare e ribellarsi affinché possano perseguire i loro sogni comunque. Mai sottovalutare il proprio valore e la volontà umana.

Trento, 9 Aprile 2017

1

Contents

Contents

Abstract

Ultracold atoms are exceptional tools to explore the physics of quantum matter. In fact, the high degree of tunability of ultracold Bose and Fermi gases makes them ideal systems for quantum simulation and for investigating macroscopic manifestations of quantum effects, such as superfluidity.

In ultracold gas research, a central role is played by collective oscillations. They can be used to study different dynamical regimes, such as superfluid, collisional, or collisionless limits or to test the equation of state of the system.

In this thesis, we present a unified description of collective oscillations in low dimensions covering both Bose and Fermi statistics, different trap geometries and zero as well as finite temperature, based on the formalism of hydrodynamics and sum rules.

We discuss the different behaviour exhibited by the second excited breathing mode in the collisional regime at low temperature and in the collisionless limit at high temperature in a 1D trapped Bose gas with repulsive contact interaction. We show how this mode exhibits a single-valued excitation spectrum in the collisional regime and two different frequencies in the collisionless limit. Our predictions could be important for future research related to the thermalization and damping phenomena in this low-dimensional system.

We show that 1D uniform Bose gases exhibit a non monotonic temperature dependence of the chemical potential characterized by an increasing-with-temperature behaviour at low temperature. This is due to the thermal excitation of phonons and reveals an interesting analogy with the behaviour of superfluids.

Finally, we investigate a gas with a finite number N of atoms in a ring geometry at $T = 0$. We discuss explicitly the deviations of the thermodynamic behaviour in the ring from the one in the large N limit.

Keywords:

quantum gases, Bose-Einstein condensates, Fermi superfluids, collective oscillations, low-dimensions, Lieb-Liniger, Yang-Yang, collisionless, hydrodynamics, thermalization, sum-rules, thermodynamics, equation of state, phonons, ring.

List of Notations

- The physical constants $\hbar$, k_B and the mass m are always present. Only in SubSec. 2.3.1 they are set equal to one: $\hbar = 2m = k_B = 1$.

- Vectors are typeset in bold math character: $\mathbf{r}, \mathbf{p}$...

- Only when necessary, hats on top of the operators are present to distinguish them from the numerical quantities: $\hat{\psi}$.

- Quantities with subscript $\perp$ are relative to the radial coordinate (of the $x - y$ plane).

- Quantities with subscript z are relative to the axial coordinate (of the z-axis).

List of Acronyms

1D one-dimensional
2D two-dimensional
3D three-dimensional
BA Bethe-Ansatz
BCS Bardeen-Cooper-Schrieffer
BEC Bose-Einstein condensation
BG Bogoliubov
BKT Berezinskii-Kosterlitz-Thouless
CIR Confinement Induced Resonance
CL collisionless
CM centre-of-mass
D dimensional
DC dipole compressional
EOS equation of state
FR Feshbach resonances
GP Gross-Pitaevskii
GPE Gross-Pitaevskii equation
HD hydrodynamic
HS hard-sphere
IBG ideal Bose gas
IFG ideal Fermi gas
LB lowest breathing
LDA Local Density Approximation
LHY Lee-Huang-Yang
LL Lieb-Liniger
LRO long range order
MF mean-field
PBC periodic boundary conditions
SF superfluid
STG Super Tonks-Girardeau
T temperature
T = 0 zero temperature
TF Thomas-Fermi
TG Tonks-Girardeau
UFG unitary Fermi gas
VS versus

List of Figures

List of Tables

Introduction

Quantum gases provide a very useful text-book tool to investigate the consequences of Quantum Mechanics. They can be exploited as *quantum simulators*, because they allow one to model other quantum matter systems, sharing the same Hamiltonian [Bloch et al., 2008, 2012]. One of the most spectacular manifestation of quantum effects, shared by quantum gases, is the phenomenon of superfluidity.

After the first realisation of Bose-Einstein condensation (BEC) in a dilute atomic gas [Anderson et al., 1995, Davis et al., 1995, Bradley et al., 1995], the experimental techniques aiming at producing and manipulating quantum gases have undergone striking progress. Today one can work with both bosonic and fermionic atomic gases and to create mixtures of different species [Pethick and Smith, 2002]. The interparticle interactions can be tuned by means Feshbach resonances [Chin et al., 2010]. By using laser light it is possible to achieve a large variety of external confinements, like harmonic, periodic, quasiperiodic, and disordered potentials. The dimensionality of the system can also be managed by applying a tight optical confinement of the atomic cloud along one or two directions. This has opened the way for the investigation of new superfluid phases like the two-dimensional Berezinskii-Kosterlitz-Thouless transition [Hadzibabic et al., 2006] and novel quantum degenerate states like the one-dimensional Tonks-Girardeau gas [Paredes et al., 2004, Kinoshita et al., 2004].

Collective oscillations in low dimensions

Harmonically trapped atomic gases exhibit *collective oscillations*, or normal modes, for which all atoms move with the same collective frequency and with a wavelength comparable to the size of the sample. Collective oscillations provide powerful tools to explore the physics of quantum many-body systems and to test fundamental theories. On one hand, normal modes can be used to investigate different dynamical regimes of the system, such as superfluid, collisional, or collisionless, for both Bose and Fermi atomic gases. On the other hand, collective frequencies are important to test the equation of state (EOS) of the system, including its temperature dependence, the thermodynamics and the presence of superfluidity.

In the last twenty years, an intense theoretical [Stringari, 1996, 1998, Bruun and Clark, 1999, Ghosh, 2000, Menotti and Stringari, 2002, Heiselberg, 2004, Stringari, 2004, Astrakharchik et al., 2005b, Baur et al., 2013] and experimental [Jin et al., 1996, Mewes et al., 1996, Jin et al., 1997, Stamper-Kurn et al., 1998, Maragò et al., 2000, Bartenstein et al., 2004b, Kinast et al., 2004, 2005, Wright et al., 2007, Altmeyer et al., 2007, Riedl

et al., 2008, Tey et al., 2013, Sánchez Guajardo et al., 2013, Fang et al., 2014] research activity was carried out aiming at the investigation of collective oscillations by considering both bosonic and fermionic atoms, different trap geometries, temperature and various dimensions.

Even if the state of the art is very rich, a unified description of collective modes in low dimensions, covering both Bose and Fermi statistics, different trap geometries and zero as well as finite temperature is still missing. Our general approach De Rosi and Stringari [2015] fills this gap and it is also able to reproduce some results of the literature in different limiting cases. Our study is based on the hydrodynamic formalism, which includes the description of the superfluid regime at zero temperature and the collisional regime in the non-superfluid phase above the critical temperature.

Thermalization and damping are a key issue for the one-dimensional (1D) Bose gas with repulsive contact interactions, due to its intrinsic integrability. They have been the object of an intense research activity [Laburthe Tolra et al., 2004, Kinoshita et al., 2006, Hofferberth et al., 2007, Mazets et al., 2008, Mazets and Schmiedmayer, 2009, 2010, Tan et al., 2010]. In harmonically trapped configurations, they affect the propagation of collective oscillations [Mazets, 2011], whose nature evolves from the collisional regime at low temperature to a collisionless regime at a higher temperature.

So far most research in collective oscillations in 1D has concerned the lowest breathing mode [Menotti and Stringari, 2002, Moritz et al., 2003, Astrakharchik, 2005, Haller et al., 2009, Hu et al., 2014, Fang et al., 2014, Gudyma et al., 2015, Gudyma, 2015, Chen et al., 2015, De Rosi and Stringari, 2015]. Since at high temperature this mode exhibits the same collective frequency in both collisional and collisionless regimes, it is not directly relevant to the investigation of thermalization in 1D trapped Bose gases.

The second excited breathing mode is still less investigated in literature [Tey et al., 2013, Hu et al., 2014]. Our results De Rosi and Stringari [2016] show that it exhibits a different behaviour in the collisional and collisionless regimes. Therefore, in contrast to the lowest breathing mode, it is a natural candidate to exploit the effects of relaxation caused by collisions and the corresponding thermalization in 1D. Our predictions are based on the sum-rule approach, which allows us to investigate both the collisionless and the hydrodynamic regimes.

Thermodynamics of a 1D Bose gas

The thermodynamic behaviour of a *superfluid* is dominated, at low temperature (T), by the thermal excitation of *phonons* [Wilks, 1967] which causes an increase of the chemical potential at low T [Papoular et al., 2012] as experimentally observed in strongly interacting Fermi gases [Ku et al., 2012].

Uniform 1D Bose gases with repulsive contact interactions exhibit a phononic spectrum at low momenta [Lieb, 1963], but they cannot be considered as a superfluid. Our results De Rosi et al. [2017] carried out in collaboration with Prof. Gregory Astrakharchik (Universitat Politècnica de Catalunya, Barcelona, Spain), show that, despite the absence of superfluidity, the chemical potential of 1D systems is characterized, at low T, by the thermal excitation of phonons, a typical feature of superfluids.

Very recently, a ring geometry with few atoms was realised [Labuhn et al., 2016]. Motivated by the experimental progress, we have investigated a gas with a small number N of atoms in a ring and the mapping with the 1D problem where calculations are carried out using periodic boundary conditions. We have studied the deviations of the thermodynamic behaviour in a ring at zero temperature from the one in the large N limit.

Our results De Rosi et al. [2017] show that finite-N corrections are important in the weakly-interacting regime, where the healing length can easily become comparable to the size of the system.

Outline

A detailed outline of the thesis follows.

Chapter 1. The first Chapter aims to introduce briefly all ultracold gas systems investigated throughout this thesis. The concept of ultracold atomic gases and their most important quantum manifestations (BEC and superfluidity) are reviewed. A special emphasis is given to interatomic interactions and how to tune them by using Fano-Feshbach resonances. Finally, the theory of interacting Bose and Fermi systems is discussed.

Chapter 2. This Chapter is completely devoted to low-dimensional quantum gases. The concept of long-range order is introduced, by pointing out how its presence is related to BEC and how it is affected by low-dimensionality. The second part presents 1D Bose gases with repulsive contact interaction, described by the Lieb-Liniger model at zero temperature ($T = 0$) and by its generalisation at finite T: the Yang-Yang theory. A special importance is given to the problem of thermalization in this system.

Chapter 3. The Chapter presents collective oscillations in low-dimensional harmonically trapped gases. We derive a general formulation of the hydrodynamic equations in the presence of an external trap in terms of the velocity field. This approach points out the central role played by the EOS in the collective frequency calculation. It reduces to a simplified form when the EOS can be approximated by a power (polytropic) law dependence on the density, allowing for an important class of analytic solutions. The Chapter is based on the publication De Rosi and Stringari [2015].

Chapter 4. This Chapter is a brief overview on the formalism of linear response functions, which is widely employed in Chap. 5.

Chapter 5. The Chapter is devoted to the investigation of the transition from the collisional, at low T, to the collisionless regime at higher T in a 1D trapped Bose gas with zero-range repulsive interactions. We predict the excitation of two different frequencies in the collisionless regime and a single frequency for the collisional regime for the second excited breathing (dipole compression) mode. Our analysis is based on the comparison of the collective frequencies calculated with both hydrodynamic and sum-rule approaches. The findings of this Chapter are published in De Rosi and Stringari [2016].

Chapter 6. The final Chapter contains some results about the thermodynamics at low T of a 1D uniform Bose gas with repulsive contact interactions. In particular, we have observed the same increasing-with-temperature behaviour of the chemical potential at low T, caused by the thermal excitation of phonons, like in superfluids, even if the system does not exhibit any superfluid phase. The investigation is based on the numerical solution of the Bethe-Ansatz equations of the Yang-Yang theory. By using the mapping with the 1D problem, we have studied a gas with a small number N of atoms in a ring, by focusing on the deviations of the thermodynamic behaviour in a ring from the one in the large N limit. The main results of this Chapter will be presented in a forthcoming paper [De Rosi et al., 2017].

List of Publications

The original results presented in this thesis have been published in the following articles:

3 **G. De Rosi**, G. E. Astrakharchik, and S. Stringari
Thermodynamic behaviour of a one-dimensional Bose gas at low temperature,
submitted to arXiv & Phys. Rev. A.
Discussed in Chap. 6 & Ref. De Rosi et al. [2017].

2 **G. De Rosi**, and S. Stringari
Hydrodynamic versus collisionless dynamics of a one-dimensional harmonically trapped Bose gas,
Phys. Rev. A **94**, 063605 (2016).
Discussed in Chap. 5 & Ref. De Rosi and Stringari [2016].

1 **G. De Rosi**, and S. Stringari
Collective oscillations of a trapped quantum gas in low dimensions,
Phys. Rev. A **92**, 053617 (2015).
Discussed in Chap. 3 & Ref. De Rosi and Stringari [2015].

Chapter 1

Overview of ultracold gases

> Life is strong and fragile. It's a paradox... It's both things, like quantum physics: It's a particle and a wave at the same time. It all exists all together.
>
> Joan Jett

The 20th-century was characterised by a deep revolution in Physics: scientists began to investigate the nature and the behaviour of atoms. This needed the introduction of a new theoretical paradigm given by Quantum Mechanics. One of the most important successes of this new theory was the explanation of the wave-particle duality exhibited by both matter (like particles, in particular, electrons) and electromagnetic radiation. The wave nature of light was first discovered in the Young experiment in 1801, through the observation of diffraction and interference phenomena. Later on, similar experiments, carried out also with electrons, lead to the same results and demonstrated the wave nature of particles. In 1905, Einstein's conjecture on photoelectric effect [Einstein, 1905] showed that light is composed of elementary particles: the photons. If one considers light of angular frequency ω, each photon carries a quantum (i.e. a packet) of energy $E = \hbar\omega$, where $\hbar = h/(2\pi)$, being h the Planck constant.

The theoretical explanation of the wave-particle duality came only in 1924 thanks to de Broglie [1925]. He showed that a particle with momentum, whose modulus is p, is associated with a wave of wavelength $\lambda_T = 2\pi\hbar/p$, known as de Broglie wavelength. If one considers a gas at temperature T, by using the Maxwell-Boltzmann distribution, one calculates the average momentum per particle $\langle p \rangle \sim \sqrt{mk_BT}$, where m is the mass of the particle and k_B is the Boltzmann constant. Therefore, one can rewrite the de Broglie wavelength as a function of temperature $\lambda_T \sim \sqrt{\hbar^2/(mk_BT)}$. If the temperature decreases, the particle slows down and its λ_T increases. In particular, at room temperature, λ_T is smaller than the atomic radius and the wave (quantum) nature of the gas does not emerge, and the particles which compose the gas behave as billiards balls. On the other hand, at temperature of few nK (reached experimentally only in the last two decades), λ_T is bigger than the average interparticle distance, therefore the wavepackets associated to particles overlap. The consequences of this are that particles lose their identity and they move all together as a giant matter wave with a very small velocity ~ 1 mm/s.

Moreover, at low temperature, the different quantum statistics of particles, namely the different behaviour of bosons and fermions, becomes apparent. In fact, similarly to waves, particles interfere. However, while bosons interfere constructively, fermions interfere destructively. This leads to distinct collective behaviours when many particles are prone to occupy the same energy levels, that is in the quantum degenerate regime. At the thermo-

dynamical level, the ground state of a system of non-interacting identical particles depends on the nature of its constituents. The BEC phase was predicted for non-interacting bosons (i.e. particles with integer spin, described by the Bose-Einstein distribution) [Einstein, 1924, 1925] on the basis of an idea on the statistical description of photons [Bose, 1924]. At $T = 0$, bosons condense in the ground state of the system described by a single wavefunction and they behave as a coherent matter wave. BEC phase is a consequence of quantum statistical effects because it occurs even without interactions. For a long time, these predictions were purely theoretical without any practical impact. Only after 70 years, in 1995, this new phase was realised experimentally by using dilute clouds of alkali atoms [Anderson et al., 1995, Davis et al., 1995, Bradley et al., 1995]. On the other hand, identical fermions (i.e. particles with half-integer spin, described by the Fermi-Dirac distribution) exhibit a different behaviour at low T: they cannot occupy the same energetic state due to the Pauli exclusion principle. Indistinguishable fermions populate the lowest energy levels from bottom-up with exactly one particle per level, forming the so-called Fermi sea. Moreover, differently from bosons, ideal fermions do not exhibit a quantum phase (like superfluidity) but only a quantum nature at $T = 0$, as first experiments with cold atoms showed, starting from 1999 [DeMarco and Jin, 1999, Schreck et al., 2001, Truscott et al., 2001].

All interacting atomic systems (except helium) undergo a phase transition to the solid state at enough low temperatures. The only way to reach a bosonic or fermionic ultracold atomic gas is in conditions of metastability (i.e. of local and not global minimum energy states). Metastability is ensured by the following criteria:

- the atomic gas is really dilute (with density $n \sim 10^{13} - 10^{15}$ atom/cm^3) such that the average interparticle spacing is much larger than the range r_0 of interactions ($n^{-1/3} \gg r_0$). This avoids three-body collisions and only elastic binary collisions between atoms are important. Since the density is really small, we need to reach very low temperatures $T \sim \mu K$ in order to appreciate quantum statistical effects.

- The atomic gas is kept far away from any material wall in order to avoid any interaction which would bring to the formation of molecules and, consequently, to the solid state.

The above conditions are satisfied if one confines a very dilute ultracold atomic gas in optical or magnetic traps [Inguscio and Fallani, 2013]. Elastic binary collisions are really important. They are fast, being their relaxation times shorter than the lifetime of the metastable atomic gas. Hence, they ensure the thermalization of the system. Moreover, binary collisions are responsible for the evaporative cooling for which, while high-energy atoms escape from the sample, the others thermalize with a redistribution of energy at lower T. In addition, collisions are responsible for the interatomic interactions which play a crucial role in the stability and the properties of quantum gases, affecting a lot of measurable properties such as the equilibrium density profiles, the ground-state energy and the collective frequencies. Differently from bosons, the presence of a superfluid quantum phase in Fermi gases depends not only on statistical effects but also on interaction.

The present Chapter is completely devoted to ultracold atomic gases which enable to investigate the manifestations of Quantum Mechanics at the many-body level.

In Sec. 1.1, we focus on non-interacting quantum gases, pointing out the effects of quantum statistics.

Since quantum gases are realised experimentally in trapped configurations, we discuss in Sec. 1.2 the concept of local density approximation which allows simplifying the treatment of trapped gases.

Given the importance of the interaction, we briefly dedicate Sec. 1.3 to the investigation of binary collisions in quantum gases, with the introduction of a single parameter a, the $s-$wave scattering length, which encodes all the information of the short-range interaction potential and how it can be tuned by means Fano-Feshbach resonances.

In Sec. 1.4, we outline some key features related to the phenomenon of superfluidity, a very peculiar quantum phase at low T and we investigate its main properties, like an unusual flow characterised by zero viscosity. Similar features are also shared by BEC.

We conclude this Chapter with interacting gases for both quantum statistics. In Sec. 1.5 we introduce the Bose gas and the two most important tools to describe it: the Bogoliubov theory and the Gross-Pitaevskii equation. In Sec. 1.6, we review the Fermi gases and all their experimentally accessible interaction regimes included in the BEC-BCS crossover.

An exhaustive treatment of these concepts is however out of the aims of this thesis; readers interested in more extended discussions can see Dalfovo et al. [1999], Pethick and Smith [2002], Giorgini et al. [2008], Walraven [2013], Pitaevskii and Stringari [2016], on which this Chapter is based.

1.1 Ideal quantum gases

Particles are of two different types: fermions and bosons. Fermions are characterised by an half-integer spin and they are the elementary components of matter: electrons, protons and neutrons which compose atoms are fermionic particles. Bosons instead have integer spin. An assembly of fermions (like an atom) may have a fermionic nature (with half-integer total spin and an odd number of fermions) or rather a bosonic nature (with integer total spin and an even number of fermions).

Bosons and fermions satisfy different quantum statistic laws. Ideal identical bosons obey the Bose-Einstein statistics, for which the energy distribution is:

$$f_B(\epsilon) = \frac{1}{e^{\beta(\epsilon - \mu)} - 1} \qquad (1.1)$$

where $\beta = 1/k_B T$ and k_B is the Boltzmann's constant. Eq. (1.1) represents the probability for a boson to occupy the state with energy ϵ at the chemical potential μ and at temperature T. Ideal fermions with the same chemical potential μ follow the Fermi-Dirac statistics:

$$f_F(\epsilon) = \frac{1}{e^{\beta(\epsilon - \mu)} + 1} \qquad (1.2)$$

which implies $f_F(\epsilon) < 1$, that is to say, the Pauli exclusion principle for which two indistinguishable fermions cannot occupy the same energy state. In the limit of low-density or high temperature, the two distributions (1.1) and (1.2) are equal to the classical Maxwell-Boltzmann statistics:

$$f_T(\epsilon) = e^{-\beta(\epsilon - \mu)} \qquad (1.3)$$

which describes a classical gas of non-interacting particles.

The quantum nature of particles appears only at low temperature and high atomic densities n, for which the interparticle distance $n^{-1/3}$ is of the order of the thermal de Broglie wavelength $\lambda_T = \sqrt{2\pi\hbar^2/(mk_B T)}$, which gives the size of the wave packet associated with each particle. When $n\lambda_T^3 \gtrsim 1$ Quantum Mechanics plays a role.

At low T, bosons occupy macroscopically the lowest energy state and there is a phase transition (BEC) characterized by a critical temperature T_C which provides, also, a scale of quantum degeneracy, for which quantum statistical effects are important. The BEC is a purely statistical phase, because it depends only on the distribution (1.1) and not on the interaction. The condition $f_B(\epsilon) > 0$ implies $\mu < \epsilon_0$, where ϵ_0 is the ground state energy. If $\mu \to \epsilon_0$, the occupation number (1.1) of the ground state diverges, marking the phase transition. The critical temperature T_C can be found from the normalization condition of the total number of particles N:

$$N = \sum_{i \neq 0} f_B(\epsilon_i, T_C, \mu = E_0) . \qquad (1.4)$$

On the other hand, at low T, ideal fermions occupy the Fermi sea, characterized by one particle per energy state. The highest energy state occupied is given by the Fermi energy $E_F = \mu(T = 0)$ and the Fermi temperature T_F. The Fermi energy can be calculated from the condition:

$$N = \sum_i f_F(\epsilon_i, T = 0, \mu = E_F) \ , \tag{1.5}$$

and one finds:

$$E_F = \frac{\hbar^2}{2m} \left(6\pi^2 n\right)^{2/3} \ . \tag{1.6}$$

For large T/T_F, (1.2) tends to be equal to Eq. (1.3), while at T = 0, all states with energy $\epsilon \leq E_F$ are occupied with probability 1, while all energy states with $\epsilon > E_F$ are empty. Therefore, T_F sets the temperature scale of quantum degeneracy. Finally, differently from the Bose case, the low temperature behaviour of an ideal Fermi gas does not imply a phase transition.

If one adds an external harmonic trap

$$V_{ext}(\mathbf{r}) = \sum_i \frac{1}{2} m \omega_i^2 r_i^2 \tag{1.7}$$

where the index $i = x, y, z$ denotes the spatial directions, both T_C and T_F, calculated from Eq. (1.4) and Eq. (1.5), respectively, are modified by the presence of the trap (1.7) [Pitaevskii and Stringari, 2016].

In Fig. 1.1, we report the different behaviours exhibited by bosons and fermions in both high and low-temperature regimes in harmonically trapped configurations.
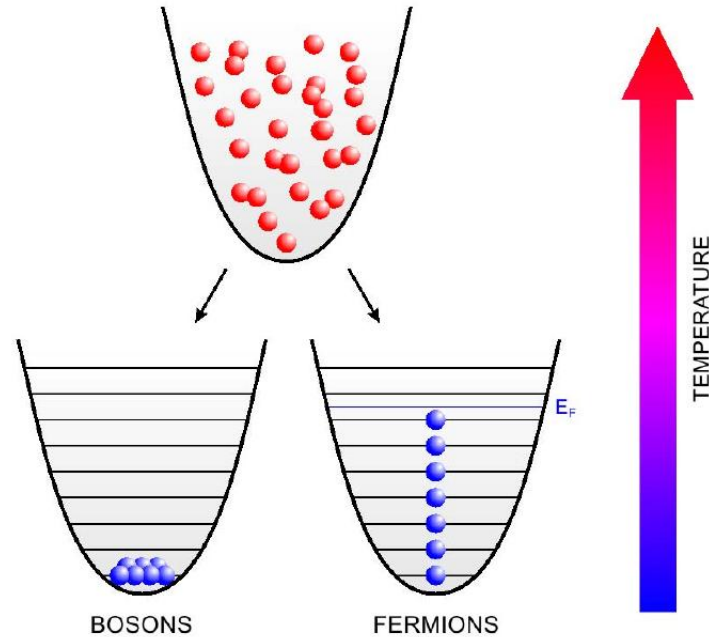
Figure 1.1: High (top) and low (bottom) temperature behaviour for bosons and fermions in an harmonic trap. "High" and "low" temperature is referred with respect to the energy spacing $\hbar\omega_{ho}$ between discretized levels of the trap with frequency ω_{ho}.

1.2   Local Density Approximation

In this Section, we investigate the Local Density Approximation (LDA) which simplifies the treatment of harmonically trapped systems. This condition holds if the system is large (with a large number of atoms N), in a weak trapping potential for which the density profile of the gas is slowly varying. At each position $\mathbf{r}$ there is a mesoscopic volume over which the local system is at equilibrium and homogeneous. Since all small volumes are in contact, they exchange heat (they are in thermal equilibrium with the temperature T) and particles (imposing a constant chemical potential μ_0 over the whole system). This simplification enables to investigate the thermodynamics of a trapped system, starting from the knowledge of its thermodynamic properties in uniform matter [Damle et al., 1996]. The global chemical potential μ_0 is written as the sum of the value $\mu[n(\mathbf{r}, T)]$ of the chemical potential, evaluated in uniform matter at the local value of the density and of the external potential $V_{ext}(\mathbf{r})$:

$$\mu_0 = \mu[n(\mathbf{r}, T)] + V_{ext}(\mathbf{r}) \ . \tag{1.8}$$

Eq. (1.8) provides an implicit equation for the density profile $n(\mathbf{r}, T)$ of the trapped gas at a given temperature T:

$$n(\mathbf{r}, T) = n[\mu(\mathbf{r}), T] = n[\mu_0 - V_{ext}(\mathbf{r}), T] \ , \tag{1.9}$$

where μ_0 is fixed by the normalization condition of the number of particles:

$$N = \int d\mathbf{r} n[\mu_0 - V_{ext}(\mathbf{r}), T] \ . \tag{1.10}$$

Starting from the knowledge of the density profile (1.9), the global chemical potential μ_0 and the temperature T, one can calculate the density profile and all thermodynamic functions. The LDA (1.8) is expected to be a reliable approximation for sufficiently large systems where finite size corrections and gradients terms in the density profile are negligible. Moreover, its interest lies also in its generality: it can be applied to a large variety of systems, independent on quantum statistics (bosons and fermions), on temperature, on interaction regime, once it is known the equation of state $\mu[n(\mathbf{r}, T)]$. For example, while in the case of BEC gases, LDA is ensured by the repulsive interaction among atoms, see Sec. 1.5, in the ideal Fermi gas, LDA can be still applied thanks to the quantum pressure related to the Pauli principle.

As we investigate in Chap. 3, LDA still applies in quasi-low-dimensional (D) (pancake and cigar) systems but does not in deep low D (two-dimensional (2D) and 1D) along the directions of tight confinement.

1.3   Binary collisions

In this Section, we recall some basic tools of the theory of scattering of slow particles [Landau, 1958], which can be applied to describe elastic binary collisions in ultracold matter. We investigate why they occur generally in the $s-$wave channel (i.e. with zero total angular momentum $\ell = 0$) and exhibit a short-range character. In particular, in SubSec. 1.3.1, we study how, given the short-range properties of the interatomic potential, we can replace it with a contact pseudopotential depending only on one parameter, the $s-$wave scattering length a, which encodes all the relevant information of the interaction.

This method can be applied to both bosons and fermions with some important differences. As a matter of fact, for example, BEC containing a large number of bosons is

stable only in the presence of interparticle repulsion. It collapses with attractive interaction when the number of bosonic atoms exceeds a critical threshold [Donley et al., 2001]. On the other hand, the Pauli exclusion principle prevents two fermions in the same energy and spin state to undergo s−wave scattering. Therefore, with attractive interactions, a Fermi system does not collapse like BEC. a can be tuned experimentally with the variation of an external magnetic field, thanks to the Feshbach resonances, introduced in SubSec. 1.3.2. Hence, if one considers two fermions of different spin states, by tuning a, one can explore the crossover from a BEC of composite molecules to a superfluid of weakly-bound Cooper pairs, described by the Bardeen-Cooper-Schrieffer (BCS) theory [Bardeen et al., 1957a,b], see SubSec. 1.6.1.

1.3.1 s-wave scattering length

Let us consider an elastic collision of two slow particles of mass m_1 and m_2, respectively. By neglecting small relativistic spin-spin and spin-orbital interactions, the solution of this two-body scattering problem reduces to that of the Schrödinger equation in the centre-of-mass frame:

$$\left[-\frac{\hbar^2}{2\mu}\nabla_{\mathbf{r}}^2 + V(r) \right] \Psi(\mathbf{r}) = E\Psi(\mathbf{r}) \ , \tag{1.11}$$

where $\mu = m_1 m_2/(m_1 + m_2)$ is the reduced mass of the two atoms and $\mathbf{r} = \mathbf{r}_1 - \mathbf{r}_2$ is the relative coordinate, whose modulus is $r = |\mathbf{r}|$, and the energy is positive $E > 0$. The relative interaction potential $V(r)$ is isotropic [1] and, therefore, depends only on r. Moreover, it can be described as a Van der Waals potential with $1/r^6$ attractive tail and short range $1/r^{12}$ repulsion. Since such potential decays fast with r, it manifests a finite-range character, in the sense that the interaction is relevant only within a region of radius r_0, the so-called range of the potential.

Let us show that at low T, the s−wave scattering is dominant in Eq. (1.11). Since $V(r)$ is a central potential, the wave function $\Psi(\mathbf{r})$ can be factorized in radial and angular contributions as $\Psi(\mathbf{r}) = \psi_\ell(r)Y_\ell^m(\theta, \phi)$, where Y_ℓ^m is the spherical harmonics with ℓ orbital angular momentum and m its projection along z−direction. Each ℓ term corresponds to a partial wave with angular momentum $\hbar\ell$. The resulting radial equation is

$$\left[-\frac{\hbar^2}{2\mu} \left(\frac{\partial^2}{\partial r^2} + \frac{2}{r}\frac{\partial}{\partial r} \right) + V_{eff}(r) \right] \psi_\ell(r) = E\psi_\ell(r) \ , \tag{1.12}$$

where we have introduced the effective potential

$$V_{eff}(r) = V(r) + \frac{\hbar^2 \ell(\ell+1)}{2\mu r^2} \tag{1.13}$$

which, for all partial waves $\ell > 0$, is given by the sum of the original central potential and a centrifugal repulsive barrier $\propto 1/r^2$. The height of this centrifugal barrier, converted in temperature, is typically of the order ~ 1 mK and below this T, p−waves ($\ell = 1$) and higher-order partial waves are suppressed, leaving only the s−wave collisions ($\ell = 0$) dominant. Since the typical ultracold range of T is $\sim \mu K \div nK$, quantum gases are in the s-wave two-body collision regime.

In the centre-of-mass frame, an incoming wave packet of wave vector $\mathbf{k}$ is scattered by the central potential $V(r)$, as represented in Fig. 1.2.

Far from the scattering center $r \gg r_0$ (for the diluteness condition), the two-body wave function, solution of Eq. (1.11), takes the asymptotic form [Landau, 1958]:

$$\Psi(\mathbf{r}) \propto e^{i\mathbf{k}\cdot\mathbf{r}} + f(k,\theta)\frac{e^{ikr}}{r} \tag{1.14}$$

---

[1]An example of anisotropic potential is provided by dipolar interaction.
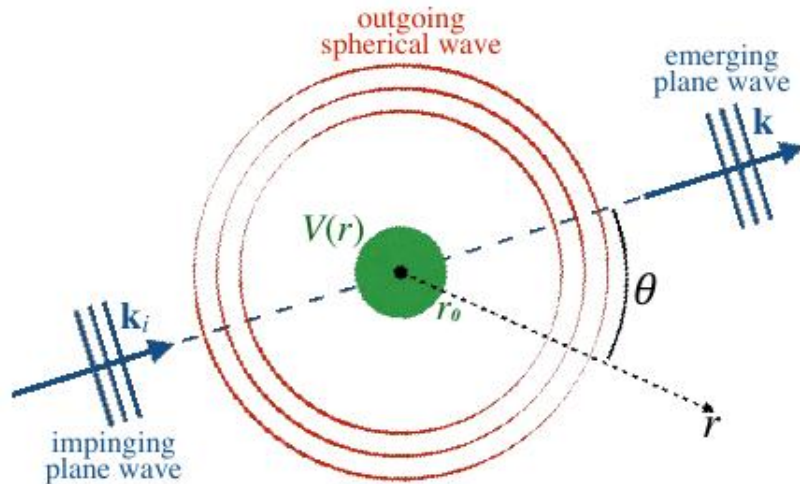
Figure 1.2: 3D scattering from a central potential $V(r)$. In the relative coordinate frame an impinging plane wave of wave vector $\mathbf{k_i}$ enters in the region $r < r_0$, where $V(r)$ is considerable. After the scattering process, and far from the scattering centre, the wave function is the superposition of an emerging plane wave of wave vector $\mathbf{k}$ and an outgoing spherical wave, whose amplitude is modulated in space depending on θ, the angle between $\mathbf{k}$ and the detection direction. From Bartolo [2014].

that is, the superposition of an ingoing plane-wave (unperturbed free particle) with wave vector $k = \sqrt{2\mu E/\hbar^2}$ and an outgoing spherical wave (scattered particle), modulated by the 3D scattering amplitude $f(k,\theta)$ (i.e. amplitude of the wave function in the scattered state).

In the $s-$wave regime, by symmetry f is independent on θ and, at low scattering energies, it becomes also independent on k, by reaching consequently a constant value:

$$\lim_{k \to 0} f(k,\theta) = -a \ , \tag{1.15}$$

where we have introduced the 3D scattering length a. Therefore, at low energies, the only parameter describing the interactions is a. This means that the details of the potential $V(r)$ do not affect the low-energy two-body Physics. As a consequence, the low-temperature scattering properties of many different atomic species are actually described by a unique Hamiltonian, that can be derived using any model potential, as long as it reproduces Eq. (1.15) and which can replace the original $V(r)$. In particular, one can choose a "universal" zero-range potential, approximating the interaction with a contact interaction:

$$V(\mathbf{r}) = \frac{2\pi\hbar^2 a}{\mu}\delta(\mathbf{r}) \ , \tag{1.16}$$

where we can define the 3D coupling constant $g_{3D} = 4\pi\hbar^2 a/m$ for $m = m_1 = m_2$ and $\delta(\mathbf{r})$ is the Dirac function [2]. We remind also that since the wave nature of atoms is relevant at low T, interactions can no longer be described by point-like collisions of particles approaching on distances $\sim r_0$, but interactions behave more as an overlap of waves with the new length scale provided by a.

---

[2]See Cohen-Tannoudji [1998-1999] for the details of the choices of the interaction potential. The $\delta(\mathbf{r})$ potential has to be regularized for the calculation of some physical quantities.

From the knowledge of f, one can compute the scattering cross-section σ:

$$\frac{d\sigma}{d\Omega} = \begin{cases} |f(k,\theta)|^2, & 0 < \theta < \pi \quad \text{distinguishable particles} \\ |f(k,\theta) \pm f(k,\pi-\theta)|^2, & 0 \leq \theta \leq \pi/2 \quad \text{identical particles} \end{cases} \qquad (1.17)$$

where $d\Omega = 2\pi\sin\theta d\theta$ is the differential solid angle and $+\ (-)$ is referred to identical bosons (fermions), ensuring that the orbital part of the wave function must be symmetric or anti-symmetric, depending on whether the total spin of the two particles is even or odd. Since f is independent on θ in the $s-$wave channel, one gets, by using Eq. (1.15):

$$\sigma = \begin{cases} 4\pi a^2 & \text{distinguishable particles} \\ 8\pi a^2 & \text{identical bosons} \\ 0 & \text{identical fermions .} \end{cases} \qquad (1.18)$$

The role played by quantum statistics is evident: for identical bosons, constructive interferences lead to an amplified cross-section, while destructive interferences cancel out the s-wave scattering for identical fermions. Thus, in the low-energy regime, two distinguishable spin-states are required for collisions to occur in a Fermi gas.

1.3.2 Fano-Feshbach resonances

In SubSec. 1.3.1 we introduced the concept of scattering length a, which characterizes the strength of the pseudopotential in the low-energy scattering. By comparing a with the average interparticle distance $n^{-1/3}$, we can conclude if the interactions are weak or strong:

$$\begin{cases} n^{1/3}a \ll 1 & \text{weak interaction} \\ n^{1/3}a \gg 1 & \text{strong interaction .} \end{cases} \qquad (1.19)$$

In this Subsection, we review the basic concepts of Fano-Feshbach resonances (FR) which are a very important experimental tool to tune the value and the sign of a, and therefore the two-body interaction in ultracold gases. This possibility to control with high precision the interaction is typical of ultracold gas experiments and it depends on the internal spin degrees of freedom of atoms which affect the interatomic interaction potential. By considering different spins, we can change the interaction by means FR, even if we have already fixed the atomic species and so their scattering potential. Even if the interaction is fixed, FR can tune a by selecting different scattering channels. The idea of FR was introduced independently by Feshbach [1958, 1962] and Fano [1935, 1961] in the field of nuclear and atomic Physics respectively (see Chin et al. [2010] for a review).

FR take place when two atoms in their initial lowest energy spin states (i.e. open channel) can be coupled to different final states (i.e. closed channel) by a collision, see Fig. 1.3. If the coupling is of hyperfine kind, the transition involves only spins and it is affected by an external magnetic field B. In this special case, we refer to magnetic FR, but in general, we refer to FR when the coupling is induced by the variation of an external parameter like B. Therefore, FR work not only for atoms in different internal (i.e. spin) states but also for identical and different atoms (i.e. of different species). The most important example is given by the magnetic FR, because, applied to fermionic atoms, lead to the realisation of strongly interacting Fermi gases and to explore the whole BCS-BEC crossover, see Sec. 1.6. In addition, FR can be obtained by coupling the open and the closed channel with radio-frequency or optical radiation. The latter method [Fedichev et al., 1996, Theis et al., 2004] suffers from heating problems and this makes it less suitable compared to magnetic FR for ultracold atoms experiments.

The open or background channel, given by the interaction potential V_{bg} and the scattering length a_{bg}, corresponds to the ground state spin configuration of the incoming particles.

We can consider also another scattering channel, described by the potential V_c, given by different spin states. Thus, the energy of the closed channel changes with an external magnetic field B. Moreover, it admits a bound state with energy E_c, Fig. 1.3.
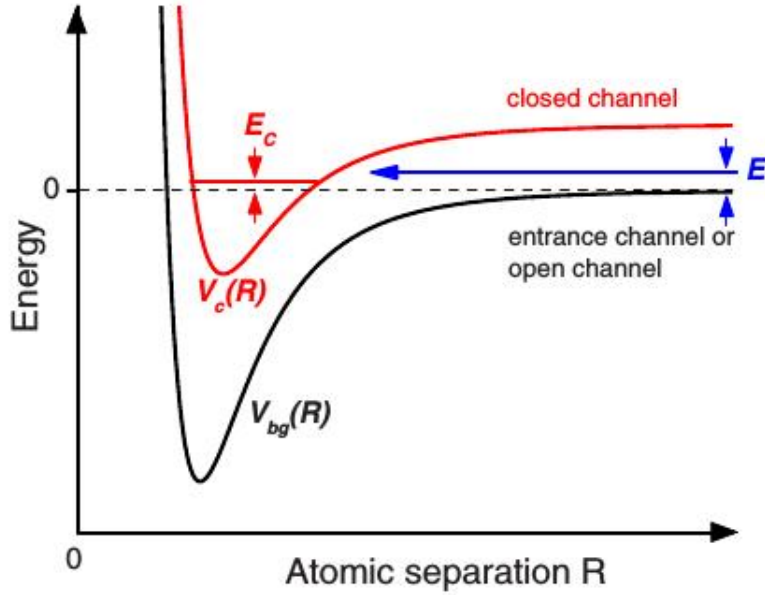
Figure 1.3: Schematic representation of the two-channel model for the Feshbach resonances (FR). Two particles scatter with energy E in the open channel, given by the background interaction potential V_{bg}. Another scattering channel given by, for instance, a different spin configuration of the incoming particles, is the closed channel described by the potential V_c. The closed channel admits a bound state with energy E_c. If $E \sim E_c$, the scattering cross section in the open channel is resonantly enhanced. From Chin et al. [2010]. Copyright © 2010, American Physical Society.

If the scattering energy E, entering in Eq. (1.11), is far from E_c, the particles do not feel the closed channel and $a = a_{bg}$. On the other hand, by tuning B, $E_c \sim E$ and we say that the closed-channel bound state is resonant with E. This leads to an enhancement of a and thus also of the cross section. From the experimental point of view, FR tune a by means a static B which changes the relative distance between the open and the closed channel.

For special values of B, if E_c crosses the zero energy point, Fig. 1.3, a is divergent and one gets the resonance. The width of the resonance Δ is expressed as a range of B and it depends on the coupling strength between the open and the closed channel. This coupling leads to a dressed bound state in the closed channel given by the open channel and features also the dependence on B of the scattering length a [Moerdijk et al., 1995]:

$$a(B) = a_{bg} \left(1 - \frac{\Delta}{B - B_0} \right) \, , \tag{1.20}$$

where at $B = B_0$, the resonance occurs: a diverges ($1/a = 0$) and drops out of the problem (unitary regime). Eq. (1.20) is plotted in Fig. 1.4. For $B = B_0 + \Delta$, $a = 0$ and one reaches the non interacting limit. If B is far from B_0, the scattering length tends to be equal to its background value $a \to a_{bg}$.

We note also that both Δ and a_{bg} can be either positive or negative like a. In particular, by changing FR adiabatically from a negative to a positive value of a, one can observe the
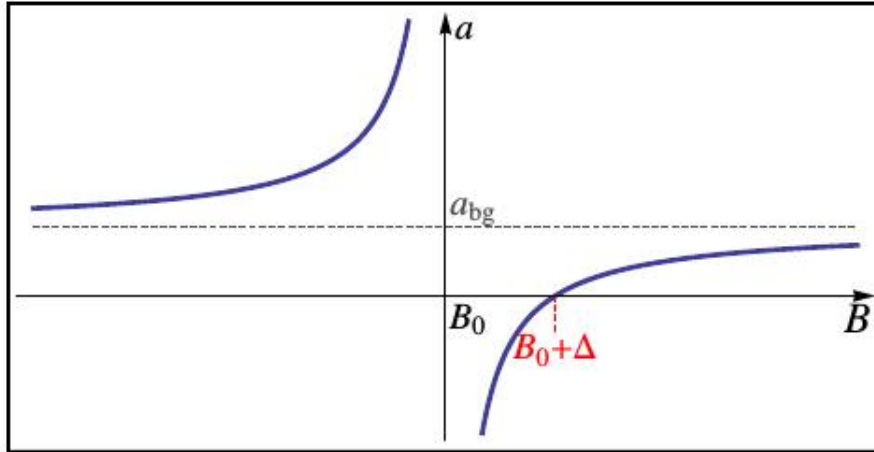
Figure 1.4: Scattering length a as a function of the external magnetic field B in a Feshbach resonance, Eq. (1.20). The resonance occurs for $B = B_0$ and has width Δ. From Ferrier-Barbut [2014].

formation of a dimer state, composed by two atoms [Chin et al., 2010]. In particular, close to the resonance, this bound state is strongly dressed, Eq. (1.20), and its binding energy takes the typical value:

$$E_b = -\frac{\hbar^2}{ma^2} \ ,$$

(1.21)

where a is also proportional to the spatial extent of the dimer wave-function.

We remark finally that as experimentally shown by Inouye et al. [1998] for the first observation of FR in an optically trapped BEC of Na atoms, we can conclude that the two most important features of FR are the tunability of a and the fast loss of atoms in the resonance region. Since this experiment investigates a BEC, it is natural to relate the resonance to a strongly enhanced three-body recombination with the consequent molecular formation for a Bose system. Therefore, when we refer to the unitary regime, we consider mainly Fermi systems which are protected to molecular losses thanks to the Pauli exclusion principle.

1.4 Superfluidity & Bose-Einstein condensation

The discovery of the superfluid state of matter marked the beginning of the exploration of Quantum Physics at thermodynamic level in quantum many-body systems. In this Section, we want to review the concept of superfluidity, its properties and how it is connected to the phenomenon of the Bose-Einstein condensation, by analysing differences and analogies between these two low-temperature quantum phases.

1.4.1 Historical Overview

Superfluidity was observed for the first time with the liquefaction of helium (with its bosonic isotope ^{4}He) in 1908 by Kamerlingh Onnes [1967]. While ^{4}He reaches liquefaction at $T = 4.2$ K, he succeeded in reaching temperatures as low as 1.5 K. Then, he used this cold reservoir of liquid to cool down other materials. This led to the discovery of superconductivity in mercury in 1911 which was marked by the absence of resistivity of the system for temperatures below 4.2 K. In 1937, the experiments of Kapitza [1938] and Allen and Misener [1938] allowed to understand that liquid ^{4}He undergoes a superfluid phase transition at 2.2 K, characterised by zero viscosity of the system. The low-temperature

absence of electric resistance and viscosity are connected each other: superconductivity is explained with the formation of Cooper pairs composed of electrons (fermions) in a metal, as prescribed by the BCS theory [Bardeen et al., 1957a,b], while the superfluidity in ^{4}He is associated to the BEC of bosonic atoms [Tisza, 1938, 1947]. For the latter case, London [1938] was the first who related superfluidity of ^{4}He to BEC, by observing that the experimental value of the superfluidity critical temperature is really close to the theoretical prediction of the critical temperature of condensation for the ideal Bose gas at the same density. A few years later, Landau [1941] provided the first theory of superfluids in terms of the spectrum of elementary excitations of ^{4}He. This led to the two-fluid hydrodynamics, first suggested by Tisza [1940]. In 1972, Osheroff et al. [1972a,b] discovered the superfluidity in the fermionic isotope ^{3}He at temperature much lower than its bosonic twin ($T < 2.6$ mK). This very low critical temperature is needed to form pairs of fermionic ^{3}He atoms. This historical step was the bridge which related the superfluid ^{4}He and superconductivity phenomena. Finally, Leggett [1975] provided the theory describing the p-wave pairing in ^{3}He, by modifying the BCS theory. In 1947, Bogoliubov developed the microscopic theory of weakly interacting Bose gases, based on the BEC phenomenon. Moreover, the concept of off diagonal long range order [Penrose, 1951, Penrose and Onsager, 1956, Landau and Lifshitz, 2013] was defined and its presence was related to BEC.

Differently from ultracold gases, liquid helium is a dense system: its average interatomic distance is of the order of the range of interatomic forces (few Angstrom). It is characterised by strong interactions which can mask most of the physical quantum features, Moreover, it exhibits short-range correlations and quantum fluctuations which allow it to remain liquid even at zero temperature. Only with the increase of the pressure, helium undergoes a liquid-solid phase transition.

Since, in general, at very low temperatures, most of the materials undergo a solid phase transition, no superfluid other than liquid helium was available until the first experimental realisation of BEC in ultracold atoms [Anderson et al., 1995, Davis et al., 1995]. The BEC phase is characterised by the velocity distribution reported in Fig. 1.5, which shows the macroscopical occupation of the state with zero momentum at low T. During the subsequent 22 years, an intense theoretical and experimental research was dedicated to the investigation of ultracold gases as quantum systems as well as their properties, sign of a superfluid phase transition, occurring at low temperatures.

In the following, we review the signatures of superfluidity shared by helium, both Fermi and Bose atomic gases as well as BEC.

1.4.2 Properties of superfluidity

Superfluidity is strongly connected to BEC and they share some common properties. The superfluid phase cannot be considered as a single phenomenon, but it is rather defined by means its properties, reviewed in this Subsection.

In general, every superfluid can flow through capillary tubes and slits without dissipation of energy: its shear viscosity is zero. When, in 1937, Kapitza, Allen and Misener discovered superfluidity in ^{4}He, they measured its viscosity in capillary tubes at $T < 2.2$ K and they found that it exhibits **non-viscous properties** [Wilks and Betts, 1987]. This phenomenon was explained by Landau [1941], who noticed that the flow in a superfluid occurs without dissipation (i.e. excitations) below a certain critical velocity, whose existence was proved by Raman et al. [1999] and Onofrio et al. [2000]. The Landau's criterion for superfluidity fixes this critical velocity:

$$v_c = \min_p \left(\frac{\epsilon(p)}{p} \right) \tag{1.22}$$
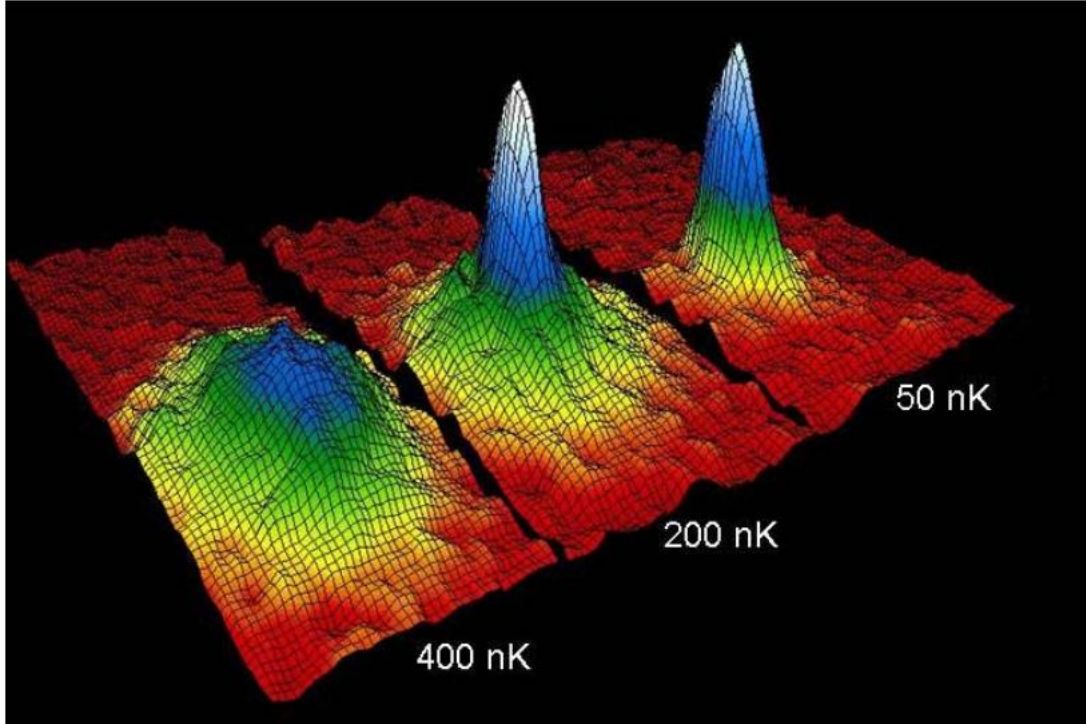
Figure 1.5: Velocity distribution of the BEC at different low T for a gas of Rubidium atoms. The BEC emerges as a peak around zero momentum, as the ground state becomes macroscopically occupied. From Anderson et al. [1995]. Copyright © 1995, American Association for the Advancement of Science.

where $\epsilon(p)$ is the dispersion relation of elementary excitations of the system.

Moreover, a superfluid is described by a macroscopic wave function $\psi(\mathbf{r})$, which implies the **phase coherence** as experimentally proved with the interferences of condensates [Andrews et al., 1997b, Bloch et al., 2000].

While the superfluid wave function can be expressed as $\psi(\mathbf{r}) = |\psi(\mathbf{r})|e^{iS(\mathbf{r})}$ in module-phase representation, the superfluid velocity is characterized by the gradient of the phase S:

$$\mathbf{v} = \frac{\hbar}{m}\nabla S(\mathbf{r}) \tag{1.23}$$

where m is the mass of the superfluid particles. Therefore, the superfluid velocity, Eq. (1.23) is always irrotational ($\nabla \times \mathbf{v} = 0$). The **irrotationality** is present also in BEC.

The phase S is always single-valued and this leads to the existence of **quantized vortices** in every superfluid, but firstly predicted in superfluid helium [Onsager, 1949, Feynman, 1953, 1954] and experimentally observed in the same system [Hall and Vinen, 1956, Rayfield and Reif, 1964] and only after even in ultracold gases [Matthews et al., 1999, Madison et al., 2000, Abo-Shaeer et al., 2001, Zwierlein et al., 2005].

At $T = 0$, the macroscopic dynamics of every superfluid is described by the **hydrodynamic theory**, which can be applied also to BEC.

This approach has been generalised at finite temperature below the critical point of superfluidity with the **two-fluid** model, first proposed for liquid helium [Tisza, 1938, Landau, 1941]. This theory provides the description of the dynamics of two fluids: a *normal* fluid behaving like a Newtonian (i.e. classical) fluid and the *superfluid* component which does not carry entropy and has no viscosity. In particular, the two-fluid hydrodynamic theory predicts the existence of a **second sound** velocity associated to the presence of the superfluid density. The second sound is an entropy wave, with constant pressure, where

the superfluid and the normal densities oscillate with opposite phases. It is present not only in ^{3}He and ^{4}He but also in quantum gases [Andrews et al., 1997a, Stamper-Kurn et al., 1998, Hou et al., 2013b, Sidorenkov et al., 2013]. The experimental investigation of second sound in quantum gases has provided a first measurement of the superfluid density.

1.5 Weakly interacting Bose-Einstein condensates

In this Section, we would like to consider the interactions in a BEC which are described by the s-wave scattering length a.

If the interactions are attractive ($a < 0$), the BEC is unstable and it collapses above a critical threshold of the number of atoms, of the order of 1000 [Bradley et al., 1997, Sackett et al., 1999, Gerton et al., 2000, Donley et al., 2001, Roberts et al., 2001]. An ideal BEC ($a = 0$) is stable, but the thermalization is forbidden because of the absence of interatomic collisions. Moreover, it is not superfluid, because its critical velocity for superfluidity vanishes, as prescribed by the Landau's criterion, see Sec. 1.4.2. The strongly interacting unitary regime ($1/a = 0$), is unstable for a BEC, due to the three-body losses depleting the gas. Finally, the weakly-interacting BEC, with atoms repelling each other ($a > 0$), has the Bogoliubov excitation spectrum fully compatible with the Landau's criterion, therefore, it can be considered as superfluid. Therefore, it exhibits some typical properties of every superfluid, like quantized vortices [Matthews et al., 1999, Madison et al., 2000, Abo-Shaeer et al., 2001] and the critical velocity [Raman et al., 1999, Onofrio et al., 2000] in a stirred BEC. For this reason, from now on, we discuss only the case of weakly-interacting BEC with $a > 0$, which can be realised experimentally on the tail of a FR. In this Section, we discuss also the basic concepts of the theory describing this interaction regime: the Bogoliubov theory and the Gross-Pitaevskii equation.

1.5.1 Bogoliubov theory

At $T = 0$, the weakly-interacting Bose gas is described by the Hamiltonian in the second quantization, obtained for a contact interaction (1.16):

$$\hat{H} = \int d\mathbf{r} \left(\frac{\hbar^2}{2m} \nabla \hat{\psi}^\dagger \nabla \hat{\psi} + \frac{g}{2} \hat{\psi}^\dagger \hat{\psi}^\dagger \hat{\psi} \hat{\psi} \right) \tag{1.24}$$

where g is the coupling constant

$$g = \frac{4\pi \hbar^2 a}{m} \ , \tag{1.25}$$

calculated within the Born approximation. Eq. (1.24) can be solved by using the Bogoliubov (BG) prescription (also called mean-field (MF)) $\hat{\psi} = \psi_0 + \delta\hat{\psi}$, with the perturbation $\langle \delta\hat{\psi} \rangle \ll 1$ [3], representing the depletion of the BEC. The ground-state condensate wavefunction ψ_0 is not anymore an operator, but it is a complex quantity, see Eq. (1.40), which assumes the role of the order parameter of the BEC, $\psi_0 = \sqrt{n}$, with n the density of the condensate, equal to the total value.

At the lowest order of approximation $\hat{\psi} = \psi_0$, the ground-state energy is

$$E_0 = \frac{1}{2} N n g \ , \tag{1.26}$$

while the pressure

$$P = -\frac{\partial E_0}{\partial V} = \frac{1}{2} g n^2 \tag{1.27}$$

---

[3] The gauge symmetry $\psi \to e^{i\alpha}\psi$ of Eq. (1.24) is broken for the onset of the BEC phase transition.

---

which shows the condition of mechanical stability $\partial n / \partial P \geq 0$ for positive compressibility, that an uniform BEC exists only for repulsive interaction $a > 0$. The chemical potential is:

$$\mu = \frac{\partial E_0}{\partial N} = gn \tag{1.28}$$

which can be combined with the LDA condition, see Eq. (1.8), to get the spatial density profile in harmonically trapped configurations:

$$n(\mathbf{r}) = \frac{\mu_0}{g} \left(1 - \sum_{i=x,y,z} \frac{r_i^2}{R_i^2} \right) \tag{1.29}$$

where $R_i = \sqrt{2\mu/(m\omega_i^2)}$ is the Thomas-Fermi radius at which the density of the BEC vanishes.

Quantum fluctuations, given by interactions, are responsible of the population of the excited states, even if the system is strictly at T = 0. At the second order of approximation in $\delta\psi$, one finally gets the BG dispersion relation of the elementary excitations of a BEC [Bogoliubov, 1947]:

$$\epsilon(p) = \sqrt{v_s^2 p^2 + \left(\frac{p^2}{2m} \right)^2} \tag{1.30}$$

where the speed of sound is $v_s = \sqrt{\frac{n}{m}\frac{\partial\mu}{\partial n}} = \sqrt{gn/m}$. Eq. (1.30) describes at low momenta p the phononic spectrum $\epsilon(p) \sim v_s p$, responsible of long wavelength excitations, while, at high-momenta, the free-particle law $\epsilon(p) \sim p^2/2m + gn$.

By considering a renormalized scattering length a and the quantum fluctuation effect, one finally finds the ground state energy per particle:

$$\frac{E_0}{N} = \frac{1}{2}gn + \frac{1}{2N} \sum_{p \neq 0} \left[\epsilon(p) - gn - \frac{p^2}{2m} + \frac{m(gn)^2}{p^2} \right] \tag{1.31}$$

where the last term in the sum is given by the renormalization of a and it is present in 3D, but not in 1D, as we discuss in Chap. 6. By replacing the sum with the integral in momentum space in Eq. (1.31), one finally finds the first correction (Lee-Huang-Yang (LHY)), given by interactions, in the ground-state energy per particle [Lee et al., 1957, Landau and Lifshitz, 1981, Pitaevskii and Stringari, 2016]:

$$\frac{E_0}{N} = \frac{1}{2}gn \left(1 + \frac{128}{15\sqrt{\pi}}\sqrt{na^3} \right) \tag{1.32}$$

and in the chemical potential

$$\mu = gn \left(1 + \frac{32}{3\sqrt{\pi}}\sqrt{na^3} \right) . \tag{1.33}$$

The LHY correction is quantified by a small value of the dimensionless gas parameter $na^3 \ll 1$. Therefore, one concludes that the MF approximation holds in the weakly-interacting regime, see SubSec. 1.3.2. In Chap. 6 a similar LHY calculation will be discussed, but in 1D. Thanks to FR, LHY correction has finally been measured in BEC [Papp et al., 2008, Navon et al., 2011].

1.5.2 Gross-Pitaevskii equation

At $T = 0$, a BEC is described by the famous time-dependent Gross-Pitaevskii equation [Gross, 1961, Pitaevskii, 1961]:

$$i\hbar \frac{d\psi}{dt} = -\frac{\hbar^2}{2m}\Delta\psi + V_{ext}(\mathbf{r})\psi + g|\psi|^2\psi \;, \qquad (1.34)$$

where $\psi(\mathbf{r}, t)$ is the wave-function of the BEC, connected to the density $n = |\psi|^2$. It coincides with the complex quantity ψ_0 of the SubSec. 1.5.1. The coupling constant is expressed by means the s-wave scattering length a, Eq. (1.25) and one considers an external potential V_{ext}, which can be of harmonic shape, Eq. (1.7). The terms in the right-hand-side of Eq. (1.34) are, respectively, the kinetic, the trapping and the interaction energy and they play an important role in the distinction of different physical regimes.

Eq. (1.34) describes also the information of the stationary states (not depending on time). Indeed, the time evolution of the order parameter is governed by the chemical potential μ

$$\psi(\mathbf{r}, t) = \psi(\mathbf{r})e^{-i\mu t/\hbar} \;, \qquad (1.35)$$

and Eq. (1.34) becomes the time-independent Gross-Pitaevskii equation

$$\left(-\frac{\hbar^2}{2m}\Delta\psi(\mathbf{r}) + V_{ext}(\mathbf{r}) + g|\psi(\mathbf{r})|^2\right)\psi(\mathbf{r}) = \mu\psi(\mathbf{r}) \qquad (1.36)$$

which has the shape of a non-linear Schrödinger equation, where the non-linearity comes from the interaction term, proportional to the particle density $n = |\psi|^2$.

If interactions can be neglected with respect to the trapping potential ($ng \ll V_{ext}$) in Eq. (1.34), one obtains the ideal gas limit, see Sec. 1.1, and the system is described by the Schrödinger equation:

$$i\hbar \frac{d\psi}{dt} = -\frac{\hbar^2}{2m}\Delta\psi + V_{ext}(\mathbf{r})\psi \;. \qquad (1.37)$$

In the stationary case, the solution of the corresponding Eq. (1.36) is the ground state of the harmonic oscillator:

$$n(\mathbf{r}) = \frac{N}{\pi^{3/2}} \frac{e^{-x^2/a_x^2}}{a_x} \frac{e^{-y^2/a_y^2}}{a_y} \frac{e^{-z^2/a_z^2}}{a_z} \qquad (1.38)$$

where $a_{i=x,y,z} = \sqrt{\hbar/(m\omega_i)}$ is the harmonic oscillator length and N is the total number of atoms in the BEC. Since a low collision rate implies a poor thermalization, these ideal non-interacting BEC are difficult to produce experimentally. Therefore, the most interesting case is when interactions are not negligible.

In the opposite limit of strong interactions, the so-called Thomas-Fermi limit, one neglects the kinetic term in the Gross-Pitaevskii equation (GPE), Eq. (1.34):

$$i\hbar \frac{d\psi}{dt} = V_{ext}(\mathbf{r})\psi + g|\psi|^2\psi \;. \qquad (1.39)$$

In this case, the solution of the stationary GPE (1.36) implies an equilibrium density distribution with an inverted parabolic shape, Eq. (1.29).

In the homogeneous limit $V_{ext}(\mathbf{r}) = 0$, the stationary GPE (1.36) returns all the results for the thermodynamics obtained with the Bogoliubov theory, see SubSec. 1.5.1. In particular, one gets the sound velocity $v_s = \sqrt{gn/m}$ which is the value obtained considering only the long-wavelength elementary excitations of the Bogoliubov spectrum (1.30).

The time-dependent GPE (1.34) describes the dynamics of the wave-function $\psi(\mathbf{r}, t)$ of the condensate. This wave-function, also called order parameter, is normalized to the total number of atoms $\int d\mathbf{r} |\psi(\mathbf{r}, t)|^2 = N$ and it can be expressed also as a complex quantity

$$\psi(\mathbf{r}, t) = \sqrt{n(\mathbf{r}, t)} e^{iS(\mathbf{r}, t)} \ , \tag{1.40}$$

with $S(\mathbf{r}, t)$ the phase of the order parameter. By defining the time-dependent superfluid velocity $\mathbf{v}(\mathbf{r}, t)$ as a function of the phase $S(\mathbf{r}, t)$, see Eq. (1.23), one can easily show that the GPE is completely equivalent to the two coupled equations of the density $n = n(\mathbf{r}, t)$ and the velocity $\mathbf{v} = \mathbf{v}(\mathbf{r}, t)$:

$$\frac{\partial n}{\partial t} + \nabla (n\mathbf{v}) = 0 \ , \tag{1.41}$$

$$m\frac{\partial \mathbf{v}}{\partial t} + \nabla \left(V_{trap}(\mathbf{r}) + gn - \frac{\hbar^2}{2m\sqrt{n}} \nabla^2 \sqrt{n} + \frac{1}{2}m\mathbf{v}^2 \right) = 0 \ , \tag{1.42}$$

called, respectively, the continuity equation and the Euler equation. Eqs. (1.41)-(1.42) have the typical structure of the dynamical equations describing a superfluid at $T = 0$ [Pitaevskii and Stringari, 2016]. In Eq. (1.42), there is only one term $\sim \hbar^2 \nabla^2 \sqrt{n}/\sqrt{n}$ which depends explicitly on the Planck constant: it is called *quantum pressure*. As we discuss in Chap. 3, these equations are used to study collective oscillations, under certain approximations.

1.6 Fermi superfluids

Differently from the bosonic case discussed in Sec. 1.5, Fermi gases are more stable in all ranges of interaction accessible. This striking stability is ensured by the Pauli exclusion principle, not present in Bose gas, responsible for the Fermi pressure which prevents the collapse at macroscopical level. This pressure is present in a lot of different systems, such as ultracold Fermi gases and neutron stars, where it can reach very high values, by counterbalancing the gravitational collapse. On the microscopical scale, the Pauli principle prevents the formation of pairs composed by two fermions with the same spin and the three-body collisions in a two-component gas.

In this Section, we discuss all interaction regimes which can be reached experimentally by means a FR in an ultracold Fermi gas with two spin components. The importance of these quantum gases lies, above all, in the fact that they can be used as quantum simulators of other more complex many-body systems, which cannot be realised or their interaction cannot be investigated easily nor manipulated, like in atomic gases.

1.6.1 BEC-BCS crossover

The experimental realisation of a degenerate [DeMarco and Jin, 1999] and superfluid [Regal et al., 2004] Fermi gas had success only after some years of the first BEC. The reason of this is related to the Pauli exclusion principle, which forbids the s-wave collisions, hence it prevents the thermalization between indistinguishable fermions at low T. Therefore, evaporative cooling techniques cannot be applied to Fermi systems. On the other hand, more advanced and recent experimental techniques have allowed the cooling of a Fermi gas. An example of these is the sympathetic cooling, where fermions thermalize with bosons, previously evaporatively cooled [Schreck et al., 2001]. Another technique consists in trapping two different fermionic species (either different atoms or spin states) between

which collisions can occur [DeMarco and Jin, 1999]. In particular, the last option is really efficient in the unitary limit, where the cross-section is large.

From now on, we consider only the two-spin-component Fermi gas. Its superfluid character depends not only on T, but also on the interaction parameter $k_F a$, where k_F is the Fermi wave vector, defined through the Fermi energy, $E_F = \hbar^2 k_F^2/(2m)$. As already discussed in SubSec. 1.3.2, the value of a can be changed by using the FR and it determines different superfluid regimes.

- If $k_F a \ll 1$, with $a > 0$, the gas is in the BEC limit. It is characterized by a strong attraction between fermions, responsible of the formation of bosonic pairs which undergo BEC [Zwierlein et al., 2003, Greiner et al., 2003, Jochim et al., 2003, Zwierlein et al., 2004, Regal et al., 2004, Bourdel et al., 2004, Bartenstein et al., 2004a, Partridge et al., 2005]. The binding energy of such molecules is given by Eq. (1.21) and, due to the Pauli exclusion principle, the interaction between dimers is repulsive with scattering length equal to $a_d = 0.6a$ [Petrov et al., 2004]. Leyronas and Combescot [2007] showed that the EOS of this dimer gas is the same of that of the BEC, also including the LHY correction, as observed experimentally by Navon et al. [2010].

- If $k_F|a| \ll 1$, with $a < 0$, the gas is in the BCS regime. It is characterised by a weak attraction between fermions of opposite momenta and spins, responsible for the formation of Cooper pairs in momentum space, as predicted by the BCS theory of superconductors [Cooper, 1956] [4]. Differently from the BEC regime, for which the pairing has a two-body character, in BCS limit, the pairing has a many-body nature, thanks to the presence of the Fermi sea. The binding energy of Cooper pairs is equal to the gap Δ appearing in the excitation spectrum at the Fermi surface. By using a variational many-body wave function, Bardeen et al. [1957a,b] have shown that fermions, with arbitrarily small attractive interaction, form Cooper pairs which exhibit a superfluid character.

- If $k_F|a| \to \infty$, the gas is in the strongly interacting (unitary) limit. Since a, which is the characteristic length of the interaction, diverges, the only remaining length scale is given by the interparticle distance $n^{-1/3}$, by making the system universal and not depending on the model. In fact, ultracold unitary fermions can be used to simulate other systems with resonant interactions, like neutron stars and complex systems [Bloch et al., 2012] or high-T_C superconductors [Randeria et al., 1989, Sá de Melo et al., 1993]. Given its universality, the unitary Fermi gas (UFG) is characterized by an EOS proportional to that of the ideal Fermi gas (IFG) at T = 0:

$$\mu = \xi_B E_F \ , \tag{1.43}$$

where ξ_B is the dimensionless Bertsch parameter, which encodes all the information of the resonant interactions of the system. From the theoretical point of view, the study of the UFG is really challenging, because, since in the theory there is no any small parameter, perturbative methods cannot be applied. Therefore, experimental measurements of ξ_B are really important in this case, by providing a benchmark for many-body approaches and allowing a comparison between theory and experiment. The value of ξ_B has been measured by Nascimbène et al. [2010], Ku et al. [2012], Van Houcke et al. [2012]:

$$\xi_B = 0.37(1) \ . \tag{1.44}$$

The three regimes described above form the so-called BEC-BCS crossover [Zwerger, 2011], Fig. 1.6. The name "crossover" derives from the fact that, by changing a and

---

[4]The BCS theory was born in order to explain firstly the existence of Cooper pairs between electrons in a superconductor. In these systems, the attractive interaction is mediated by phonons of the crystalline lattice [Frohlich, 1952, Bardeen and Pines, 1955], while neutral atoms in a superfluid interact each other, without any "mediator".

(a) BEC regime   (b) BCS regime   (c) Unitary regime
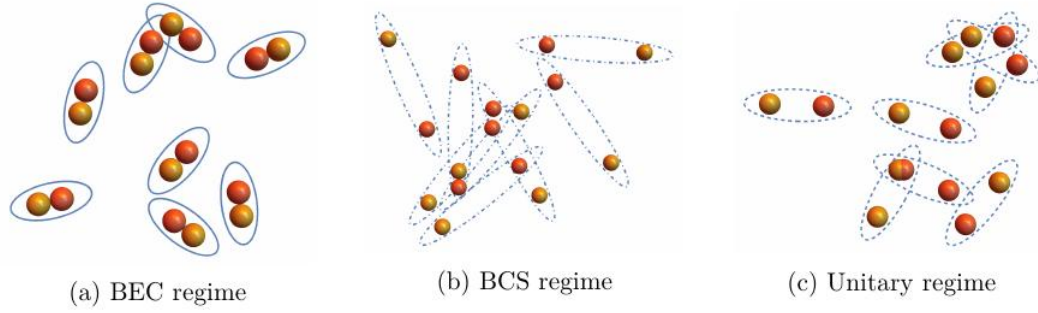
Figure 1.6: Three regimes of the whole BEC-BCS crossover. Fermionic pairs are bounded by a blue line. In the BEC limit (a), the pair size is much smaller than the interparticle distance, while the opposite occurs in the BCS regime (b). In the unitary limit (c), the two typical lengths are of the same order. From Delehaye [2016].

regime, there is no additional phase transition. The experimental realization of the BEC-BCS crossover was early suggested by Leggett [1980], Nozières and Schmitt-Rink [1985]. The whole crossover exhibits superfluidity at $T = 0$, with the presence of quantized vortices [Zwierlein et al., 2005] and of the critical velocity [Miller et al., 2007, Weimer et al., 2015, Delehaye et al., 2015]. As discussed in Fig. 1.6, the size of pairs varies along the crossover [Veeravalli et al., 2008]. Even the critical temperature T_C of superfluidity varies from a weak dependence on a (as shown for atomic BECs by Baym et al. [2001] and Smith et al. [2011]) in the BEC limit to an exponentially small value in the BCS regime $T_C \propto T_F e^{-\pi/(2k_F|a|)}$, by crossing its maximum value in the unitary limit [Haussmann et al., 2007].

The BEC-BCS crossover can be studied also at finite T. In this regime, the UFG has been investigated by Nascimbène et al. [2010], Ku et al. [2012] and its EOS agrees with the diagrammatic Monte-Carlo method [Van Houcke et al., 2012]. Finally, the presence of a superfluid phase transition was proven with the critical temperature $T_C = 0.167(13)T_F$ [Nascimbène et al., 2010, Ku et al., 2012, Navon et al., 2013].

Chapter 2

Ultracold gases in low dimensions

> By dimension, we simply mean an independent direction in which, in principle, you can move; in which motion can take place. In an everyday world, we have left-right as one dimension; we have back-forth as a second one; and we have up-down as a third.
>
> Brian Greene

In the typical experimental situations, an ultracold gas is trapped. If the trapping is tight along one or two spatial directions, the atomic cloud reaches low dimensional configurations. The interest in low dimensional Physics is related to the presence of striking phenomena, not present in the 3D counterpart. For example, new superfluid phase transitions emerge, like the Berezinskii-Kosterlitz-Thouless (BKT) in 2D. Moreover, new quantum degenerate states can be observed like the quasi-condensate and the Tonks-Girardeau regime, where the last one is typical of 1D configurations.

This Chapter is entirely devoted to low dimensional atomic gases. First of all, we discuss in Sec. 2.1 how realizing experimentally both quasi-low D as well as deep low-D geometries, for one- and two-dimensions.

In Sec. 2.2, we introduce the concept of long range order (LRO) which describes the correlations between distant points in a gas. Its presence is related to BEC and superfluidity. We discuss also how low dimensionality affects the behaviour of the LRO and, consequently, the onset of the low-T phase transition.

Given its stunning Physics, Sec. 2.3 is fully dedicated to 1D and to the Lieb-Liniger model. We stress how this theory is more general than the Bogoliubov approach, discussed in the last Chapter, by including also the strongly-interacting regime which corresponds to the Tonks-Girardeau (TG). In this limit, the gas behaves like an ideal Fermi system. In addition, we study the peculiar spectrum of elementary excitations, which exhibits a two-fold nature, and some interesting analogies with the Bogoliubov spectrum, the soliton and the ideal Fermi gas, depending on the strength of the interatomic interaction. We investigate also the finite-temperature generalisation of the Lieb-Liniger model, whose theory was formulated by Yang and Yang in 1969. This Chapter is closed with a very general overview of the problem of thermalization in 1D.

Readers interested in more extended discussions can see Mazets et al. [2008], Mazets and Schmiedmayer [2009, 2010], Mazets [2011], Pitaevskii and Stringari [2016], on which this Chapter is based.

2.1 Low dimensions

In the first Chapter we have studied 3D systems. For harmonically trapped gases, see Eq. (1.7), this is achieved by the constraint that the chemical potential be much larger than the trapping oscillator frequencies: $\mu \gg \hbar\omega_i$ with $i = x, y, z$ [1]. Under this condition the equation of state of 3D uniform system can be used in the LDA (1.8), which takes into account the inhomogeneities caused by the external trapping potential.

By tuning the shape and the intensity of the trapping potential one can realise experimentally dilute and cold gases in highly anisotropic configurations where the motion of particles is quenched in one or two dimensions. This is accomplished by using optical and magnetic techniques which can be applied to both Bose and Fermi gases. These new low dimensional systems can show a deeply different behaviour, for the equilibrium and the dynamical properties.

Low dimensional systems always live in the 3D world and their actual realisation is based on proper trapping conditions. It is then important to distinguish between configurations which seem to be low dimensional only from a geometrical point of view (with the ratio between the axial R_z and radial $R_\perp$ size much smaller or larger than unity, but from a local point of view they have a 3D nature) and true low dimensional systems whose quantum and thermal motion is frozen in one or two directions. In the first case, we use the notation of pancake ($R_z \ll R_\perp$) and cigar ($R_z \gg R_\perp$) configurations, while in the latter case we use the notation of 2D and 1D systems. Let us discuss all possible cases in detail.

We firstly investigate a 3D gas which occupies a surface A and it is axially confined by the harmonic potential $m\omega_z^2 z^2/2$.

If one considers the pancake regime [Petrov et al., 2000a], the system is effectively 3D and many configurations of the harmonic oscillator Hamiltonian are excited in the axial (z) direction. In this limit, the system keeps locally its original 3D feature even though, from a geometrical point of view, it looks 2D if $\sqrt{A} \gg R_z$, see Fig. 2.1.
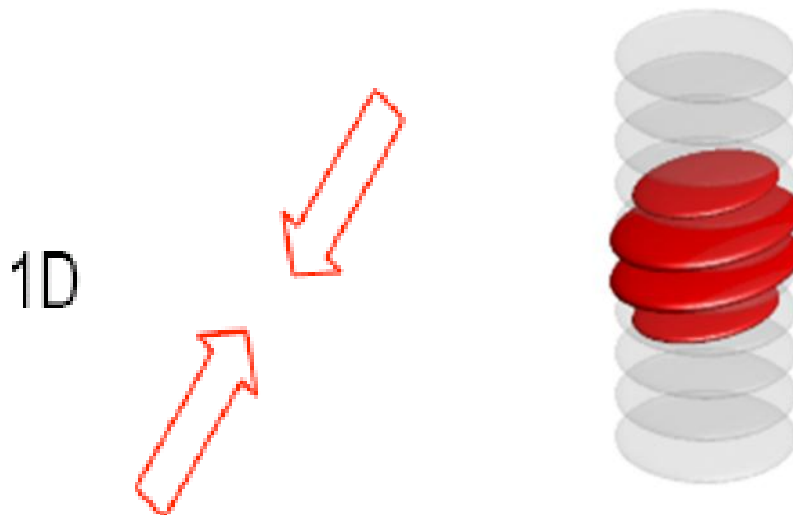
Figure 2.1: A collection of pancakes. From IQOQI.

The local 3D nature ($\mu \gg \hbar\omega_z$) is ensured by the application of the LDA (1.8) along

---

[1]This condition holds at T = 0. At high T, one requires also $k_B T \gg \hbar\omega_i$.

the z-axis, which allows the derivation of the 2D EOS with the integration over z of the 3D EOS, see Appendix A.

If the axial trapping is tight, a deep 2D regime can be reached. The many-body wave function approaches the Gaussian ground-state of the axial harmonic oscillator. The system has lost its local 3D nature ($\mu \ll \hbar\omega_z$) and, consequently, LDA cannot be applied along the z-direction. In this case, the 2D EOS is derived from low-dimensional approaches, see Appendix A.

If the gas is isotropically trapped also in the plane, one should consider the harmonic potential of the form $m\omega_\perp^2 r_\perp^2/2$, with $\omega_\perp = \omega_x = \omega_y$ and $r_\perp = \sqrt{x^2 + y^2}$. Both pancake and 2D geometries are reached with the condition that the planar trapping is weaker than the axial confinement $\omega_z \gg \omega_\perp$. In addition, LDA can be applied along the $r_\perp$ direction for large enough systems satisfying the condition $\mu \gg \hbar\omega_\perp$.

A similar analysis can be carried out for a system of length Z confined radially by the harmonic potential of the shape $m\omega_\perp^2 r_\perp^2/2$.

In 3D cigar geometry, many states of the harmonic oscillator Hamiltonian are excited in the radial direction. In this limit, the gas keeps locally its original 3D nature although, from a geometrical point of view, it looks 1D if $L \gg R_\perp$, see Fig. 2.2.
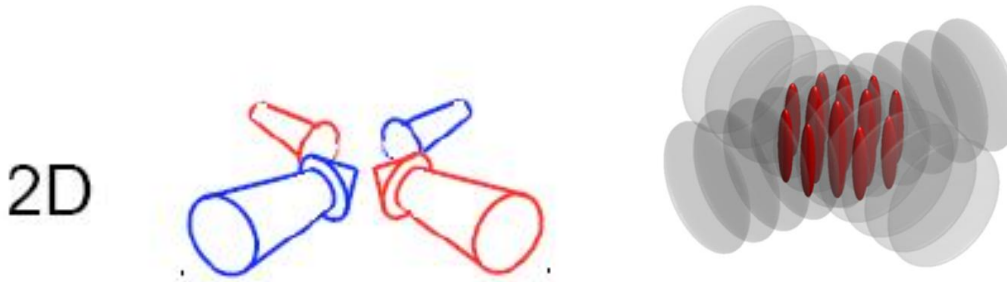
Figure 2.2: A collection of cigars. From IQOQI.

The local 3D nature ($\mu \gg \hbar\omega_\perp$) is ensured by the application of the LDA (1.8) along the $r_\perp$-axis, which allows the derivation of the 1D EOS with the integration over $r_\perp$ of the 3D EOS, see Appendix A.

The 1D regime is reached for tight radial trapping. In this case, the solution of the many-body problem approaches the Gaussian ground-state of the radial harmonic oscillator. The system has lost its local 3D nature ($\mu \ll \hbar\omega_\perp$) and, consequently, LDA cannot be applied along the radial direction. The 1D EOS is derived from low-dimensional approaches, see Appendix A.

If the gas is harmonically trapped along the z-direction by the potential $m\omega_z^2 z^2/2$, with $\omega_z \ll \omega_\perp$, the 1D equilibrium density profile can be calculated by applying the LDA along the z-direction ($\mu \gg \hbar\omega_z$).

LDA regimes (pancake and cigar) have been realized both for Bose [Jin et al., 1996, Mewes et al., 1996, Burger et al., 2002] and Fermi [Kinast et al., 2004, Bartenstein et al., 2004a, Weimer et al., 2015] trapped gases. 2D [Görlitz et al., 2001, Rychtarik et al., 2004, Desbuquois et al., 2012] and 1D [Görlitz et al., 2001, Greiner et al., 2001, Schreck et al., 2001, Paredes et al., 2004] geometries have been also achieved experimentally.

Another way to obtain experimentally pancake geometries is to exploit the fast rotation of the atomic cloud which leads to an increase of the number of atoms in planar directions [Schweikhard et al., 2004].

In Chap. 3, we investigate the dynamics in these deep-low-D and quasi-low-D systems. While the difference between these two kinds of geometries lies in the EOS, as we discuss in

the next Chapter, they share the same deep-low-D nature for the lowest energy dynamics (like collective oscillations). Therefore, both LDA regimes, even if locally are considered as 3D systems, they behave as deep low-D configurations from the kinematic point of view.

2.2 One-body density matrix and long range order in low dimensions

As we have discussed in the last Chapter, symmetry breaking and the order parameter are the underlying concepts of BEC. In this Section, we introduce the concept of LRO exhibited by the one-body density matrix in the presence of BEC, and by the two-body density matrix for the BEC-BCS crossover. We investigate how the behaviour of LRO changes in low dimensionality.

Let us introduce the one-body density matrix [Pitaevskii and Stringari, 2016]:

$$n^{(1)}(\mathbf{r}, \mathbf{r}') = \langle \psi^{\dagger}(\mathbf{r}) \psi(\mathbf{r}') \rangle \tag{2.1}$$

where $\psi(\mathbf{r})$ and $\psi^{\dagger}(\mathbf{r})$ are the annihilation and the creation field operators of a particle at position $\mathbf{r}$. Moreover, $n^{(1)}(\mathbf{r}, \mathbf{r}')$ is an hermitian matrix and it is defined on the average $\langle ... \rangle$. Eq. (2.1) is a very general definition holding for every trapped as well as homogeneous system, for every quantum statistics, in equilibrium and in dynamical evolution [2]. By considering the diagonal components $\mathbf{r} = \mathbf{r}'$ of the one-body density matrix (2.1), one finds the density of the system $n(\mathbf{r}) = n^{(1)}(\mathbf{r}, \mathbf{r})$, which provides the total number of particles $N = \int d\mathbf{r} n(\mathbf{r})$.

At finite T, in the thermodynamic equilibrium, the average $\langle ... \rangle$ in Eq. (2.1) is weighted on the probability of the system to occupy n different states $(e^{-E_n/(k_B T)})$. The eigenstates ψ_n of the Hamiltonian are associated to the eigenvalues E_n and the one-body density matrix becomes:

$$n^{(1)}(\mathbf{r}, \mathbf{r}') = \frac{1}{Q} \sum_n e^{-E_n/(k_B T)} n_n^{(1)}(\mathbf{r}, \mathbf{r}') \ , \tag{2.2}$$

normalized to the partition function $Q = \sum_n e^{-E_n/(k_B T)}$.

We define the momentum $\mathbf{p}$ distribution

$$n(\mathbf{p}) = \langle \psi^{\dagger}(\mathbf{p}) \psi(\mathbf{p}) \rangle \tag{2.3}$$

which can be connected to Eq. (2.1) by a Fourier transform

$$n^{(1)}(|\mathbf{r} - \mathbf{r}'|) = \frac{1}{L^D} \int d\mathbf{p} \, n(\mathbf{p}) e^{i\mathbf{p} \cdot (\mathbf{r} - \mathbf{r}')/\hbar} \tag{2.4}$$

holding for an uniform (without an external trap) and isotropic system with dimension D and length L. From Eq. (2.4), we observe that the one-body density matrix depends only on the modulus of the relative distance $|\mathbf{r} - \mathbf{r}'|$ between two points in the system [Dalibard, 2015-2016].

Let us consider a 3D ($D = 3$) uniform and isotropic system of bosons. For a normal gas, $n(\mathbf{p})$ exhibits a smooth behaviour at low momenta and, from Eq. (2.4), one observes that $n^{(1)}(|\mathbf{r}-\mathbf{r}'|)$ vanishes at divergent relative distance $|\mathbf{r}-\mathbf{r}'| \to +\infty$. On the other hand, in the BEC phase, since $n(\mathbf{p})$ contains a delta-function which marks the macroscopic occupation of the single-particle ground state $\mathbf{p} = \mathbf{0}$, Eq. (2.4) implies that at large distance the one-body density matrix tends to a finite value

$$\lim_{|\mathbf{r}-\mathbf{r}'| \to +\infty} n^{(1)}(|\mathbf{r} - \mathbf{r}'|) = n_0 \tag{2.5}$$

---

[2]Out of equilibrium, Eq. (2.1) depends on time t.

where n_0 is exactly the density of the condensate fraction. This peculiar behaviour of $n^{(1)}(|\mathbf{r} - \mathbf{r}'|)$ is the off-diagonal-LRO, since it involves the non-diagonal components $\mathbf{r} \neq \mathbf{r}'$ of Eq. (2.1) [Penrose, 1951, Penrose and Onsager, 1956, Landau and Lifshitz, 2013]. The off-diagonal LRO (2.5) holds also in the presence of repulsive interactions and finite T by which n_0 is modified. In fact, while in an ideal Bose gas all atoms are in the BEC at T = 0, with interactions $n_0 < n$ even at T = 0. Moreover, for T above the critical temperature T_C of BEC, $n_0 = 0$, because the gas is in the normal phase.

In the case of BEC-BCS crossover for a 3D Fermi gas, see SubSec. 1.6.1, despite the different nature of the regimes in this crossover, they all exhibit superfluidity at low T. They all share the off-diagonal LRO at big relative distances, for the two-body density matrix [Gor'kov, 1958]:

$$\lim_{r \to +\infty} \langle \psi_\uparrow^\dagger(\mathbf{r}_2 + \mathbf{r}) \psi_\downarrow^\dagger(\mathbf{r}_1 + \mathbf{r}) \psi_\downarrow(\mathbf{r}_1) \psi_\uparrow(\mathbf{r}_2) \rangle = |F(\mathbf{r}_1, \mathbf{r}_2)|^2 \tag{2.6}$$

where we have introduced the pairing field $F(\mathbf{R}, \mathbf{s}) = \langle \psi_\downarrow(\mathbf{R} + \mathbf{s}/2) \psi_\uparrow(\mathbf{R} - \mathbf{s}/2) \rangle$, referring to the spin-singlet pairing. The pairing field $F(\mathbf{R}, \mathbf{s})$ defines also the order parameter [Pitaevskii and Stringari, 2016]. The vectors $\mathbf{R} = (\mathbf{r}_1 + \mathbf{r}_2)/2$ and $\mathbf{s} = \mathbf{r}_1 - \mathbf{r}_2$ are, respectively, the centre-of-mass and the relative coordinate. Differently from the case of the BEC, Eq. (2.1), the off-diagonal LRO for a Fermi superfluid involves the expectation value of the product of two field operators, Eq. (2.6).

In the following, we discuss the behaviour of LRO in low D for both quantum statistics as well as T = 0 and finite T. For example, in a homogeneous Bose gas, the dimensionality strongly affects the presence and also the nature of the BEC. Indeed, the absence of a true condensate in both 2D and 1D at finite T is due to the long-wave fluctuations of the phase S of the order parameter [Popov, 2001], as prescribed by the Hohenberg-Mermin-Wagner theorem [Mermin and Wagner, 1966, Hohenberg, 1967].

We study briefly how, while the presence of an external harmonic trap favours the BEC, the T, the interactions as well as the low D tend to destroy the condensate. The combination of these effects has as consequence the birth of new quantum degenerate states not present in 3D, like the quasi-condensate in 2D and both the quasi-condensate and the TG in 1D.

2.2.1 LRO in two dimensions

In the uniform 2D Bose gas a true BEC can exist only at T = 0 regime, for which bosons occupy the condensate. The gas exhibits LRO for both the ideal and the weakly-interacting case.

In this Subsection, we focus more on the behaviour of the LRO for a 2D Bose gas at finite T. For the Hohenberg-Mermin-Wagner theorem [Hohenberg, 1967], in uniform 2D configurations, the thermal fluctuations of the phase S of the order parameter (1.40) destroy the BEC and $n^{(1)}$ (2.1) vanishes with a power law at large relative distances, without exhibiting LRO [Kane and Kadanoff, 1967]. The exponent of this power law depends explicitly on T, by showing the important role played by thermal fluctuations. The long-wavelength (i.e. small momenta) fluctuations of the phase S destroy the condensate, but they preserve the irrotationality condition $\nabla \times \mathbf{v} = 0$ ensuring the superfluid behaviour. For this reason, every system exhibiting a power-law decay of the one-body density matrix is called quasi-condensate. This new quantum state, not present in 3D, describes a condensate with fluctuating phase, by exhibiting a true BEC only locally. Experimental evidence for quasi-condensation in a 2D atomic hydrogen gas has been reported by Safonov et al. [1998].

In a uniform 2D ideal Bose gas, there is no phase transition at finite T. If one considers repulsive interactions, they favour the presence of a peculiar superfluid phenomenon at

sufficiently low T. In fact, one can define the BKT critical temperature T_{BKT}, which characterizes the superfluid BKT transition [Berezinskii, 1971, 1972, Kosterlitz and Thouless, 1973, Kosterlitz, 1974], observed experimentally by Bishop and Reppy [1978, 1980], Hadzibabic et al. [2006], Cladé et al. [2009] and Tung et al. [2010]. For $T > T_{BKT}$ [Nelson and Kosterlitz, 1977], there is the thermal [3] (and spontaneous) creation of free vortices which characterizes a normal phase with an exponentially decay of $n^{(1)}$ (2.1) at large distances. The absence of superfluid (SF) phase in this T regime has been observed by Choi et al. [2013]. For $T < T_{BKT}$, these vortices are bound in pairs with opposite circulation and the system exhibits a quasi-condensate phase.

If one adds an external harmonic trap, the situation changes drastically. The trap, by providing a finite size of the system, introduces a lower bound for the moment and reduces the phase fluctuations. In this way, the macroscopic occupation of the zero-momentum ground state and so the BEC are favoured. At finite T, differently from the uniform gas, the BEC phase transition occurs with a critical temperature T_C proportional to the trapping frequency [Pitaevskii and Stringari, 2016]. This is true for the ideal Bose gas, while in the weakly-interacting case, one has to distinguish between the true BEC taking place at $T \ll T_C$ and the quasi-condensate at $T < T_C$.

We close this Subsection by pointing out that the interaction, the T and the presence of the trap affect the onset of a phase transition. The discrete nature of the lowest trap levels emerges only if the interaction between particles which occupy a given level, is much smaller than the level spacing. Otherwise, the interaction smears out the discrete nature of the energy spectrum. The same happens for T. If the thermal energy $k_B T$ is much smaller than the level spacing, the discrete structure of levels appears.

2.2.2 LRO in one dimension

In compressible 1D systems, the LRO is absent for quantum fluctuations of the phase S, Eq. (1.40), even at T = 0 [Pitaevskii and Stringari, 1991, 2016]. In fact, as what happens in 2D, the one-body density matrix $n^{(1)}$ decays with a power law at large relative distance [Schwartz, 1977, Haldane, 1981]. On the other hand, differently from 2D at $T \neq 0$, for 1D at T = 0 the exponent of this power law depends explicitly on the sound velocity, pointing out the quantum nature of fluctuations at T = 0. This sound velocity varies according to the interaction regime, from the weakly to strongly repulsive. In the latter case, the system exhibits a novel quantum regime, typical of 1D: the Tonks-Girardeau (TG), which is discussed in Sec. 2.3 and whose $n^{(1)}$ exhibits the same behaviour of that of a 1D ideal Fermi gas [Mehta, 2004]. In the case of strongly attractive 1D Bose gas, the system enters in the Super Tonks-Girardeau (STG) regime [Astrakharchik et al., 2005a], for which correlations decay faster than in the TG case.

Let us consider now the finite T. Phase transitions cannot occur in 1D at finite T [Landau and Lifshitz, 2013]. Indeed, the one-body density matrix $n^{(1)}$ decreases exponentially at large distance [Reatto and Chester, 1967, Kane and Kadanoff, 1967], by showing the crucial role of thermal fluctuations in destroying the LRO. Moreover, this decrease is faster for higher T.

For what concerns the ideal Bose gas in uniform configurations, there is no BEC at finite T. If one adds the trap to this system, one has a sharp crossover to BEC. In this case, the decrease of T below an effective critical temperature T_C, proportional to the trapping frequency, gives rise to the increase of the population of atoms in the ground state, which becomes macroscopic, as observed by Ketterle and van Druten [1996].

---

[3]We notice that in 3D the thermal creation of quantized vortices is forbidden, because it implies a macroscopic cost of energy, which is proportional to their diameter.

In the weakly interacting regime at low T, the density fluctuations are suppressed and the gas is in the quasi-condensate state (even at T = 0 [Luxat and Griffin, 2003]). The use of Bogoliubov theory in this system is discussed by Mora and Castin [2003].

By adding the harmonic trap in the interacting Bose gas at T = 0, there is the true BEC, with the density profile calculated from the GPE, see SubSec. 1.5.2. At finite T, one has to define two T scales: the phase fluctuation T, T_ϕ, and the degeneracy T, T_d. These two temperatures define three different regimes: at $T \ll T_\phi$, the system exhibits a true BEC, for $T_\phi < T < T_d$, there is the quasi-condensate, while for $T \gg T_d$, the gas is in the classical regime [Petrov et al., 2000b].

The exponential decay behaviour of $n^{(1)}$ is exhibited also by trapped cigar configurations, but with some important differences given by the quasi-1D geometry. In particular, one can consider a quasi-condensation T, T_Φ, and the 3D critical T of the BEC, T_C. For $T < T_\Phi$, these elongated systems are characterised by the presence of a true BEC, since thermal fluctuations are small. For $T_\Phi < T < T_C$, there is the appearance of a quasi-condensate, as observed experimentally by Dettmer et al. [2001], Hellweg et al. [2001], Richard et al. [2003], Gerbier et al. [2003], Hellweg et al. [2003]. The theory of phase fluctuations in these highly elongated trapped Bose gases was developed by Petrov et al. [2001].

Before ending this Subsection, let us consider the case of 1D Fermi gases whose one-body density matrix [Haldane, 1981] behaves differently from the bosonic case. For an ideal Fermi gas, the one-body density matrix $n^{(1)}$ decays as $\sin(\pi n |z - z'|)/|z - z'|$, where n is the 1D density and $|z - z'|$ denotes the relative distance along the axial direction. This behaviour reflects the typical jump from 1 to 0 in the momentum distribution at the Fermi surface $k = \pm k_F$. In the interacting case, the $n^{(1)}$ decays faster and the jump at the Fermi surface disappears [Pitaevskii and Stringari, 2016].

2.3 Lieb-Liniger model

In this Section we investigate the Lieb-Liniger model, which describes N identical bosons interacting with s-wave contact repulsive force, in uniform 1D configurations at T = 0. At finite T, this system has been generalised by Yang and Yang [1969], see SubSec. 2.3.1. Moreover, it is integrable and, consequently, it does not exhibit thermalization as discussed in SubSec. 2.3.2.

The Lieb-Liniger model is more general than the 1D mean-field Gross-Pitaevskii (GP) theory, because it takes into account also small values of the density [Pitaevskii and Stringari, 2016]. In the high density limit [4], the model reproduces the same results of GP theory.

The research of 1D bosons began with Girardeau [1960] who studied only the case of infinite repulsion. This limit, present only in 1D, is the Tonks-Girardeau (TG) regime. After some years, Lieb and Liniger [1963] provided the whole description of 1D Bose gases. These particles are characterised by a repulsive zero-range interaction. The Lieb-Liniger model describes an exact solution of the many-body problem. This solution is numerical and it depends on the interaction strength, but it has two analytical limits:

- **Bogoliubov regime** (BG): weak interaction and high density;
- **Tonks-Girardeau regime** (TG): strong interaction and small density.

---

[4]The validity of the 1D mean-field theory requires that the condition $\xi/d \gg 1$ for the ratio between the healing length $\xi \sim \hbar/(m v_s)$ and the interparticle distance $d = n^{-1}$ be satisfied. This gives the condition $n|a_{1D}| \gg 1$ ensured for large values of the 1D density n. a_{1D} is the 1D scattering length. We notice that this inequality is opposite to the 3D weakly-interacting gas, compare Eq. (1.19).

In the TG regime, the deviations from the mean-field BG regime are relevant and the gas exhibits the ideal Fermi gas behaviour.

The Lieb-Liniger Hamiltonian is

$$H = -\frac{\hbar^2}{2m} \sum_{i=1}^{N} \frac{\partial^2}{\partial z_i^2} + g_{1D} \sum_{i>j}^{N} \delta(z_i - z_j) \tag{2.7}$$

where the 1D coupling constant can be expressed as

$$g_{1D} = 2a\hbar\omega_\perp = \frac{2\hbar^2}{m} \frac{a}{a_\perp^2} = -\frac{2\hbar^2}{ma_{1D}} \tag{2.8}$$

where we have used $a_{1D} = -a_\perp^2/a$, being a and a_{1D} the 3D and the 1D scattering length, respectively, while $a_\perp = \sqrt{\hbar/m\omega_\perp}$ is the radial harmonic oscillator length. In the Lieb-Liniger model, since the interaction is repulsive, the coupling constant is positive $g_{1D} > 0$, which implies a negative scattering length $a_{1D} < 0$. Eq. (2.8) holds only if $a_\perp \gg a$. In this regime, Eq. (2.8) has been obtained by averaging the 3D interaction over the radial Gaussian density profile [Olshanii, 1998, Petrov et al., 2000b].

If the condition $a_\perp \gg a$ is not satisfied, the a_{1D} should be renormalized and the 1D coupling constant becomes:

$$g_{1D} = \frac{2\hbar^2 a}{ma_\perp^2} \frac{1}{1 - Ca/a_\perp} , \tag{2.9}$$

with $C \simeq 1.0326$. For $a \to a_{CIR} = a_\perp/C$, g_{1D} is divergent and one reaches the so-called Confinement Induced Resonance (CIR). For repulsive interaction, one should require $0 < a < a_{CIR}$. Eq. (2.9) points out that one can tune the coupling constant g_{1D} by varying the strength of the radial harmonic trapping.

The Hamiltonian (2.7) can be diagonalized via Bethe-Ansatz in an exact way [Lieb and Liniger, 1963]. Therefore, one can calculate the EOS of the system at $T = 0$, for every positive value of g_{1D}. The ground state energy per particle is

$$\frac{E_0}{N}(\gamma) = \frac{\hbar^2}{2m} n^2 e(\gamma(n)) , \tag{2.10}$$

where n is the 1D particle density. In Eq. (2.10), the interaction parameter γ is defined as:

$$\gamma = \frac{mg_{1D}}{\hbar^2 n} = -\frac{2}{na_{1D}} \tag{2.11}$$

and, as we study in the following, it plays a crucial role in determining the interaction regime of the Lieb-Liniger model.

In order to calculate numerically the ground state energy per particle $e(\gamma)$ of Eq. (2.10), one should solve the following system of integral equations [Lieb and Liniger, 1963, Menotti and Stringari, 2002]:

$$g_\lambda(x) = \frac{1}{2\pi} + \frac{1}{\pi} \int_{-1}^{1} g_\lambda(y) \frac{\lambda}{\lambda^2 + (x - y)^2} dy, \tag{2.12}$$

$$\gamma(\lambda) = \lambda \left(\int_{-1}^{1} g_\lambda(x) dx \right)^{-1} , \tag{2.13}$$

$$e(\gamma) = \frac{\gamma^3}{\lambda^3} \int_{-1}^{1} g_\lambda(x) x^2 dx . \tag{2.14}$$

From Eq. (2.10), one calculates the chemical potential $\mu = \partial E_0/\partial N$.

In the BG regime of high density $n|a_{1D}| \gg 1$, corresponding to the weak repulsive limit $\gamma \ll 1$, Eq. (2.11), one gets the ground state energy:

$$\left(\frac{E_0}{N}\right)_{BG} = \frac{1}{2}g_{1D}n \tag{2.15}$$

and for the chemical potential

$$\mu_{BG} = g_{1D}n \ . \tag{2.16}$$

Both of the above results have the same shape of the corresponding quantities in the BG theory for a 3D case, SubSec. 1.5.1, provided the 1D coupling constant and density.

In the opposite TG regime, the density is low $n|a_{1D}| \ll 1$ and the interaction is strongly repulsive $\gamma \gg 1$. In this case, one gets:

$$\left(\frac{E_0}{N}\right)_{TG} = \frac{\hbar^2\pi^2 n^2}{6m} \ , \tag{2.17}$$

and

$$\mu_{TG} = E_F = \frac{\hbar^2\pi^2 n^2}{2m} \ , \tag{2.18}$$

where we recover the result that, at $T = 0$, the chemical potential is equal to the Fermi energy E_F. Since the interaction potential is highly repulsive, the bosons behave as impenetrable. In order to explain the physical interpretation of this regime, let us discuss a scattering process in 1D. In this low-D, the scattering angle is always zero, therefore the process is described only by the reflection probability of the two colliding particles. When the energies of the two particles tend to be zero, the reflection probability tends to be one. In the TG regime, since the T is zero, the only relevant energy scale is given by E_F which tends to be zero in the small density TG limit. In the TG limit, the eigenfunctions Ψ_B of the interacting Bose gas can be mapped into the eigenstates Ψ_F of the 1D ideal Fermi gas [Girardeau, 1960]

$$\psi_B(z_1, ..., z_N) = |\Psi_F(z_1, ..., z_N)| \tag{2.19}$$

where Ψ_F are given by the Slater determinants. The modulus in Eq. (2.19) ensures the symmetry of the Bose-Einstein statistics, while, for $z_i = z_j$, $\Psi_B = 0$ for any pair of bosons, reflecting the impenetrability in the TG regime. The mapping (2.19) is reported in Fig. 2.3.

$$\Psi_B(z_1, \ldots, z_N) = |\Psi_F(z_1, \ldots, z_N)|$$
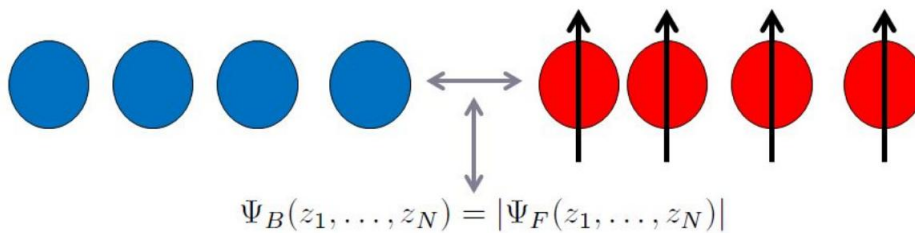
Figure 2.3: Mapping between the strongly repulsive spinless bosons (blue spheres) and the ideal fermions (red spheres). We notice also that all fermions have all equal spins in order to satisfy the Pauli exclusion principle.

The mapping (2.19) ensures also that all local physical quantities A have the same average if calculated with the bosonic and the fermionic eigenfunctions:

$$\langle\Psi_B|A|\Psi_B\rangle = \langle\Psi_F|A|\Psi_F\rangle \ . \tag{2.20}$$

For this reason, we conclude that the TG gas behaves really as an ideal Fermi gas (IFG) in 1D, since they share a lot of physical observables like the density profile, the energies

and the thermodynamic functions. Moreover the TG-IFG mapping holds also at finite T as one can show, for example, by calculating the specific heat [Pitaevskii and Stringari, 2016].

On the other hand, the non-local observables of the TG regime cannot be calculated by using Eq. (2.20). For example, the momentum distribution $n(p)$ of the TG system does not coincide with that of the IFG, which exhibits the typical step behaviour, because, for low momenta $p \to 0$, the TG $n(p)$ diverges [Vaidya and Tracy, 1979].

The TG regime was observed experimentally firstly in 2004 by Kinoshita et al. [2004] and Paredes et al. [2004].

The spectrum of the elementary excitations of the Lieb-Liniger model was investigated by Lieb [1963]. For every value of the interaction parameter γ, there are always two different branches (an upper and lower one), which coincide, at small momenta p, with the linear phononic spectrum $\epsilon = v_s p$. In the BG regime, the upper branch tends to be equal to the Bogoliubov spectrum (1.30), while the lower one is characterised by the same dispersion relation of the solitonic excitations of the GPE [Kulish et al., 1976, Ishikawa and Takayama, 1980]. In the opposite TG limit, the upper and the lower branch coincides with the single-particle and the hole spectrum of the IFG, respectively. In Fig. 2.4, we report the Lieb-Liniger excitation spectrum for two different values of the interaction parameter γ.

For attractive interactions $g_{1D} < 0$, the ground-state (not uniform in space) describes a bright soliton with negative values of energy [McGuire, 1964]. Moreover, for strongly attractive interactions, there is the presence of an uniform and metastable gas, the Super-Tonks-Girardeau (STG) regime [Astrakharchik et al., 2005a]. In addition, the energy of the STG corresponds to that of hard-rods of length a_{1D} [5]. The STG regime was realized experimentally firstly by Haller et al. [2009].

2.3.1 Yang-Yang thermodynamics

At finite arbitrary T, the Lieb-Liniger model has to be generalised with the Yang-Yang theory [Yang and Yang, 1969].

In the thermodynamic limit, the Bethe-Ansatz solution for the Hamiltonian (2.7) can be obtained by solving the following system of three coupled equations [Yang and Yang, 1969, Yang, 1970, Lang et al., 2015]:

$$\epsilon(k) = -\mu(c,T) + k^2 - \frac{Tc}{\pi} \int_{-\infty}^{+\infty} \frac{dq}{c^2 + (k-q)^2} \times \ln\left\{1 + \exp\left[-\frac{\epsilon(q)}{T}\right]\right\} , \qquad (2.21)$$

$$2\pi f_p(k) \left\{1 + \exp\left[\frac{\epsilon(k)}{T}\right]\right\} = 1 + 2c \int_{-\infty}^{+\infty} dq \frac{f_p(q)}{c^2 + (k-q)^2} , \qquad (2.22)$$

$$\int_{-\infty}^{+\infty} dk f_p(k) = n , \qquad (2.23)$$

where we have set $\hbar = 2m = k_B = 1$ and the coupling constant $c = g_{1D}/2$, for simplicity. In Eqs. (2.21) - (2.22) - (2.23), $\epsilon(k)$ is the excitation spectrum energy, k are the quasi-momenta, $f_p(k)$ is the particle quasi-momenta distribution function, and $\exp[\epsilon(k)/T] \equiv f_h/f_p$, with f_h the hole quasi-momenta distribution function. From Eq. (2.23), we notice also that the $f_p(k)$ distribution is normalized to the density n.

From the above equations, one can calculate all the thermodynamic functions, with some important limits [Yang and Yang, 1969]. At T = 0 this approach reproduces the

---

[5]Differently from the Lieb-Liniger model, in the STG regime, the coupling constant is negative $g_{1D} < 0$ and so the scattering length is positive $a_{1D} > 0$.
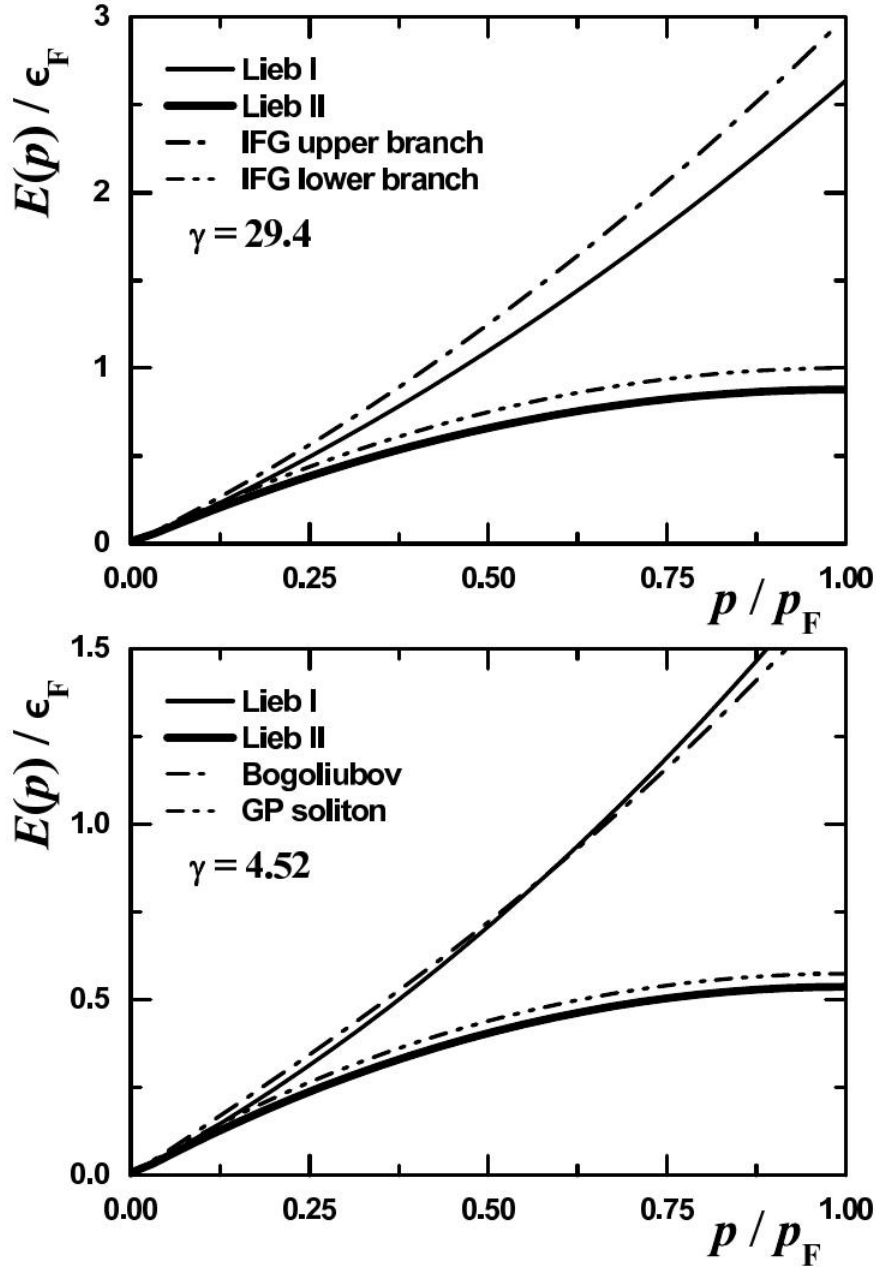
Figure 2.4: Particle (thin solid line) and hole (bold solid line) dispersion relations of the Lieb-Liniger model for $\gamma = 29.4$ (upper panel) and $\gamma = 4.52$ (lower panel). Upper panel: dashed-dot and dashed-dot-dot curves are the ideal Fermi gas particle and hole excitation energies, respectively. Lower panel: the dashed-dot line corresponds to the Bogoliubov spectrum (1.30), while the dashed-dot-dot curve gives the GP soliton dispersion. From Pitaevskii and Stringari [2016]. Copyright © 2016, Oxford University Press.

Lieb-Liniger theory results, while for $c = 0$ and for $c = +\infty$, it provides the description of a free Bose and Fermi gas, respectively.

In Chap. 6, we calculate the chemical potential as a function of T for a broad range of values of γ, by using the correspondence $c \equiv \gamma n$ from the above equations. We observe that the chemical potential increases for larger values of γ, compare Eq. (2.16) with Eq. (2.18).

2.3.2 Problem of thermalization

The Lieb-Liniger model at T = 0 is a special example of integrable model [Thacker, 1981, Yurovsky et al., 2008], which has the number of conserved quantities equal to that of the degrees of freedom. For this reason, it can be exactly solved by Bethe-Ansatz [Lieb and Liniger, 1963]. This has as consequence that if one considers its dynamical evolution, the system always remembers its initial configuration and it does not thermalize by means collisions between atoms. The absence of thermalization is a direct consequence of the deep 1D geometry. As already anticipated in Sec. 2.3, during every collision in 1D, since the scattering angle is always zero, bosons can simply weakly repel (BG regime) or being impenetrable (TG) each other. During a scattering process, the moduli of the momenta of the two colliding particles remain the same or are exchanged. For this reason, without a redistribution of kinetic energy, the system cannot thermalize locally (and, consequently, globally) through collisions.

The absence of thermalization for arrays of trapped 1D Bose gases has been experimentally observed by Kinoshita et al. [2006]. In particular, by preparing the system in an out-of-equilibrium configuration, this experiment showed that thermal equilibrium is not reached (the momentum distribution never becomes a Gaussian) even after thousands of collisions between atoms. This is true for a broad range of values of the interaction strength (from TG to intermediate coupling regime). The experiment of Kinoshita et al. [2006] was particularly insightful because it was the first which demonstrated the lack of thermalization in 1D Bose gases, which is compromised, together with the integrability, by both harmonic trap and not perfect contact interactions.

In the following, we discuss what are the factors responsible for the breakdown of integrability and also the entity of their action on the thermalization of 1D Bose gas [Mazets et al., 2008, Mazets and Schmiedmayer, 2009, 2010, Mazets, 2011].

Let us consider the finite T, see SubSec. 2.3.1, and the axial harmonic trap:

$$V_{trap}(z) = \frac{1}{2}m\omega_z^2 z^2 \; , \qquad (2.24)$$

in the Lieb-Liniger model. As already discussed in Sec. 2.1, the presence of the radial trapping is always ensured in order to reach the 1D regime. We require that the trap is highly elongated $\omega_\perp \gg \omega_z$. To implement the deep 1D quantum physics we require the following conditions:

$$\mu \ll \hbar\omega_\perp \qquad k_B T \ll \hbar\omega_\perp \qquad (2.25)$$

for the chemical potential and the thermal energy, respectively. Since we want to investigate how the T and the radial trapping may influence the integrability, let us relax the above conditions in order to reach a quasi-1D regime:

$$\mu < \hbar\omega_\perp \qquad k_B T < \hbar\omega_\perp \; . \qquad (2.26)$$

Let us consider a collision of two identical bosons which are initially in the transverse ground state of the radial trapping. If the collision is purely 1D, both atoms remain in this ground state after the scattering process and thermalization does not occur. In order to observe an energy exchange and a consequent thermalization, there should be a radial excitation after the collision. In this case, the 1D condition $a/a_\perp \ll 1$ is violated, since $\omega_\perp$ is small and the 1D coupling constant g_{1D} of pairwise collisions depends on the radial trapping due to the radial excitations, see Eq. (2.9) [Olshanii, 1998]. In particular, g_{1D} increases for higher values of the ratio $a/a_\perp$. If one calculates the population rate of the radial modes given by two-body collisions and compares it with the experimental values [Hofferberth et al., 2008], the contribution to the thermalization of pairwise collisions is negligible [Mazets et al., 2008, Mazets and Schmiedmayer, 2009, 2010].

Let us look for the thermalization contribution in the three-body collisions mediated by radial excited states. This kind of scattering really leads to a non-negligible violation of the integrability of the system [Mazets and Schmiedmayer, 2010] and so, it should be considered as a correction to the Lieb-Liniger model, being responsible for thermalization processes. The three-body population rate of radial modes is dominant compared with the two-body one discussed above, by considering the typical experimental values [Hofferberth et al., 2008].

Thermalization is affected also by the interaction strength because three-body collisions require the presence of three atoms at the same location. Hence, thermalization is easier for the BG regime, differently from the TG limit for which atoms behave as ideal fermions. Therefore, the stronger is the delta-like pairwise repulsive interaction, the smaller is the probability of finding three particles close and, consequently, thermalization is suppressed [Mazets and Schmiedmayer, 2009, 2010]. Thus, a quasi-1D system close to the TG limit is almost integrable.

Finally, we would like to discuss the influence of a weak ($\omega_\perp \gg \omega_z$) axial trapping (2.24) on the integrability of the 1D Bose gas [Mazets, 2011]. For this purpose, we neglect the radial excitations. By considering the typical experimental values [Kinoshita et al., 2006] of quantities entering in the theory [Olshanii, 1998], one can calculate the timescale on which the integrability breakdown due to the axial trap can be neglected. This time scale is too long compared with the typical duration of an experiment in an ultracold atom lab. Therefore, the effect of the longitudinal trap on the thermalization can be neglected [Mazets, 2011].

We conclude this Subsection by summarising that the main source of the breakdown of integrability with a consequent thermalization in trapped 1D Bose gases is provided by the radial excitation modes. This is strictly connected to the occurring of three-body collisions which allow the redistribution of moment of colliding particles [Mazets et al., 2008, Mazets and Schmiedmayer, 2010, Tan et al., 2010].

Chapter 3

Collective oscillations of a trapped quantum gas in low dimensions

> I'm attracted to ensembles: you get a lot of really good moving pieces. It's sort of like a horse race in a way, especially when you know that everyone is on this collision course. It's like, "Who's going to make it?" And you can put people together in unexpected pairings.
>
> Noah Hawley

In recent years the study of low-dimensional quantum gases has been the object of significant experimental and theoretical research [Pricoupenko et al., 2004, Pitaevskii and Stringari, 2016]. As discussed in the last Chapter, the main interest is due to the increase of quantum correlations and fluctuations caused by the reduced dimensionality which makes the properties of these systems significantly different from their 3D counterpart [Bloch et al., 2008]. For example, in 2D, thermal fluctuations rule out the existence of LRO at finite T (Hohenberg-Mermin-Wagner theorem) [Mermin and Wagner, 1966, Hohenberg, 1967] and novel aspects of superfluid phenomena, like the BKT transition, take place. In compressible 1D systems the occurrence of LRO is ruled out by quantum fluctuations even at $T = 0$ [Pitaevskii and Stringari, 1991, 2016].

The goal of this Chapter is to focus on the collective oscillations of a low dimensional atomic gas. Their study is of paramount importance for the investigation of properties of quantum many-body systems, like superfluidity and thermodynamics. During the last twenty years, collective oscillations have been the object of systematic theoretical and experimental investigations in different trap geometries, dimensionality and atomic species [Stringari, 1996, Jin et al., 1996, Mewes et al., 1996, Jin et al., 1997, Stamper-Kurn et al., 1998, Maragò et al., 2000, Chevy et al., 2002, Cozzini et al., 2003, Pollack et al., 2010].

While some of the results discussed in this Chapter have been already derived in the literature, a unified description covering both Bose and Fermi statistics at zero as well as at finite temperature in different regimes of axial and radial trapping is still missing. Our analysis can help in providing useful links and comparisons among different regimes of experimental and theoretical interest.

Our investigation is based on the hydrodynamic formalism applicable to various regimes, including the superfluid regime at zero temperature and the collisional regime in the non-superfluid phase above the critical temperature. To this purpose, we derive a general formulation of the hydrodynamic equations in presence of an external trapping potential

in terms of the velocity field. This approach explicitly points out the irrotational vs rotational nature of the solutions and the role of the equation of state. It reduces to a simplified form when the EOS exhibits a polytropic dependence on the density, allowing for an important class of analytic solutions. Our results are also compared with the predictions for the frequencies of the normal modes in the collisionless regime.

The original results presented in this Chapter have been published in the paper De Rosi and Stringari [2015]. The Chapter is organised as follows.

In Sec. 3.1 we introduce the concept of the polytropic equation of state, both in terms of the pressure and, at $T = 0$, of the chemical potential. The values of the polytropic coefficient q, fixing the power law isoentropic dependence of the EOS on the density, are discussed in some relevant cases of different dimensionality for both Bose and Fermi gases at zero as well as at finite temperature. We consider geometrical configurations corresponding to pancake and cigar profiles, whose equation of state can be derived starting from the 3D EOS, employing the local density approximation along the directions of the confinement. We also discuss the case of deep 2D and 1D configurations where the motion of the gas is instead frozen along the directions of the confinement.

In Sec. 3.2, we provide an overview of collective modes, by including the case of the ideal gas model.

In Sec. 3.3 we derive a general equation obeyed by the velocity field associated with the collective motion, starting from the hydrodynamic theory in the presence of external trapping. This equation holds both for a superfluid gas at zero temperature, where the macroscopic dynamic behaviour is described by the hydrodynamic theory of superfluids, and in the normal phase, in the collisional regime, characterised by the condition $\omega\tau \ll 1$, where τ is a typical collisional time. We show that the equation for the velocity field acquires a particularly simple form if the equation of state of the gas exhibits a polytropic dependence on the density.

In Secs. 3.4, 3.5, 3.6 and 3.7 we derive the discretized oscillation frequencies in the presence of additional harmonic trapping in the plane (in the case of 2D configurations) and along the axis (in the case of 1D configurations). Special emphasis is given to the lowest breathing modes whose frequency, differently from the divergency free solutions, is explicitly sensitive to the value of the polytropic coefficient and can exhibit a temperature dependence even in the hydrodynamic regime.

3.1 Polytropic equation of state

A useful feature, which allows for a significant simplification of the theoretical analysis, is the fact that in several configurations, corresponding to different dimensional, interaction and temperature regimes and quantum statistics, the equation of state of the atomic gas exhibits a simple power law dependence on the density n in the form

$$P(n, \bar{s}) = n^q p(\bar{s}) \,, \tag{3.1}$$

where P is the pressure of the gas, q is called the polytropic coefficient, $\bar{s}$ is the entropy per particle and $p(\bar{s})$ is a function of $\bar{s}$, fixed by the thermodynamic behaviour of the gas at zero ($\bar{s} = 0$) as well as at finite temperature. As we will show in the following Sections, the polytropic coefficient q plays a crucial role in determining the frequency of the discretized collective oscillations in the presence of harmonic trapping. Viceversa, the value of the function $p(\bar{s})$ determines the adiabatic sound velocity v_s, according to the thermodynamic law

$$m v_s^2 = \left(\frac{\partial P}{\partial n}\right)_{\bar{s}} = q n^{q-1} p(\bar{s}) = q \frac{P}{n} \,. \tag{3.2}$$

Starting from Eq. (3.1) and using the thermodynamic relation $(\partial U/\partial n)_{\bar{s}} = P/n^2$, one can write the following relationship between the energy per particle and the pressure of the gas:

$$U = \frac{1}{q-1}\frac{P}{n} \, , \qquad (3.3)$$

which has been obtained by integration on the density.

At $T = 0$ the scaling law (3.1) can be also written in the form

$$\mu(n, T = 0) = \frac{q}{q-1}n^{q-1}p(\bar{s} = 0) \qquad (3.4)$$

where μ is the chemical potential of the gas related to the pressure by the Gibbs-Duhem thermodynamic relation

$$dP = nd\mu + sdT \qquad (3.5)$$

where $s = n\bar{s}$ is the entropy density. The sound velocity at zero temperature, where $dP = nd\mu$, can be rewritten in terms of the chemical potential as

$$mv_s^2 = n\left(\frac{\partial \mu}{\partial n}\right)_{\bar{s}} = (q-1)\mu \, . \qquad (3.6)$$

When applied to configurations of lower dimensions the pressure and the density entering (3.1) should be replaced by the corresponding 2D or 1D pressure and density of the gas.

The parametrization (3.1) for the equation of state applies to an important class of physical systems. The values of the corresponding polytropic index q are explicitly derived in Appendix A and are reported in the Tables 3.1 and 3.2. For example, in a 3D Fermi gas at unitarity [Giorgini et al., 2008] (as well as in the ideal 3D Fermi gas and in the ideal 3D Bose gas above the critical temperature) simple dimensionality arguments permit to identify the value $q = 5/3$ for the polytropic coefficient. The 3D weakly interacting Bose gas [Dalfovo et al., 1999], at zero temperature, is instead characterized by the different value $q = 2$, in fully agreement with the EOS (3.4) and (1.28) within the Bogoliubov theory. On the other hand, Eq. (3.1) does not hold for the ideal Bose gas below the condensation temperature since this system has an infinite compressibility and its pressure vanishes in the limit of zero temperature.

In the presence of axial or radial confinement, one should distinguish between the case when the 3D equation of state can be still applied locally within the local density approximation (LDA) (1.8) and the case where the motion is instead frozen along the directions of confinement, see Sec. 2.1.

The first case includes the so-called pancake geometry (where the equation of state can be expressed in terms of the 2D density and pressure) and the so-called cigar geometry (where the equation of state can be expressed in terms of the 1D density and pressure). Both configurations have been realised experimentally both for bosons [Jin et al., 1996, Mewes et al., 1996] as well as for fermions [Kinast et al., 2004, Bartenstein et al., 2004a, Weimer et al., 2015] and are characterised by different values of the polytropic coefficient (see Table 3.1). The second case includes the deep 2D and 1D configurations where the thermodynamic behaviour cannot be derived starting from the 3D equation of state in the LDA, as discussed in Chap. 2. These configurations are particularly interesting from the many-body and thermodynamic point of view. In 2D they exhibit the Berezinski-Kosterlitz-Thouless transition [Desbuquois et al., 2012], while in the 1D case for bosons, at zero temperature, they are described by Lieb-Lininger theory [Lieb and Liniger, 1963, Lieb, 1963]. Some of these low-dimensional regimes are also characterised by well-defined values of the polytropic coefficient which are reported in Table 3.2.

Table 3.1: Polytropic index q for the weakly interacting Bose gas at T = 0 and for the unitary Fermi gas in different LDA regimes. The results for the unitary Fermi gas hold also for the ideal Fermi gas at all temperatures and for the ideal Bose gas above T_c. From De Rosi and Stringari [2015]. Copyright © 2015, American Physical Society.

	Bose gas (T = 0)	Unitary Fermi gas
3D uniform	2	5/3
pancake (LDA)	5/3	3/2
cigar (LDA)	3/2	7/5

Table 3.2: Polytropic index q for a Bose gas for different 2D and 1D regimes in the presence of tight confinement. The 2D mean field value $q = 2$ holds also for the interacting Fermi gas in the BCS and BEC limits. From De Rosi and Stringari [2015]. Copyright © 2015, American Physical Society.

	T = 0	high T
2D mean field	2	2
1D mean field	2	3
1D Tonks-Girardeau	3	3

It is finally interesting to compare the adiabatic sound velocity $v_{s_{3D}}$ of 3D uniform systems with the sound velocity v_s for the lower dimensional regimes reported in Table 3.1. At T = 0, for equal values of the chemical potential (which, in the case of the LDA regimes, would correspond to equal values of the central density), one finds the following relationship

$$\frac{v_s^2}{v_{s_{3D}}^2} = \frac{q-1}{q_{3D}-1} \, , \tag{3.7}$$

where q_{3D} is the polytropic coefficient of the equation of state of 3D uniform matter. In the special case of a cigar trap (see Table 3.1), the above equation gives the value $v_s^2/v_{s_{3D}}^2 = 1/2$ for a weakly interacting Bose gas and $v_s^2/v_{s_{3D}}^2 = 3/5$ for the unitary Fermi gas. The above reduction factors of the sound velocity were first theoretically derived by Zaremba [1998] and by Capuzzi et al. [2006]. They were confirmed experimentally by Andrews et al. [1997a] and Joseph et al. [2007] for cigar Bose and Fermi gases, respectively. In the classical regime of high temperature, where $P = nk_BT$, one instead find the result

$$\frac{v_s^2}{v_{s_{3D}}^2} = \frac{q}{q_{3D}} \, , \tag{3.8}$$

where the sound velocities are calculated at the same temperature.

3.2   Overview of collective modes

In the last Chapters, we mainly discuss uniform atomic gases, without an external harmonic trap. In this Section, we would like to investigate the differences and the analogies of elementary excitations with and without a harmonic confinement. In this way, we introduce the concept of *collective oscillations* in trapped atomic systems, which is the main topic of the present Chapter. Finally, in SubSec. 3.2.1, we discuss the special case of normal excitations in the ideal gas.

In uniform systems, the lowest energy excitations have a phononic nature, characterised by a linear dispersion $\epsilon(p) = v_s p$, where v_s is the sound velocity. As we have studied in Sec. 3.1, v_s depends strongly on the EOS and, therefore, it changes from one system to another. For example, for the Bogoliubov spectrum (1.30), the sound velocity is given by the value $v_s = \sqrt{gn/m}$. We remind that we got the linear phononic dispersion relation exactly by taking the low-energy limit of Eq. (1.30), which corresponds to long-wavelength excitations. The symmetries of the system always leave their footprint on the excitations. Since the gas is homogeneous and therefore translationally invariant, the sound dispersion relation is a continuous function of momentum. Moreover, the sound propagates by means a series of oscillating compressions and expansions of the cloud at local level. At finite T, this process is adiabatic and one calculates the sound velocity starting from the adiabatic compressibility, see Eq. (3.2), while at $T = 0$, the isothermal and adiabatic compressibilities are equal, and v_s is provided by Eq. (3.6). The excitation of the sound in highly elongated geometry (cigar) is carried out with a laser pulse at the centre of the trap, which is responsible for a small shift in density followed by the propagation of sound wave packets in both positive and negative z-directions. With this excitation method, the sound velocity has been measured both for Bose [Andrews et al., 1997a] as well as for Fermi [Joseph et al., 2007] gases in cigar configurations.

Let us investigate how the lowest energy elementary excitations change by adding an external harmonic trap (1.7). Given the nature of the confinement, the excitation spectrum is discrete and this is an important difference with respect to the phononic spectrum discussed above. These discrete excitations are called *collective oscillations* or *normal modes* with *collective frequencies* ω. The presence of the trap enters directly the expressions of ω which are of the same order of the trapping frequency.

Normal modes are small oscillations characterised by both small amplitudes and velocities and long wavelengths (of the order of the size of the cloud). These excitations are linear (low-energy) oscillations for which the density, during its dynamical evolution, is slowly varying in both time and space. If one considers the GP gas at $T = 0$, see SubSec. 1.5.2, in the linear regime, the quantum pressure term in Eq. (1.42) is negligible. Actually, the two equations (1.41) and (1.42) are more general by considering a generic chemical potential $\mu(n)$ instead of the value gn holding for the GP gas. In fact, with this important generalisation, they describe every ultracold gas in the hydrodynamic regime at $T = 0$, where $\mu(n)$ plays the role of the EOS, Eq. (3.4). Actually, as we will investigate in the following Section, Eqs. (1.41) and (1.42) hold also for a normal gas with T above the critical point of condensation or superfluidity $T > T_C$. In this case, the role of the EOS in Eq. (1.42) is played by the pressure $P(n)$ and, at finite T, we require that the dynamics is adiabatic, by considering also a continuity equation for the entropy, really similar to that of the density n, Eq. (3.14).

Another remarkable property of collective frequencies is that they do not depend explicitly on the actual value of the interaction coupling constant, even if their values depend on the interaction regime. For example, as we will discuss in the following, in the collisionless regime, the frequency ω of the ideal gas is different from the result predicted in the hydrodynamic regime.

We close this Section by reminding that the investigation of collective oscillations allowed to characterise some properties of the atomic gas, like, for example, the superfluidity in a Bose [Maragò et al., 2000, De Rossi et al., 2016] or in a Fermi [Bartenstein et al., 2004b, Nascimbène et al., 2009] gas and also the dimensionality of the system [Merloti et al., 2013, Fang et al., 2014].

3.2.1 Ideal gas frequencies and harmonic trapping

In this Subsection, we summarise the behaviour of excitation frequencies of the ideal gas model, in the presence of harmonic trapping (see Eq. (1.37)). This model describes a gas in the absence of mean-field interaction and of collisions.

The eigenenergies of the harmonic oscillator (1.38) in 2D are:

$$\epsilon_{n_x,n_y} = \left(n_x + \frac{1}{2}\right)\hbar\omega_x + \left(n_y + \frac{1}{2}\right)\hbar\omega_y \ , \tag{3.9}$$

where $n_x, n_y = 0, 1, 2...$ are the quantum numbers which identify the energy levels in x and y spatial direction, respectively. While the values $n_x = n_y = 0$ characterize the ground state (1.38), the non-zero integers $n_x = n_y = 1, 2, 3...$ describe the excitations of the harmonic oscillator system. In an isotropic harmonic trap $\omega_\perp = \omega_x = \omega_y$, the corresponding frequencies of the elementary excitations can be written as:

$$\omega_{cl}(n, m) = \omega_\perp(2n + |m|) \ , \tag{3.10}$$

with $2n + |m| = n_x + n_y$. While n is associated with the number of radial nodes of the density oscillation, m is the z-component of the angular momentum.

In 1D, one can carry out a similar analysis:

$$\epsilon_{n_z} = \left(n_z + \frac{1}{2}\right)\hbar\omega_z \ , \tag{3.11}$$

and the frequency is

$$\omega_{cl}(k) = (k + 1)\omega_z \ , \tag{3.12}$$

with $k + 1 = n_z$ and the quantum number $k = 0, 1, 2...$ is associated to the number of radial nodes.

3.3 Hydrodynamic equations in the presence of external trapping

In this Section, we discuss the hydrodynamic (HD) equations for the velocity field describing the collective motion of the gas in the presence of an external confining potential and in the dissipationless (entropy conserving) regime. Even if these equations have a classical shape, because they do not contain the Planck constant, quantum mechanical effects deeply affect their solutions, being responsible for important changes in the behaviour of the equation of state and, in particular, in the value of the polytropic coefficients, as discussed in Sec. 3.1. These equations describe correctly the dynamic behaviour of an interacting system at zero temperature, where they coincide with the irrotational ($\nabla \times \mathbf{v} = 0$) hydrodynamic equations of superfluids and apply to interacting Bose and Fermi superfluid gases, as well as to strongly interacting superfluids like ^4He [Pitaevskii and Stringari, 2016]. In particular, for dilute weakly interacting Bose gases, HD equations can be derived

explicitly from the time-dependent Gross-Pitaevskii equation with the Thomas-Fermi approximation which enables to neglect the quantum pressure term, see SubSec. 1.5.2. At $T = 0$, HD equations have been used in predicting the frequencies of the collective oscillations [Stringari, 1996], in fair agreement with the experimental findings. For the ideal Fermi gas the HD equations were derived in the collisional limit by Minguzzi and Tosi [2001] at $T = 0$. They also apply above the critical temperature T_C for superfluidity, in the collisional regime where $\omega\tau \ll 1$, with τ the collisional time, and the equation of state can still depend in a crucial way on quantum statistical effects [Griffin et al., 1997]. In this regime, the velocity field admits the presence of rotational components ($\nabla \times \mathbf{v} \neq 0$), forbidden in every superfluid phase. For finite temperature, below T_C, the hydrodynamic equations should be instead generalised to include the coupled description of the normal and superfluid components (Landau's two-fluid hydrodynamic equations), allowing for the propagation of first and second sound [Pitaevskii and Stringari, 2016]. Therefore, they hold only in the presence of one component (superfluid or normal). Finally, in the absence of the trap, HD equations reproduce sound waves with dispersion $\omega = v_s q$, where v_s is the sound velocity, Eq. (3.2), see Sec. 3.2.

The hydrodynamic equations include the equation of continuity

$$\frac{\partial n(\mathbf{r},t)}{\partial t} + \nabla \cdot [n_0(\mathbf{r})\mathbf{v}(\mathbf{r},t)] = 0, \tag{3.13}$$

which expresses the conservation of density, the continuity equation for the entropy density ensuring the dissipationless dynamics,

$$\frac{\partial s(\mathbf{r},t)}{\partial t} = -\nabla [s_0(\mathbf{r})\mathbf{v}(\mathbf{r},t)], \tag{3.14}$$

and the equation for the current density $\mathbf{j}(\mathbf{r},t) = mn_0(\mathbf{r})\mathbf{v}(\mathbf{r},t)$

$$\frac{\partial \mathbf{j}(\mathbf{r},t)}{\partial t} = - [\nabla P(\mathbf{r},t) + n(\mathbf{r},t)\nabla V_{ext}(\mathbf{r})], \tag{3.15}$$

which has the same shape of the Euler's equation for the flow of a non-viscous liquid in the presence of an external potential $V_{ext}(\mathbf{r})$. Eq. (3.15) provides a non-trivial solution for the equilibrium configuration ($\mathbf{v} = 0$), for which the ground state density profile satisfies the LDA (1.8) at $T = 0$.

In the above equations n_0 and s_0 are the equilibrium values of the density and of the entropy density, respectively and, for simplicity, we have considered the limit of small amplitude oscillations and small velocities from the equilibrium configuration. At zero temperature, where the equation for the entropy identically vanishes, the hydrodynamic equations reduce to two coupled equations for the density and the velocity field. HD equations can be used only for the study of macroscopic phenomena with long wavelength excitations of phononic nature, for which all fields entering Eqs. (3.13)-(3.15) vary slowly in space and time. For these phenomena, the wavelength must be larger than the healing length ξ, whose value depends on the system considered. For example, for the BEC, the Bogoliubov dispersion law (1.30) tends to the phonon spectrum for wavelengths larger than $\xi \sim \hbar/(mv_s)$. In the BCS limit, ξ is given by the pairing gap $\xi \sim \hbar v_F/\Delta_{\text{gap}}$. Close to the resonance $k_F|a| \to +\infty$, the only characteristic length of the system is determined by the average interatomic distance and for wavelengths bigger than this, HD theory holds.

Starting from the above equations and using suitable thermodynamic relations, it is possible to derive the following equation for the stationary solutions of the velocity field characterized by the time dependence $\mathbf{v}(\mathbf{r},t) = \mathbf{v}(\mathbf{r})e^{-i\omega t}$ (see Appendix B):

$$m\omega^2\mathbf{v} = -\nabla \left[\left(\frac{\partial P}{\partial n}\right)_{\bar{s}}(\nabla \cdot \mathbf{v})\right] + (\gamma_{ad} - 1)(\nabla V_{ext})(\nabla \cdot \mathbf{v}) + \nabla(\mathbf{v} \cdot \nabla V_{ext}) \tag{3.16}$$

where the adiabatic coefficient

$$\gamma_{ad} = \left(\frac{\partial P}{\partial n}\right)_{\bar{s}} / \left(\frac{\partial P}{\partial n}\right)_T \tag{3.17}$$

provides the ratio between the isothermal and the adiabatic compressibilities. Equation (3.16) holds for configurations of different dimensionality and for arbitrary external potentials compatible with the applicability of the local density approximation along the direction of the velocity flow. It shows that the eigenfrequencies ω of the collective oscillations can be determined once the adiabatic and the isothermal compressibilities are known. These quantities depend on the nature of the system, on temperature and, of course, on the dimensionality of the configuration. Result (3.16) shows explicitly the emergence of rotational components in the velocity field $\mathbf{v}$ caused by the presence of the external potential [term proportional to $(\gamma_{ad} - 1)$]. This term exactly vanishes if the adiabatic and isothermal compressibilities coincide ($\gamma_{ad} = 1$), a condition ensured only at T $= 0$. In this limit Eq. (3.16) actually coincides with the hydrodynamic equation of irrotational superfluids. To our knowledge, the equations of linearized hydrodynamics, in the presence of an external potential, have never been derived so far in the general form (3.16). Their derivation represents one of the main results of the present PhD thesis and the principal findings are reported in De Rosi and Stringari [2015].

Starting from the equations of hydrodynamics it is also possible to derive (see Appendix B) the equation

$$\frac{\partial T(\mathbf{r}, t)}{\partial t} = -\frac{T}{c_v}\left(\frac{\partial P}{\partial T}\right)_n \frac{\nabla \cdot \mathbf{v}(\mathbf{r}, \mathbf{t})}{n_0} , \tag{3.18}$$

for the time dependence of the temperature of the gas, where c_v is the specific heat at constant volume. Eq. (3.18) shows that, for divergency free solutions ($\nabla \cdot \mathbf{v} = 0$), like the surface modes (Sec. 3.4), the temperature of the trapped gas is constant during the oscillation.

For systems obeying the polytropic behaviour (3.1) the equation for the temperature takes the simplified form

$$\frac{\partial T(\mathbf{r}, t)}{\partial t} = -(q - 1)T\nabla \cdot \mathbf{v}(\mathbf{r}, t) \tag{3.19}$$

which follows directly from Eq. (3.3) and from the thermodynamic relation $c_v = (\partial U / \partial T)_n$. Equation (3.19) coincides with the result derived by Griffin et al. [1997] for a 3D ideal Bose gas at $T \geq T_c$, where $q = 5/3$.

For systems obeying the polytropic law (3.1), the equation for the velocity field (3.16) takes the further simplified expression (see Appendix B)

$$m\omega^2\mathbf{v} = -\left(\frac{\partial P}{\partial n}\right)_{\bar{s}}\nabla\left(\nabla \cdot \mathbf{v}\right) + (q - 1)\left(\nabla V_{ext}\right)\nabla \cdot \mathbf{v} + \nabla\left(\mathbf{v} \cdot \nabla V_{ext}\right) \tag{3.20}$$

in terms of the adiabatic compressibility and the polytropic coefficient q. Equation (3.20) coincides with the result derived by Griffin et al. [1997] for a 3D ideal Bose gas for $T \geq T_c$ with $q = 5/3$. At T $= 0$, where $\gamma_{ad} = 1$, it reduces to

$$m\omega^2\mathbf{v} = -(q - 1)\nabla\left[\mu(n)\nabla \cdot \mathbf{v}\right] + \nabla\left[\mathbf{v} \cdot \nabla V_{ext}\right] \tag{3.21}$$

where we have used the T $= 0$ expression (3.4) for the chemical potential $\mu(n)$.

In the form (3.20) (and (3.21) at T $= 0$) the equation for the velocity field admits a useful class of analytical solutions that will be discussed in the following Sections where we will consider an external potential of the shape

$$V_{\text{ext}}(x, y) = \frac{1}{2}m\left(\omega_x^2 x^2 + \omega_y^2 y^2\right) \tag{3.22}$$

for the investigation of the collective oscillations of 2D configurations and of the form

$$V_{\text{ext}}(z) = \frac{1}{2}m\omega_z^2 z^2 \tag{3.23}$$

in the case of 1D configurations.

The solution of Eqs. (3.20) and (3.21) is the velocity field $\mathbf{v}$. As we will discuss in the following, we choose a proper ansatz for $\mathbf{v}$ which reflects not only the symmetries of the atomic cloud but also the kind of mode of which we want to calculate the collective frequency ω. By inserting this ansatz in Eqs. (3.20) and (3.21) we calculate the frequency ω.

3.4 Surface modes

In this Section, we discuss the surface modes, which involve only the surface of the atomic cloud, without any change of its volume (compression or expansion). They are completely independent on the EOS.

These modes are divergency free oscillations ($\nabla \cdot \mathbf{v} = 0$) and, therefore, the hydrodynamic equation (3.16) takes the simplified form

$$m\omega^2 \mathbf{v} = \nabla \left(\mathbf{v} \cdot \nabla V_{ext} \right) \tag{3.24}$$

independent of the equation of state, quantum statistics and temperature.

First of all, we consider the case of 2D isotropic confinement, where the trapping frequency is the same in all directions ($\omega_x = \omega_y \equiv \omega_\perp$). An important class of solutions of Eq. (3.24) is given by the irrotational choice ($\nabla \times \mathbf{v} = 0$) [Stringari, 1996]:

$$\mathbf{v}(r_\perp, \phi) \propto \nabla \left[r_\perp^{|m|} e^{\pm im\phi} \right], \tag{3.25}$$

where m is z-th component of angular momentum. The resulting eigenfrequencies take the form

$$\omega^2(m) = \omega_\perp^2 |m| . \tag{3.26}$$

The lowest energy surface mode is the *dipole* or *centre-of-mass* mode with $m = 1$ in Eq. (3.26). This mode corresponds to the oscillation of the centre-of-mass of the atomic cloud. Its frequency is always equal to that of the trap ($\omega_D = \omega_\perp$), independently on the system and on its EOS. The reason of this peculiar property is directly provided by the Kohn's theorem: the centre-of-mass oscillation is affected only by the external potential (the trap), and not by the internal forces of the system since the internal and the external degrees of freedom are completely decoupled. The dipole mode is reported in Fig. 3.1.
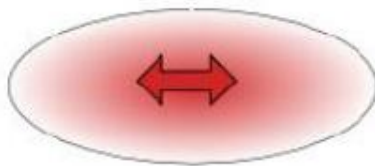
Figure 3.1: Dipole mode. From De Rossi [2016].
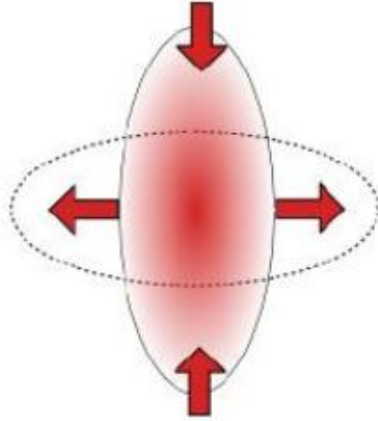
Figure 3.2: Quadrupole mode. From De Rossi [2016].

Another interesting mode is the *quadrupole* oscillation. It is a surface deformation without volume change, see Fig. 3.2. Like every surface mode, the frequency of the quadrupole is independent on the EOS. The frequency is however different if one calculates it in the HD interacting gas, from Eq. (3.26) with $m = 2$: $\omega_Q = \sqrt{2}\omega_\perp$ or in the ideal gas (collisionless regime) $\omega_Q = 2\omega_\perp$ (see Eq. (3.10) with $n = 0$ and $m = 2$). This difference is very useful, because through the measurement of this mode, one can distinguish between the hydrodynamic and the collisionless regime.

In the case of anisotropic potentials ($\omega_x \neq \omega_y$) an important example of divergency free oscillations is described by the ansatz:

$$\mathbf{v}(x, y) \propto \nabla(xy) \tag{3.27}$$

yielding the result

$$\omega_S^2 = \omega_x^2 + \omega_y^2 \tag{3.28}$$

for the collective frequency. This is the so-called *scissors* mode corresponding to an oscillating rotation of the atomic cloud in the x-y plane, see Fig. 3.3. This mode can be excited by means a sudden rotation of the trap by a small angle θ. Since it preserves the shape of the gas during the oscillation, it is independent on the EOS. It has the same value in 3D as well as in 2D configurations described by the hydrodynamic formalism. It was first predicted by Guéry-Odelin and Stringari [1999] and experimentally observed in both 3D Bose [Maragò et al., 2000], where it was used to investigate the superfluid character of the system, and in Fermi superfluids [Wright et al., 2007].

3.5 Compressional oscillations in pancake and 2D isotropic traps

In this Section, we discuss the collective oscillations exhibiting a change of volume of the atomic cloud. Since these modes are characterised by a compression of the gas, their frequencies depend explicitly on the EOS.

Let us first consider the superfluid regime at T = 0 for which, as already pointed out in the Section 3.3, the irrotationality condition for the velocity field holds. For systems whose equation of state is characterized by the polytropic density dependence (3.4), the velocity field obeys the hydrodynamic Eq. (3.21). For isotropic 2D traps one can easily
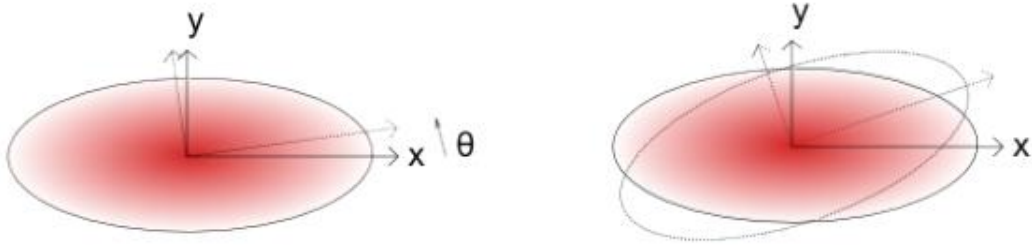
Figure 3.3: The scissors mode is excited by turning the trapping axis. From De Rossi [2016].

check that this equation is solved by the following irrotational ansatz for the velocity field [Stringari, 1998]:

$$\mathbf{v}(r_\perp, \phi) \propto \nabla \left[(r_\perp^{2n} + ...)r_\perp^{|m|} e^{\pm im\phi} \right] \tag{3.29}$$

where n fixes the number of the radial nodes of the density modulations occurring during the oscillation and m is z-th component of angular momentum. The resulting hydrodynamic eigenfrequencies take the form

$$\omega^2(n, m, q) = \omega_\perp^2 [2n + |m| + 2n(q-1)(n+|m|)]. \tag{3.30}$$

Result (3.30) can be applied to a rich variety of physical situations whose equation of state is simply incapsulated in the polytropic q index and differs from the predicted values of the ideal gas model in the collisionless regime, see SubSec. 3.2.1:

$$\omega_{cl}(n, m) = \omega_\perp(2n + |m|). \tag{3.31}$$

Moreover, result (3.30) should be compared with the hydrodynamic dispersion law holding in the presence of a 3D isotropic harmonic potential ($\omega_x = \omega_y = \omega_z \equiv \omega_{ho}$)

$$\omega^2(n, l, q) = \omega_{ho}^2 [2n + l + (q-1)(2n^2 + 2nl + n)] \tag{3.32}$$

where l is the angular momentum. Eq. (3.32) reduces to the results of Stringari [1996] and Bruun and Clark [1999], Baranov and Petrov [2000], Minguzzi and Tosi [2001] in the case of the weakly interacting Bose ($q = 2$) and Fermi ($q = 5/3$) gases, respectively. Result (3.30) reduces to the dispersion (3.26) of surface modes in the case $n = 0$.

The most important solution accounted for by (3.30) is the 2D *monopole* or *breathing* mode ($n = 1$ and $m = 0$), for which one finds the result

$$\omega_M^2(q) = 2q\omega_\perp^2. \tag{3.33}$$

Its name is taken from biology, because the evolution of this mode remembers the respiration mode of a biological cell, see Fig. 3.4. Differently from the surface modes discussed in the previous Section, the frequency of the breathing mode (3.33) depends explicitly on the polytropic index q. Therefore, it is consequently sensitive to the EOS obeyed by the gas and on all the information carried by it: the T, the D, the quantum statistics of atoms, the shape of the trap and the interaction. For example, the monopole collective frequency is different for a Bose and a Fermi gas. The frequency (3.33) of the 2D breathing mode differs from the one in the 3D isotropic case (see Eq. (3.32) with $n = 1$ and $l = 0$) which yields the value $\omega_M^2(q) = (3q - 1)\omega_{ho}^2$.
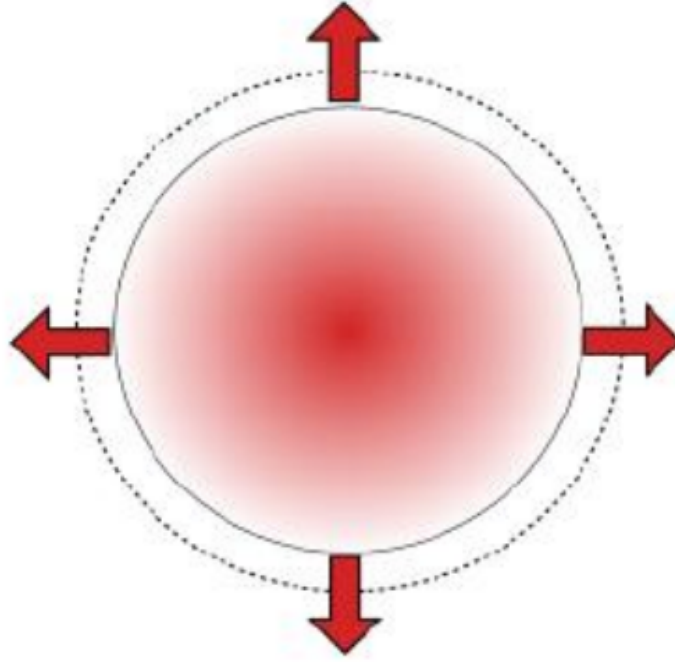
Figure 3.4: Monopole mode. From De Rossi [2016].

For the unitary Fermi gas in the pancake regime ($q = 3/2$), one gets the value $\omega_M = \sqrt{3}\omega_\perp$. Actually, this value turns out to be independent of temperature, as a consequence of the fact that, at unitarity, the scaling solution for the breathing mode is exactly satisfied by the hydrodynamic equations at all temperatures [Hou et al., 2013a]. Notice that this result differs from the value $\omega_M = 2\omega_{ho}$ holding for the unitary Fermi gas with 3D isotropic trapping ($q = 5/3$). In this latter case, an exact solution of the time-dependent Schrödinger equation is available for the monopole breathing mode, independent not only of temperature but also of the amplitude of the oscillation and holding in all collisional regimes (scale invariance) [Castin, 2004]. A similar situation holds also for the 2D regime of a weakly interacting Bose gas ($q = 2$) in the presence of isotropic trapping where one also finds the result $\omega_M = 2\omega_\perp$, independent of temperature and of the amplitude of oscillations [Pitaevskii, 1996, Pitaevskii and Rosch, 1997]. In the case of the 2D Fermi gas the result $\omega_M = 2\omega_\perp$, following from the $q = 2$ value of the polytropic coefficient, holds both in the BEC and BCS regime and, with high accuracy, along the whole crossover, revealing an apparent scale invariance [Taylor and Randeria, 2012, Levinsen and Parish, 2015], as proven experimentally by Vogt et al. [2012].

The temperature dependence of the frequency of the breathing mode takes instead place for the pancake weakly interacting Bose gas. At T = 0 ($q = 5/3$) one finds $\omega_M = \sqrt{10/3}\omega_\perp$ [Stringari, 1996]. This result differs from the value obtained at high temperature, where the thermodynamic behaviour of the gas can be approximated by the ideal Bose gas ($q = 3/2$) and the hydrodynamic frequency takes the value $\omega_M = \sqrt{3}\omega_\perp$. The frequency of the monopole mode of the pancake Bose gas is then expected to exhibit a temperature dependence. The temperature dependence of this mode was pointed out in the first experiments on the collective oscillations carried out at Jila [Jin et al., 1997] where, however, due to the small number of atoms, the system enters soon the collisionless regime for $T > T_c$, rather than the collisional one. Achieving the hydrodynamic condition $\omega\tau \ll 1$ is, in general, a difficult task in weakly interacting Bose gases, due to the small available values of the density of the gas. A simple estimate, based on the classical evaluation of the collisional time,

Table 3.3: Hydrodynamic frequencies of the breathing mode in different LDA regimes. The values reported for the unitary Fermi gas hold also for the ideal Bose gas above T_C. From De Rosi and Stringari [2015]. Copyright © 2015, American Physical Society.

	Bose gas (T = 0)	Unitary Fermi gas
3D isotropic	$\sqrt{5}\omega_{ho}$	$2\omega_{ho}$
pancake (LDA)	$\sqrt{10/3}\omega_\perp$	$\sqrt{3}\omega_\perp$
cigar (LDA)	$\sqrt{5/2}\omega_z$	$\sqrt{12/5}\omega_z$

Table 3.4: Hydrodynamic frequencies of the breathing mode for a Bose gas in low dimensions and tight trapping regimes. The 2D mean field value $\omega_M = 2\omega_\perp$ holds also for the interacting Fermi gas in the BCS and BEC limits. From De Rosi and Stringari [2015]. Copyright © 2015, American Physical Society.

	T = 0	high T
2D mean field	$2\omega_\perp$	$2\omega_\perp$
1D mean field	$\sqrt{3}\omega_z$	$2\omega_z$
1D Tonks-Girardeau	$2\omega_z$	$2\omega_z$

yields, for frequencies of the order of the trapping frequency ω_{ho}, the condition [Dalfovo et al., 1999] $l_{mph} \ll R_T$, where $l_{mph} = (n\sigma)^{-1}$ is the mean free path. Here n is the local 3D density, $\sigma = 8\pi a^2$ is the s-wave cross section, while $R_T = \sqrt{2k_B T/m\omega_{ho}^2}$ is the thermal radius.

A summary of the frequencies of the breathing mode in the most relevant cases discussed in this Section is presented in Tables 3.3 and 3.4.

3.6 Coupled compressional and surface modes in anisotropic traps

In this Section we investigate the case of anisotropic trapping $(\omega_x \neq \omega_y)$, where the breathing and the quadrupole oscillations discussed in the previous Sections are coupled. The coupling is accounted for by the ansatz

$$\mathbf{v}(x, y) = \nabla(\alpha x^2 + \beta y^2), \tag{3.34}$$

where the relative value of the parameters α and β have to be determined by solving the hydrodynamic equation (3.20). Since $\nabla(\nabla \cdot \mathbf{v}) = 0$ the frequency of the coupled modes, for a given value of the polytropic coefficient q, are given by

$$\omega_\pm^2(q) = \frac{(q+1)}{2}(\omega_x^2 + \omega_y^2) \pm \frac{\sqrt{(q+1)^2(\omega_x^2 + \omega_y^2)^2 - 16q\omega_x^2\omega_y^2}}{2}. \tag{3.35}$$

In the isotropic limit ($\omega_x = \omega_y = \omega_\perp$) Eq. (3.35) reproduces the results (3.33) and (3.26) for the monopole and the quadrupole, respectively, derived in the previous Sections. In the case of the 2D mean field regime, where the polytropic coefficient takes the value $q = 2$, result (3.35) was derived by Ghosh [2000] and by Baur et al. [2013] for bosons and fermions, respectively.

Result (3.35) gives general predictions for the collective frequencies in 2D configurations for arbitrary values of the deformation of the trap. It is interesting to consider the limit of highly deformed 2D trapping potentials. For $\omega_x \ll \omega_y$ the lower solution takes the form

$$\omega_-^2 = \frac{4q}{(q+1)}\omega_x^2, \tag{3.36}$$

while the upper solution is given by

$$\omega_+^2 = (q+1)\omega_y^2 . \tag{3.37}$$

Of course a symmetric result takes place in the opposite limit $\omega_x \gg \omega_y$.

In the 2D mean field case ($q = 2$), Eq. (3.36) provides the result $\omega_- = \sqrt{8/3}\omega_x$, in agreement with the findings of Ghosh [2000]. In the pancake regime, Eq. (3.36) instead reduces to the frequency of the axial breathing mode of a cigar configuration (see next Section).

Equation (3.37) instead coincides with the solution of the 3D hydrodynamic equations for triaxial harmonic trapping [Pitaevskii and Stringari, 2016] in the intermediate regime $\omega_z \gg \omega_y \gg \omega_x$.

3.7 Collective frequencies in cigar and 1D traps

In this Section, we complete the discussion on the collective frequencies of harmonically trapped gases considering 1D configurations.

Similarly to the 2D case, two different regimes can be considered also in 1D. The first one, called cigar regime, corresponds to systems described locally by the 3D equation of state, but the radial confinement is enough tight to ensure a 1D nature to the low-energy dynamic behaviour. This configuration is particularly suited to investigate the propagation of sound [Andrews et al., 1997a, Joseph et al., 2007, Horikoshi et al., 2010].

A second case is the deep 1D (hereafter simply called 1D) regime where the radial motion is frozen (for a general review on 1D systems see, for example, Giamarchi [2004, 2016]). The role of correlations is particularly important in this regime and, in the case of Bose gases at $T = 0$, is described by Lieb-Liniger theory [Lieb and Liniger, 1963], see Sec. 2.3. A key question in 1D is the role of thermalization, see SubSec. 2.3.2. From this point of view, the comparison between experiments and the predictions of hydrodynamic theory (which assumes local thermalization at finite temperature) would be particularly insightful. Another important feature of 1D systems is the absence of phase transitions at finite temperature [Landau and Lifshitz, 2013], see SubSec. 2.2.2.

The equations of hydrodynamics derived in Sect. 3.3 become particularly simple in 1D, the velocity field being a function of the variable z and all the gradients acting only on the z-direction. Looking for solutions of the form

$$v = z^k + \alpha_{k-2}z^{k-2} + ... \tag{3.38}$$

one finds that the hydrodynamic equation (3.20), in the presence of the polytropic equation of state (3.1), admits simple analytic solutions in the presence of the harmonic trapping (3.23).

At $T = 0$, where one can conveniently use Eq. (3.21) with the chemical potential given by (A.1), the dispersion law takes the form

$$\omega^2(k, q) = (k + 1)\left[(q - 1)\frac{k}{2} + 1\right]\omega_z^2 \ . \tag{3.39}$$

Equation (3.39) was first derived by Menotti and Stringari [2002] in the context of 1D Bose gases.

In the classical limit of high temperature, where one can use the equation of state $P_{1D} = n_{1D}k_BT$, the hydrodynamic equation (3.20) gives rise instead to the following dispersion relation

$$\omega^2(k, q) = (qk + 1)\omega_z^2 \ . \tag{3.40}$$

Result (3.39) should be also compared with the dispersion

$$\omega_{cl}(k) = (k + 1)\omega_z \tag{3.41}$$

holding in the collisionless regime of a non interacting 1D gas, see SubSec. 3.2.1.

Let us first consider the case of the cigar unitary Fermi gas. In this case the polytropic coefficient is equal to $q = 7/5$ at all temperatures and the $k = 1$ hydrodynamic solution, corresponding to the lowest breathing (LB) mode, is equal to $\omega_{LB} = \sqrt{12/5}\omega_z$ [Heiselberg, 2004, Stringari, 2004] at both zero and finite temperature. The situation is different for the higher nodal modes ($k > 1$) where the hydrodynamic frequencies at $T = 0$ and in the classical limit are different revealing an interesting temperature dependence [Hou et al., 2013b] that was investigated experimentally by Tey et al. [2013] in good agreement with the predictions of the theory. The case of the cigar Bose gas is different. In fact in this case the polytropic coefficient depends on temperature, being equal to $q = 3/2$ at $T = 0$ and to $q = 7/5$ in the classical limit. As a result, the frequency of the $k = 1$ lowest breathing mode takes the value $\omega_{LB} = \sqrt{5/2}\omega_z$ [Stringari, 1996, 1998] while in the high temperature classical limit one finds the smaller hydrodynamic value $\omega_{LB} = \sqrt{12/5}\omega_z$. In the collisionless limit, one instead finds the value $2\omega_z$. The $T = 0$ value $\sqrt{5/2}\omega_z$ was measured experimentally by Stamper-Kurn et al. [1998] in excellent agreement with the prediction of theory. At finite temperature, these authors found that the frequency slightly drops below the low-temperature limit. At even higher temperatures they observed a significant increase of ω, likely due to the breakdown of the hydrodynamic condition $\omega\tau \ll 1$.

The comparison between the lowest compressional mode in the cigar geometry ($k = 1$) and the lowest solution (3.36) holding in the pancake geometry with highly anisotropic 2D trapping, allows for the non trivial relationship

$$q_{cigar} + 1 = \frac{4q_{pancake}}{q_{pancake} + 1} \tag{3.42}$$

between the polytropic coefficients in the cigar and pancake geometries. The relationship is confirmed by the results reported in Table 3.1.

The behaviour of the collective frequencies in the deep 1D regime is also very interesting. In the case of bosons, one should distinguish between the mean field case, where $q = 2$ at $T = 0$, and the TG limit [Girardeau, 1960], where $q = 3$. In the former case the frequency of the $k = 1$ breathing mode takes the value $\omega_{LB} = \sqrt{3}\omega_z$, while in the TG limit one finds $\omega_{LB} = 2\omega_z$. The behaviour of the lowest breathing frequencies, in the intermediate regimes between the mean-field and the TG limits, was theoretically investigated by Menotti and Stringari [2002] and experimentally observed by Haller et al. [2009]. At high temperatures, both regimes predict the frequency $\omega_{LB} = 2\omega_z$ for the same $k = 1$ mode. One then concludes that, differently from the 1D mean field, the frequency of the breathing mode in

the TG regime is temperature independent. The result is not surprising since in the TG limit bosons behave like 1D non-interacting fermions where scaling invariance applies. It is worth noting, however, that the hydrodynamic frequencies of the higher nodal modes depend on temperature even in the TG limit. For example, the $k = 2$ mode has frequency $\omega_{k=2} = 3\omega_z$ at $T = 0$ and $\omega_{k=2} = \sqrt{7}\omega_z$ in the classical limit. The temperature dependence of the $k = 1$ breathing mode in the 1D mean field has been recently measured by Fang et al. [2014].

Chapter 4

Linear response theory

> Everything, however complicated - breaking waves, migrating birds, and tropical forests - is made of atoms and obeys the equations of quantum physics. But even if those equations could be solved, they wouldn't offer the enlightenment that scientists seek. Each science has its own autonomous concepts and laws.
>
> Martin Rees

In this Chapter we introduce some basic concepts of the linear response theory, which is really useful to investigate the dynamics of many-body systems at $T = 0$ as well as at finite T. It can be applied to several kinds of systems, ranging from atomic nuclei to interacting quantum gases, just to mention some examples.

The main goal of linear response theory is to provide the description of the excitation spectrum by applying an external perturbation to the system. The perturbation is usually described by a one-body operator and it is enough weak, such that the linear regime holds. The response of the system depends on the nature of the external perturbation as well as, of course, on the properties of the system.

In the case of uniform systems, depending on the value of the transferred momentum from the external probe, one can investigate different regimes. For small momentum transfer, the constituents of the system move coherently in the form of sound waves. In the case of high momentum transfer, the external probe instead scatters from the individual constituents in an incoherent way.

In the case of isotropically trapped systems, the external perturbation is usually associated to transfer of angular momentum l and the collective oscillations correspond to small values of l.

The present Chapter is organised as follows.

In Sec. 4.1 we present a general analysis of the formalism, by introducing the concepts of dynamic polarizability, dynamic structure factor and sum rules.

In Sec. 4.2 a special emphasis is given to density excitations.

Finally, in Sec. 4.3, we discuss general inequalities, based on the formalism of linear response theory, which give useful bounds for the excitation energies as well as for the fluctuations of physical observables.

An exhaustive treatment of these concepts is however out of the aims of this thesis; readers interested in more extended discussions can see Pitaevskii and Stringari [2016], on which this Chapter is based.

4.1   Dynamic structure factor and sum rules

We consider a many-body system described by the unperturbed Hamiltonian H, and two linear operators F and G, which represent physical observables, with vanishing ground-state expectation values.

The system is coupled to the external perturbation G through the time-dependent Hamiltonian:

$$H_{pert}(t) = -\lambda G e^{-i\omega t} e^{\eta t} - \lambda^* G^\dagger e^{+i\omega t} e^{\eta t} \ , \tag{4.1}$$

where $\lambda \ll 1$ represents the strength of the external field, which, following the above considerations, is small enough in order to apply linear response theory. The factor $e^{\eta t}$, with η positive and small, guarantees that at time $t = -\infty$ the system is described by the unperturbed Hamiltonian H, because, from Eq. (4.1), it is clear that $H_{pert}(t = -\infty) = 0$.

Let us now calculate the fluctuation $\delta \langle F^\dagger \rangle$ induced by the presence of the external field. This fluctuation oscillates in time with the same frequency ω as the external perturbation (4.1), and it can be written as

$$\delta \langle F^\dagger \rangle = \lambda e^{-i\omega t} e^{\eta t} \chi_{F^\dagger, G}(\omega) + \lambda^* e^{+i\omega t} e^{\eta t} \chi_{F^\dagger, G^\dagger}(-\omega) \ , \tag{4.2}$$

where we have introduced the linear response function, also called dynamic polarizability of the system, $\chi_{F^\dagger, G}(\omega)$. It satisfies the property $\chi^*_{F^\dagger, G}(\omega) = \chi_{F, G^\dagger}(-\omega)$. The response function $\chi_{F^\dagger, G}(\omega)$ gives information about the properties of the system in the absence of the external perturbation, and it can be evaluated using perturbation theory. If the system is in thermal equilibrium at temperature T at $t = -\infty$, then one finds the result [Kubo, 1956, 1957]:

$$\chi_{F^\dagger, G}(\omega) = -\frac{1}{\hbar} Q^{-1} \sum_{m,n} e^{-\beta E_m} \left[\frac{\langle m| F^\dagger |n \rangle \langle n| G |m \rangle}{\omega - \omega_{n,m} + i\eta} - \frac{\langle m| G |n \rangle \langle m| F^\dagger |n \rangle}{\omega + \omega_{n,m} + i\eta} \right] \ , \tag{4.3}$$

where $|n\rangle$ and $\omega_{n,m} = (E_n - E_m)/\hbar$ are, respectively, the eigenstates and the excitation frequencies of the unperturbed Hamiltonian ($H |n\rangle = E_n |n\rangle$), and $Q = \sum_m e^{(-\beta E_m)}$ is the partition function. The Boltzmann factor $e^{(-\beta E_m)}$ takes into account the thermal equilibrium of the initial state.

The quantity which describes the properties of the excited system is called the dynamic structure factor:

$$S_F(\omega) = Q^{-1} \sum_{m,n} e^{(-\beta E_m)} |\langle n| F |m \rangle|^2 \delta(\hbar\omega - \hbar\omega_{nm}) \tag{4.4}$$

from which it is clear that depends not only on the perturbation F, but also on how F interacts with the system at atomic levels $|\langle n| F |m \rangle|^2$ and it is responsible of atomic transitions. The delta function in Eq. (4.4) describes that the frequency ω of the fluctuation of the system (4.2) is selected starting from the proper atomic transition frequency ω_{nm}. The contribution of the terms with $m \neq 0$ is more important if T is high. At T = 0, the dynamic structure factor reduces to

$$S_F(\omega) = \sum_n |\langle n| F |0 \rangle|^2 \delta(\hbar\omega - \hbar\omega_{n0}) \ . \tag{4.5}$$

In Eq. (4.5), the quantity $|\langle n| F |0 \rangle|^2$ is the strength of the operator F relative to the state $|n\rangle$. Notice also that Eq. (4.5) vanishes at $\omega < 0$ since the excitation energies $\hbar\omega_{n0}$ are always positive, the system being initially in its ground state. Therefore, at T = 0, the system can only gain energy and not release it, differently from the finite T case. At

finite T, from Eq. (4.4), by interchanging the indices m and n in the sum, one finds the principle of detailed balancing:

$$S_F(\omega) = e^{\beta\hbar\omega} S_{F^\dagger}(-\omega) \tag{4.6}$$

which states that the probabilities (proportional to $S_F(\omega)$ and $S_F^\dagger(-\omega)$, respectively) that the system gains and releases energy after the coupling with the external perturbation, are connected each other by the Boltzmann factor $e^{\beta\hbar\omega}$. As discussed above, from Eq. (4.6), one finds again that at $T = 0$, $\beta = 1/(k_B T) = +\infty$, and therefore $S_F^\dagger(-\omega) = 0$, with $\omega > 0$.

In the simplest case when the two operators coincide $F = G$, the response function $\chi_F \equiv \chi_{F^\dagger,F}$ can be written in terms of the dynamic structure factor S_F as

$$\chi_F(\omega) = - \int_{-\infty}^{+\infty} d\omega' \left[\frac{S_F(\omega')}{\omega - \omega' + i\eta} - \frac{S_{F^\dagger}(\omega')}{\omega + \omega' + i\eta} \right] . \tag{4.7}$$

By using the Dirac relation

$$\lim_{\eta \to 0} \frac{1}{x - a + i\eta} = P\frac{1}{x - a} - i\pi\delta(x - a) , \tag{4.8}$$

where P is the principal part, the function χ_F can be separated into its real and imaginary parts

$$\chi_F(\omega) = \chi'_F(\omega) + i\chi''_F(\omega) . \tag{4.9}$$

From Eq. (4.7), one finds for the real part

$$\chi'_F(\omega) = - \int_{-\infty}^{+\infty} d\omega' \left[S_F(\omega') P\frac{1}{\omega - \omega'} - S_{F^\dagger}(\omega') P\frac{1}{\omega + \omega'} \right] \tag{4.10}$$

and for the imaginary part

$$\chi''_F(\omega) = \pi \left[S_F(\omega) - S_{F^\dagger}(-\omega) \right] . \tag{4.11}$$

From Eqs. (4.10) - (4.11), one deduces that the real χ' and the imaginary χ'' are even and odd functions with respect to the change of ω and F into $-\omega$ and $F^\dagger$. By using Eq. (4.6), Eq. (4.11) can be rewritten as

$$\chi''_F(\omega) = \pi \left(1 - e^{-\beta\hbar\omega} \right) S_F(\omega) \tag{4.12}$$

which is called also the dissipative component of the response function. From Eq. (4.12), it is clear that at $T = 0$, the two functions χ''_F and S_F are equal, up to a factor π, for positive ω. This implies that, at $T = 0$, only processes which increase energy in the system are allowed. On the other hand, at finite T, the two functions χ''_F and S_F can differ a lot, especially at high T when $\beta\hbar\omega$ is small. In particular, the dynamic structure factor has a much stronger dependence on T with respect to χ''_F, which is consequently considered a more fundamental quantity from the many-body point of view.

The causal nature of the response of the perturbation is described by the Kramers-Kronig relations [Kronig, 1926, Kramers, 1927, Pitaevskii and Stringari, 2016]:

$$\chi'_F(\omega) = -\frac{1}{\pi} \int_{-\infty}^{+\infty} d\omega' \chi''_F(\omega') P\frac{1}{\omega - \omega'} \tag{4.13}$$

$$\chi''_F(\omega) = \frac{1}{\pi} \int_{-\infty}^{+\infty} d\omega' \chi'_F(\omega') P\frac{1}{\omega - \omega'} . \tag{4.14}$$

In order to evaluate explicitly the response function or, equivalently, the dynamic structure factor, one needs to solve the Schrödinger equation and find the eigenstates and the eigenfrequencies of the many-body system. This yields to the calculation of the matrix elements in Eq. (4.3). However, one can obtain information on the behaviour of the dynamic structure factor by applying the method of sum rules, which gives an algebraic way to evaluate the moments of the dynamic structure factor

$$m_p(F) = \hbar \int_{-\infty}^{+\infty} (\hbar\omega)^p S_F(\omega) d\omega \tag{4.15}$$

which at finite T, by using Eq. (4.4), becomes:

$$m_p(F) = Q^{-1} \sum_{m,n} e^{-\beta E_m} |\langle n| F |m\rangle|^2 (E_n - E_m)^p \tag{4.16}$$

while at T = 0, by using Eq. (4.5):

$$m_p(F) = \sum_n (E_n - E_0)^p |\langle n| F |0\rangle|^2 . \tag{4.17}$$

An important advantage of this method is that it can reduce the calculation of the dynamical properties of the many-body problem to the knowledge of a few key parameters relative to its initial unperturbed configuration. Indeed, by using the completeness relation $\sum_n |n\rangle \langle n| = 1$, one easily gets the exact identities for finite T:

$$m_0(F) + m_0(F^\dagger) = \langle \{F^\dagger, F\} \rangle \tag{4.18}$$

$$m_0(F) - m_0(F^\dagger) = \langle [F^\dagger, F] \rangle \tag{4.19}$$

$$m_1(F) + m_1(F^\dagger) = \langle [F^\dagger, [H, F]] \rangle \tag{4.20}$$

$$m_1(F) - m_1(F^\dagger) = \langle \{F^\dagger, [H, F]\} \rangle \tag{4.21}$$

where the average is taken on the equilibrium thermal state, and we have taken into account only the lowest moments. In general, $S_F \neq S_F^\dagger$ so the sum rules (4.19) and (4.21) differ from zero. The sum rules (4.19) and (4.20) are connected to the high-frequency expansion of the dynamic response function (4.7) which is provided by

$$\chi_F(\omega)_{\omega\to\infty} = -\frac{1}{\hbar\omega} \langle [F^\dagger, F] \rangle - \frac{1}{(\hbar\omega)^2} \langle [F^\dagger, [H, F]] \rangle , \tag{4.22}$$

showing that the leading term of the expansion, which depends on $1/\omega$, vanishes if F commutes with its adjoint, as in the case of the density operator (see Sec. 4.2). Another property is that the sum-rules (4.18) and (4.21) which contain the anticommutators do not enter the above expansion. In the limit of small ω, the dynamic polarizability reproduces its static limit (static polarizability $\chi_F(0)$) according to the law

$$\chi_F(0) \equiv \chi_F(\omega)_{\omega\to 0} = m_{-1}(F) + m_{-1}(F^\dagger) , \tag{4.23}$$

where we have introduced the inverse energy-weighted moment m_{-1} of the dynamic structure factor. Differently from the moments with $p \geq 0$, the inverse energy-weighted moments cannot be calculated in terms of commutators, and they are evaluated with the direct calculation of the static response $\chi_F(0)$.

By combining Eq. (4.12) with the antisymmetry property $\chi_F^*(\omega) = \chi_{F^\dagger}(-\omega)$, one derives the fluctuation-dissipation theorem:

$$\langle \{F^\dagger, F\} \rangle = \hbar \int_{-\infty}^{+\infty} d\omega [S_F(\omega) + S_{F^\dagger}(\omega)] = \frac{\hbar}{\pi} \int_{-\infty}^{+\infty} d\omega \chi_F''(\omega) \coth\left(\frac{\beta\hbar\omega}{2}\right) , \tag{4.24}$$

which connects the dissipative component χ_F'' of the response function to the fluctuation $\langle \{F^\dagger, F\} \rangle$ of the operator F. By using the property $\chi_F''(\omega) \coth\left(\frac{\beta\hbar\omega}{2}\right) \geq \chi_F''(\omega)\frac{2}{\beta\hbar\omega}$ which holds for both positive and negative values of ω and the equation

$$\chi_F(0) = \frac{1}{\pi} \int_{-\infty}^{+\infty} d\omega \frac{\chi_F''(\omega)}{\omega} \tag{4.25}$$

coming from Eq. (4.13), one derives the inequality

$$\langle \{F^\dagger, F\} \rangle \geq 2k_B T \chi_F(0) \, , \tag{4.26}$$

which becomes an equality for $\coth\left(\frac{\beta\hbar\omega}{2}\right) = \frac{2}{\beta\hbar\omega}$ in the classical regime of high T.

4.2   Density response function

In this Section, we apply the linear response theory to the density response function [Pines and Nozières, 1999], which is the most important problem.

We consider the **q**-component of the Fourier transform

$$\rho_{\mathbf{q}} = \sum_{i=1}^{N} e^{-i\mathbf{q}\cdot\mathbf{r}_i} = \int d\mathbf{r} e^{-i\mathbf{q}\cdot\mathbf{r}} n(\mathbf{r}) \tag{4.27}$$

of the density operator

$$n(\mathbf{r}) = \sum_{i=1}^{N} \delta(\mathbf{r} - \mathbf{r}_i) \, , \tag{4.28}$$

where $\mathbf{r}_i$ is the coordinate operator of the i-th particle.

As we discuss in the following, the above operator, within the framework of the sum-rule approach, describes the propagation of sound in uniform configurations which has to be compared with collective modes in trapped systems, investigated in Chap. 5.

The density response function $\chi(\mathbf{q}, \omega)$ is calculated by making the choice $F = G = \delta\rho_{\mathbf{q}}^\dagger$, with $\delta\rho_{\mathbf{q}}^\dagger = \rho_{\mathbf{q}}^\dagger - \langle\rho_{\mathbf{q}}^\dagger\rangle_{eq}$, in Eq. (4.3). Notice that the expectation value $\langle\rho_{\mathbf{q}}^\dagger\rangle_{eq}$ is taken at equilibrium and it is zero in uniform configurations if $\mathbf{q} \neq 0$. At T $= 0$, the equilibrium configuration coincides with the ground-state. For low-momentum transfer, the response function $\chi(\mathbf{q}, \omega)$ is sensitive to the collective oscillations of the system, which are phonons (sound) in uniform configurations. On the other hand, for high momentum, the collective character is not anymore relevant, since the external probe scatters incoherently from the individual components of the system. This regime is suitable to explore the momentum distribution $n(\mathbf{p})$ of the atomic cloud.

Analogously, one can calculate the dynamic structure factor $S(\mathbf{q}, \omega)$ by using $F = \delta\rho_{\mathbf{q}}^\dagger$ in Eq. (4.4). The importance of the dynamic structure factor resides in the fact that it describes the cross-section of inelastic reactions where the scattering probe transfers momentum $\hbar\mathbf{q}$ and energy $\hbar\omega$ to the system, as happens in neutron scattering from liquid helium [Pitaevskii and Stringari, 2016].

We study now the moments

$$m_p(\mathbf{q}) = \hbar \int_{-\infty}^{+\infty} (\hbar\omega)^p S(\mathbf{q}, \omega) d\omega \tag{4.29}$$

of the dynamic structure factor. In many situations, they can be calculated explicitly through the method of sum rules, which is useful if the dynamic structure factor $S(\mathbf{q}, \omega)$

is characterized by a sharp peak. Moreover, the derivation of sum rules for the density operator can be simplified if the unperturbed configuration is invariant under both parity and time reversal transformations, in which case the following identity holds:

$$S(\mathbf{q}, \omega) = S(-\mathbf{q}, \omega) \ . \tag{4.30}$$

A very relevant sum rule is given by the energy-weighted moment, which can be calculated by combining the completeness relation with Eq. (4.30)

$$m_1(\mathbf{q}) = \hbar^2 \int_{-\infty}^{+\infty} S(\mathbf{q}, \omega) \omega d\omega = \frac{1}{2} \langle [\delta\rho_{\mathbf{q}}^\dagger, [H, \delta\rho_{\mathbf{q}}]] \rangle \ . \tag{4.31}$$

The energy-weighted moment (4.31) determines the high ω behaviour of the response function

$$\lim_{\omega \to \infty} \chi(\mathbf{q}, \omega) = \frac{2}{(\hbar\omega)^2} m_1(\mathbf{q}) \tag{4.32}$$

as one can derive from Eq. (4.22) where the term $1/\omega$ vanishes.

To calculate the double commutator of Eq. (4.31), we observe that, for velocity-independent potentials, only the kinetic energy term contributes to the inner commutator $[H, \delta\rho_{\mathbf{q}}]$, yielding to the double commutator $[\delta\rho_{\mathbf{q}}, [H, \delta\rho_{-\mathbf{q}}]] = N\hbar^2 q^2/m$. Then, one gets the model-independent result

$$m_1(\mathbf{q}) = \hbar^2 \int_{-\infty}^{+\infty} S(\mathbf{q}, \omega) \omega d\omega = N \frac{\hbar^2 q^2}{2m} \ , \tag{4.33}$$

which is called the f-sum rule [Placzek, 1952, Nozières and Pines, 1958]. This is the analogue of the famous dipole Thomas-Reich-Kuhn sum rule for atomic spectra, and it is a very remarkable result. First, it can be applied to a wide class of many-body systems, independent of statistics and temperature. Second, as we shall see later, it can be used, combined with other moments, to calculate the frequency of the collective oscillations. In addition, the f-sum rule is also deeply related to the equation of continuity (3.13). For this reason, the f-sum rule describes also the conservation of the particle number.

Finally, let us discuss the inverse energy-weighted moment

$$m_{-1}(\mathbf{q}) = \int_{-\infty}^{+\infty} S(\mathbf{q}, \omega) \frac{1}{\omega} d\omega \ , \tag{4.34}$$

which is connected to the static response of the system, see Eq. (4.23), and therefore it determines its low frequency limit

$$N\chi(\mathbf{q}) \equiv \chi(\mathbf{q}, 0) = 2m_{-1}(\mathbf{q}) \ , \tag{4.35}$$

where we have used Eq. (4.30). In uniform systems the low-$\mathbf{q}$ limit of the static response can be connected to the thermodynamic isothermal compressibility κ_T. Indeed, the deformations induced by the external force can be expressed as local changes of the pressure, and a straightforward calculation provides the compressibility sum-rule

$$\lim_{\mathbf{q} \to 0} \int_{-\infty}^{+\infty} S(\mathbf{q}, \omega) \frac{1}{\omega} d\omega = \frac{N\kappa_T}{2} = \frac{N}{2mv_T^2} \tag{4.36}$$

where κ_T is expressed in terms of the isothermal velocity v_T: $\kappa_T = 1/(mv_T^2)$.

If one applies the density operator to the fluctuation-dissipation theorem (4.24), one gets

$$NS(\mathbf{q}) = \hbar \int_{-\infty}^{+\infty} d\omega S(\mathbf{q}, \omega) = \frac{\hbar}{2\pi} \int_{-\infty}^{+\infty} d\omega \chi''(\mathbf{q}, \omega) \coth\left(\frac{\beta\hbar\omega}{2}\right) \ . \tag{4.37}$$

For small values of $\mathbf{q}$, the integral (4.37) is given by the classical contribution $|\omega| \ll k_B T$ for which $\coth\left(\frac{\beta \hbar \omega}{2}\right) = \frac{2k_B T}{\hbar \omega}$. By using Eqs. (4.12) and (4.36), one gets the low-$\mathbf{q}$ behaviour of the static structure factor at finite T

$$\lim_{\mathbf{q} \to 0} S(\mathbf{q}) = \frac{k_B T}{m v_T^2} \ . \tag{4.38}$$

For low T, Eq. (4.38) holds for very small ranges of the wave vectors $\mathbf{q}$. In this special case, for some values of $\mathbf{q}$, the integral (4.37) is not exhausted by the classical region $|\omega| \ll k_B T$ and the static structure factor $S(\mathbf{q})$ is sensitive to quantum fluctuations.

4.3 General inequalities

The formalism of the linear response function is really general, so it can be applied to derive some relations of broad validity. In particular, in this Section, we discuss some inequalities which will be useful to describe the collective response of the system after an external perturbation.

At T $= 0$, where the dynamic structure factor vanishes for $\omega < 0$, see Eq. (4.5), one can find rigorous upper bounds for the energy $\hbar \omega_{min}$ of the lowest state excited by the operator F:

$$\hbar \omega_{min} \leq \frac{m_{p+1}(F)}{m_p(F)} \tag{4.39}$$

and

$$\hbar \omega_{min} \leq \sqrt{\frac{m_{p+1}(F)}{m_{p-1}(F)}} \tag{4.40}$$

both holding for any value of p.

Moreover, the moments (4.15) of the excitation operator F satisfy

$$\frac{m_{p+1}(F)}{m_p(F)} \geq \frac{m_p(F)}{m_{p-1}(F)} \ . \tag{4.41}$$

All the previous inequalities become identities only if an unique excited state exhausts the strength of the operator F or if the dynamic structure factor has a delta shape like $S_F(\omega) \propto \delta(\hbar \omega - \hbar \bar{\omega})$. In this situation $\omega_{min} = \bar{\omega}$ and the ratios of the moments on the right-hand side of Eqs. (4.39) and (4.40) coincide with $\hbar \bar{\omega}$ for any value of p.

By choosing the density operator for F, see Sec. 4.2, and by considering Eq. (4.40) with $p = 0$, in the low-momenta limit $q \to 0$ one gets that the lowest excitation frequency vanishes as

$$\omega_{min}(q) \leq v_s q \tag{4.42}$$

where we have introduced the sound velocity $v_s = \sqrt{\kappa^{-1}/m}$, being κ the compressibility.

The above finding has been derived on a very general basis. No hypothesis on the exact nature of the system has been made, except for the validity of the f-sum rule and the fact that the compressibility is finite. With these assumptions, we showed that the excitation spectrum is gapless with the bound (4.42) which becomes an identity if all the moments are exhausted by a single excited state. For example, this is true for both dilute Bose gas and superfluid helium.

In the following, we will briefly discuss how the linear response theory is also of a paramount importance in order to show the occurrence or the absence of the BEC in low dimensions, see Sec. 2.2, both at zero and finite T.

At finite T, from the formalism of the response function, one can derive the Bogoliubov inequality [Bogoliubov, 1962]

$$|\chi_{F^\dagger G}(0)|^2 \leq \chi_F(0)\chi_G(0) \tag{4.43}$$

which contains the static response function, Eq. (4.3) with $\omega = 0$, of two operators F and G with $\chi_F \equiv \chi_{F^\dagger F}$ and $\chi_G \equiv \chi_{G^\dagger G}$.

By combining Eq. (4.43) and Eq. (4.26), one finally finds (see the detailed derivation in Pitaevskii and Stringari [2016]):

$$\langle\{F^\dagger, F\}\rangle \geq 2k_B T \frac{|\langle[F^\dagger, C]\rangle|^2}{\langle[C^\dagger, [H, C]]\rangle} \tag{4.44}$$

where the operator C is defined by means $G = [H, C]$. Eq. (4.44) is called Bogoliubov inequality and provides a rigorous lower bound to the fluctuations of any general operator F in terms of the operator C. It has been used to show the absence of LRO in 2D and 1D systems with continuous symmetry [Mermin and Wagner, 1966, Hohenberg, 1967].

Bogoliubov inequality can be applied in order to study the infrared divergent behaviour exhibited by the particle distribution $n_{\mathbf{p}}$ of a BEC system, for which it becomes [Pitaevskii and Stringari, 2016]:

$$2n_{\mathbf{p}} + 1 \geq m \frac{2k_B T}{p^2} n_0 \tag{4.45}$$

where n_0 is the condensate density. Inequality (4.45) was used by Hohenberg [1967] to rule out the existence of BEC in 2D and 1D, for the $1/p^2$ infrared divergency responsible for the absence of LRO. Moreover, result (4.45) has been derived by assuming that the system is in thermal equilibrium and holds only at finite T for which thermal fluctuations of the phase, taken into account by Eq. (4.44), are present.

On the other hand, at T $= 0$, only quantum fluctuations survive but they are not described by the Bogoliubov inequality (4.44). The effects of quantum fluctuations are properly taken into account by the uncertainty inequality [Pitaevskii and Stringari, 2016]:

$$\langle\{F^\dagger, F\}\rangle \geq \frac{|\langle[F^\dagger, C]\rangle|^2}{\langle\{C^\dagger, C\}\rangle} \tag{4.46}$$

which provides a lower bound for the fluctuations of the general operator F in terms of the operator C. Let us compare the uncertainty inequality (4.46) with the Bogoliubov inequality (4.44): both provide rigorous bounds. Differently from Eq. (4.44), Eq. (4.46) does not depend on T and therefore, it can be also used at T $= 0$.

By considering a BEC as above, one finds that the fluctuations of the phase and those of the density cannot be simultaneously small [Pitaevskii and Stringari, 1991]. Moreover, at T $= 0$, for low momenta $p \to 0$, the particle distribution function $n_{\mathbf{p}}$ diverges as $1/p$:

$$n_{\mathbf{p}} \geq \frac{n_0 m v_s}{2p} , \tag{4.47}$$

where v_s is the sound velocity. This infrared divergency is the result of two-body interactions which make the compressibility of the system finite. The $1/p$ divergency in the momentum distribution of a BEC was firstly investigated by Gavoret and Nozières [1964]. Inequality (4.47) rules out the occurrence of LRO in 1D Bose systems at T $= 0$.

Chapter 5

Hydrodynamic versus collisionless dynamics of a 1D harmonically trapped Bose gas

> I must confess that, at that time, I had absolutely no knowledge of the slowness of the relaxation processes in the ground state, processes which take place in collisions with the wall or with the molecules of a foreign gas.

> Alfred Kastler

Thermalization and relaxation phenomena represent a key issue in 1D systems [Popov, 2001, Giamarchi, 2004] of identical bosons with zero-range repulsive interaction due to the intrinsic integrability [Thacker, 1981, Rigol et al., 2007, Yurovsky et al., 2008, Rigol, 2009] of this many-body system and have been the object of recent experimental and theoretical investigations [Laburthe Tolra et al., 2004, Kinoshita et al., 2006, Hofferberth et al., 2007, 2008, van Amerongen et al., 2008, Mazets et al., 2008, Mazets and Schmiedmayer, 2009, 2010, Tan et al., 2010], see SubSec. 2.3.2. They play an important role not only for the achievement of equilibrium but also for the propagation of collective modes [Mazets, 2011] whose nature, in harmonically trapped configurations, is expected to evolve from the HD regime at low temperature to a collisionless (CL) regime at higher temperature. At low temperature, the applicability of the hydrodynamic description is ensured by the phononic nature of the elementary excitations. Phonons are in fact known to characterise the long wavelength dispersion of the excitation spectrum in one-dimensional interacting Bose gases, see Sec. 2.3 [Lieb and Liniger, 1963, Lieb, 1963] and their description has the same form as the one given by the hydrodynamic theory of superfluids, see Chap. 3 [Menotti and Stringari, 2002, De Rosi and Stringari, 2015]. At high temperature[1], the density profile is provided by the Maxwell-Boltzmann distribution:

$$n_T(z) = n(0)e^{-z^2/Z_T^2}, \tag{5.1}$$

where the peak density is fixed by the normalization condition $n(0) = N/(\sqrt{\pi}Z_T)$ and the thermal radius Z_T characterizes the width of the Gaussian $Z_T = \sqrt{2k_BT/(m\omega_z^2)}$ and it contains most of atoms in the trap at finite T. Eq. (5.1) decays exponentially due to the

---

[1] High temperature regime implies that the thermal energy is much higher than the degeneracy energy $E_{deg} \sim \hbar^2 n^2/m$: $k_BT \gg E_{deg}$. On the other hand, the temperature should not be too high in order to ensure the 1D condition: $k_BT \ll \hbar\omega_\perp$, where $\omega_\perp$ is the radial trapping frequency.

presence of the trap. Therefore, the collisional rate $\Gamma = n\sigma v_{th}$, with $v_{th} \sim \sqrt{T}$ the thermal velocity and σ the s-wave cross-section, decreases as $\sim \sigma/T$ at high T, collisions become rare and the system enters the collisionless regime described by the ideal gas model [2]. One then expects a transition between the HD and the CL regime which could provide valuable information on the collisional effects in 1D configurations.

So far most of the attention in the collective features of 1D harmonically trapped Bose gases has concerned the lowest breathing (LB) mode. The frequency of this mode was calculated at T = 0 within the Lieb-Liniger model using a sum-rule approach [Menotti and Stringari, 2002], exploring the transition from the weakly interacting BG gas to the TG limit of strongly repulsive bosons [Tonks, 1936, Girardeau, 1960]. The experimental results of Haller et al. [2009] have confirmed with good accuracy the predictions of the theory. Recent studies of this mode have also focused on the so-called STG regime of hard rods [Astrakharchik, 2005, Haller et al., 2009] and on the regime of small number of particles (or small coupling constant g_{1D}) where the LDA, usually employed to calculate the density profiles using the equation of state of uniform matter, is not applicable [Gudyma et al., 2015, Gudyma, 2015, Chen et al., 2015]. The temperature dependence of the frequency of the lowest breathing mode has also been the object of recent theoretical [Hu et al., 2014, Chen et al., 2015] and experimental [Moritz et al., 2003, Fang et al., 2014] work. The theoretical predictions are usually based on a hydrodynamic description where the relevant thermodynamic quantities are calculated using the Yang-Yang theory [Yang and Yang, 1969, Yang, 1970], which generalises the Lieb-Liniger theory [Lieb and Liniger, 1963, Lieb, 1963] of interacting 1D bosons to finite temperature. A characteristic feature of the hydrodynamic theory applied to the lowest breathing mode is that, at high temperatures, it predicts [Hu et al., 2014, Fang et al., 2014, De Rosi and Stringari, 2015] the same frequency $\omega = 2\omega_z$ as given by the non-interacting gas model, see Table 5.1. This rules out the possibility of a simple identification of the hydrodynamic versus (VS) the collisionless nature of the oscillation.

In this Chapter, we exploit the different behaviour exhibited by the dipole compressional (DC) mode, identified as the lowest compression mode with the same parity as the centre-of-mass (dipole) mode. Differently from the centre-of-mass mode, which oscillates with the model independent frequency $\omega = \omega_z$, the dipole compression mode is sensitive to the equation of state and, differently from the lowest breathing mode, is characterized by a different excitation spectrum at high temperatures, when investigated in the hydrodynamic or in the collisionless regimes, see Table 5.2. This mode, whose frequency has been already measured at low temperature in elongated configurations in the case of the unitary Fermi gas [Tey et al., 2013], is consequently a natural candidate to exploit the effects of relaxation caused by collisions and the corresponding thermalization effects in 1D configurations. Numerical calculations for the DC frequencies at zero and finite temperature in the hydrodynamic framework have been carried out by Hu et al. [2014].

In the following, we will use the Lieb-Liniger Hamiltonian [Kheruntsyan et al., 2005]

$$H = H_{kin} + H_{int} + H_{trap} = -\frac{\hbar^2}{2m} \sum_{i=1}^{N} \frac{\partial^2}{\partial z_i^2} + g_{1D} \sum_{i>j}^{N} \delta(z_{ij}) + \sum_{i=1}^{N} V_{ext}(z_i) , \qquad (5.2)$$

describing a gas of 1D interacting Bose particles in the presence of the harmonic potential $V_{ext}(z) = m\omega_z^2 z^2/2$. Here $z_{ij} \equiv z_i - z_j$ is the relative coordinate and g_{1D} is the relevant 1D coupling constant. In the presence of radial harmonic trapping and in the absence of confinement induced resonance [Olshanii, 1998, Petrov et al., 2000b], the interaction parameter g_{1D} can be written as $g_{1D} = 2\hbar^2 a/ma_\perp^2$ where a is the three-dimensional scattering length and $a_\perp$ is the radial oscillator length, see Sec. 2.3.

[2]The opposite situation happens in uniform configurations: since the density is constant in space, the collisional rate increases with T.

The original results presented in this Chapter have been published in the paper De Rosi and Stringari [2016]. This Chapter is organised as follows.

In Sec. 5.1 we summarise the basic results of the hydrodynamic theory of 1D gases confined by a harmonic potential. This theory allows for analytic results for the collective frequencies if the equation of state exhibits a polytropic dependence on the density [De Rosi and Stringari, 2015]. Furthermore, it can be conveniently formulated using a variational procedure allowing for an easy determination of the collective frequencies in the intermediate regimes of temperature and interaction.

In Sec. 5.2 we formulate a sum rule approach to describe the frequency of the collective oscillations in the presence of harmonic trapping. This approach provides a useful insight on the physical features of the collective oscillations, both at zero and finite temperature. In this Section we also provide a valuable derivation of the 1D virial theorem, holding in all regimes of temperature and interaction. An extension of the virial theorem, which turns out to be useful for the study of the dipole compression mode, is also presented.

In Sec. 5.3 we discuss the dipole compression frequency and point out the different behaviour exhibited in the hydrodynamic and in the collisionless regime of high temperature. In particular, in the latter case, this mode exhibits a characteristic beating effect involving two different frequencies which are expected to be of easy experimental identification.

In Sec. 5.4 we investigate some important issues for the experimental measurement of our theoretical predictions of Sec. 5.3.

5.1 Variational formulation of the hydrodynamic theory for an harmonically trapped 1D Bose gas

In this Section, we introduce the variational formulation of the HD approach, which provides the same results for the breathing mode frequencies, already derived in Sec. 3.7.

We consider the 1D version

$$m(\omega^2 - \omega_z^2)nv + \frac{\partial}{\partial z}\left[n\left(\frac{\partial P}{\partial n}\right)_{\bar{s}}\frac{\partial v}{\partial z}\right] = 0 \qquad (5.3)$$

of the linearized hydrodynamic equation [Griffin et al., 1997, Taylor et al., 2009, De Rosi and Stringari, 2015] for the velocity field $v(z)$, where $(\partial P/\partial n)_{\bar{s}}$ is the adiabatic compressibility ($\bar{s}$ being the entropy per particle) evaluated at the local value of the 1D equilibrium density profile $n \equiv n(z)$ whose z-dependence, caused by the external potentials $V_{ext}(z)$, can be determined in the Local Density Approximation (A.1), through the solution of the equilibrium ($v = 0$) Euler equation, see Eq. (3.15)

$$\left(\frac{\partial P(z)}{\partial n}\right)_T \frac{\partial n(z)}{\partial z} + n(z)\frac{\partial V_{ext}(z)}{\partial z} = 0 \; , \qquad (5.4)$$

for a fixed value of the temperature of the gas.

The above equations show that the eigenfrequencies ω of the collective oscillations are determined once the adiabatic and the isothermal $(\partial P/\partial n)_T$ compressibilities, calculated at the local value $n(z)$ of the density, are known. These quantities depend on the interaction and on the temperature of the gas.

In the uniform case ($V_{ext} = 0$) Eq. (5.3) admits a plane wave solution $v \propto e^{iqz}$ yielding the phonon dispersion relation $\omega = v_s q$, where $v_s = \sqrt{(\partial P/\partial n)_{\bar{s}}/m}$ is the adiabatic sound velocity.

It is worth noticing that, since in 1D there is no superfluid phase transition, see Sub-Sec. 2.2.2 [Mermin and Wagner, 1966, Hohenberg, 1967], Eq. (5.3) can be applied to all temperatures provided the dynamic behaviour of the gas is correctly described by the

hydrodynamic theory. This represents an important difference with respect to 2D and 3D systems where hydrodynamic theory, for temperatures below the critical value, should be generalised to the Landau theory of two fluids, see Sec. 3.3 [Pitaevskii and Stringari, 2016].

It is immediate to show that Eq. (5.3) can be derived [Hou et al., 2013b] from the variational approach $\delta\omega^2/\delta v = 0$ (and small velocity variation $\delta v \ll 1$) with [3]

$$\omega^2 = \omega_z^2 + \frac{\int dz n \left(\frac{\partial P}{\partial n}\right)_{\bar{s}} \left(\frac{\partial v}{\partial z}\right)^2}{\int dz m n v^2} \ , \tag{5.5}$$

first developed in 3D systems [Taylor and Griffin, 2005, Taylor et al., 2008, 2009]. The advantage of using the variational approach, Eq. (5.5), rather than the differential hydrodynamic equation, Eq. (5.3), is that one can easily estimate the collective frequencies, at zero as well as at finite temperature, with a suitable ansatz for the velocity field. This method has been recently implemented by Hu et al. [2014].

In addition to the universal dipole result $\omega(D) = \omega_z$ for the centre-of-mass oscillation (Kohn mode), corresponding to the choice $v = const$, useful expressions for the frequencies of the relevant collective modes concern the lowest breathing mode

$$\omega_{HD}^2(LB) = \omega_z^2 + \frac{\int dz n \left(\frac{\partial P}{\partial n}\right)_{\bar{s}}}{\int dz m n z^2} \ , \tag{5.6}$$

corresponding to the ansatz $v = z$, and the dipole compression mode

$$\omega_{HD}^2(DC) = \omega_z^2 + \frac{\int dz n \left(\frac{\partial P}{\partial n}\right)_{\bar{s}} 4z^2}{\int dz m n (z^2 - \langle z^2 \rangle)^2} \ , \tag{5.7}$$

corresponding to the ansatz $v = z^2 - \langle z^2 \rangle$ where $\langle z^2 \rangle$ is the average value of z^2 calculated at equilibrium. The term $\langle z^2 \rangle$ ensures the orthogonality between the dipole compression mode and the centre-of-mass oscillation. This is easily proven by noticing that the density variations $\delta n(z) = \partial_z[vn]$, derived from Eq. (3.13), associated with the DC mode give rise to a vanishing dipole moment: $\int dz z \delta n(z) = 0$ [4].

Predictions (5.6) and (5.7) for the lowest breathing and the dipole compression modes are expected to provide an accurate approximation to the exact solutions of the hydrodynamic equation (5.3) in all regimes of interaction and temperature. This is the consequence of the fact that the corresponding ansatz for the velocity field coincides with the exact solution of the hydrodynamic equation in important asymptotic regimes, where the equation of state exhibits a polytropic dependence on the density [De Rosi and Stringari, 2015], like the T = 0 weakly interacting limit, the T = 0 Tonks-Girardeau limit as well as in the classical regime of high temperatures [De Rosi and Stringari, 2015]. One then expects that the same ansatz for v will be accurate also in the intermediate regimes of interaction and temperature. Such accuracy was recently proven numerically by Hu et al. [2014]. The values of the hydrodynamic frequencies calculated in the above three asymptotic regimes [De Rosi and Stringari, 2015] are reported in Table 5.1 for the lowest breathing mode and in Table 5.2 for the dipole compressional mode, see also Sec. 3.7 and Appendix C for the detailed calculation. Finally, we notice that the LB HD frequencies of Table 5.1 were obtained also by Bouchoule et al. [2016] using scaling arguments starting from the HD equations.

---

[3]By applying the variational procedure to Eq. (5.5) and by using Eq. (5.4) and the definition of the adiabatic coefficient (3.17), one can find the hydrodynamic equation (3.16), which is completely equivalent to Eq. (5.3).

[4]Since the DC mode has the same parity of the centre-of-mass mode, the velocity ansatz can be chosen as $v(z) = \alpha_2 z^2 + \alpha_0$. By imposing the vanishing dipole moment condition, one finally finds $\alpha_0 = -\alpha_2 \langle z^2 \rangle$, for which the DC ansatz does not excite the centre-of-mass oscillation.

Table 5.1: Hydrodynamic VS collisionless frequencies of the lowest breathing mode (LB) for a 1D Bose gas. From De Rosi and Stringari [2016]. Copyright © 2016, American Physical Society.

	Hydrodynamic		Collisionless
	T = 0	**high T**	**Collisionless**
1D weakly interact. (BG)	$\sqrt{3}\omega_z$	$2\omega_z$	$2\omega_z$
1D Tonks-Girardeau	$2\omega_z$	$2\omega_z$	$2\omega_z$

5.2 Sum rules and collective oscillations

In this Section, we apply the sum-rule approach to calculate the collective frequencies of the centre-of-mass (SubSec. 5.2.1), the lowest breathing (SubSec. 5.2.2) and the dipole compression (SubSec. 5.2.3) modes.

As discussed in Chap. 4, sum rules represent a powerful tool to describe the collective behaviour exhibited by quantum many-body systems [Lipparini and Stringari, 1989, Stringari, 1996, Pitaevskii and Stringari, 2016], perturbed by an external excitation with low momentum transfer. Their main merit is that, in many cases, they provide accurate predictions for the collective frequencies avoiding the full solution of the quantum many-body problem. Furthermore, being based on the algebra of commutators, see Appendix D, they emphasize the symmetry properties of the problem and the role of conservation rules. In general sum rules provide compact expressions for the p-moments

$$m_p(F) = \hbar \int_{-\infty}^{+\infty} (\hbar\omega)^p S_F(\omega) d\omega \qquad (5.8)$$

of the dynamic structure factor

$$S_F(\omega) = Q^{-1} \sum_{n,m=1}^{N} e^{-\beta E_m} |\langle m| F |n\rangle|^2 \delta(\hbar\omega - \hbar\omega_{nm}) , \qquad (5.9)$$

where $F = \sum_{k=1}^{N} f(z_k)$ is the relevant excitation operator, $Q = \sum_{m=1}^{N} \exp[-\beta E_m]$ is the partition function and $\omega_{nm} = (E_n - E_m)/\hbar$ are the Bohr transition frequencies, relative to the Hamiltonian, Eq. (5.2).

An important sum rule, widely employed in many-body calculations, concerns the inverse-energy weighted moment m_{-1} of the dynamic structure factor. This moment is directly related to the static response $\chi(F)$ defined in terms of the fluctuation $\delta\langle F \rangle = \lambda\chi(F)$, induced by an external static perturbation of the form $H_{pert} = -\lambda F$ applied to the

Table 5.2: Hydrodynamic VS collisionless frequencies of the dipole compressional mode (DC) for a 1D Bose gas. From De Rosi and Stringari [2016]. Copyright © 2016, American Physical Society.

	Hydrodynamic		Collisionless
	T = 0	**high T**	**Collisionless**
1D weakly interact. (BG)	$\sqrt{6}\omega_z$	$\sqrt{7}\omega_z$	$3\omega_z$ & $1\omega_z$
1D Tonks-Girardeau	$3\omega_z$	$\sqrt{7}\omega_z$	$3\omega_z$ & $1\omega_z$

system, according to the relationship [Pitaevskii and Stringari, 2016] $\chi(F) = 2m_{-1}(F)$. The calculation of m_{-1} for the classical gas is reported in Appendix E.

The m_{-1} sum rule can be combined with the energy weighted sum rule, which in general can be reduced in the form of a double commutator involving the Hamiltonian H and the excitation operator F, yielding the simple result

$$m_1(F) = \frac{1}{2}\langle[F,[H,F]]\rangle = \frac{\hbar^2}{2m}N\langle|\nabla_z f(z)|^2\rangle \ , \tag{5.10}$$

to provide an estimate of the collective frequency through the ratio

$$\hbar^2 \omega_{1,-1}^2 = \frac{m_1}{m_{-1}} \ . \tag{5.11}$$

The cubic energy weighted moment can be written in the form of a double commutator involving the Hamiltonian H and the commutator $[H, F]$:

$$m_3(F) = \frac{1}{2}\langle[[F,H],[H,[H,F]]]\rangle \ . \tag{5.12}$$

It can be combined with the energy weighted moment (5.10), in order to calculate the collective frequency

$$\hbar^2 \omega_{3,1}^2 = \frac{m_3}{m_1} \ . \tag{5.13}$$

Both the ratios (5.11) and (5.13) are given by an equality and not an upper bound, since the dynamic structure factor (5.9) has a delta structure, see Sec. 4.3.

In the presence of harmonic trapping, the choice for the excitation operator depends on the nature of the collective mode. In the following Subsections, we will calculate the collective frequencies of some modes.

5.2.1 Centre-of-mass mode

For the simplest case of the centre-of-mass (dipole) mode, we choose the excitation operator $F_D = \sum_{k=1}^{N} z_k$ [5]. We remind that its frequency is always equal to that of the trap $\omega(D) = \omega_z$.

The inverse energy weighted moment m_{-1} can be calculated from Eq. (E.4):

$$m_{-1} = \frac{N}{2m\omega_z^2} \tag{5.14}$$

which turns to be independent on T and so holding for all temperature regimes.

Moreover, the energy weighted moment m_1 is estimated from Eq. (5.10):

$$m_1 = \frac{N\hbar^2}{2m} \ . \tag{5.15}$$

By combining Eq. (5.14) and Eq. (5.15) in Eq. (5.11), one gets the trapping frequency.

From Eq. (5.12), one calculates the cubic energy weighted moment:

$$m_3 = \frac{\hbar^4 \omega_z^2 N}{2m} \tag{5.16}$$

and from the ratio (5.13) one finds again the frequency ω_z.

The model independence of the dipole mode is well reflected by the fact that Eqs. (5.14), (5.15) and (5.16) are independent on T and on the gas regime.

The most interesting cases of LB and DC modes will be discussed in the following Subsections.

---

[5]The excitation operator $F = \sum_{k=1}^{N} f(z_k)$ is related to the velocity field v, defined in Sec. 5.1, by $v(z) \propto \nabla_z f(z)$.

5.2.2 Lowest breathing mode

For the lowest breathing mode the natural choice is provided by the operator $F_{LB} = \sum_{k=1}^{N}(z_k^2 - \langle z^2 \rangle)$ which ensures the condition $\langle F_{LB} \rangle = 0$ at equilibrium. In this case the inverse energy weighted moment can be easily calculated since the static perturbation $-\lambda F_{LB}$ consists of a simple renormalization of the harmonic trapping frequency. One then finds the following result [Menotti and Stringari, 2002, Pitaevskii and Stringari, 2016]:

$$m_{-1}(LB) = -\frac{N}{m}\frac{\partial \langle z^2 \rangle}{\partial \omega_z^2} \ , \tag{5.17}$$

for the inverse energy weighted moment. On the other hand, the energy weighted moment (5.10), relative to the same excitation operator, yields the result

$$m_1(LB) = \frac{2N\hbar^2}{m}\langle z^2 \rangle \ , \tag{5.18}$$

so that the ratio between the two sum rules provides the expression

$$\omega_{1,-1}^2(LB) = -2\frac{\langle z^2 \rangle}{\partial \langle z^2 \rangle / \partial \omega_z^2} \tag{5.19}$$

for the squared collective frequency.

Result (5.19) was successfully employed to evaluate the LB frequency in 1D Bose gases at zero temperature [Menotti and Stringari, 2002]. In particular, by using the Local Density Approximation to evaluate the ω_z-dependence of the average square radius, this equation accounts for the transition of the collective frequency from the value $\sqrt{3}\omega_z$ holding in the weakly interacting Bose gas to the value $2\omega_z$ holding in the Tonks-Girardeau limit, see Table 5.1 [6]. Since Eq. (5.19) does not assume the Local Density Approximation, it can be also used to estimate the collective frequencies when the coupling constant g_{1D} or the number of atoms are small [Gudyma et al., 2015, Gudyma, 2015], a relevant situation in experiments where one usually works with arrays of 1D tubes, each of them containing $N \sim 25$ atoms, see Sec. 2.1.

One should however notice that result (5.19) is not adequate to describe the frequency of the LB mode at finite temperature. This is best understood in the classical limit of high temperatures where Eq. (5.19) provides the result $\sqrt{2}\omega_z$ for the collective frequency to be compared with the exact value $2\omega_z$ holding in the classical limit where the Hamiltonian of the system reduces to the ideal gas value (see Table 5.1) [7]. The discrepancy between the two values is due to the fact that, at finite temperature, the operator F_{LB} excites zero-frequency modes which provide a finite contribution to the inverse energy weighted moment sum rule.

---

[6]For the BG regime, one must to take into account the profile (C.3), from which one calculates:

$$\begin{cases} \langle z^2 \rangle_{\text{BG}} = \frac{3^{5/3}}{15}\left(\frac{g_{1D}N}{2m\omega_z^2}\right)^{2/3} \\ \frac{\partial \langle z^2 \rangle_{\text{BG}}}{\partial \omega_z^2} = -\frac{2}{3}\frac{\langle z^2 \rangle_{\text{BG}}}{\omega_z^2} \ . \end{cases} \tag{5.20}$$

For the TG regime, the density profile is (C.4), from which one finds

$$\begin{cases} \langle z^2 \rangle_{\text{TG}} = \frac{\hbar N}{2m\omega_z} \\ \frac{\partial \langle z^2 \rangle_{\text{TG}}}{\partial \omega_z^2} = -\frac{\langle z^2 \rangle_{\text{TG}}}{2\omega_z^2} \ . \end{cases} \tag{5.21}$$

[7]For the classical gas at high T, one must to take into account the Maxwell-Boltzmann distribution (5.1), from which one derives

$$\begin{cases} \langle z^2 \rangle_T = \frac{k_B T}{m\omega_z^2} \\ \frac{\partial \langle z^2 \rangle_T}{\partial \omega_z^2} = -\frac{\langle z^2 \rangle_T}{\omega_z^2} \ . \end{cases} \tag{5.22}$$

A similar situation takes place in uniform matter, where a natural choice for the excitation operator is $F = \rho(q) = \sum_{k=1}^{N} e^{iqz}$, see Eq. (4.27). Eq. (5.11) yields, for small wavevectors q, the result $\omega_{1,-1}(q) = v_T q$ with $mv_T^2 = (\partial P/\partial n)_T$, see Eq. (4.42), related to the *isothermal* sound velocity v_T. In this case, we have used the well-known result for the model-independent f-sum rule for m_1, Eq. (4.33), and for the compressibility sum rule, Eq. (4.36) [Pines and Nozières, 1999, Pitaevskii and Stringari, 2016]:

$$m_{-1}(q)_{q\to 0} = \frac{N}{2}\left(\frac{\partial n}{\partial P}\right)_T \, , \qquad (5.23)$$

for the inverse-energy weighted sum-rule which is fixed, at small wavevector q, by the *isothermal* compressibility of the system. At zero temperature Eq. (5.11) provides the exact result for the sound velocity in interacting Bose systems, being the isothermal and the adiabatic compressibilities equal. The situation is different at high temperature, where the propagation of sound is provided, in the collisional regime, by the adiabatic rather than by the isothermal compressibility. The inadequacy of the ratio (5.11) in providing the correct value of the sound velocity at finite temperature is due to the existence of a diffusive (zero-sound) mode, located at very low excitation energies, which provides a crucial contribution to the inverse energy weighted sum rule [Pines and Nozières, 1999]. The drawback of the inverse energy weighted sum rule in providing the propagation of sound at finite temperature is not peculiar of uniform systems, but it also shows up in the study of the collective excitations in the presence of harmonic trapping, as we have observed above.

The correct value of the collective frequency at finite temperature is recovered if, instead of calculating the inverse energy weighted sum rule, one evaluates the cubic energy weighted sum rule $m_3(F)$, Eq. (5.12). Differently from $m_{-1}(F)$, the cubic energy weighted moment is not sensitive to the zero frequency modes excited by the operator F at high temperature. Evaluation of the triple commutator (5.12) with the Lieb-Liniger Hamiltonian (5.2) yields the following result for the m_3 sum rule relative to the excitation operator $F_{LB} = \sum_{k=1}^{N}(z_k^2 - \langle z^2 \rangle)$:

$$m_3(LB) = \frac{2\hbar^4}{m^2}\left(4\langle H_{kin}\rangle + 4\langle H_{trap}\rangle + \langle H_{int}\rangle\right) \, . \qquad (5.24)$$

A useful simplification of Eq. (5.24) is provided by the virial theorem [Stringari, 1996, Gudyma, 2015, Pitaevskii and Stringari, 2016], which can be derived by imposing the general condition $\langle [H, G] \rangle = 0$ holding at equilibrium for any choice of the operator G. By making the choice of the hermitian operator $G = \sum_{k=1}^{N}(z_k p_{z,k} + p_{z,k} z_k)$ corresponding to an unitary scaling deformation of the many-body wave function, one derives the exact relationship, see Appendix G:

$$2\langle H_{kin}\rangle - 2\langle H_{trap}\rangle + \langle H_{int}\rangle = 0 \, . \qquad (5.25)$$

Thanks to the virial theorem (5.25) the cubic energy weighted sum rule (5.24) can be further simplified and, combined with the energy weighted sum rule (5.18), yields the following expression for the LB collective frequency [Gudyma, 2015]

$$\hbar^2\omega_{3,1}^2(LB) = \frac{m_3(LB)}{m_1(LB)} = \hbar^2\omega_z^2\left(4 - \frac{\langle H_{int}\rangle}{2\langle H_{trap}\rangle}\right) \, , \qquad (5.26)$$

or, equivalently [Gudyma, 2015],

$$\omega_{3,1}^2(LB) = \omega_z^2\left(3 + \frac{\langle H_{kin}\rangle}{\langle H_{trap}\rangle}\right) \, , \qquad (5.27)$$

holding also beyond LDA. Eq. (5.26) explicitly shows that, if the average value of the interaction energy is negligible, as happens in the TG regime and in the collisionless regime of high temperatures, one recovers the correct value $2\omega_z$ for the lowest compression mode (see Table 5.1). In the case of the weakly interacting Bose gas one can neglect, at $T = 0$, the kinetic energy term and Eq. (5.27) correctly reproduces the hydrodynamic value $\sqrt{3}\omega_z$. In conclusion, one expects that the sum rule result m_3/m_1 will provide an excellent estimate of the frequency of the lowest compression mode in all ranges of temperature, interaction and number of particles. At $T = 0$ it is expected to provide results of similar accuracy as prediction (5.19) based on the ratio between the energy weighted and the inverse energy weighted sum rule. The expression (5.26) for the LB collective frequency was already considered by Fang et al. [2014] to analyse their experimental data at finite temperature.

A further interesting expression for the $\omega_{3,1}^2$ ratio can be obtained by using the Hellmann-Feynman expression $\langle H_{int} \rangle = g_{1D}\partial F/\partial g_{1D}$ for the interaction energy, where F is the free energy of the system [8]. In this way Eq. (5.26) takes the form

$$\omega_{3,1}^2(LB) = \omega_z^2 \left[4 + \frac{\hbar^2 \mathcal{C} a_{1D}}{2m\langle H_{trap} \rangle} \right] \tag{5.28}$$

where we have introduced the 1D Tan's contact parameter $\mathcal{C} = (m/\hbar^2)\partial F/\partial a_{1D}$ with $a_{1D} = -2\hbar^2/mg_{1D}$ the 1D scattering length. The same result can be obtained by using the Tan's contact 1D virial theorem (see, for example, Valiente [2012]):

$$E = \frac{\beta + 2}{2}\langle H_{\text{trap}} \rangle - \frac{\hbar^2 \mathcal{C}}{2m} a_{1D} \tag{5.29}$$

where $H_{trap} \propto z^\beta$ and E is the total energy of the system. By combining Eq. (5.29) with $\beta = 2$ and Eq. (5.25), one gets

$$\langle H_{\text{trap}} \rangle - \langle H_{\text{kin}} \rangle = -\frac{\hbar^2 \mathcal{C} a_{1D}}{2m} , \tag{5.30}$$

which used with Eq. (5.27) provides the relation (5.28).

The Tan's contact [Tan, 2008] characterizes the large momentum tail of the momentum distribution. In its more general definition, it is expressed as:

$$\mathcal{C} = \Omega \lim_{|\mathbf{k}| \to \infty} k^4 n_\sigma(\mathbf{k}) \tag{5.31}$$

where $\Omega = L^D$ is the volume, D is the dimension and σ is the spin component. Eq. (5.31) is defined for both bosonic and fermionic systems with zero-range interactions in any dimension [Olshanii and Dunjko, 2003, Combescot et al., 2009, Werner and Castin, 2010, Valiente et al., 2011, Barth and Zwerger, 2011]. In 1D, the contact $\mathcal{C}$ can be also expressed in terms of the pair short-distance correlation function [Olshanii and Dunjko, 2003, Gangardt and Shlyapnikov, 2003].

---

[8]The Hellmann-Feynman theorem enables to calculate the derivative of the eigenvalue E_λ with respect to a continuous parameter λ:

$$\frac{dE_\lambda}{d\lambda} = \int dV \psi_\lambda^* \frac{dH_\lambda}{d\lambda} \psi_\lambda$$

where H_λ is the Hamiltonian and ψ_λ the eigenfunction of H_λ both depending on λ and dV represents the integration over the domain of the wavefunction. By considering the finite T, one introduces the free energy $F = E - TS$ and the above expression becomes:

$$\frac{dF}{dg_{1D}} = \int_{-\infty}^{+\infty} dz \frac{dH_{\text{int}}}{dg_{1D}} n_T(z) = \frac{d\langle H_{\text{int}} \rangle}{dg_{1D}}$$

where we have considered the interaction energy of the Hamiltonian (5.2) and the Maxwell-Boltzmann distribution (5.1), independent on the coupling constant g_{1D}.

Result (5.28) relates the frequency of the lowest compression mode, fixed with high accuracy by the ratio $\omega^2_{3,1}(LB)$, to independently measurable quantities, like the contact and the trapping energy. Thus, from Eqs. (5.29) and (5.30), one can calculate also the kinetic and the interaction energies.

5.2.3 Dipole compression mode

A similar analysis can be worked out for the dipole compression mode excited by the operator $F_{DC} = \sum^N_{k=1} f_{DC}(z_k)$ with $f_{DC}(z) = z^3/3 - z\langle z^2\rangle$. The choice ensures that the operator F_{DC} will not excite the centre-of-mass (dipole) oscillation, thanks to the presence of the term $z\langle z^2\rangle$. This can be easily shown by checking that the crossed energy weighted sum rule $\langle[F_D,[H,F_{DC}]]\rangle$, with $F_D = \sum^N_{k=1} z_k$, identically vanishes [9].

In the case of the DC mode the static response, and hence the inverse energy weighted sum rule, can be easily calculated only in the LDA (A.1) where, in the presence of the external perturbation $-\lambda F_{DC}$, the chemical potential is modified according to $\mu \to \mu - \lambda f_{DC}(z)$ and the density profile is, accordingly, modified as $n(z) \to n(z) + \lambda f_{DC}(z)(\partial n/\partial\mu)_T$. The inverse energy weighted sum rule relative to the DC mode then takes the useful form [10] (see Appendix H for the detailed calculation)

$$m_{-1}(DC) = \frac{1}{2}\int dz \left(\frac{z^3}{3} - z\langle z^2\rangle\right)^2 \left(\frac{\partial n}{\partial\mu}\right)_T . \qquad (5.32)$$

Using Eq. (5.10), the energy weighted moment is also easily evaluated and takes the form:

$$m_1(DC) = \frac{\hbar^2 N}{2m}(\langle z^4\rangle - \langle z^2\rangle^2) . \qquad (5.33)$$

It is straightforward to verify that, at $T = 0$, the ratio m_1/m_{-1} provides the correct (squared) hydrodynamic frequencies both in the weakly interacting Bose gas ($\sqrt{6}\omega_z$), where $\partial\mu/\partial n = g_{1D}$, Eq. (A.15), and in the Tonks-Girardeau limit ($3\omega_z$), where $\partial\mu/\partial n = \hbar^2\pi^2 n/m$, Eq. (A.18). At high temperatures, where $\partial\mu/\partial n_{|T} = \partial P/\partial n_{|T}/n = k_B T/n$, one instead finds that the frequency $\omega_{1,-1}$ takes the value $\sqrt{3}\omega_z$ which is smaller than the hydrodynamic value $\sqrt{7}\omega_z$, similarly to the case of the LB mode discussed above, see Appendix I. This result is the consequence of the fact that the DC operator F_{DC} excites, at high temperature, two modes with frequency equal to ω_z and $3\omega_z$, respectively. The corresponding strengths σ_1 and σ_3 characterizing the dynamic structure factor $S_F(\omega)$ can be easily evaluated through the identification of the weighted combination of the two excited frequencies [11] with the calculated result $\sqrt{3}\omega_z$:

$$\omega^2_{1,-1}(DC) = \frac{\sigma_1\omega_z + \sigma_3 3\omega_z}{\sigma_1/\omega_z + \sigma_3/(3\omega_z)} = 3\omega^2_z , \qquad (5.35)$$

---

[9] $[H,F_{DC}] = \frac{i\hbar}{m}\sum^N_{i=1}\left[\left(\langle z^2\rangle - z^2_i\right)p_i + i\hbar z_i\right]$.

[10] The same procedure, applied to the lowest breathing mode, should take into account a further position independent correction $\delta\mu = -\int dz f(z)(\partial n/\partial\mu)_T / \int dz(\partial n/\partial\mu)_T$, which is required to ensure the particle number conservation $\int dz\delta n = 0$. This yields the general expression

$$m_{-1} = \frac{1}{2}\int dz f(z)\left[f(z) + \delta\mu\right]\left(\frac{\partial n}{\partial\mu}\right)_T ,$$

for the inverse energy weighted sum rule holding, in the LDA, for any choice of $f(z)$, see Appendix H.

[11] The sum-rules can be expressed as weighted combinations by combining Eq. (5.8) and Eq. (5.9):

$$\begin{cases} m_1 = \sum_{i=1,3}\sigma_i E_i \\ m_3 = \sum_{i=1,3}\sigma_i E^3_i \\ m_{-1} = \sum_{i=1,3}\frac{\sigma_i}{E_i} \end{cases} \qquad (5.34)$$

where σ_i are the strengths relative to the excitation energy $E_i = \hbar\omega_i$. In our case, the excited frequencies are just two: ω_z and $3\omega_z$.

---

yielding the relationship $\sigma_1 = \sigma_3$. The above result for the strengths σ_1 and σ_3 permits to predict, in the same regime of high temperature, the value of the ratio between the cubic and the energy weighted moments. Indeed, by expressing the sum-rules as combinations of the two frequencies ω_z and $3\omega_z$:

$$\omega_{3,1}^2(DC) = \frac{\sigma_1\omega_z^3 + \sigma_3(3\omega_z)^3}{\sigma_1\omega_z + \sigma_3 3\omega_z} = 7\omega_z^2 \ , \tag{5.36}$$

we find the correct hydrodynamic frequency at high T, $\sqrt{7}\omega_z$.

As in the case of the LB mode also for the dipole compression mode the cubic energy weighted sum rule can be calculated on a general basis in all regimes of temperature by carrying out explicitly the algebra of commutators. We find the result (see Appendix I):

$$m_3(DC) = \frac{\hbar^4 N}{m^2}[g_{1D}\langle z^2\rangle\langle\delta(z_{ij})\rangle + g_{1D}\langle Z_{ij}^2\delta(z_{ij})\rangle - $$
$$ - \frac{3}{2}m\omega_z^2\langle z^2\rangle^2 + \frac{1}{m}\langle z^2\rangle\langle p_z^2\rangle + \frac{3}{m}\langle p_z z^2 p_z\rangle + \frac{3}{2}m\omega_z^2\langle z^4\rangle - \frac{\hbar^2}{m}] \ , \tag{5.37}$$

where $Z_{ij} = (z_i + z_j)/2$ is the centre-of-mass coordinate and we have defined the intensive quantities $\langle\delta(z_{ij})\rangle \equiv \langle\sum_{i>j}^N \delta(z_{ij})\rangle/N$ and $\langle Z_{ij}^2\delta(z_{ij})\rangle \equiv \langle\sum_{i>j}^N Z_{ij}^2\delta(z_{ij})\rangle/N$. Eq. (5.37) holds also for a small number of particles N because its derivation does not imply the validity of the LDA. Similarly to the case of the LB mode discussed above, also for the DC mode one can obtain a useful relationship among the various contributions entering (5.37) with the help of a generalized virial theorem derivable by imposing the condition $\langle[H,G]\rangle = 0$, with the choice $G = \sum_{k=1}^N \left(z_k^3 p_{z,k} + p_{z,k} z_k^3\right)$, see Appendix G. This yields the relationship:

$$\frac{6}{m}\langle p_z z^2 p_z\rangle + 6g_{1D}\langle\delta(z_{ij})Z_{ij}^2\rangle - 2m\omega_z^2\langle z^4\rangle - \frac{3\hbar^2}{m} = 0 \ . \tag{5.38}$$

It is easy to verify that the ratio m_3/m_1 provides the correct square excitation energy in some relevant limits at zero temperature. These include the weakly interacting Bogoliubov gas, where the kinetic energy contribution to (5.25), (5.37) and (5.38) vanishes and the DC excitation frequency takes the T = 0 hydrodynamic value $\sqrt{6}\omega_z$, and in the Tonks-Girardeau limit, where the contribution due to the interaction vanishes and the frequency takes the value $3\omega_z$ [Hu et al., 2014, De Rosi and Stringari, 2015]. At T = 0 the ratio m_3/m_1 also accounts for the regimes of small coupling constant g_{1D} or small atomic numbers N where the LDA is no longer applicable [Chen et al., 2015]. At high temperature, where interaction effects are negligible, the ratio m_3/m_1 reproduces the hydrodynamic result $\sqrt{7}\omega_z$ for the average excitation frequency, consistently with the derivation of result (5.36), (see Appendix I for the full calculation and Table 5.2).

In the next Section, we will provide a more detailed description of the excitation spectrum of the dipole compression mode, by studying the response of the trapped gas to a sudden density perturbation, giving rise to observable signatures of the collisional VS collisionless nature of the gas.

5.3   Exciting the dipole compression mode

In this Section we exploit the peculiar behaviour exhibited by the dipole compression mode resulting from a sudden small density perturbation of the form $H_{pert}(z,t) = \lambda F_{DC}(z)\Theta(t)$ with $F_{DC} = \sum_{k=1}^{N} f_{DC}(z_k)$, $f_{DC}(z) = z^3/3 - z\langle z^2\rangle$ and $\Theta(t)$ the Heaviside function. Perturbations of similar form can be tailored with laser techniques and have been already implemented in the case of highly elongated Fermi gases [Tey et al., 2013]. The form of the DC perturbation $f_{DC}(z)$ is shown in Fig. 5.1 where we have expressed the variable z in units of the thermal radius $Z_T = \sqrt{2k_B T/(m\omega_z^2)}$. As pointed out in the previous Section, the excitations produced by this perturbation are exactly decoupled from the centre-of-mass motion.
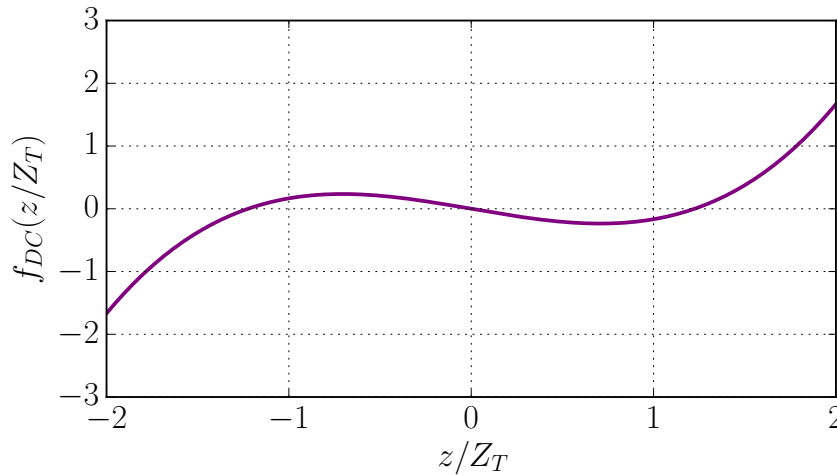
Figure 5.1: External perturbation $f_{DC}(z) = z^3/3 - z\langle z^2\rangle$ exciting the dipole compression (DC) mode. The value of $\langle z^2\rangle$ is calculated using a Maxwell-Boltzmann distribution (5.1) with thermal radius $Z_T = \sqrt{2k_B T/(m\omega_z^2)}$. From De Rosi and Stringari [2016]. Copyright © 2016, American Physical Society.

From the continuity equation (3.13) where we have identified the velocity $v(z) \propto \nabla_z f(z)$ with the gradient of the excitation operator, one can express the spatial density change caused by the external perturbation $f(z)$ as follows:

$$\delta n(z) \propto \nabla_z \left[(\nabla_z f(z)) n(z)\right] \ . \tag{5.39}$$

Let us calculate Eq. (5.39) for the DC perturbation $f(z) = f_{DC}(z)$ and in the high-T regime. For this purpose, we consider the Maxwell-Boltzmann distribution (5.1) and Eq. (5.39) is reported in Fig. 5.2. We observe that since the DC excitation operator is an odd function in space, see Fig. 5.1, this symmetry is transmitted to the density change (5.39) and the decay is fast for the presence of the gaussian classical distribution, Fig. 5.2. For this reason, the signal is not relevant for $|z/Z_T| > 2$. Since the density perturbation (5.39) has been derived starting from the continuity equation which holds in the hydrodynamic regime, Fig. 5.2 is referred only to the single mode excited with frequency $\sqrt{7}\omega_z$, see Table 5.2, and not to the CL limit where two different modes are present at high temperatures. For our discussion, the excitation operator f_{DC} is the same for both the HD as well as the CL regime. Actually, for the latter collisionless limit, one should calculate the two excitation operators responsible of the two decoupled modes with frequencies ω_z and $3\omega_z$. In this way, one gets two density perturbations $\delta n(z,t) = \delta n(z)e^{-i\omega t}$ relative to the two frequencies.
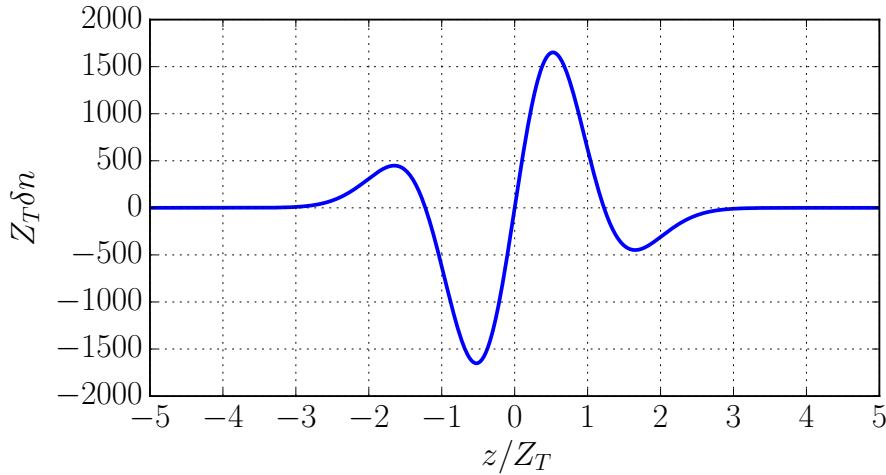
Figure 5.2: Density change in space for the dipole compression mode at high temperature in the hydrodynamic regime. $Z_T = \sqrt{2k_BT/(m\omega_z^2)}$ is the thermal radius.

According to linear response theory [Pitaevskii and Stringari, 2016] the time evolution of the expectation value $\delta\langle F\rangle(t) = \int dz \delta n(z,t) f_{DC}(z)$ follows the law [Zambelli and Stringari, 2001] (see Appendix J for its derivation):

$$\delta\langle F\rangle(t) = \frac{\lambda\hbar}{k_BT} \int_{-\infty}^{+\infty} d\omega' S_F(\omega') \left[1 - \cos(\omega' t)\right] \ , \qquad (5.40)$$

where $S_F(\omega)$ is the dynamic structure factor relative to the excitation operator F, see Eq. (5.9).

In the hydrodynamic regime a single frequency, provided by Eq. (5.7), will appear in the time evolution of the signal. According to the results of Table 5.2, this frequency will evolve continuously from the low temperature T value $\sqrt{6}\omega_z$ (weakly interacting limit) or $3\omega_z$ (Tonks-Girardeau limit) to the large T value $\sqrt{7}\omega_z$. In Fig. 5.3(a) we show the time dependence of the signal $\delta\langle F\rangle(t)$ predicted in the high T hydrodynamic limit, for which the dynamic structure factor is $S(\omega) = \sigma\delta(\omega - \sqrt{7}\omega_z)$ and Eq. (5.40) becomes:

$$\delta\langle F\rangle_{HD}(t) = \frac{\hbar\lambda\sigma}{k_BT} \left[1 - \cos(\sqrt{7}\omega_z t)\right] \ , \qquad (5.41)$$

being σ the excitation strength.

If instead the system is in the collisionless regime of high temperature, the dynamic structure factor carries the contributions of both frequencies $S_F(\omega) = \sigma[\delta(\omega - \omega_z) + \delta(\omega - 3\omega_z) + \omega \to -\omega]$ (we have set $\sigma_1 = \sigma_3 \equiv \sigma$, according to the discussions presented at the end of the previous Sec. 5.2), the signal will exhibit a typical beating involving the two frequencies

$$\delta\langle F\rangle_{CL} = \frac{\hbar\lambda\sigma}{k_BT} \left[2 - \cos(\omega_z t) - \cos(3\omega_z t)\right] \qquad (5.42)$$

as reported in Fig. 5.3(b).

The observation of the transition between a single frequency signal to the beating regime can then be considered a signature of the transition between the hydrodynamic to the collisionless regime. A transition of similar nature was observed in the study of the scissors mode of 3D Bose gases in a deformed harmonic potential where the frequency has a single value at low temperature in the superfluid Bose-Einstein condensed phase, while the spectrum exhibits a beating between two frequencies for temperatures larger than the critical temperature where the system is in the non-superfluid collisionless regime [Guéry-Odelin and Stringari, 1999, Maragò et al., 2000].
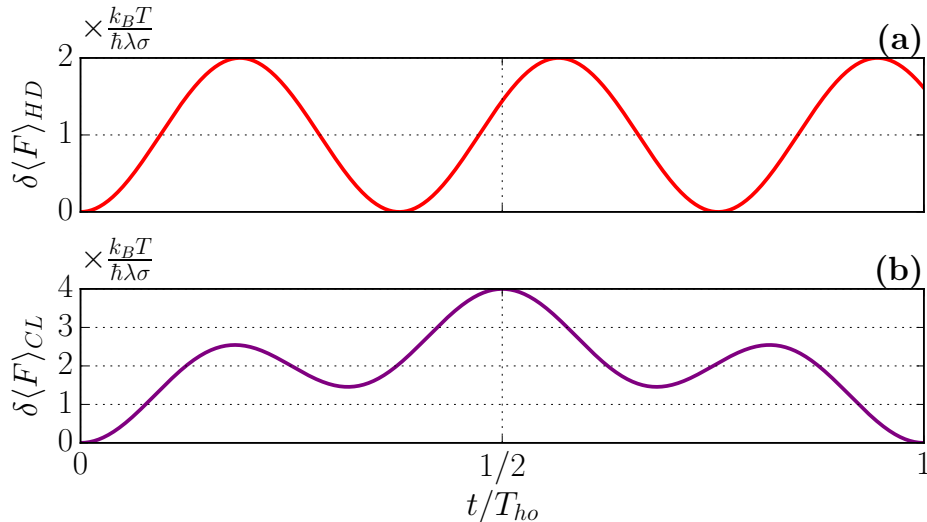
Figure 5.3: Time evolution of the expectation value $\delta\langle F\rangle(t)$, in units of oscillator time $T_{ho} = 2\pi/\omega_z$, following the perturbation of the dipole compression mode (see text).
In the hydrodynamic regime of high temperatures **(a)** the signal is characterized by the single frequency $\sqrt{7}\omega_z$, while in the collisionless regime of high T **(b)** by a periodic beating of the two frequencies ω_z and $3\omega_z$. From De Rosi and Stringari [2016]. Copyright © 2016, American Physical Society.

5.4 Experimental issues

In this Section, we discuss some experimental issues relative to our theoretical predictions about the DC mode reported in previous Secs. 5.2 and 5.3.

Even if we have chosen the DC excitation operator

$$F_{DC} = \sum_{k=1}^{N} f_{DC}(z_k) = \sum_{k=1}^{N} \frac{z_k^3}{3} - z_k\langle z^2\rangle \qquad (5.43)$$

such that the centre-of-mass (dipole) mode is not excited, see SubSec. 5.2.3, this does not reflect the experimental situation. In fact, in a laboratory, it is extremely difficult to generate a perturbation which reproduces exactly Eq. (5.43). Therefore, in most cases, even the dipole mode is excited [Tey et al., 2013]. The major experimental problem is to distinguish always the extra dipole frequency ω_z from the other modes of interest in all regimes.

The case of zero temperature is trivial. As a matter of fact, the system is always in the hydrodynamic regime, characterised by a single excitation frequency: $\sqrt{6}\omega_z$ or $3\omega_z$ in the BG or TG interaction limit, respectively, see Table 5.2. Therefore, it is easy to distinguish the dipole mode, being its frequency different from both the expected HD frequencies.

The situation at high T is more complicated. In the collisionless regime, we expect a beating of two frequencies for the DC mode. One of them is exactly equal to the centre-of-mass (CM) frequency ω_z even if the CM is not excited by the operator (5.43). Since, experimentally, one cannot easily realize the perturbation in the exact form (5.43), the CM will be unavoidably excited and one cannot, consequently, distinguish if the frequency ω_z, appearing in the resulting signal, really belongs to the CM or to the DC mode. A possible way to solve this problem is to measure the higher frequency present in the oscillation: if it is equal to $3\omega_z$, one can conclude that the system is in the CL regime; if instead one measures the frequency $\sqrt{7}\omega_z$ the gas is in the HD limit.

A better solution to this problem is provided by the measurement of the signal in the integral form:

$$\delta\langle F\rangle(t) = \int dz\,\delta n_{\mathrm{DC}}(z,t)f(z) \tag{5.44}$$

where the density perturbation δn_{DC} is given by Eq. (5.39) relative to the DC mode. Let us considers the dipole mode $f_D(z) = z$ in Eq. (5.44). By construction one gets that the CM signal is not excited: $\delta\langle F\rangle_D(t) = 0$. Therefore, the observation of the $\omega = \omega_z$ component in the signal (5.44) is a proof that we are in the collisionless regime. In other words, the integrated signal (5.44) acts like a "filter" for the centre-of-mass mode.

Chapter 6

Thermodynamic behaviour of a 1D Bose gas at low temperature

> Life isn't one-dimensional. The world isn't simply divided into good versus evil. I think we're all capable of both.

<div align="right">Alexander Skarsgard</div>

It is well known that the thermodynamic behaviour of a superfluid is dominated, at low temperature, by the thermal excitation of phonons [Wilks, 1967]. This explains, in particular, the peculiar behaviour exhibited at low temperature by the specific heat as well as by other fundamental thermodynamic functions. A non-trivial (and less investigated in the literature) consequence of superfluidity shows up in the non-monotonic behaviour of the chemical potential [Papoular et al., 2012]. At low temperature T the chemical potential increases with T as a consequence of the thermal excitation of phonons. At high temperature, in the ideal gas classical regime, the chemical potential is instead a decreasing function of T. This non-monotonic behaviour has been recently measured in a strongly interacting atomic Fermi gas [Ku et al., 2012] where it was shown that the chemical potential exhibits a maximum in the vicinity of the superfluid critical temperature.

It is consequently interesting to explore the low-temperature thermodynamic behaviour of other systems, like one-dimensional (1D) interacting Bose gases, which are known to exhibit a phononic excitation spectrum, despite the fact that they cannot be considered superfluids according to standard definition. By investigating the drag flow caused by a moving external perturbation Astrakharchik and Pitaevskii [2004] have in fact shown that 1D Bose gases interacting with contact potential exhibit a traditional superfluid behaviour, characterized by the absence of friction force, only in the weakly interaction regime, where Bogoliubov theory applies and the gas can be locally considered Bose-Einstein condensed, despite the absence of true long range order.

In this Chapter, we investigate the low-temperature expansion of the chemical potential μ for a 1D Bose gas with contact repulsive interaction in uniform configurations for the whole crossover, ranging from the weak to the strong interaction limit. We find that for all intermediate interaction regimes, described at T = 0 by Lieb-Liniger (LL) theory, the increase of the chemical potential at low temperature follows the law $\mu \propto T^2$ and is actually caused by the phononic nature of the long wavelength elementary excitations, as in usual superfluids [Papoular et al., 2012]. The relevant coefficient fixing the T^2 law depends on the density derivative of the T = 0 sound velocity which can be calculated using Lieb-Liniger theory. This feature strengthens the analogy with superfluids even in

1D dimension. Importantly, our results can be also generalised to every Luttinger liquid at low temperature whose macroscopic elementary excitations can be described in terms of non-interacting phonons.

Recently, a ring geometry has been experimentally realized for a microscopic system of $N = 8 - 20$ atoms [Labuhn et al., 2016]. Motivated by the experimental progress, we study in details also the behaviour of a gas containing a finite number of atoms in a ring, focusing on the deviations of its thermodynamic behaviour from the one in the large N limit.

Our system is a uniform gas of bosons interacting with a repulsive contact interaction

$$H = -\frac{\hbar^2}{2m} \sum_{i=1}^{N} \frac{\partial^2}{\partial x_i^2} + 2c \sum_{i>j}^{N} \delta(x_i - x_j) \qquad (6.1)$$

where the interaction parameter c is related to the 1D coupling constant $g_{1D} = -2\hbar^2/(ma_{1D})$ through $c = mg_{1D}/\hbar^2$, where a_{1D} is the 1D scattering length. The system (6.1) has been realized experimentally for the whole interaction crossover by suitably tuning the interaction strength [Kinoshita et al., 2004, 2006, Cazalilla et al., 2011], described by the dimensionless parameter

$$\gamma = \frac{c}{n} = -\frac{2}{na_{1D}} \qquad (6.2)$$

from weak ($\gamma \to 0$) to strong ($\gamma \gg 1$) interactions [Kinoshita et al., 2004, 2006, Haller et al., 2009, 2010, 2011]. The first case is described by Bogoliubov (BG) theory, while the latter corresponds to the so-called Tonks-Girardeau (TG) regime where bosons are impenetrable and their wave function can be mapped onto that of an ideal Fermi gas [Girardeau, 1960].

The original results presented in this Chapter will appear in the forthcoming paper De Rosi et al. [2017]. This Chapter is organised as follows.

In Sec. 6.1 we derive the low-temperature expansion of the chemical potential, starting from the free energy of an ideal phononic gas. This assumption is fully justified by the low-momenta behaviour of the Lieb-Liniger excitation spectrum. The low-temperature expansion exhibits a T^2-dependence on temperature, with the coefficient related to the density derivative of the LL sound velocity at zero temperature. The Bethe-Ansatz results for the chemical potential are shown to agree very well with the low-temperature expansion, for the whole BG-TG crossover.

In Sec. 6.2 we investigate the BG weakly-interacting gas. By considering the quantum fluctuation contribution in the ground-state energy at T = 0, we explore the behaviour of the chemical potential and of the sound velocity. While this correction is important at T = 0, it does not affect the low-temperature expansion of the chemical potential.

Similarly to Sec. 6.2, we calculate in Sec. 6.3 the first corrections in the interaction parameter γ to the TG strongly interacting gas. The starting point is the expansion, for large values of γ, of the ground-state energy of a hard-sphere gas.

In Sec. 6.4 we derive the low-temperature expansions of both the adiabatic and the isothermal inverse compressibilities. The coefficients of the T^2 laws are studied as a function of the interaction parameter γ and analytically calculated in the BG and TG limits.

In Sec. 6.5 we consider a ring configuration with a finite number of particles at zero temperature and calculate the finite-size corrections with respect to the thermodynamic limit for the energy, the chemical potential and the sound velocity.

6.1 Low-temperature expansion of the chemical potential

As discussed in Sec. 2.3, the elementary excitations of an interacting 1D Bose gas at $T = 0$ have a phononic character at small momenta [Lieb and Liniger, 1963, Lieb, 1963, Pitaevskii and Stringari, 2016], characterized by the linear dispersion relation

$$\epsilon(p)_{p \to 0} = v_s(\gamma)p . \tag{6.3}$$

The sound velocity is related to the inverse compressibility [Lieb and Liniger, 1963, Lieb, 1963]

$$v_s(\gamma) = \sqrt{\frac{n}{m}\frac{\partial\mu(\gamma)}{\partial n}} = \sqrt{\frac{\hbar^2 n^2}{2m^2}\left(6e(\gamma) - 4\gamma\frac{\partial e(\gamma)}{\partial\gamma} + \gamma^2\frac{\partial^2 e(\gamma)}{\partial\gamma^2}\right)} , \tag{6.4}$$

where $n = N/L$ denotes the linear density and the chemical potential μ is calculated at $T = 0$ within the Lieb-Liniger model from the ground-state energy per particle $E_0(\gamma)/N = \hbar^2 n^2 e(\gamma)/(2m)$ (2.10) [Lieb and Liniger, 1963, Lieb, 1963]:

$$\mu(\gamma) = \frac{\partial E_0(\gamma)}{\partial N} = \frac{\hbar^2 n^2}{2m}\left[3e(\gamma) - \gamma\frac{\partial e(\gamma)}{\partial\gamma}\right] . \tag{6.5}$$

The ratio between the sound velocity and the Fermi velocity $v_F = \hbar\pi n/m$ is known as the Luttinger parameter, $K_L = v_F/v_s$, and plays an important role in defining the long-range properties of one-dimensional systems. Figure 6.1 shows the dependence of the speed of sound on the interaction parameter γ, Eq. (6.4), for the Lieb-Liniger model, described by the Hamiltonian (6.1). There is a smooth crossover between the mean-field value defined as $v_s = \sqrt{g_{1D}n/m} = v_F\sqrt{\gamma}/\pi$ for weak interactions to the Tonks-Girardeau (ideal Fermi gas) value $v_s = v_F$ in the limit of strong repulsion, see Appendix K.
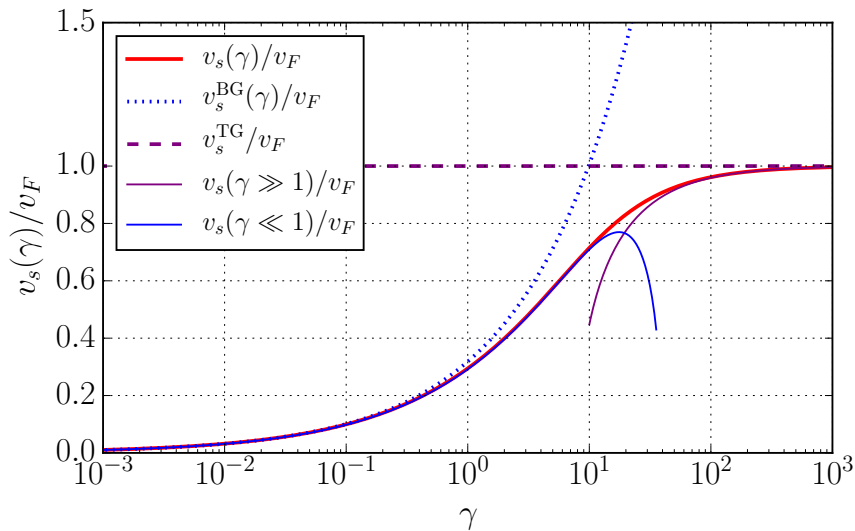
Figure 6.1: Sound velocity v_s at $T = 0$ in units of Fermi velocity v_F (red solid line) as a function of the interaction parameter γ, calculated by solving the Lieb-Liniger equations. The Bogoliubov (blue dotted line, $v_s^{BG}(\gamma)/v_F = \sqrt{\gamma}/\pi$) and Tonks-Girardeau (purple dashed line, $v_s^{TG} = v_F$) limits, including their first-order corrections (blue solid line $v_s(\gamma \ll 1)/v_F = v_s^{BG}(\gamma)/v_F\sqrt{1 - \sqrt{\gamma}/(2\pi)}$ and purple solid line $v_s(\gamma \gg 1)/v_F = \sqrt{1 - 8/\gamma}$, respectively) are present too, see Secs. 6.2 and 6.3. From De Rosi et al. [2017].

For larger momenta, the 1D excitation spectrum is characterised by a continuous structure, bounded by two branches of elementary excitations [Lieb and Liniger, 1963, Lieb, 1963, Yang and Yang, 1969, Pitaevskii and Stringari, 2016], which have been the object of recent measurements [Meinert et al., 2015]. For small values of γ, the Lieb-I particle-like branch corresponds to the Bogoliubov excitation spectrum [Lieb and Liniger, 1963, Lieb, 1963, Kulish et al., 1976, Pitaevskii and Stringari, 2016]. The Lieb-II hole-like branch is instead associated with the dark soliton dispersion predicted by Gross-Pitaevskii theory [Kulish et al., 1976, Ishikawa and Takayama, 1980, Pitaevskii and Stringari, 2016]. The two branches merge into the phononic spectrum for $p \ll m v_s$, Fig. 6.2 and Sec. 2.3.
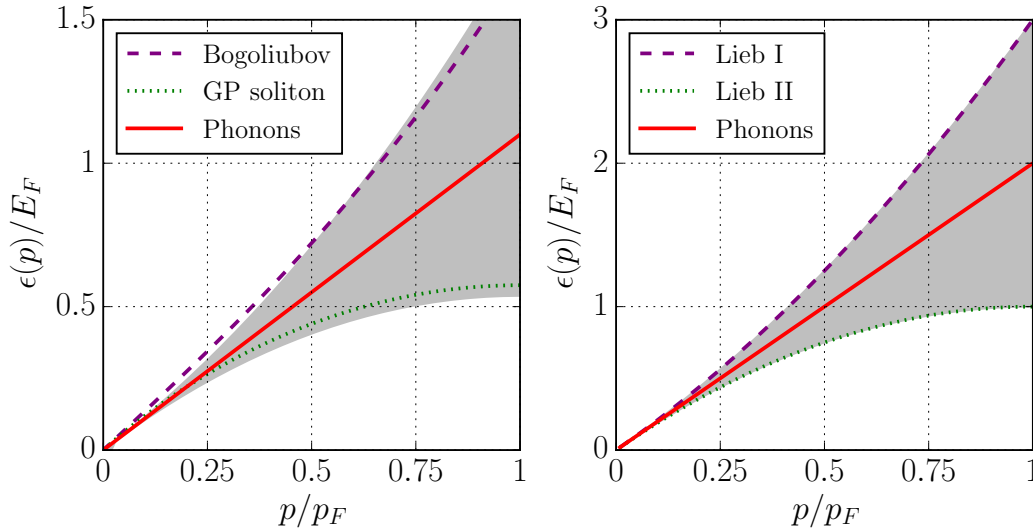
Figure 6.2: Lieb-Liniger excitation spectrum in the BG regime with $\gamma = 4.52$ (left) and in the deep TG regime with $\gamma = +\infty$ (right). The units are the Fermi energy E_F and the Fermi momentum $p_F = m v_F$. The shaded region represents the continuum of the excitations and it is delimited by the upper (Lieb-I) and the lower (Lieb-II) branch of the spectrum. On the left, Lieb-I and II branches are not reported and the purple dashed line gives the Bogoliubov dispersion and the green dotted line describes the mean-field (GP) soliton spectrum. In the limit $\gamma \to 0$, Lieb-I branch tends to be equal to the BG dispersion, while Lieb-II one coincides with the soliton spectrum. The red solid line is the Lieb-Liniger phononic spectrum calculated with $\gamma = 4.52$. On the right, Lieb-I and Lieb-II branches are reported and they coincide with the particle (purple dashed line) and hole (green dotted line) ideal Fermi gas excitations, respectively. The red solid line is the phononic spectrum calculated with the Fermi velocity. From De Rosi et al. [2017].

At low temperature ($k_B T \ll m v_s^2$) we expect that the thermodynamic behaviour of the system can be calculated in terms of a gas of non-interacting phonons. The free energy $A = E - TS$ of this ideal Bose gas is then given by

$$A(T, L) = E_0(\gamma) + \frac{k_B T L}{2\pi\hbar} \int_{-\infty}^{\infty} \log\left[1 - e^{-\beta\epsilon(p)}\right] dp^1 \qquad (6.6)$$

where $\epsilon(p)$ is dispersion (6.3) and we have added the energy $E_0(\gamma)$ calculated at T = 0 with the Lieb-Liniger theory, Eq. (2.10). Notice that the thermal contribution to A is affected by two-body interactions through the dependence of $\epsilon(p)$ on the interaction parameter γ. The integral of Eq. (6.6) yields the following low-T expansion for the free energy

$$A(T, L) = E_0(\gamma) - \frac{\pi}{6} \frac{(k_B T)^2 L}{\hbar v_s(\gamma)} , \qquad (6.7)$$

---

[1]This equation is more general, because it holds also for the Planck radiation composed by photons.

which differs from the usual T^4-behaviour exhibited by 3D superfluids [Pitaevskii and Stringari, 2016] because of the 1D structure of the integral (6.6). Starting from result (6.7) one can calculate the low-T expansion of the chemical potential:

$$\mu(T, \gamma) = \left(\frac{\partial A}{\partial N}\right)_{T,L} = E_F \left[\alpha(\gamma) + \beta(\gamma)\left(\frac{T}{T_F}\right)^2\right] \tag{6.8}$$

where we have introduced the energy scale $E_F = k_B T_F = \hbar^2 \pi^2 n^2 / 2m$ given by the Fermi energy of a 1D Fermi gas, which exhibits the same density dependence as the quantum degeneracy temperature of the system. We have also defined the relevant dimensionless parameters of the expansion

$$\alpha(\gamma) = \frac{\mu(\gamma)}{E_F} \tag{6.9}$$

and

$$\beta(\gamma) = \frac{\pi E_F}{6\hbar v_s^2(\gamma)} \frac{\partial v_s(\gamma)}{\partial n} , \tag{6.10}$$

which are functions of the interaction parameter γ and can be calculated at zero temperature using Lieb-Liniger theory and Eq. (6.4) and Eq. (6.5). It is worth noticing that the parameter $\beta(\gamma)$, which is the most relevant because it fixes the leading coefficient of the low-T expansion, depends on the density derivative of the sound velocity. The two numerical functions $\alpha(\gamma)$, Eq. (6.9), and $\beta(\gamma)$, Eq. (6.10), have been calculated within LL theory and their values are reported in Figs. 6.3 and 6.4 with their BG and TG limits, see Appendix K. In particular, the TG limits for $\alpha(\gamma)$ and $\beta(\gamma)$ reproduce the low-T Sommerfeld expansion of the chemical potential for the 1D ideal Fermi gas, Eq. (6.25).
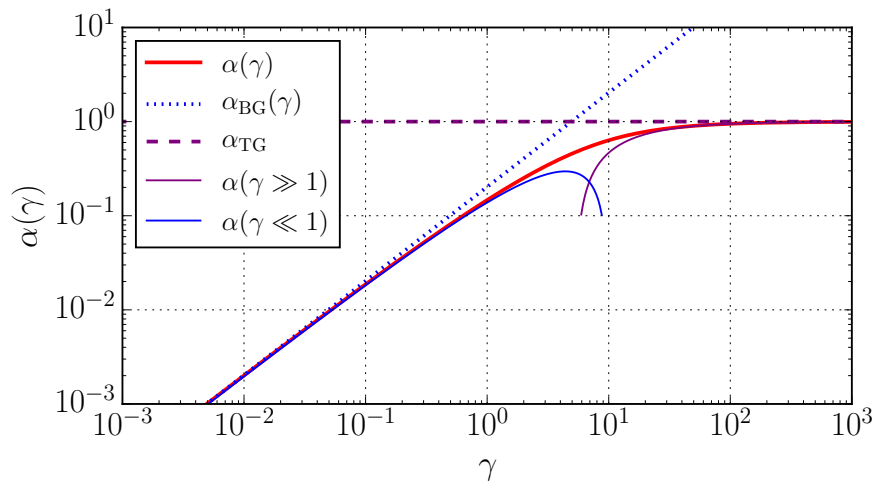
Figure 6.3: $\alpha(\gamma)$ (red solid line) with leading dependence (purple dashed line, $\alpha_{\mathrm{TG}} = 1$ and blue dotted line, $\alpha_{\mathrm{BG}}(\gamma) = 2\gamma/\pi^2$) and first-order corrections [purple solid line, $\alpha(|\gamma| \gg 1) = 1 - 16/(3\gamma)$ and blue solid line, $\alpha(\gamma \ll 1) = \alpha_{\mathrm{BG}}(\gamma)(1 - \sqrt{\gamma}/\pi)$] for Tonks-Girardeau and Bogoliubov limits, respectively. From De Rosi et al. [2017].

In Figs. 6.5-6.6 we report the temperature dependence of the chemical potential of the system described by Hamiltonian (6.1) as obtained from the Bethe-Ansatz (BA) approach first developed by Yang-Yang [Yang and Yang, 1969, Yang, 1970, Kheruntsyan et al., 2005, Lang et al., 2015] for several characteristic values of γ, see SubSec. 2.3.1. The crossover from mean-field to Tonks-Girardeau regimes (see Fig. 6.1) introduces two distinct energy scales. Correspondingly, we rescale the chemical potential in units of the Fermi energy E_F in Fig. 6.5 and in units of the mean-field zero-temperature chemical potential $\mu_{\mathrm{BG}} = g_{\mathrm{1D}} n$ in Fig. 6.6.
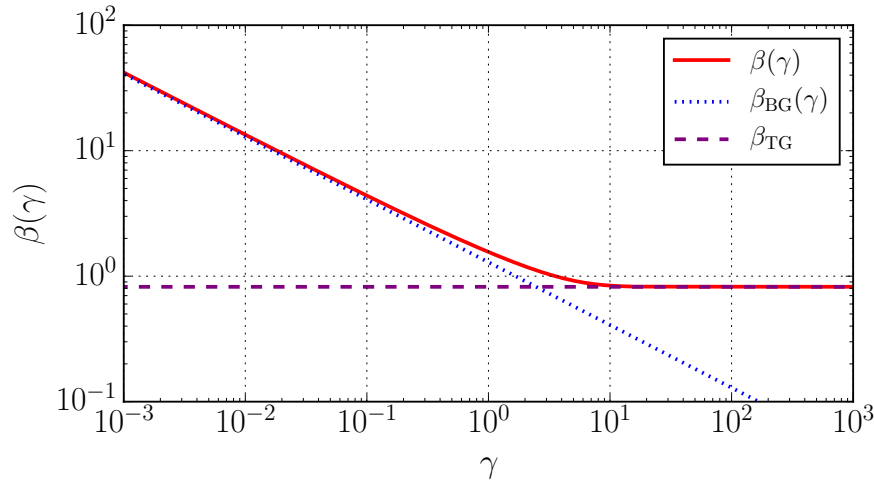
Figure 6.4: $\beta(\gamma)$ (red solid line) with the Tonks-Girardeau (purple dashed line, $\beta_{\mathrm{TG}} = \pi^2/12$) and Bogoliubov (blue dotted line, $\beta_{\mathrm{BG}}(\gamma) = \pi^3/(24\sqrt{\gamma})$) limits. From De Rosi et al. [2017].

The first choice provides natural units in TG regime in which strongly repulsive bosons behave similarly to ideal fermions (IFG) in the limit of $\gamma \to \infty$. In this regime, the chemical potential as a function of T is calculated by inverting the Fermi-Dirac distribution (magenta dashed line in Fig. 6.5):

$$n_{\mathrm{IFG}}(p) = \frac{1}{e^{\frac{1}{k_B T}\left(\frac{p^2}{2m} - \mu\right)} + 1} \ , \tag{6.11}$$

and, despite the absence of superfluidity, it still exhibits the quadratic low-temperature dependence $\mu \propto T^2$, which follows from the low-temperature Sommerfeld expansion, Eq. (6.25).

By reducing the interaction parameter γ, the system becomes softer and the limit of vanishing interactions ($\gamma \to 0$) corresponds to an ideal Bose gas (IBG) with the chemical potential $\mu(T)$ fixed by the relationship (red dashed line in Fig. 6.5):

$$n_{\mathrm{IBG}}(p) = \frac{1}{e^{\frac{1}{k_B T}\left(\frac{p^2}{2m} - \mu\right)} - 1} \ . \tag{6.12}$$

Notice that, because of the absence of Bose-Einstein condensation [Mermin and Wagner, 1966, Hohenberg, 1967], the chemical potential of the 1D ideal Bose gas is always negative and approaches the value $\mu = 0$ as $T \to 0$.

Remarkably, for all finite interaction strengths, the temperature dependence is not monotonic. Moreover, the initial increase is perfectly described by the quadratic low-temperature expansion (6.8), thereby proving that the model based on a gas of independent phonons well accounts for the thermodynamic behaviour of the 1D interacting Bose gas. This is a non-trivial result due to the complex structure of the elementary excitations at larger wavevectors exhibiting a double branch converging into the phonon law (6.3) only at small momenta. We notice also that the chemical potential for high temperatures, which is a decreasing function of T, can be considered as a shift of the ideal Bose chemical potential, Eq. (6.12), for every value of γ.

While Fig. 6.5 shows very well the whole crossover from the weakly to strongly interacting regime, it is not appropriate for small values of γ, since the low-T expansion breaks down at very low T. Therefore, for the BG regime, in addition to the new energy scale
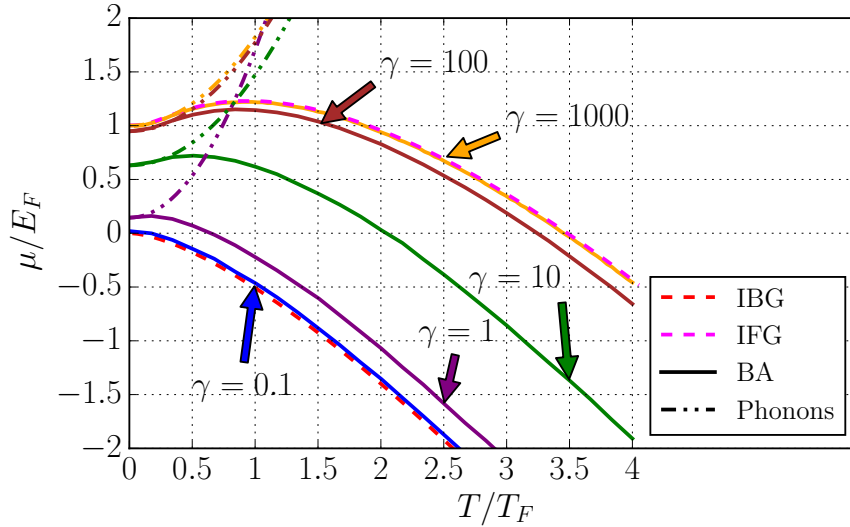
Figure 6.5: Chemical potential as a function of temperature T in Fermi units for several values of γ. The solid lines represent the Bethe-Ansatz (BA) solutions for different values of γ. The dot-dashed lines are the low-temperature expansions of the chemical potential taking into account only the phononic contribution, Eq. (6.8). The low-T expansions for $\gamma \geq 1000$ are equal to the analytical Sommerfeld expansion of Eq. (6.25). Both the chemical potential as a function of T for the ideal Fermi (magenta dashed line) and ideal Bose (red dashed line) gas are also reported, Eq. (6.11) and (6.12), respectively. From De Rosi et al. [2017].

$g_{1D}n$ for the chemical potential, we introduce the following T unit, see Fig. 6.6:

$$T_{\mathrm{BG}}(\gamma) = \frac{\hbar k_F v_s^{\mathrm{BG}}(\gamma)}{k_B} = T_F \frac{2\sqrt{\gamma}}{\pi} \; . \tag{6.13}$$

Eq. (6.13) has been derived from the phononic linear dispersion law, with wave vector fixed equal to the Fermi value k_F ($E_F = \hbar^2 k_F^2/(2m)$) and sound velocity $v_s^{\mathrm{BG}}(\gamma)$, provided by Bogoliubov theory.

In the natural units for the BG regime, the low-T expansion (6.8) can be rewritten as:

$$\mu(T, \gamma) = g_{1D}n \left[\alpha(\gamma)\frac{\pi^2}{2\gamma} + 2\beta(\gamma) \left(\frac{T}{T_{\mathrm{BG}}(\gamma)} \right)^2 \right] \; , \tag{6.14}$$

which breaks at very small values of γ. For this reason, the curve (6.14) is not reported in Fig. 6.6 for $\gamma = 0.001$.

For the weakly-interacting regime ($\gamma \ll 1$), we point out from Fig. 6.5 that, for low temperatures $T \ll \mu$ with $\mu \propto T^2$, the gas behaves like a quasicondensate, exhibiting typical features of superfluids. For $\mu \ll T \ll T_F$, the gas is in a thermal degenerate state, while for $T \gg T_F$ the gas behaves classically with $\mu < 0$. The above conditions, rewritten in the more natural BG units of Fig. 6.6 becomes:

$$\frac{T}{T_{\mathrm{BG}}(\gamma)} \ll \frac{\mu}{g_{1D}n} \frac{\sqrt{\gamma}}{\pi} \; , \tag{6.15}$$

holding in the quasicondensate,

$$\frac{\mu}{g_{1D}n} \frac{\sqrt{\gamma}}{\pi} \ll \frac{T}{T_{\mathrm{BG}}(\gamma)} \ll 1 \; , \tag{6.16}$$
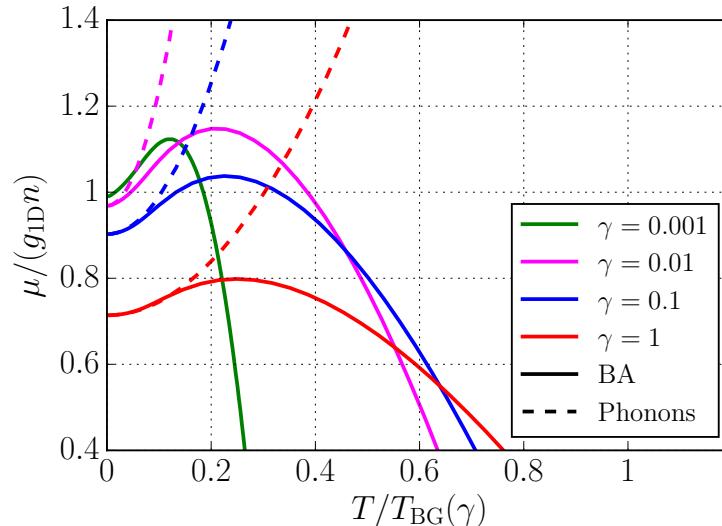
Figure 6.6: Chemical potential as a function of temperature in BG units for several small values of γ. The solid lines represent the Bethe-Ansatz (BA) solutions. The dashed lines are the low-temperature expansions of the chemical potential taking into account the phononic excitations, Eq. (6.14). We notice also that the phononic expansion (6.14) does not hold for very small γ, like $\gamma = 0.001$, for which value the low-T expansion is not reported. From De Rosi et al. [2017].

for the thermal degenerate gas and

$$\frac{T}{T_{\text{BG}}(\gamma)} \gg \frac{\pi}{2\sqrt{\gamma}} \ , \tag{6.17}$$

in the classical regime. A similar classification of the quantum degeneracy states in 1D trapped configurations was first proposed by Petrov et al. [2000b], see SubSec. 2.2.2.

6.2 Bogoliubov regime $\gamma \to 0$

In the mean-field theory, the chemical potential is linear in density, $\mu_{\text{BG}}(T = 0) = g_{1D}n$ and the velocity of sound takes the value $v_s^{\text{BG}}(\gamma) = \hbar n\sqrt{\gamma}/m = v_F\sqrt{\gamma}/\pi$, see Fig. 6.1 and Appendix K.

The first correction to the mean-field expression for the equation of state comes from the quantum fluctuations [Lee et al., 1957, Lee and Yang, 1957, Pitaevskii and Stringari, 2016]. Differently from the 3D case, see SubSec. 1.5.1, in 1D the renormalization of the scattering length due of the absence of ultraviolet divergences is not required in the calculation of the ground-state energy, see Appendix L. Therefore in 1D one can consider all ranges of momenta and one finds [Lieb and Liniger, 1963, Lieb, 1963]:

$$\frac{E_0}{N} = \frac{1}{2}g_{1D}n + \frac{2}{2N}\sum_{p>0}^{+\infty}\left[\epsilon(p) - g_{1D}n - \frac{p^2}{2m}\right] \tag{6.18}$$

where

$$\epsilon(p) = \sqrt{\frac{g_{1D}n}{m}p^2 + \left(\frac{p^2}{2m}\right)^2} \tag{6.19}$$

is the Bogoliubov excitation spectrum. By considering the thermodynamic limit of Eq. (6.18) and by solving the integral in momentum space, one finally finds the first-order correction

in the interaction parameter for the ground-state energy [Lieb and Liniger, 1963, Lieb, 1963]

$$\frac{E_0}{N}(\gamma \ll 1) = \frac{\hbar^2 n^2}{2m} \gamma \left(1 - \frac{4}{3\pi}\sqrt{\gamma} \right) \; . \tag{6.20}$$

The same result can be also found by performing a power series expansion of the Lieb-Liniger equations [Kaminaka and Wadati, 2011, Gudyma, 2015]. Contrarily to the usual 3D case, in one dimension the correction steaming from quantum fluctuations is negative.

Equation (6.20) allows one to calculate the higher-order corrections for the other thermodynamic quantities at T = 0. For the chemical potential (6.5), one finds the result

$$\mu(\gamma \ll 1) \approx \frac{\hbar^2 n^2 \gamma}{m} \left(1 - \frac{\sqrt{\gamma}}{\pi} \right) \tag{6.21}$$

which implies the result

$$\alpha(\gamma \ll 1) \approx \alpha_{\mathrm{BG}}(\gamma) \left[1 - \frac{\sqrt{\gamma}}{\pi} \right] \tag{6.22}$$

for the expansion of the coefficient $\alpha(\gamma)$, where $\alpha_{\mathrm{BG}}(\gamma) = 2\gamma/\pi^2$ is the mean-field (BG) value. The corresponding result has been plotted in Fig. 6.3 and well reproduces the exact value of $\alpha(\gamma)$ up to values $\gamma \sim 1$.

From Eq. (6.4) and Eq. (6.21), one can calculate also the correction to the sound velocity [Lieb and Liniger, 1963, Lieb, 1963]

$$v_s(\gamma \ll 1) \approx v_s^{\mathrm{BG}}(\gamma)\sqrt{1 - \frac{\sqrt{\gamma}}{2\pi}} \tag{6.23}$$

which is also reported in Fig. 6.1, yielding the expression

$$\beta(\gamma \ll 1) \approx \beta_{\mathrm{BG}}(\gamma) \; , \tag{6.24}$$

for the coefficient $\beta(\gamma)$, Eq. (6.10), with $\beta_{\mathrm{BG}}(\gamma) = \pi^3/(24\sqrt{\gamma})$ the Bogoliubov value. Notice that, differently from the case of $\alpha(\gamma)$ [see Eq. (6.22)], the first correction $\beta_{\mathrm{BG}}(\gamma)$ vanishes because of an exact cancellation between the corrections provided by the terms $\partial v_s/\partial n$ and v_s^2 of Eq. (6.10). This explains why the Bogoliubov approximation describes correctly the value of $\beta(\gamma)$ for a large interval of values of γ, up to $\gamma \sim 1$ (see Fig. 6.4).

6.3 Tonks-Girardeau regime $\gamma \to \infty$

For $\gamma \to \infty$, the TG regime describes a gas whose energetic behaviour coincides with that of an ideal Fermi gas: the thermodynamic quantities do not depend on the coupling constant $g_{1\mathrm{D}}$, but only on the density n, encoded in the Fermi energy E_F. This regime can be interpreted as a unitary Bose gas which behaves like an ideal Fermi gas (or a unitary Fermi gas with Bertsch parameter equal to 1). Therefore, the chemical potential is equal to the Fermi energy $\mu_{\mathrm{TG}}(T = 0) = E_F$, while the sound velocity is equal to the Fermi velocity $v_s^{\mathrm{TG}} = v_F = \sqrt{2E_F/m}$, see Fig. 6.1 and Appendix K. The low-T expansion of the chemical potential in this limit is equal to the first terms of Sommerfeld expansion (orange dot-dashed line for $\gamma = 1000$ in Fig. 6.5) of the 1D ideal Fermi gas, as already pointed out by Lang et al. [2015]:

$$\mu_{Somm}(T) = E_F \left[1 + \frac{\pi^2}{12} \left(\frac{T}{T_F} \right)^2 \right] \tag{6.25}$$

which contains the TG limits of $\alpha(\gamma)$ and $\beta(\gamma)$ parameters, Figs. 6.3 and 6.4.

First-order corrections to the TG regime can be calculated by starting from the ground state energy per particle of a gas of hard-sphere (i.e. impenetrable) bosons with diameter $a_{1D} > 0$ [Girardeau, 1960]:

$$\frac{E_0}{N} = \frac{\pi^2 \hbar^2}{6m} \frac{n^2}{(1 - na_{1D})^2} \ .$$ (6.26)

In the limit of point-like bosons $a_{1D} = 0$, Eq. (6.26) reproduces the ground state energy of the free Fermi gas, Eq. (K.10).

It is natural to apply expression (6.26) for the energy of a strongly interacting 1D Bose gas also to the case of negative scattering lengths a_{1D} corresponding to large and positive values of γ, see Eq. (6.2), i.e to the case of a strongly repulsive 1D Bose gas. The quantity $n|a_{1D}|$ is interpreted as gas parameter in 1D and, in the TG regime, it is small, Eq. (6.2). By expanding Eq. (6.26) for $n|a_{1D}| \ll 1$, in terms of γ, one can then write

$$\frac{E_0}{N}(|\gamma| \gg 1) \approx \frac{\pi^2 \hbar^2 n^2}{6m} \left(1 - \frac{4}{\gamma}\right)$$ (6.27)

holding for both the Super Tonks-Girardeau [Astrakharchik et al., 2005a] ($\gamma < 0$) and the strongly repulsive [Gudyma, 2015] ($\gamma > 0$) regimes, see Sec. 2.3.

From Eq. (6.27), one easily calculates the correction of the chemical potential at $T = 0$, Eq. (6.5):

$$\mu(|\gamma| \gg 1) \approx E_F \left(1 - \frac{16}{3\gamma}\right)$$ (6.28)

which implies the result [Gudyma, 2015]

$$\alpha(|\gamma| \gg 1) \approx 1 - \frac{16}{3\gamma}$$ (6.29)

for $\alpha(\gamma)$, including the first correction to the TG result $\alpha_{TG} = 1$. Prediction (6.29) is reported in Fig. 6.3 for positive values of γ, its accuracy being good for value of γ larger than ~ 10.

From Eq. (6.4) and Eq. (6.28), one can calculate also the first correction, at large γ, to the sound velocity [Gudyma, 2015, Valiente and Öhberg, 2016]:

$$v_s(|\gamma| \gg 1) \approx v_F \sqrt{1 - \frac{8}{\gamma}}$$ (6.30)

which is reported in Fig. 6.1. For the coefficient $\beta(\gamma)$, which provides the T^2-correction in the expansion of the chemical potential, we find again an exact cancellation between the $1/\gamma$ correction (provided by the term $\partial v_s / \partial n$) and v_s^2 entering the expression (6.10) for $\beta(\gamma)$, similarly to what happens in the small γ expansion discussed in the previous Section 6.2 in the case of the Bogoliubov gas. We then find that the Tonks-Girardeau expression $\beta_{TG} = \pi^2/12$ provides a very accurate estimate of $\beta(\gamma)$ for values of γ larger than ~ 10 (see Fig. 6.4).

6.4 Low-temperature expansion of the inverse compressibilities

In this Section, we provide the phononic low-T expansions of both the adiabatic and isothermal inverse compressibilities, discussed in SubSec. 6.4.1 and 6.4.2, respectively. Both quantities provide relevant information about the equation of state of the gas under investigation. In particular, the adiabatic inverse compressibility is of a paramount importance, being directly related to the adiabatic sound velocity, measured in the experiments in cigar configurations.

6.4.1   Adiabatic inverse compressibility and sound velocity

From the Gibbs-Duhem relation $dP = nd\mu + sdT$, one finds

$$\left(\frac{\partial P}{\partial n}\right)_{\bar{s}} = n\left(\frac{\partial \mu}{\partial n}\right)_{\bar{s}} + n\bar{s}\left(\frac{\partial T}{\partial n}\right)_{\bar{s}} \tag{6.31}$$

where s is the entropy density and $\bar{s} = s/n$ is the entropy per particle.

At low temperature the entropy per particle of a non-interacting gas of phonons takes the form [2] [Pitaevskii and Stringari, 2016]

$$\bar{s}(T) = \frac{\pi k_B^2 T}{3\hbar v_s n} \ , \tag{6.32}$$

which depends on the T $= 0$ value (6.4) of the sound velocity.

Using Eq. (6.32), one derives the result

$$\left(\frac{\partial T}{\partial n}\right)_{\bar{s}} = \frac{3\hbar v_s \bar{s}}{\pi k_B^2}\left(1 + \frac{6\hbar n v_s \beta(\gamma)}{\pi E_F}\right) \ , \tag{6.33}$$

where we have used Eq. (6.10) for the density derivative of the sound velocity at constant entropy.

From the low-T expansion (6.8), Eq. (6.32), the coefficient (6.9) and by introducing the interaction parameter (6.2), one calculates the adiabatic density variation of the chemical potential

$$\left(\frac{\partial \mu}{\partial n}\right)_{\bar{s}} = \frac{m}{n}v_s^2 + \frac{(k_B T)^2}{nE_F}\left(\frac{12n\hbar v_s}{\pi E_F}\beta^2(\gamma) - \gamma\frac{\partial \beta(\gamma)}{\partial \gamma}\right) \ . \tag{6.34}$$

By inserting (6.33) and (6.34), in Eq. (6.31), one finally finds the low-temperature expansion

$$\left(\frac{\partial P(T,\gamma)}{\partial n}\right)_{\bar{s}} = \left(\frac{\partial P}{\partial n}\right)_{T=0} + E_F\delta(\gamma)\left(\frac{T}{T_F}\right)^2 \tag{6.35}$$

of the adiabatic inverse compressibility, where

$$\left(\frac{\partial P(\gamma)}{\partial n}\right)_{T=0} = mv_s^2(\gamma) \tag{6.36}$$

is the T $= 0$ value of the inverse compressibility and we have defined the positive quantity

$$\delta(\gamma) = \frac{24}{\pi^2}\beta^2(\gamma)\frac{v_s(\gamma)}{v_F} - \gamma\frac{\partial \beta(\gamma)}{\partial \gamma} + \frac{\pi^2}{6}\frac{v_F}{v_s(\gamma)} + 2\beta(\gamma) \ , \tag{6.37}$$

---

[2]From the entropy

$$\frac{S}{k_B} = \sum_i \left[\frac{\beta\left(\epsilon_i - \mu\right)}{e^{\beta(\epsilon_i - \mu)} - 1} - \ln\left(1 - e^{\beta(\mu - \epsilon_i)}\right)\right]$$

one considers the low-T description of a gas of non-interacting phonons $\mu = 0$ with linear dispersion $\epsilon(p) = v_s p$. By replacing the sum with an integral in momentum space, one finally finds Eq. (6.32). The same equation can be also calculated starting from the expression of energy [Pitaevskii and Stringari, 2016]:

$$E = \sum_i \frac{\epsilon_i}{e^{\beta(\epsilon_i - \mu)} - 1}$$

and its low-T expansion:

$$E(T) = \frac{\pi L \left(k_B T\right)^2}{6\hbar v_s}$$

which, combined with Eq. (6.7) of the free energy, reproduces Eq. (6.32).

---

which is reported in Fig. 6.7 together with its asymptotic limits in the Bogoliubov and Tonks-Girardeau regimes. The first corrections $\gamma \ll 1$ and $\gamma \gg 1$ for small and large interaction parameter, respectively, vanish like for the $\beta(\gamma)$ coefficient. Indeed, the BG limit describes very well the curve (6.37) up to $\gamma \sim 1$ and the TG regime holds for values larger than $\gamma \sim 10$ of the interaction parameter.
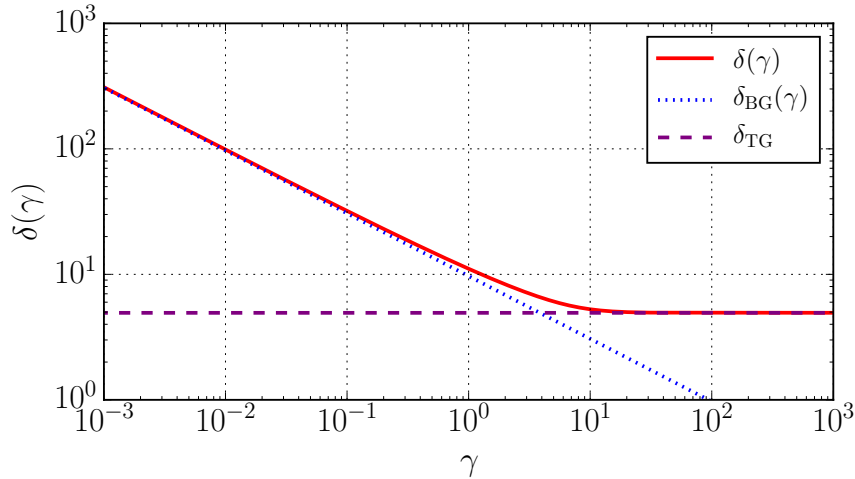
Figure 6.7: Curvature $\delta(\gamma)$ of the low-temperature expansion of the adiabatic inverse compressibility (red solid line). Both BG (blue dotted line) and TG (purple dashed line) analytical limits $\delta_{\text{BG}}(\gamma) = \frac{5}{16}\frac{\pi^3}{\sqrt{\gamma}}$ and $\delta_{\text{TG}} = \frac{\pi^2}{2}$, respectively, are also reported. From De Rosi et al. [2017].

The adiabatic inverse compressibility provides directly the sound velocity at finite temperature $mv_s^2 = (\partial P/\partial n)_{\bar{s}}$. From Eq. (6.35), one can calculate the phononic low-T expansion of the adiabatic sound velocity

$$v_s(T, \gamma) = \sqrt{v_s^2(\gamma) + \frac{E_F}{m}\delta(\gamma)\left(\frac{T}{T_F}\right)^2}\,, \tag{6.38}$$

being $v_s(\gamma)$ the $T = 0$ Lieb-Liniger sound speed (6.4).

6.4.2 Isothermal inverse compressibility

By fixing the temperature T in Eq. (6.31) and by considering the expansion of the chemical potential (6.8), one can also calculate the low-T expression for the isothermal inverse compressibility

$$\left(\frac{\partial P(T, \gamma)}{\partial n}\right)_T = \left(\frac{\partial P}{\partial n}\right)_{T=0} + E_F\eta(\gamma)\left(\frac{T}{T_F}\right)^2 \tag{6.39}$$

where we have defined the negative dimensionless coefficient

$$\eta(\gamma) = -2\beta(\gamma) - \gamma\frac{\partial\beta(\gamma)}{\partial\gamma}\,. \tag{6.40}$$

Notice that the thermal corrections to the isothermal and adiabatic inverse compressibilities have opposite sign, being the coefficient $\eta(\gamma)$ always negative. The absolute value of $\eta(\gamma)$ is reported in Fig. 6.8 together with its asymptotic limits in the Bogoliubov and Tonks-Girardeau regimes. The negative value of $\eta(\gamma)$ is the consequence of the peculiar temperature dependence of the free energy (6.7). As in the case of $\delta(\gamma)$, the first corrections for small $\gamma \ll 1$ and large $\gamma \gg 1$ interaction parameter vanish in $\eta(\gamma)$.
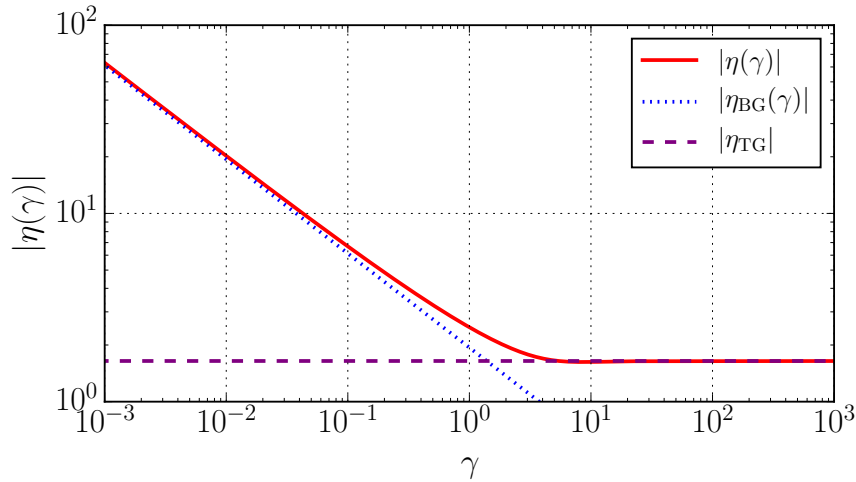
Figure 6.8: Absolute value of the curvature $\eta(\gamma)$ of the low-temperature expansion of the isothermal inverse compressibility (red solid line). Both BG (blue dotted line) and TG (purple dashed line) analytical limits $\eta_{\mathrm{BG}}(\gamma) = -\pi^3/(16\sqrt{\gamma})$ and $\eta_{\mathrm{TG}} = -\pi^2/6$, respectively, are also reported. From De Rosi et al. [2017].

6.5   Gas on a ring

The physics in one dimension is unusual in many aspects. The mean–field regime is reached at *large* densities contrarily to what happens in three dimensions where the weakly–interacting limit corresponds to small densities, according to the limit $na^3 \to 0$. For a fixed number of particles N the mean–field limit in one dimension, $n|a_{1D}| \to \infty$, can be obtained either increasing the linear density $n = N/L$, by decreasing the system size L, or by increasing the s–wave scattering length a_{1D}, i.e. decreasing the coupling constant $g_{1D} = -2\hbar^2/ma_{1D}$. Asymptotically, at a certain point, the size of the system L will become comparable to the healing length

$$\xi = \sqrt{\frac{\hbar^2}{2mg_{1\mathrm{D}}n}} \tag{6.41}$$

and finite–size effects will become important. This should be contrasted to the three-dimensional case where the mean–field regime is instead achieved by increasing the system size L which consequently becomes larger than the healing length.

Finite–size effects depend on the system geometry. Interestingly, periodic boundary conditions (PBC), commonly used as a mathematical tool in three–dimensional world, in one dimension can be explicitly realized in a ring and have consequently a direct physical interest. This is another peculiarity of the one–dimensional world. In the following we calculate the finite–size dependence of thermodynamic quantities for a gas confined in a ring whose properties are then equivalent to the ones of a linear 1D system satisfying PBC. If one considers a plane wave $\propto e^{ikz}$ and one imposes PBC, one finds that the momentum is quantized according to

$$p_i = \hbar k_i = \frac{2\pi\hbar n_i}{L} \tag{6.42}$$

where $n_i = 0, \pm$ are integers. Moreover, in 1D, all the integrals in momentum space, defined in the thermodynamic limit ($N, L \to +\infty$, $n = $ finite), are replaced by a sum over

the discretized momenta (6.42) as:

$$\int_{-\infty}^{+\infty} dp \to \frac{2\pi\hbar}{L} \sum_{p=-\infty}^{+\infty} \quad . \tag{6.43}$$

In the following, we calculate the finite-size corrections in both BG and TG regimes at zero temperature for a finite number of particles.

6.5.1 Bogoliubov regime at $T = 0$

Let us consider the T = 0 ground-state energy per particle given by

$$\frac{E_0}{N} = \frac{1}{2}g_{1D}n + \frac{1}{2N} \sum_{p=-\infty}^{+\infty} \left[\epsilon(p) - g_{1D}n - \frac{p^2}{2m} \right] \tag{6.44}$$

corresponding to the Bogoliubov regime of small γ, where $\epsilon(p)$ is provided by the Bogoliubov spectrum (6.19). Equation (6.44) differs from Eq. (6.18) because it contains the $p = 0$ term in the sum. This term has been included in order to avoid self-interaction effects in the leading mean-field term of Eq. (6.18) which should be replaced by $g_{1D}(N-1)/(2L)$.

By introducing the discretized values of p (6.42), the energy can be rewritten in the form

$$\frac{E_0}{N} = \frac{1}{2}g_{1D}n \left[1 + \sqrt{\gamma}G(y) \right] \tag{6.45}$$

where we have introduced the dimensionless variable

$$y = \gamma N^2, \tag{6.46}$$

depending on the interaction parameter γ and the function

$$G(y) = \frac{2}{y\sqrt{y}} \sum_{n_i=0}^{+\infty} \left[2\pi n_i \sqrt{y + (\pi n_i)^2} - 2(\pi n_i)^2 - y \right] + \frac{1}{\sqrt{y}} \quad , \tag{6.47}$$

where the adding of the quantity $1/\sqrt{y}$ ensures that the term $n_i = 0$ in the sum is counted just once.

By using the Euler Mac-Laurin expansion (see Appendix M), one can calculate the expression for the series (6.47) for large values of y:

$$G(y \gg 1) \approx -\frac{4}{3\pi} - \frac{\pi}{3y} \quad . \tag{6.48}$$

In Fig. 6.9 we report the comparison of the series (6.47) with its expansion (6.48). We notice that the two curves agree in excellent way for $y > 10$. The thermodynamic limit $-4/(3\pi)$ is also reported.

For large number of particles, the ground-state energy per particle (6.45) then takes the form:

$$\frac{E_0}{N}(\gamma N^2 \gg 1, \gamma \ll 1) \approx \frac{1}{2}g_{1D}n \left[1 - \frac{4}{3\pi}\sqrt{\gamma} - \frac{\pi}{3N^2\sqrt{\gamma}} \right] \tag{6.49}$$

and, in the thermodynamic limit, reproduces Eq. (6.20). The condition $y = \gamma N^2 \gg 1$ is equivalent to requiring that the healing length (6.41) be smaller than the size L of the system.

The ground-state energy contains three contributions: the leading term corresponds to the usual mean field energy, the second contribution arises from the quantum fluctuations
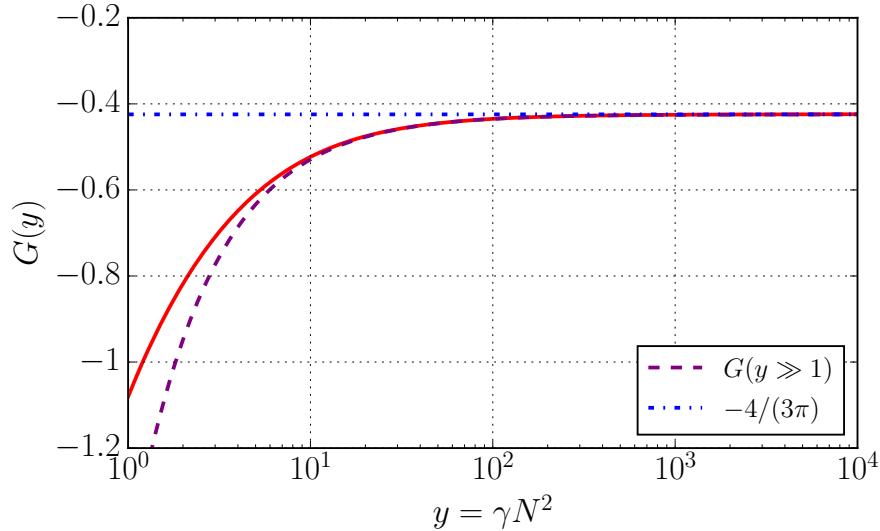
Figure 6.9: Comparison of the numerical series $G(y)$ (6.47) (red solid line) and its analytical expansion (6.48) (purple dashed line) holding for $y \gg 1$. The blue dot-dashed line represents the thermodynamic value. From De Rosi et al. [2017].

and is a one-dimensional analog of the Lee-Huang-Yang correction in 3D, while the last term accounts for finite-size effects and depends explicitly on the interaction parameter γ.

Finite size corrections can be sizeable, as clearly shown by Fig. 6.10 where we report the energy per particle as a function of y for the thermodynamic limit (6.20) (dot-dashed line), the Bethe-Ansatz (BA) calculation (circle), the Bogoliubov expression (6.45) (solid line) and the expansion (6.49) (dashed line). The figure reveals a general good agreement between the BA and the Bogoliubov predictions (6.45), except for $\gamma = 1$, where Eq. (6.45), being based on the Bogoliubov approach, is no longer adequate.
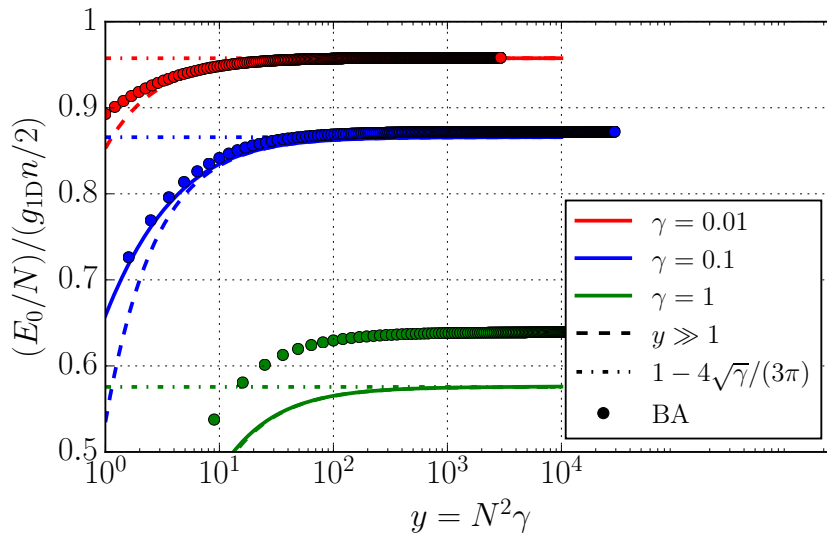
Figure 6.10: Comparison of the ground state energy per particle, in BG units, as a function of $y = \gamma N^2$ in the thermodynamic limit of Bogoliubov theory (6.20) (dot-dashed line), the Bethe-Ansatz (BA) calculation (circle), the Bogoliubov expression (6.45) (solid line) and the $y \gg 1$ expansion (6.49) (dashed line), for several values of the interaction parameter γ. From De Rosi et al. [2017].

The chemical potential can be obtained by deriving Eq. (6.44) with respect to N, at fixed L. One finds

$$\mu = \left(\frac{\partial E_0}{\partial N}\right)_L = g_{1D}n\left[1 + \frac{1}{2N}\sum_{p=-\infty}^{+\infty}\left(\frac{p^2}{2m}\frac{1}{\epsilon(p)} - 1\right)\right] \qquad (6.50)$$

which can be rewritten as $\mu = g_{1D}n[1 + \sqrt{\gamma}F(y)]$, where y is provided by Eq. (6.46) and we have introduced the series

$$F(y) = \frac{1}{\sqrt{y}}\sum_{n_i=0}^{+\infty}\left(\frac{\pi n_i}{\sqrt{y + (n_i\pi)^2}} - 1\right) + \frac{1}{2\sqrt{y}} \qquad (6.51)$$

depending on the quantized momenta (6.42) and such that the zero-momentum term is accounted once. The Euler Mac-Laurin expression, applied to the sum (6.51), yields

$$F(y \gg 1) \approx -\frac{1}{\pi} - \frac{\pi}{12y} \qquad (6.52)$$

holding in the $y \gg 1$ limit. In Fig. 6.11 we report the comparison of the series (6.51) with its expansion (6.52) holding for $y \gg 1$. The two curves agree very well for $y > 10$.
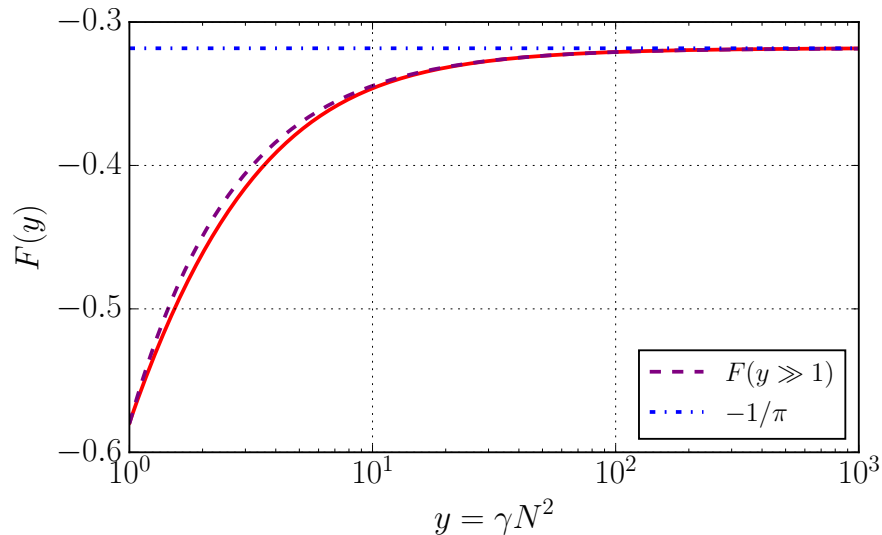
Figure 6.11: Comparison of the numerical series $F(y)$ (6.51) (red solid line) and its analytical expansion (6.52) (purple dashed line) holding for $y \gg 1$. The blue dot-dashed line represents the thermodynamic value. From De Rosi et al. [2017].

Using Eq. (6.52), one can finally write the following expansion for the chemical potential

$$\mu(\gamma N^2 \gg 1, \gamma \ll 1) \approx g_{1D}n\left[1 - \frac{\sqrt{\gamma}}{\pi} - \frac{\pi}{12N^2\sqrt{\gamma}}\right] . \qquad (6.53)$$

In Fig. 6.12 we report the results for the chemical potential as a function of y (6.46) for the thermodynamic limit (6.21) (dot-dashed line), the BA calculation (symbols) and the Bogoliubov expression (6.50) (solid line). The $y \gg 1$ expansion (6.53) practically coincides with the full series (6.50). The square symbol corresponds to the "forward" definition $\mu_+ = E_0(N+1) - E_0(N)$ of the chemical potential, the star symbol to the "backward" expression $\mu_- = E_0(N) - E_0(N-1)$, while the circles to the "symmetric" value $\bar{\mu} = (\mu_+ + \mu_-)/2$. While the three definitions of the chemical potential coincide in the

thermodynamic limit $N \to \infty$, they are different in a finite system [3]. In particular, the symmetric definition $\bar{\mu}$ well agrees with the calculation (6.50), based on the differential definition $\mu = (\partial E_0/\partial N)_L$, except for the $\gamma = 1$ case.
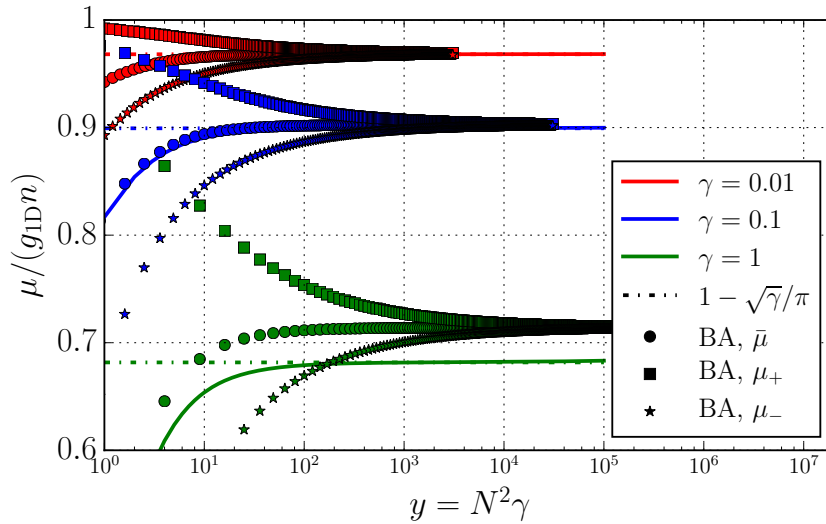
Figure 6.12: Comparison of the chemical potential in BG units as a function of $y = \gamma N^2$ in the thermodynamic limit (6.21) (dot-dashed line), the Bethe-Ansatz (BA) calculation (symbols) and the Bogoliubov expression (6.50) (solid line), for several values of the interaction parameter γ. For the BA: $\mu_+ = E_0(N+1) - E_0(N)$ (square), $\mu_- = E_0(N) - E_0(N-1)$ (star) and $\bar{\mu} = (\mu_+ + \mu_-)/2$ (circle). From De Rosi et al. [2017].

From Eq. (6.50), one can also calculate the sound velocity (6.4), corresponding to the density derivative of the chemical potential for a fixed value of L. The resulting expression,

$$v_s(\gamma) = v_s^{\mathrm{BG}}(\gamma) \sqrt{1 - \frac{g_{1\mathrm{D}} n}{2N} \sum_{p=-\infty}^{+\infty} \left(\frac{p^2}{2m} \right)^2 \frac{1}{\epsilon^3(p)}} \tag{6.54}$$

with $v_s^{\mathrm{BG}}(\gamma)$ the sound velocity defined in the Bogoliubov regime, used in Fig. 6.1. The above expression can be rewritten as $v_s(\gamma) = v_s^{\mathrm{BG}}(\gamma)\sqrt{1 - \sqrt{\gamma} H(y)}$ where we have defined the series

$$H(y) = \frac{\sqrt{y}}{2} \sum_{n_i=0}^{+\infty} \frac{\pi n_i}{[y + (\pi n_i)^2]^{3/2}} , \tag{6.55}$$

after introducing the variable y (6.46) and the quantized momenta (6.42). As before, we apply the Euler Mac-Laurin formula and we find the expansion

$$H(y \gg 1) \approx \frac{1}{2\pi} - \frac{\pi}{24y} \tag{6.56}$$

holding in the $y \gg 1$ limit, yielding the asymptotic expansion

$$v_s(\gamma N^2 \gg 1, \gamma \ll 1) \approx v_s^{\mathrm{BG}}(\gamma) \sqrt{1 - \frac{\sqrt{\gamma}}{2\pi} + \frac{\pi}{24N^2 \sqrt{\gamma}}} \tag{6.57}$$

for the sound velocity.

---

[3]Important differences between μ_+ and μ_- are known to occur in nuclear physics [Bohr and Mottelson, 1969], where they are also employed to identify pairing effects of superfluid nature.

6.5.2 Tonks–Girardeau regime at $T = 0$

According to Girardeau [1960], the ground-state energy of the gas in the strongly-interacting limit is the same as that of an ideal Fermi gas. The energy for finite number of particles N in a box with periodic boundary conditions is obtained by summing the energy of the single-particle levels in the box,

$$\frac{E_0}{N}(N) = \frac{\hbar^2}{mN} \sum_{n_i=1}^{\frac{1}{2}(N-1)} \left(\frac{2\pi n_i}{L}\right)^2 = \frac{1}{6}\left(1 - \frac{1}{N^2}\right)\frac{\pi^2\hbar^2 n^2}{m} \ . \tag{6.58}$$

In the thermodynamic limit, $N = \infty$, Eq. (6.58) results in $E_{\text{TG}} = \pi^2\hbar^2 n^2/(6m)$. The "excluded volume" correction should be present for a finite interaction strength, see the hard–sphere like expression, Eq. (6.26), and the discussion below it. In order to incorporate the leading finite-size correction close to Tonks-Girardeau regime we replace L with $L - Na_{1D}$ in Eq. (6.58) resulting in the following expression for the energy per particle

$$\frac{E_0}{N}(N, \gamma) = \frac{1}{6}\frac{\pi^2\hbar^2 n^2}{m}\left(1 - \frac{1}{N^2}\right)\left(1 + \frac{2}{\gamma}\right)^{-2} \ . \tag{6.59}$$

For large values of the interaction parameter γ one can replace the factor $(1 + 2/\gamma)^{-2}$ with $(1 - 4/\gamma)$. In Fig. 6.13 we report the energy per particle as a function of N for the TG regime (6.58) (solid line), the hard-sphere (HS) like model (6.59) (dashed and dotted lines) and the BA solution (symbols) for several values of γ. We observe a very good agreement between the BA solution and the analytical hard-sphere (6.59) expression. For $\gamma = 1000$ the BA results are indistinguishable from the TG limit (6.58) and they are not reported in the figure. The comparison between Eq. (6.59) and Eq. (6.49) reveals that finite-size effects are less important in the TG regime since in the weakly interacting Bogoliubov regime, the correction $1/(N^2\sqrt{\gamma})$ is amplified by the smallness of γ.
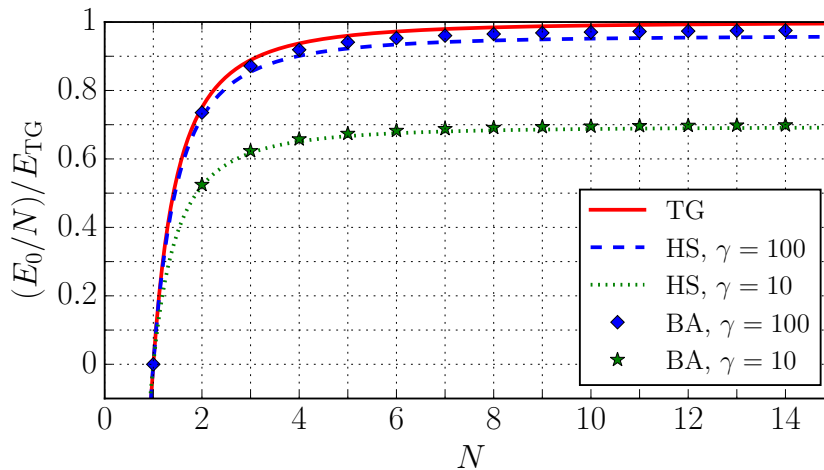
Figure 6.13: Energy per particle in units of the TG gas energy $E_{\text{TG}} = \pi^2\hbar^2 n^2/(6m)$ as a function of N. Bethe-Ansatz (BA) results (symbols) with different values of the interaction parameter γ are compared with the TG gas (6.58) (red solid line) and the hard–sphere (HS) model (6.59) (dashed and dotted lines). From De Rosi et al. [2017].

For strong repulsion we obtain the finite-size correction to the chemical potential

$$\mu(N, |\gamma| \gg 1) = \left(\frac{\partial E_0}{\partial N}\right)_L \approx E_F\left[1 - \frac{16}{3\gamma} - \frac{1}{3N^2}\left(1 - \frac{8}{\gamma}\right)\right] \tag{6.60}$$

and to the sound velocity (6.4):

$$v_s(N, |\gamma| \gg 1) \approx v_F \sqrt{1 - \frac{8}{\gamma} + \frac{4}{3\gamma N^2}} \ . \tag{6.61}$$

It is interesting to note that while the finite-size correction to the energy (6.59) and the chemical potential (6.60) scales as $1/N^2$ with the number of particles, such a correction is instead asymptotically vanishing in the sound velocity (6.61).

From Eq. (6.59), one calculates the explicit expression for the chemical potential $\mu = (\partial E_0/\partial N)_L$:

$$\mu(N, \gamma) = \frac{E_F}{\left(1 + \frac{2}{\gamma}\right)^3} \left[1 + \frac{2}{3\gamma} - \frac{1}{3N^2}\left(1 - \frac{2}{\gamma}\right)\right] \tag{6.62}$$

which, in the thermodynamic limit, gives

$$\mu(\gamma) = \frac{E_F}{\left(1 + \frac{2}{\gamma}\right)^3}\left(1 + \frac{2}{3\gamma}\right) \tag{6.63}$$

and for large values of the interaction parameter γ provides Eq. (6.60).

In Fig. 6.14, we plot the chemical potential (6.62) (solid line) as a function of N for different values of γ. In the same figure we plot also the values of μ_+ and μ_- which differ from the symmetric value $\bar\mu = (\mu_+ + \mu_-)/2$ for small values of N (See note 3), similarly to the case of the weakly interacting Bose gas. Differently from the weakly interacting BG gas, the symmetric value $\bar\mu$ however exhibits significant deviations with respect to the differential estimate $(\partial E_0/\partial N)_L$, for small values of N.
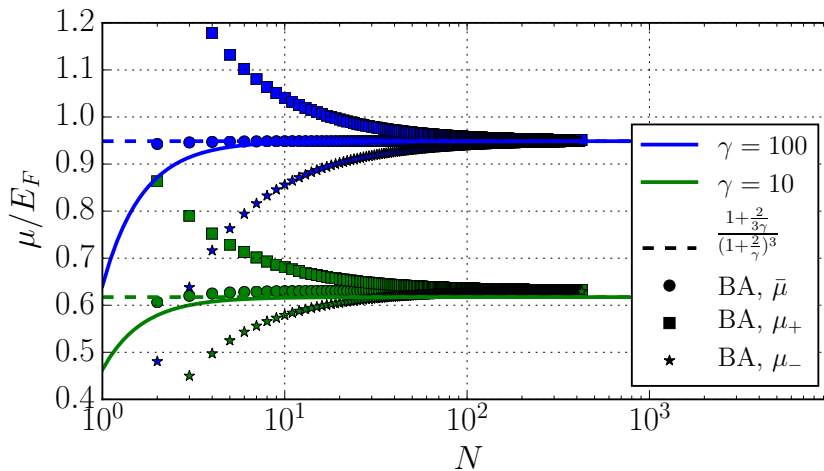
Figure 6.14: Chemical potential at $T = 0$ in Fermi units as a function of the number of particles N in the TG regime (6.62) for fixed values of γ (solid line). The dashed lines correspond to the thermodynamic limit $[1 + 2/(3\gamma)]/(1 + 2/\gamma)^3$ of the TG model (6.63). The symbols correspond to the Bethe-Ansatz (BA) calculation: $\mu_+ = E_0(N+1) - E_0(N)$ (square), $\mu_- = E_0(N) - E_0(N-1)$ (star) and $\bar\mu = (\mu_+ + \mu_-)/2$ (circle). From De Rosi et al. [2017].

Conclusions & Perspectives

In the course of describing my formative moment in 1978, I have already implicitly given my four basic rules for research. Let me now state them explicitly, then explain. Here are the rules:
1. Listen to the Gentiles
2. Question the question
3. Dare to be silly
4. Simplify, simplify.

Paul Krugman - *"How I Work"*,
American Economist (1993)

This thesis is dedicated to the theoretical investigation of collective oscillations in low-dimensional harmonically trapped atomic gases and the thermodynamics of the 1D uniform Bose gas.

In the first part, we have derived a unified description of the discretized collective oscillations of quantum gases in different conditions of trapping and dimensionality.

A major result is given by the derivation of a general hydrodynamic equation for the velocity field [Eq. (3.16)], depending solely on the adiabatic and isothermal compressibilities of the gas. This equation takes a particularly simple form in the case of systems exhibiting a polytropic equation of state, characterised by a power law dependence of the pressure on the density ($P \propto n^q$), for a fixed value of the entropy. The polytropic equation of state characterises a significant class of many-body configurations of either bosonic and fermionic nature.

We analytically calculated the collective frequencies for pancake and cigar configurations, where the equation of state can be obtained from the 3D equation of state using the local density approximation, as well as in the deep 2D and 1D regimes where the motion is instead frozen along the direction of the confinement. Special emphasis is given to the lowest breathing mode, whose frequency has been shown to depend explicitly on the value of the polytropic coefficient q, and to its coupling with the quadrupole oscillations in anisotropic external potentials.

We have emphasised, in particular, the comparison between the $T = 0$ results, characterising the behaviour of superfluids, and the high-temperature behaviour, both in the hydrodynamic and collisionless regime.

Our results can be used as a starting point to calculate the collective frequencies in systems whose equation of state deviates from the polytropic law and the solution of the hydrodynamic equations can be handled using a perturbative approach. This procedure, first employed to estimate the frequency shifts of dilute Bose gases caused by beyond mean-field effects [Pitaevskii and Stringari, 1998], was developed in a systematic way by Astrakharchik [2005] in a variety of configurations of different dimensionality and quantum statistics. It was recently applied by Merloti et al. [2013] to explore the breakdown of scale invariance in a quasi-two-dimensional Bose gas due to the presence of the third dimension.

Another interesting perspective of our results is given by the study of the collective frequencies in 1D harmonically trapped Bose gases at finite temperature which can provide a useful test for the achievement of the collisional (hydrodynamic) condition at finite temperature. This outlook has been developed in the second part of the present thesis, by considering different regimes of interaction, temperature and number of particles.

For this purpose, we have developed two different theoretical methods: the hydrodynamic approach, rewritten in an easier variational formulation, and the more microscopic sum-rule approach. While the first method, which can be applied only within the Local Density Approximation (LDA), enabled us to calculate the hydrodynamic frequencies for all interaction and temperature regimes, the sum-rule approach allowed us to calculate the collective frequencies even beyond the LDA and in the collisionless regime of high temperatures.

The inverse energy weighted (m_{-1}), the energy weighted (m_1) and the cubic energy weighted (m_3) sum rules are calculated and their applicability to exploit the behaviour of the collective frequencies at zero as well as at finite temperature have been explicitly discussed. We have furthermore developed the formalism of the virial theorem which permits the derivation of more compact expressions for the average excitation frequencies, defined by the ratio $\hbar^2 \omega^2 = m_3/m_1$.

The combined use of the hydrodynamic and sum-rule approaches enabled us to draw important conclusions about the temperature dependence of the collective frequencies. While in the case of the lowest breathing mode the frequencies in the high-temperature hydrodynamic and collisionless regimes coincide and are equal to $2\omega_z$, where ω_z is the oscillator frequency; a different scenario emerges in the case of the dipole compression mode excited by the operator $f_{DC}(z) = z^3/3 - z\langle z^2 \rangle$. In the dipole compression case, the hydrodynamic approach, in fact, predicts the value $\sqrt{7}\omega_z$ for the collective frequency, while in the collisionless regime the same operator gives rise to the excitation of two different frequencies given by ω_z and $3\omega_z$. By calculating the response of the system to a sudden perturbation of the form $\lambda f_{DC}(z)\Theta(t)$, we predict a typical beating between the two frequencies whose experimental observation would provide a useful signature of the achievement of the collisionless regime. The investigation of the temperature dependence of the dipole compression mode is then expected to provide valuable information on the transition between the hydrodynamic and collisionless regime and on the role of collisions in 1D interacting Bose gases.

The sum-rule approach is also expected to provide a useful tool to explore the behaviour of the dipole compression frequencies when the Local Density Approximation is not available at zero as well as at finite temperature and for different interaction regimes. This could be the object of a future investigation.

An interesting perspective is the application of our results to quantum fluids of light [Carusotto and Ciuti, 2013], which exhibit some analogies with BECs. We would like to provide the theoretical description of normal modes in light within nonlinear photonics [Larré and Carusotto, 2015], by including also the finite temperature case [Chiocchetta et al., 2016]. The final goal of this project is not only the building of the still missing theoretical framework of collective oscillations in quantum fluids of light but also the first measurement of normal modes in this system and a better understanding of nature (like the EOS) of the light itself. This project will be carried out in collaboration with Prof. Iacopo Carusotto (University of Trento, Italy) and Dr. Pierre-Élie Larré (Laboratoire Kastler–Brossel, UPMC, Paris, France).

In the last Chapter we have investigated the low-temperature properties of 1D Bose gases along the whole Bogoliubov (BG) — Tonks-Girardeau (TG) crossover.

We have shown that, at low temperature, the chemical potential exhibits a typical T^2 behavior, which follows from the leading contribution to thermodynamics arising from the

thermal excitation of phonons, similarly to what happens in superfluids. The chemical potential is always a decreasing function of T at high temperature, thus the T^2 increase exhibited by the chemical potential at low temperature is responsible for a typical non-monotonic behaviour as a function of T. The coefficient of the T^2 law has been calculated using the Lieb-Liniger results for the sound velocity and the resulting behaviour has been successfully compared with thermodynamic functions obtained from the Yang-Yang theory of 1D interacting Bose gases. We have also presented results for the temperature dependence of the isothermal and adiabatic inverse compressibilities. In particular we have shown that the T^2 correction has opposite sign in the two cases.

In the second part of the Chapter we have focused on the corrections to the thermodynamic functions caused by the finite size of the system. To this purpose, we have considered the useful ring geometry and the mapping with the 1D problem where calculations are carried out using periodic boundary conditions. Explicit results have been obtained in the weakly and strongly interacting regimes where, at zero temperature, the first corrections to the thermodynamic limit, due to finite-size effects, can be calculated in analytic form, in excellent agreement with the numerical results provided by the Bethe-Ansatz. We have found that finite-size corrections are particularly important in the weakly interacting regime where the healing length can easily become comparable to the size of the system.

Appendices

Appendix A

EOS and polytropic coefficient

In this Appendix we identify the polytropic coefficient q characterizing the equation of state (3.1) of a uniform gas in different low-dimensional configurations and for different quantum statistics (see Tables 3.1 and 3.2).

Let us first consider the ideal situation of zero temperature. As already discussed in Section 3.1, a first interesting two-dimensional regime is the so-called pancake where the system keeps, locally, its 3D nature in the sense that the chemical potential is much larger than axial oscillator energy $\mu \gg \hbar\omega_z$. In this case, we can apply the local density approximation (LDA) along the axial direction and write the chemical potential in the form

$$\mu_0 = \mu(n) + \frac{m}{2}\omega_z^2 z^2 \tag{A.1}$$

which allows us to determine the z-dependence of the density profile. The value of μ_0 coincides with the chemical potential $\mu(n)$ calculated at $z = 0$ and is fixed by the normalization condition $n_{2D} = \int dz\, n(\mathbf{r})$. The quantity μ_0 plays consequently the role of the 2D chemical potential and exhibits an explicit dependence on the 2D density n_{2D}. This dependence characterises the 2D equation of state and, for simplicity, we will omit the suffix 0 in μ_0 and use the simpler notation $\mu(n_{2D})$ to characterise the equation of state of the two-dimensional gas.

The 2D equation of state of a pancake gas is easily derived in the case of dilute Bose gas where the 3D equation of state has the form $\mu = gn$ and the use of the LDA procedure (A.1) gives the result [Pitaevskii and Stringari, 2016]

$$\mu^B(n_{2D}) = \left(\frac{3\pi\hbar^2\omega_z a n_{2D}}{\sqrt{2m}}\right)^{2/3} , \tag{A.2}$$

characterized by the value $q = 5/3$ for the polytropic coefficient, see Eq. (3.1) and (3.4).

An analogous calculation can be carried out for a pancake Fermi gas at unitarity, where the 3D equation of state has the form $\mu = \xi_B \frac{\hbar^2}{2m}(3\pi^2 n)^{2/3}$, with ξ_B the Bertsch parameter, yielding [Pitaevskii and Stringari, 2016]

$$\mu^F(n_{2D}) = \left(2\pi\xi_B^{\frac{3}{2}}\omega_z \frac{\hbar^3}{m} n_{2D}\right)^{1/2} , \tag{A.3}$$

and hence the value $q = 3/2$ for the polytropic coefficient.

Similar results can be obtained in cigar 1D-like configurations where the gas is harmonically trapped along the $x - y$ directions and satisfies the LDA along the radial direction

$$\mu_0 = \mu(n) + \frac{m}{2}\omega_\perp^2 r_\perp^2 , \tag{A.4}$$

where, for simplicity, we have considered an isotropic trap $\omega_\perp = \omega_x = \omega_y$ in the plane and we have defined the radial coordinate $r_\perp = \sqrt{x^2 + y^2}$. In this case, after integrating the radial 3D Thomas-Fermi profile, one finds [Pitaevskii and Stringari, 2016]

$$\mu^B(n_{1D}) = 2\hbar\omega_\perp (an_{1D})^{1/2} \tag{A.5}$$

and

$$\mu^F(n_{1D}) = \left(\frac{\xi_B \hbar^2}{2m}\right)^{3/5} \left(\frac{15}{4}\pi m\omega_\perp^2 n_{1D}\right)^{2/5} \tag{A.6}$$

for the chemical potential of the cigar Bose and unitary Fermi gas respectively where $n_{1D} = \int dxdy n(\mathbf{r})$. From the above equations, one derives the values $q = 3/2$ and $q = 7/5$ for the polytropic coefficients in the Bose and unitary Fermi cigars, respectively which are reported in the Table 3.1.

The results $q = 3/2$ and $q = 7/5$ for the polytropic coefficients of the pancake and cigar Fermi gas at unitarity holds also at finite temperature. In fact the 3D result for the equation of state, given by Eq. (3.1) with $q = 5/3$, can be usefully rewritten in the form [Ho, 2004, Hou et al., 2013b]

$$P_{3D}(x,T) = f_p(x)\frac{k_B T}{\lambda_T^3} \tag{A.7}$$

and

$$n_{3D}(x,T) = \frac{f'_p(x)}{\lambda_T^3} = \frac{f_n(x)}{\lambda_T^3} \tag{A.8}$$

where the temperature dependence of the 3D pressure and density follows from dimensionality arguments. We have here introduced the thermal wavelength $\lambda_T = \sqrt{2\pi\hbar^2/mk_B T}$, the dimensionless functions $f_p(x)$ and its derivative $f_n(x) = f'_p(x)$. The dimensionless parameter $x = \mu/k_B T$, fixed by the ratio between the chemical potential and the temperature of the gas, determines the entropy per particle $\bar{s}$ according to the relationship

$$\frac{\bar{s}(x)}{k_B} = \frac{5}{2}\frac{f_p(x)}{f_n(x)} - x \ . \tag{A.9}$$

The above results reflect the universality of the 3D uniform Fermi gas at unitarity.

By applying the local density approximation (A.1) along the z-direction in the pancake geometry and along the $x - y$ plane (A.4) in the cigar geometry, after integration of the density and of the pressure profile along the same directions, from Eq. (A.7) and Eq. (A.8) one easily finds a new temperature dependence of the 2D and 1D pressure and density for a given value of the entropy, fixed by the ratio $x = \mu/k_B T$. For the pancake configuration one finds

$$P_{2D}(x_{2D},T) = \frac{k_B T}{\lambda_T^3}\sqrt{\frac{2k_B T}{m\omega_z^2}}F_p^{2D}(x_{2D}) \tag{A.10}$$

and

$$n_{2D}(x_{2D},T) = \frac{1}{\lambda_T^3}\sqrt{\frac{2k_B T}{m\omega_z^2}}F_n^{2D}(x_{2D}) \tag{A.11}$$

while for the cigar 1D configuration the result is [Hou et al., 2013b]

$$P_{1D}(x_{1D},T) = \frac{k_B T}{\lambda_T^3}\frac{2k_B T}{m\omega_\perp^2}F_p^{1D}(x_{1D}) \tag{A.12}$$

and

$$n_{1D}(x_{1D},T) = \frac{1}{\lambda_T^3}\frac{2k_B T}{m\omega_\perp^2}F_n^{1D}(x_{1D}) \tag{A.13}$$

holding at all temperatures. From the above results one easily finds, using Eq. (3.1) the values $q = 3/2$ and $q = 7/5$ for the polytropic coefficient in the 2D and 1D cases, independent of temperature. In Eq. (A.10) and (A.11), we have defined the integrated functions $F_{n,p}^{2D}(x_{2D}) = \int_{-\infty}^{+\infty} dz' f_{n,p}(x')$ with $x_{2D} = \mu_0/k_B T$, while in Eq. (A.12) and (A.13) the analogous 1D integrated functions are $F_{n,p}^{1D}(x_{1D}) = 2\pi \int_0^{+\infty} dr'_\perp r'_\perp f_{n,p}(x')$ with $x_{1D} = \mu_0/k_B T$. The same results for the values of q hold also for the ideal Fermi gas as well as for the ideal Bose gas above T_c where the thermodynamic functions can be written in the same form as for the unitary Fermi gas, the functions f_n and f_p being of course different.

So far we have considered the pancake and cigar geometries where the local density approximation allows us to safely use the 3D equation of state locally. The situation is different in the opposite regime of tight axial or radial confinement where the motion is frozen to the lowest harmonic oscillator wave function along the tight directions. At zero temperature the condition for being in these deep 2D and 1D regimes is given by $\mu \ll \hbar\omega_z$ and $\mu \ll \hbar\omega_\perp$, respectively. At high temperature the conditions are, instead, $k_B T \ll \hbar\omega_z$ and $k_B T \ll \hbar\omega_\perp$, respectively, see Sec. 2.1. At $T = 0$ these low dimensional regimes are easily described in the case of a weakly interacting Bose gas where the use of Gross-Pitaevskii theory yields the simple results for the 2D and 1D equations of state

$$\mu^B(n_{2D}) = g_{2D} n_{2D} \tag{A.14}$$

and

$$\mu^B(n_{1D}) = g_{1D} n_{1D} \tag{A.15}$$

apart from unimportant additional constant terms. In Eq. (A.14) the 2D coupling constant is given by [Pitaevskii and Stringari, 2016]

$$g_{2D} = \sqrt{8\pi} \frac{\hbar^2}{m} \frac{a}{a_z} \tag{A.16}$$

and is fixed by the ratio a/a_z between the 3D $s-$wave scattering length and the axial harmonic oscillator length $a_z = \sqrt{\hbar/m\omega_z}$, while in the 1D case one finds the result [Pitaevskii and Stringari, 2016]

$$g_{1D} = 2a\hbar\omega_\perp . \tag{A.17}$$

Result (A.14) for the equation of state of the 2D Bose gas holds only in the limit of weak coupling ($a \ll a_z$), ensuring the absence of quantum anomaly effects [Papoular and Stringari, 2015]. The 1D equation of state (A.15) instead holds provided $n_{1D} a_\perp^2/a \gg 1$. In both cases (also called 2D and 1D mean field regimes) one identifies the value $q = 2$ for the polytropic coefficient. Both the 2D and 1D mean field regimes have been achieved experimentally by Desbuquois et al. [2012] and Kinoshita et al. [2004], Paredes et al. [2004], respectively.

In the 1D case, extensive experimental and theoretical work has been done also to explore regimes beyond the mean field condition $n_{1D} a_\perp^2/a \gg 1$ where the many-body properties of the gas are described by Lieb-Liniger theory. In the limit $n_{1D} a_\perp^2/a \ll 1$, the gas enters the limit of impenetrable bosons also called Tonks-Girardeau regime where the gas acquires a Fermi-like behaviour and its equation of state exhibits a quadratic density dependence [Girardeau, 1960], see also Sec. 2.3:

$$\mu^{TG}(n_{1D}) = \pi^2 \frac{\hbar^2}{2m} n_{1D}^2 . \tag{A.18}$$

In this regime, the value of the polytropic coefficient is $q = 3$.

In the case of interacting Fermi gases, the theoretical description of the lower dimensional regimes is more difficult with respect to the Bose case. In two dimensions one can

still identify a BCS-BEC crossover like in the 3D case, see SubSec. 1.6.1. However, in the two-body problem, the presence of a resonance always corresponds to the occurrence of a bound state, differently from what happens in 3D where this is ensured only for positive values of the 3D scattering length, see SubSec. 1.3.2. Far from the resonance, the chemical potential of the 2D Fermi gas is described by a linear dependence on the density, both on the BEC side, where the gas is described by a 2D system of bosonic molecules, and on the deep BCS limit, where the gas approaches the ideal Fermi gas behaviour. In both cases, the value of the polytropic coefficient is $q = 2$. The same value of q characterises the equation of state of the classical gas at high temperature.

Tables 3.1 and 3.2 summarise the main results of this Appendix, reporting the values of the polytropic coefficients q in a class of interesting configurations.

Appendix B

HD equations in the presence of an external potential

In this Appendix, we derive the most relevant hydrodynamic equations used in Chap. 3 to calculate the collective frequencies in the presence of external harmonic trapping.

In order to derive Eq. (3.16), we first take the time derivative of Eq. (3.15) yielding, in the limit of small amplitude oscillations,

$$mn_0 \frac{\partial^2}{\partial t^2}\mathbf{v} = -\nabla \frac{\partial}{\partial t}P - \nabla V_{ext}\left(\frac{\partial}{\partial t}n\right) \ . \tag{B.1}$$

The time derivative of the pressure can be written as:

$$\frac{\partial P}{\partial t} = \left(\frac{\partial P}{\partial n}\right)_T \frac{\partial n}{\partial t} + \left(\frac{\partial P}{\partial T}\right)_n \frac{\partial T}{\partial t} \tag{B.2}$$

and requires the knowledge of the time derivative of the temperature.

In order to calculate $\partial T/\partial t$ it is convenient to rewrite the equation for the entropy density (3.14) in terms of the entropy per particle $\bar{s} = s/n$. By using the equation of continuity (3.13), it is immediate to find the equation

$$\frac{\partial \bar{s}(\mathbf{r},t)}{\partial t} = -\mathbf{v}(\mathbf{r},t)\nabla \bar{s}_0(\mathbf{r}) = \frac{1}{n_0^2}\left(\frac{\partial P}{\partial T}\right)_n \mathbf{v} \cdot \nabla n_0 \tag{B.3}$$

where, in deriving the second equality, we have used the thermodynamical relation

$$Td\bar{s} = c_v dT - \frac{T}{n^2}\left(\frac{\partial P}{\partial T}\right)_n dn \tag{B.4}$$

applied to equilibrium ($dT = 0$), where

$$c_v = \frac{T}{n_0^2}\left(\frac{\partial P}{\partial T}\right)_n \left(\frac{\partial n}{\partial T}\right)_{\bar{s}} \tag{B.5}$$

is the specific heat at constant volume.

On the other hand, by considering $\bar{s}$ as a function of density and temperature, one can also write

$$\frac{\partial \bar{s}}{\partial t} = \left(\frac{\partial \bar{s}}{\partial n}\right)_T \frac{\partial n}{\partial t} + \left(\frac{\partial \bar{s}}{\partial T}\right)_n \frac{\partial T}{\partial t} \ . \tag{B.6}$$

Using the equation of continuity (3.13) and thermodynamic relation (B.3), one finally obtains the useful equation

$$\frac{\partial T(\mathbf{r},t)}{\partial t} = -\frac{T}{c_v}\left(\frac{\partial P}{\partial T}\right)_n \frac{\nabla \cdot \mathbf{v}(\mathbf{r},\mathbf{t})}{n_0} \tag{B.7}$$

for the time derivative of the temperature, holding also in the presence of external trapping.

Using the equilibrium condition ($\mathbf{v} = 0$) in the Eq. (3.15)

$$\nabla P_0 = \left(\frac{\partial P_0}{\partial n_0}\right)_T \nabla n_0 = -n_0 \nabla V_{ext} \tag{B.8}$$

and the thermodynamic relation

$$\left(\frac{\partial P}{\partial n}\right)_{\bar{s}} = \left(\frac{\partial P}{\partial n}\right)_T + \left(\frac{\partial P}{\partial T}\right)_n \left(\frac{\partial T}{\partial n}\right)_{\bar{s}} \tag{B.9}$$

relating the adiabatic and isothermal compressibilities, it is easy to recast the hydrodynamic equation (B.1) in the useful form

$$m\omega^2 \mathbf{v} = -\nabla \left[\left(\frac{\partial P}{\partial n}\right)_{\bar{s}} (\nabla \cdot \mathbf{v})\right] + (\gamma_{ad} - 1)(\nabla V_{ext})(\nabla \cdot \mathbf{v}) + \nabla (\mathbf{v} \cdot \nabla V_{ext}) \tag{B.10}$$

where γ_{ad} is the adiabatic coefficient defined by Eq. (3.17) and we have considered velocity fields oscillating as $\mathbf{v}(\mathbf{r}, t) = \mathbf{v}(\mathbf{r})e^{-i\omega t}$.

Starting from Eq. (B.10), one can derive Eq. (3.20) in the case of a polytropic equation of state for which Eq. (3.2) holds. By considering, moreover, Eq. (3.5) at constant temperature, Eq. (A.1) and Eq. (3.17), one can finally rewrite:

$$\nabla \left[\left(\frac{\partial P}{\partial n}\right)_{\bar{s}} (\nabla \cdot \mathbf{v})\right] = \left(\frac{\partial P}{\partial n}\right)_{\bar{s}} \nabla (\nabla \cdot \mathbf{v}) + q (\nabla \cdot \mathbf{v}) \nabla V_{ext} \left(\frac{\gamma_{ad}}{q} - 1\right) \tag{B.11}$$

which plugged into Eq. (B.10) yields Eq. (3.20).

Appendix C

Collective frequencies from variational hydrodynamics

In this Appendix, we report the detailed calculation of the LB and the DC collective frequencies by using the variational approach, Eq. (5.5) for different interaction and T regimes.

C.1 Lowest breathing mode

Let us consider the LB mode, whose variational hydrodynamic equation is (5.6). For gases described by the polytropic EOS, Eq. (3.1), by using Eq. (3.2) holding at finite T, one gets:

$$\omega_{\mathrm{HD}}^2(LB) = \omega_z^2 + \frac{\int dz q P}{\int dz m n z^2} \tag{C.1}$$

while, at $T = 0$, from Eq. (3.6), one calculates the variational expression:

$$\omega_{\mathrm{HD}}^2(LB) = \omega_z^2 + \frac{\int dz n(q-1)\mu}{\int dz m n z^2} \; . \tag{C.2}$$

In the following, we consider the regimes of T and interaction, for which the density profile $n(z)$ can be calculated analytically.

For the classical regime of high T, $P = n k_B T$, from the Euler equation at equilibrium (5.4), one finds the density profile $n_T(z)$, Eq. (5.1). By considering the polytropic index $q = 3$ (see Table 3.2) in the variational expression, Eq. (C.1), one finally calculates the frequency $\omega_{\mathrm{HD}}(LB) = 2\omega_z$ which is the high-T HD result of Table 5.1.

We consider now the BG regime of weak interaction at $T = 0$. The density profile can be found either from Eq. (5.4) or by considering the EOS (A.15) in the LDA (A.1). It exhibits the typical inverted parabola shape of the Thomas-Fermi (TF) regime:

$$n_{\mathrm{BG}}(z) = n(0) \left(1 - z^2/Z_{TF}^2\right), \tag{C.3}$$

and $n_{\mathrm{BG}}(z) = 0$ for $|z| \geq Z_{TF}$. The peak density and the TF radius are, respectively, $n(0) = \left(9mN^2\omega_z^2/(32g_{1D})\right)^{1/3}$ and $Z_{TF} = \left(3Ng_{1D}/(2m\omega_z^2)\right)^{1/3}$. By using the polytropic index $q = 2$ (see Table 3.2) in Eq. (C.2), one finds the hydrodynamic frequency $\omega_{\mathrm{HD}}(LB) = \sqrt{3}\omega_z$, reported in Table 5.1.

Finally, we study the TG regime of strong repulsion at $T = 0$. By combining Eq. (A.18) with Eq. (A.1), we calculate the density profile:

$$n_{\mathrm{TG}}(z) = n(0)(1 - z^2/Z^2)^{1/2}, \tag{C.4}$$

and $n(z) = 0$ for $|z| \geq Z$. The peak density and the radius of the cloud are, respectively, $n(0) = \left(2mN\omega_z/(\pi^2\hbar)\right)^{1/2}$ and $Z = (2\hbar N/(m\omega_z))^{1/2}$. With the polytropic index $q = 3$ (Table 3.2) in Eq. (C.2), one calculates the LB mode frequency $\omega_{\mathrm{HD}}(LB) = 2\omega_z$, present in Table 5.1.

C.2   Dipole compression mode

We consider in this Section the DC mode, whose collective frequency can be calculated with Eq. (5.7) in the hydrodynamic regime. For polytropic EOS at finite T, one gets:

$$\omega_{\mathrm{HD}}^2(DC) = \omega_z^2 + \frac{4q \int dz P z^2}{m \int dz n \left(z^2 - \langle z^2 \rangle\right)^2} \tag{C.5}$$

while, at $T = 0$, the hydrodynamic equation becomes

$$\omega_{\mathrm{HD}}^2(DC) = \omega_z^2 + \frac{4(q-1) \int dz n \mu z^2}{m \int dz n \left(z^2 - \langle z^2 \rangle\right)^2} \tag{C.6}$$

where the average $\langle z^2 \rangle = \int dz z^2 n(z)/N$ is calculated by using the suitable density profile, according to the interaction and T regime [Kheruntsyan et al., 2005].

In a completely analogous way to the previous Section, one calculates all the collective frequencies which coincide with results of Table 5.2 of the classical, BG and TG limits.

Appendix D

Properties of commutators

In this Appendix, we report the most common properties of commutators, largely used for the calculation of sum-rules in Chap. 5.

- $[A, BC] = B[A, C] + [A, B]C$;
- $[AB, C] = A[B, C] + [A, C]B$;
- $[ABC, D] = AB[C, D] + A[B, D]C + [A, D]BC$;
- $[A, [B, C]] + [B, [C, A]] + [C, [A, B]] = 0$;
- $[z, \frac{d}{dz}]A(z) = -A(z)$, for every $A(z)$;
- $[z, A(p_z)] = i\hbar \frac{dA}{dp_z}$;
- $[p_z, A(z)] = -i\hbar \frac{dA}{dz}$;
- $[z, p] = i\hbar$;
- $[z, p_z^n] = i\hbar n p_z^{n-1}$;
- $[z^n, p_z] = i\hbar n z^{n-1}$,

where z and p_z are the position and the momentum operators in z-direction, respectively. $A(z)$ denotes a function of z and A, B and C are generic operators.

Appendix E

m_{-1} for the classical gas

In this Appendix, we report the explicit calculation of the inverse energy weighted moment m_{-1} for a classical gas at high temperature.

The small perturbation of the Hamiltonian $H_{pert} = -\lambda F$, with $\lambda \ll 1$, becomes a perturbation of the density profile, which, for high temperatures, is described by the Maxwell-Boltzmann distribution (5.1):

$$n_T^{pert}(z) = \frac{N}{\sqrt{\pi}Z_T} e^{-(\langle H_{trap}\rangle - \lambda F)/k_B T}, \tag{E.1}$$

where the trap energy is $\langle H_{trap}\rangle = m\omega_z^2 \langle z^2\rangle/2$.

By expanding Eq. (E.1) for small perturbation strengths $\lambda \ll 1$, we calculate the average perturbation

$$\delta\langle F\rangle = \frac{\int_{-\infty}^{+\infty} dz F n_T^{pert}(z)}{N} \tag{E.2}$$

with the constraint that at equilibrium it must be zero:

$$\langle F\rangle_{eq} = \frac{\int_{-\infty}^{+\infty} dz n_T(z) F}{N} = 0 \tag{E.3}$$

where $n_T(z)$ is the unperturbed Maxwell-Boltzmann distribution (Eq. (5.1) or Eq. (E.1) with $\lambda = 0$). Therefore, one can calculate the static response function $\chi(F) = \delta\langle F\rangle/\lambda$, and finally the moment $m_{-1} = \chi(F)/2$, holding only at high T:

$$m_{-1}(T \gg 1) = \frac{1}{2k_B TN}\int_{-\infty}^{+\infty} dz n_T(z) F^2 = \frac{N}{2k_B T}\langle |f(z)|^2\rangle , \tag{E.4}$$

where in the second equality we have used the excitation operator $f(z)$ defined by $F = \sum_{k=1}^{N} f(z_k)$.

Appendix F

Ideal gas model in 1D

In this Appendix, we discuss the ideal gas in 1D, which is relevant for rewriting the virial theorem and the sum-rules beyond the LDA for a small number of particles N or small values of the coupling constant g_{1D}. In this regime, the interaction is negligible and the ideal gas is described by the harmonic oscillator model.

The ground-state wavefunction, which corresponds to the eigenvalue (3.11) with $n_z = 0$ of the 1D harmonic oscillator is:

$$\psi_0(z) = \frac{1}{\pi^{1/4}\sqrt{a_z}} e^{-\frac{z^2}{2a_z^2}} \tag{F.1}$$

where a_z is the harmonic oscillator length along the $z-$direction $a_z = \sqrt{\hbar/m\omega_z}$ and it corresponds to the width of the Gaussian (F.1). The wavefunction (F.1) is normalized $\int_{-\infty}^{+\infty} dz|\psi_0(z)|^2 = 1$ and it defines the density distribution of the N-body system:

$$n(z) = N|\psi_0(z)|^2 \tag{F.2}$$

from which one observes that $n(z)$ increases with N.

We can use Eq. (F.2) for the calculation of averages of a generic quantity x:

$$\langle x \rangle_{ho} = \frac{\int_{-\infty}^{+\infty} dz\, x\, n(z)}{N} = \int_{-\infty}^{+\infty} dz\, x |\psi_0(z)|^2 \ . \tag{F.3}$$

In the following, we report some averages (F.3) which will be useful in Appendix G. By using the momentum operator $p_z = -i\hbar\nabla_z$ and the ground-state wave function (F.1), one calculates:

$$\begin{cases} \langle z^2 \rangle_{ho} = \frac{\hbar}{2m\omega_z} \\ \langle p_z^2 \rangle_{ho} = -\hbar^2 \int_{-\infty}^{+\infty} dz\, \psi_0(z)\nabla_z^2\psi_0(z) = \frac{m\omega_z\hbar}{2} \\ \langle p_z z \rangle_{ho} = i\hbar \int_{-\infty}^{+\infty} dz\, z\left(\nabla_z\psi_0(z)\right)\psi_0(z) = -\frac{i\hbar}{2} \\ \langle p_z^2 z^2 \rangle_{ho} = -\hbar^2 \int_{-\infty}^{+\infty} dz\, z^2\psi_0(z)\nabla_z^2\psi_0(z) = -\frac{\hbar^2}{4} \\ \langle z^4 \rangle_{ho} = \frac{3}{4}\left(\frac{\hbar}{m\omega_z}\right)^2 \\ \langle p_z z^2 p_z \rangle_{ho} = \frac{3}{4}\hbar^2 \ . \end{cases} \tag{F.4}$$

Appendix G

Virial theorem

In this Appendix, we report the explicit derivation of the virial theorem (5.25) even in its generalised form (5.38). We show that both expressions hold even beyond the LDA.

G.1 Virial theorem

The virial theorem connects the average contributions of the kinetic, trapping and interaction energies. We want to find its formulation for the 1D trapped Bose gas, whose Hamiltonian is (5.2). According to the quantum version of the virial theorem, we have to impose that the average $\langle[\sum_i z_i p_i, H]\rangle = 0$, with the momentum operator $p_i = -i\hbar\partial/\partial z_i$, must be zero. The average is performed over the thermal state for the classical gas and over the ground state at $T = 0$.

By applying the commutator properties, see Appendix D, we arrive at the following expression:

$$\sum_i \langle z_i[p_i, H_{trap}]\rangle + \sum_i \langle[z_i, H_{kin}]p_i\rangle + \sum_i \langle z_i[p_i, H_{int}]\rangle = 0 . \tag{G.1}$$

By using the properties of Dirac delta $(x\partial\delta(x)/\partial x = -\delta(x))$ and the centre-of-mass and relative coordinates in the calculation with H_{int}, we find:

$$\begin{cases} z_i[p_i, H_{trap}] = z_i\left(-i\hbar\frac{\partial H_{trap}}{\partial z_i}\right) = -i\hbar(2H_{trap}) ; \\ [z_i, H_{kin}]p_i = \left(i\hbar\frac{\partial H_{kin}}{\partial p_i}\right)p_i = i\hbar(2H_{kin}) ; \\ z_i[p_i, H_{int}] = z_i\left(2i\hbar\frac{H_{int}}{z_i-z_j}\right) = i\hbar H_{int} . \end{cases}$$

Therefore, Eq. (G.1) provides the virial theorem, Eq. (5.25).

It easy to show that result (5.25) can be obtained also with the hermitian operator $G = \sum_{k=1}^N (z_k p_{z,k} + p_{z,k} z_k)$ which commutes with the Hamiltonian $\langle[H, G]\rangle = 0$.

Let us show now that the virial theorem (5.25) holds also beyond the LDA. The limiting case is a system with just one particle $N = 1$, for which the interaction energy is zero $H_{int} = 0$ in the Hamiltonian (5.2). In this regime, one exploits the harmonic oscillator model discussed in Appendix F and the virial theorem reduces to:

$$\frac{\langle p_z^2\rangle_{ho}}{m} - m\omega_z^2\langle z^2\rangle_{ho} = 0 , \tag{G.2}$$

where all averages are calculated on the ground-state state (F.1) of the harmonic oscillator. By using the suitable expressions of Eq. (F.4), one finds that Eq. (G.2) is verified.

G.2   Generalized virial theorem

Let us find a generalisation of the virial theorem, Eq. (5.38), particularly useful for the calculation of the cubic energy weighted moment m_3 for the DC mode.

We impose $\langle[\sum_i z_i^3 p_i, H]\rangle = 0$, where we have used the Hamiltonian (5.2). By performing similar calculations of above we find the expression:

$$\frac{3}{m}\langle p_z^2 z^2\rangle + 3g_{1D}\langle\delta(z_{ij})Z^2\rangle - m\omega_z^2\langle z^4\rangle + \frac{9i\hbar}{m}\langle p_z z\rangle - \frac{3\hbar^2}{m} = 0 \ , \tag{G.3}$$

whose notation is the same used in Eq. (5.37) and Eq. (5.38).

If we consider the symmetrized form of the generalized virial theorem $\langle[\sum_i z_i^3 p_i + p_i z_i^3, H]\rangle = 0$, Eq. (G.3) becomes

$$\frac{6}{m}\langle p_z^2 z^2\rangle + 6g_{1D}\langle\delta(z_{ij})Z^2\rangle - 2m\omega_z^2\langle z^4\rangle + \frac{12i\hbar}{m}\langle p_z z\rangle - \frac{3\hbar^2}{m} = 0 \ . \tag{G.4}$$

By using the commutator $[z^2, p_z] = 2i\hbar z$, we can rewrite Eq. (G.4) in a more symmetrized and hermitian way, see Eq. (5.38). We have preferred this final expression, because it is fully hermitian and it does not contain any imaginary term.

All the different forms of the generalized virial theorem (G.3), (G.4) and (5.38) hold beyond LDA. In order to show it, as already discussed in Sec. G.1, we consider the harmonic oscillator case of $N = 1$ particle and zero interaction energy. In this limit, Eq. (5.38) is fully satisfied by using the averages (F.4).

Appendix H

General expressions for m_{-1}

In this Appendix, we derive some general expressions for the inverse energy weighted moment m_{-1}, holding in the LDA, for all modes, interaction and temperature regimes. Their high-T limit corresponds to the relation derived in Appendix E, for the classical gas.

Let us consider the LDA, Eq. (A.1). We add the external perturbation $-\lambda F$, with $F = \sum_{k=1}^{N} f(z)$ to the Hamiltonian (5.2). The LDA becomes:

$$\mu_0 = \mu(n) + \frac{1}{2} m \omega_z^2 z^2 - \lambda f(z) \tag{H.1}$$

where we have introduced $\mu(n) = \mu(n_{eq}) + \delta\mu = \mu(n_{eq}) + (\partial\mu/\partial n)\delta n_{tot}$ and $\mu_0 = \mu_{00} + \delta\mu_0$ and the total density perturbation $\delta n_{tot} = \delta n_F + \delta n_V$, given by the perturbation and the external trap. By using the LDA at equilibrium $\mu(n_{eq}) + \frac{1}{2} m \omega_z^2 z^2 = \mu_{00}$, we recall $\delta n = \delta n_F$ which is equal to:

$$\delta n = \lambda \left(f(z) + C \right) \left(\frac{\partial n}{\partial \mu} \right)_T . \tag{H.2}$$

By imposing the usual normalization condition $\int dz \delta n = 0$, we calculate the constant C:

$$C = -\frac{\int dz f(z) \left(\frac{\partial n}{\partial \mu} \right)_T}{\int dz \left(\frac{\partial n}{\partial \mu} \right)_T} . \tag{H.3}$$

The normalization constant (H.3), which ensures the conservation of the number of particles after the perturbation, for symmetry reasons of the integral, it is different from zero only in the case of the LB mode, for which $f_{\text{LB}}(z) = z^2 - \langle z^2 \rangle$.

We observe that all above equations hold for both BG and TG regimes at T = 0. In each case, one has to take into account the suitable density profile $n(z)$: Eqs. (C.3) or (C.4). By calculating the quantities $\delta\langle F \rangle$ (E.2) and $\langle F \rangle_{eq}$ (E.3), for each regime, one finally finds the inverse energy weighted moment:

$$m_{-1} = \frac{1}{2\lambda} \int dz f(z) \delta n = \frac{1}{2} \int dz f(z) \left(f(z) + C \right) \left(\frac{\partial n}{\partial \mu} \right)_T . \tag{H.4}$$

Let us generalize result (H.4) for the classical regime of high T. By using the Gibbs-Duhem relation (3.5) at fixed T, we can write $\partial\mu/\partial n_{|T} = (\partial P/\partial n)_{|T}/n$. Therefore, Eq. (H.2) becomes:

$$\delta n = \lambda n \left(f(z) + C \right) \left(\frac{\partial n}{\partial P} \right)_T . \tag{H.5}$$

By imposing the normalization condition $\int_{-\infty}^{+\infty} dz \delta n = 0$, we finally find that, at high T, $C = 0$ always even for the LB mode. This implies that the addition of C quantity

119

is necessary only at $T = 0$ where LDA applies. On the other hand, this problem is not present with the other two momenta m_1 and m_3, for which we have used the more general commutator expressions (5.10) and (5.12), without assuming the LDA. Differently from the commutators, the LDA does not automatically satisfy the normalisation of the number of particles, because it is a local law, defined point by point.

The more general expression for m_{-1} holding for all regimes of T and interaction is:

$$m_{-1} = \frac{1}{2} \int dz f(z) n \left(f(z) + C \right) \left(\frac{\partial n}{\partial P} \right)_T . \tag{H.6}$$

From Eq. (H.6), by using the EOS of a classical gas $P = n k_B T$, we finally find again the classical limit (E.4).

Appendix I

Sum-rules for the DC mode

In this Appendix, we report some detailed calculations of the sum rules for the DC mode.

For the BG regime at $T = 0$, we use the density profile (C.3) and Eq. (5.20), from which one finds:

$$\langle z^4 \rangle_{\text{BG}} = \frac{15}{7} \langle z^2 \rangle_{\text{BG}}^2 \tag{I.1}$$

which, combined with Eq. (5.33), gives the following expression for the energy weighted moment in the BG regime:

$$m_1(DC) = \frac{4}{7} \frac{\hbar^2 N}{m} \langle z^2 \rangle_{\text{BG}}^2 . \tag{I.2}$$

The inverse energy weighted moment (5.32) becomes:

$$m_{-1}(DC) = \frac{2}{21} \frac{N}{m\omega_z^2} \langle z^2 \rangle_{\text{BG}}^2 . \tag{I.3}$$

By considering the ratio m_1/m_{-1}, one finally finds the hydrodynamic frequency $\omega_{1,-1}(DC) = \sqrt{6}\omega_z$, see Table 5.2.

For the TG regime, by considering the density (C.4) and Eq. (5.21), one calculates the average

$$\langle z^4 \rangle_{\text{TG}} = 2\langle z^2 \rangle_{\text{TG}}^2 . \tag{I.4}$$

From Eq. (5.33), we find the relation

$$m_1(DC) = \frac{\hbar^2 N \langle z^2 \rangle_{\text{TG}}^2}{2m} . \tag{I.5}$$

For the inverse energy weighted moment (5.32), one calculates

$$m_{-1}(DC) = \frac{1}{2} \frac{N\hbar^2}{m} \langle z^2 \rangle_{\text{TG}}^2 . \tag{I.6}$$

With the ratio m_1/m_{-1}, we finally find the hydrodynamic frequency $\omega_{1,-1}(DC) = 3\omega_z$, see Table 5.2.

Finally, we perform the same calculations for the classical gas (5.1) and Eq. (5.22):

$$\langle z^4 \rangle_T = 3\langle z^2 \rangle_T^2 . \tag{I.7}$$

From Eq. (5.33) we find the energy weighted moment:

$$m_1(DC) = \frac{N\hbar^2}{2m} 2\langle z^2 \rangle_T^2 . \tag{I.8}$$

121

On the other hand, from Eq. (E.4) or (5.32), we get:

$$m_{-1}(DC) = \frac{N}{3m\omega_z^2}\langle z^2\rangle_T^2 \ . \tag{I.9}$$

From the ratio m_1/m_{-1} we finally find $\omega_{1,-1}(DC) = \sqrt{3}\omega_z$, which is different from the hydrodynamic value by comparing with Table 5.2, similarly to the case of the LB mode discussed in Chap. 5.

Concerning the cubic energy weighted moment (5.12), by applying the properties of the commutators reported in Appendix D, one finds:

$$m_3 = \frac{\hbar^4 N}{m^2}[g_{1D}\langle z^2\rangle\langle\delta(z_{ij})\rangle + g_{1D}\langle Z_{ij}^2\delta(z_{ij})\rangle - \frac{3}{2}m\omega_z^2\langle z^2\rangle^2 +$$
$$+ \frac{1}{m}\langle z^2\rangle\langle p_z^2\rangle + \frac{3}{m}\langle p_z^2 z^2\rangle + \frac{3}{2}m\omega_z^2\langle z^4\rangle - \frac{\hbar^2}{m} + \frac{6i\hbar}{m}\langle p_z z\rangle] \tag{I.10}$$

where we have used the same notation of Eq. (5.37). By using the commutator $[z^2, p_z] = 2i\hbar z$, one can rewrite Eq. (I.10) in the more symmetric way (5.37), where imaginary parts are not present.

Let us calculate now the cubic energy weighted moment m_3 for several interactions and T regimes. For simplicity, we neglect in (5.37) the term $\sim \hbar^6 N/m^3$, which is relevant only in the small number of particle N regime.

For the BG regime, the kinetic energy is zero and one gets the following relations between the interaction and the trapping energies: $\langle H_{int}\rangle = 2\langle H_{trap}\rangle$ and $g_{1D}\langle\delta(z_{ij})Z_{ij}^2\rangle = m\omega_z^2\langle z^4\rangle/3$, derived respectively from Eq. (5.25) and (5.38), where in the last equation we have neglected the small N correction $\sim 3\hbar^2/m$. Eq. (5.37) becomes:

$$m_3(DC) = \frac{\hbar^4 N\omega_z^2}{2m}\left[\frac{11}{3}\langle z^4\rangle_{\mathrm{BG}} - \langle z^2\rangle_{\mathrm{BG}}^2\right] \ , \tag{I.11}$$

which combined with the Eq. (5.33), provides the ratio:

$$\hbar^2\omega_{3,1}^2(DC) = \frac{m_3}{m_1} = \frac{\hbar^2\omega_z^2}{3}\left[\frac{11\langle z^4\rangle_{\mathrm{BG}} - 3\langle z^2\rangle_{\mathrm{BG}}^2}{\langle z^4\rangle_{\mathrm{BG}} - \langle z^2\rangle_{\mathrm{BG}}^2}\right] \ . \tag{I.12}$$

By using the averages (5.20) and (I.1), one finds the hydrodynamic frequency $\omega_{3,1}(DC) = \sqrt{6}\omega_z$ of Table 5.2.

If one considers the non-interacting case $\langle H_{int}\rangle = 0$, one can write $\langle H_{kin}\rangle = \langle H_{trap}\rangle$ and $\langle p_z z^2 p_z\rangle = m^2\omega_z^2\langle z^4\rangle/3$, respectively from Eq. (5.25) and (5.38) in the large N limit. One then finds the cubic energy weighted moment (5.37):

$$m_3(DC) = \frac{\hbar^4 N}{m^2}\frac{1}{2}m\omega_z^2\left(5\langle z^4\rangle - \langle z^2\rangle^2\right) \tag{I.13}$$

holding for the TG regime and for the classical gas. By using Eq. (5.33) we find the ratio:

$$\hbar^2\omega_{3,1}^2(DC) = \frac{m_3}{m_1} = \hbar^2\omega_z^2\left[\frac{5\langle z^4\rangle - \langle z^2\rangle^2}{\langle z^4\rangle - \langle z^2\rangle^2}\right] \ . \tag{I.14}$$

By considering the TG regime and by using Eqs. (5.21) and (I.4), one finds

$$m_3(DC) = \frac{9\hbar^4 N\omega_z^2\langle z^2\rangle_{TG}^2}{2m} \tag{I.15}$$

which combined with the energy weighted moment (I.5) gives the hydrodynamic frequency $\omega_{3,1}(DC) = 3\omega_z$ of Table 5.2. This result is obtained also directly from Eq. (I.14) in the strongly repulsive regime.

Let us consider now the classical gas. From Eq. (I.13), by considering Eqs. (5.22) and (I.7), we finally get

$$m_3(DC) = \frac{7\hbar^4 N \omega_z^2 \langle z^2 \rangle_T^2}{m} \tag{I.16}$$

which combined with Eq. (I.8), provides the hydrodynamic frequency $\omega_{3,1}(DC) = \sqrt{7}\omega_z$, obtained also from Eq. (I.14) and reported in Table 5.2.

Finally, we discuss the collisionless regime, described by the harmonic oscillator model, see Appendix F. The ideal gas limit can be reached for one particle $N = 1$, which implies that the interaction is equal to zero in the Hamiltonian (5.2). We consider the cubic energy weighted moment (5.37), holding also for small N and without any approximation. By using the averages (F.4), one finds the expression for m_3:

$$m_3(DC) = 9\omega_z^2 \frac{\hbar^4}{m} \langle z^2 \rangle_{ho}^2 \ , \tag{I.17}$$

while the energy weighted moment (5.33) in the same limit is:

$$m_1(DC) = \frac{\hbar^2}{m} \langle z^2 \rangle_{ho}^2 \ . \tag{I.18}$$

By using Eqs. (I.17) and (I.18) and from the ratio m_3/m_1, we easily find $\omega_{3,1}(DC) = 3\omega_z$, which is the same collisionless frequency of the DC mode, see Table 5.2. We observe also that the result $3\omega_z$ is completely independent of the number of particles N: we have calculated it for $N = 1$, but it is the same for every N in the harmonic oscillator model.

Appendix J

Time evolution of the DC signal

In this Appendix we derive the time evolution of the expectation value (5.40) [Zambelli and Stringari, 2001].

Starting from the expression of the perturbation of the Hamiltonian $H_{pert}(z,t) = \lambda F(z)\Theta(t)$, we express the Heaviside step function $\Theta(t)$ in terms of its Fourier component and we find:

$$\delta\langle F\rangle = \lambda\chi_F(\omega)\Theta(t) = \frac{i\lambda}{4\pi}\int_{-\infty}^{+\infty}d\omega\chi_F(\omega)\frac{e^{-i\omega t}}{\omega+i\eta} + c.c. . \tag{J.1}$$

We integrate Eq. (J.1) in the complex plane: $\delta\langle F\rangle = \lambda\chi_F(0)$.

According to the linear response theory [Pitaevskii and Stringari, 2016] and Chap. 4, we can rewrite the static polarizability as a complex quantity, see Eq. (4.9): $\chi_F(0) = \chi_F'(0) + i\chi_F''(0)$, where the real part can be expressed in terms of the imaginary one by using the Kramers-Kronig relation, Eq. (4.13):

$$\chi_F'(0) = -\frac{1}{\pi}\int_{-\infty}^{+\infty}d\omega'\chi_F''(\omega')P\left(-\frac{1}{\omega'}\right) \tag{J.2}$$

where P is the principal value which can be expressed through the Dirac relation (4.8).

By exploiting the properties of the Dirac delta, included its representation in terms of the Fourier transform, we finally find

$$\delta\langle F\rangle(t) = \frac{\lambda}{\pi}\int_{-\infty}^{+\infty}d\omega'\frac{\chi_F''(\omega')}{\omega'}\left(1-e^{i\omega't}\right) , \tag{J.3}$$

where we have used the fact that Eq. (J.3) is completely symmetric to the exchange of the sign of the frequency $e^{i\omega t}\rightarrow e^{-i\omega t}$. By using the fluctuation-dissipation theorem (4.24) in the classical (high-T) regime, we finally approximate:

$$\frac{1}{\pi}\frac{\chi_F''(\omega)}{\omega} \approx \frac{\hbar S_F(\omega)}{k_B T} \tag{J.4}$$

where the dynamic structure factor $S_F(\omega)$, relative to the excitation operator F, is an even function in ω for high temperatures for the property: $S_F(\omega) = e^{\hbar\omega/(k_B T)}S_F(-\omega)$, see Eq. (4.6). In addition, by using the Euler relation ($e^{i\omega t} = \cos(\omega t) + i\sin(\omega t)$), we finally find that, for symmetry reason, only the cosine contributes in the integral (J.3) and we obtain Eq. (5.40), where we observe that $\delta\langle F\rangle(t=0) = 0$ for causality, because the perturbation F is turned on at $t=0$ time.

Appendix K

Analytical limits for BG and TG regimes

In this Appendix, we report the BG and TG analytical limits of the thermodynamic quantities investigated in Chap. 6.

First of all, by using Eq. (6.4) and (6.5), one can rewrite the coefficients (6.9) and (6.10) of the phononic expansion (6.8) as:

$$\alpha(\gamma) = \frac{1}{\pi^2}\left(3e(\gamma) - \gamma\frac{\partial e(\gamma)}{\partial\gamma}\right) \tag{K.1}$$

and

$$\beta(\gamma) = \frac{\pi^3 f(\gamma)}{12\sqrt{2}} \tag{K.2}$$

where we have defined the dimensionless function

$$f(\gamma) = \frac{12e(\gamma) - 10\gamma\frac{\partial e(\gamma)}{\partial\gamma} + 4\gamma^2\frac{\partial^2 e(\gamma)}{\partial\gamma^2} - \gamma^3\frac{\partial^3 e(\gamma)}{\partial\gamma^3}}{\left[6e(\gamma) - 4\gamma\frac{\partial e(\gamma)}{\partial\gamma} + \gamma^2\frac{\partial^2 e(\gamma)}{\partial\gamma^2}\right]^{3/2}} \ . \tag{K.3}$$

In this way, it is more clear that the functions $\alpha(\gamma)$ and $\beta(\gamma)$ depends on γ through the dimensionless energy per particle $e(\gamma)$, see Eq. (2.10), and its derivatives.

K.1   Bogoliubov regime

In the weakly-interacting BG regime, the dimensionless energy per particle (2.10) is equal to the value [Lieb and Liniger, 1963, Lieb, 1963]

$$e_{\mathrm{BG}}(\gamma) = \gamma \tag{K.4}$$

from which one can calculate all analytical limits of the relevant physical quantities discussed in the following.

The ground-state energy per particle is derived from Eq. (2.10)

$$\left(\frac{E_0}{N}\right)_{\mathrm{BG}} = \frac{1}{2}g_{1\mathrm{D}}n \ . \tag{K.5}$$

From Eq. (6.5), the BG limit of the chemical potential at T = 0 is

$$\mu_{\mathrm{BG}}(T=0) = g_{1\mathrm{D}}n \ , \tag{K.6}$$

as expected from Bogoliubov theory.

One calculates also the Bogoliubov sound velocity (6.4)

$$v_s^{\mathrm{BG}}(\gamma) = \sqrt{\frac{g_{1\mathrm{D}}n}{m}} = v_F \frac{\sqrt{\gamma}}{\pi} \tag{K.7}$$

where, in the second equality, we have introduced the interaction parameter γ (6.2) and the Fermi velocity v_F (K.12).

From Eqs. (K.1)-(K.2)-(K.3), one calculates the following BG limits:

$$\begin{cases} f_{\mathrm{BG}}(\gamma) = \frac{1}{\sqrt{2\gamma}} \\ \alpha_{\mathrm{BG}}(\gamma) = \frac{2\gamma}{\pi^2} \\ \beta_{\mathrm{BG}}(\gamma) = \frac{\pi^3}{24\sqrt{\gamma}} \end{cases} \tag{K.8}$$

K.2 Tonks-Girardeau regime

For the strongly-interacting TG limit, the dimensionless energy per particle (2.10) is [Lieb and Liniger, 1963, Lieb, 1963]

$$e_{\mathrm{TG}} = \frac{\pi^2}{3} \,, \tag{K.9}$$

independent on the interaction parameter γ as expected. From Eq. (K.9) we calculate all analytical TG limits of the same quantities discussed in the previous Section.

The ground-state energy per particle (2.10) becomes:

$$\left(\frac{E_0}{N}\right)_{\mathrm{TG}} = \frac{\hbar^2 \pi^2 n^2}{6m} \,. \tag{K.10}$$

The chemical potential (6.5) in the TG limit is equal to the Fermi energy:

$$\mu_{\mathrm{TG}}(T=0) = E_F = \frac{\hbar^2 \pi^2 n^2}{2m} \,. \tag{K.11}$$

Correspondingly, the sound speed (6.4) at T = 0 is provided by the Fermi velocity

$$v_s^{\mathrm{TG}}(\gamma) = v_F = \sqrt{\frac{2E_F}{m}} = \frac{\hbar \pi n}{m} \,. \tag{K.12}$$

The numerical functions (K.1)-(K.2)-(K.3) are independent on γ in the strongly interacting regime

$$\begin{cases} f_{\mathrm{TG}} = \frac{\sqrt{2}}{\pi} \\ \alpha_{\mathrm{TG}} = 1 \\ \beta_{\mathrm{TG}} = \frac{\pi^2}{12} \,, \end{cases} \tag{K.13}$$

where the last two coefficients are the same appearing in the Sommerfeld expansion (6.25).

Appendix L

Bogoliubov theory in 1D: the quantum fluctuation correction

In this Appendix we calculate explicitly the correction due to the quantum fluctuations in the 1D energy per particle (6.20) for small values of γ.

First of all, we write the Hamiltonian of the 1D system at T = 0 in terms of the field operators ψ:

$$H = \int dz \left(\frac{\hbar^2}{2m} \nabla_z \psi^\dagger \nabla_z \psi \right) + \frac{1}{2} \int dz dz' \psi^\dagger \psi'^\dagger V(z - z') \psi \psi' \tag{L.1}$$

where

$$V(z - z') = g_{1D} \sum_{i>j} \delta(z - z') \tag{L.2}$$

is the two-body contact interaction. If we consider an uniform system of length L, the field operators can be written in terms of plane-waves:

$$\psi(z) = \frac{1}{\sqrt{L}} \sum_{p_i} a_{p_i} e^{i p_i z / \hbar} \tag{L.3}$$

where a_{p_i} is the annihilation operator which destroys a particle in the single-particle state with momentum p, and p satisfies the cyclic boundary conditions. By inserting Eq. (L.2) and Eq. (L.3) in Eq. (L.1), we finally find

$$H = \sum_p \frac{p^2}{2m} a_p^\dagger a_p + \frac{g_{1D}}{2L} \sum_{p_1, p_2} a_{p_1}^\dagger a_{p_2}^\dagger a_{p_1} a_{p_2}{}^1 \; . \tag{L.4}$$

We use the Bogoliubov prescription in H: $a_0 = a_0^\dagger \equiv \sqrt{N_0}$, where we have replaced the operators a_0 and $a_0^\dagger$ with a $c-$number.

In first approximation, we neglect the $p \neq 0$ terms in H (L.4) and we get the ground state of the BG limit, see Sec. K.1.

---

[1] In 3D, differently from the 1D case, this equation contains the real potential characterized by a short range term which makes it difficult to get the solution of the Schrödinger equation at microscopic level. In particular, the scattering of slow particles cannot be studied by applying perturbation theory. Since in 3D the weakly-interacting Bose gas is dilute, the actual form of the two-body potential is not important for the description of the macroscopic properties of the gas, provided the potential reproduces the correct value of the s-wave scattering length. Therefore, one replaces the microscopic potential with an effective, soft one without the hard-core at small distances and for which the perturbation theory can be applied. Since the physics of the system depends only on the scattering length, this method in 3D provides the correct many-body description, see SubSec. 1.3.1.

In second approximation, we retain in (L.4) all the terms quadratic in a_p with $p \neq 0$, while the terms containing only one a_p operator with $p \neq 0$ do not enter for the momentum conservation.

By using the Bose commutation rules

$$\begin{cases} [a_p^\dagger, a_p'^\dagger] = [a_p, a_p'] = 0 \\ [a_p, a_p'^\dagger] = \delta_{p,p'} \end{cases} \tag{L.5}$$

Eq. (L.4) becomes:

$$H = \frac{g_{1D}}{2L} a_0^\dagger a_0^\dagger a_0 a_0 + \sum_p \frac{p^2}{2m} a_p^\dagger a_p + \frac{g_{1D}}{2L} \sum_{p \neq 0} \left(4 a_0^\dagger a_p^\dagger a_0 a_p + a_p^\dagger a_{-p}^\dagger a_0 a_0 + a_0^\dagger a_0^\dagger a_p a_{-p} \right) . \tag{L.6}$$

By combining the normalization condition $\sum_p a_p^\dagger a_p = N$, the Bogoliubov prescription and Eq. (L.5) and by neglecting next-order terms, we find

$$a_0^\dagger a_0^\dagger a_0 a_0 = N^2 - 2N \sum_{p \neq 0} a_p^\dagger a_p \tag{L.7}$$

which used together with Eq. (L.6), finally gives

$$H = \frac{g_{1D} N^2}{2L} + \sum_p \frac{p^2}{2m} a_p^\dagger a_p + \frac{1}{2} g_{1D} n \sum_{p \neq 0} \left(2 a_p^\dagger a_p + a_p^\dagger a_{-p}^\dagger + a_p a_{-p} \right) \tag{L.8}$$

where we have introduced the density $n = N/L$ [2].

Since the Hamiltonian (L.8) is quadratic in $a_p^\dagger$ and a_p, it can be diagonalized by the linear Bogoliubov transformation

$$\begin{cases} a_p = u_p b_p + v_{-p}^* b_{-p}^\dagger \\ a_p^\dagger = u_p^* b_p^\dagger + v_{-p} b_{-p} . \end{cases} \tag{L.9}$$

By using Eq. (L.5) and by imposing the same Bose commutation rules for the new operators $b_p^\dagger$ and b_p, we finally find

$$|u_p|^2 - |v_{-p}|^2 = 1 \tag{L.10}$$

which is satisfied by imposing

$$\begin{cases} u_p = \cosh \alpha_p \\ v_{-p} = \sinh \alpha_p . \end{cases} \tag{L.11}$$

The parameter α_p is chosen to make the coefficient of the non-diagonal terms $b_p^\dagger b_{-p}^\dagger$ and $b_p b_{-p}$ in the Hamiltonian (L.8) vanish. This condition yields

$$\frac{g_{1D} n}{2} \left(|u_p|^2 + |v_{-p}|^2 \right) + \left(\frac{p^2}{2m} + g_{1D} n \right) u_p v_{-p} = 0 \tag{L.12}$$

where we have used the symmetry properties $\sum_{p \neq 0} u_p u_{-p} = \sum_{p \neq 0} |u_p|^2$ and $\sum_{p \neq 0} v_p v_{-p} = \sum_{p \neq 0} |v_{-p}|^2$. In Eq. (L.12) we use Eq. (L.11) and the properties

$$\begin{cases} \cosh 2\alpha_p = \cosh^2 \alpha_p + \sinh^2 \alpha_p \\ \sinh 2\alpha_p = 2 \cosh \alpha_p \sinh \alpha_p \end{cases} \tag{L.13}$$

---

[2]In 3D, one has to use also the renormalization of the scattering length [Landau, 1958], which contains the divergency for large values of the momenta. This ultraviolet behaviour is the consequence of the replacement of the Fourier transform of the effective potential with its value at zero wavevector, because only small momenta are involved in slow-particle scattering.

---

and by introducing $\coth \alpha_p = \cosh \alpha_p / \sinh \alpha_p$, we get the condition

$$\coth 2\alpha_p = -\frac{\frac{p^2}{2m} + g_{1D}n}{g_{1D}n} \tag{L.14}$$

in which we use Eqs. (L.13)-(L.10)-(L.11) and we find the explicit form of the coefficient u_p and v_p

$$u_p, v_{-p} = \pm \sqrt{\frac{\frac{p^2}{2m} + g_{1D}n}{2\epsilon(p)} \pm \frac{1}{2}} \tag{L.15}$$

where we have defined the Bogoliubov dispersion law for the elementary excitations of the system (6.19). From Eq. (L.15) we calculate the quantities

$$\begin{cases} |u_p|^2 = \frac{\frac{p^2}{2m} + g_{1D}n}{2\epsilon(p)} + \frac{1}{2} \\ |v_{-p}|^2 = \frac{\frac{p^2}{2m} + g_{1D}n}{2\epsilon(p)} - \frac{1}{2} \\ u_p v_{-p} = -\frac{g_{1D}n}{2\epsilon(p)} \end{cases} \tag{L.16}$$

which used in Eq. (L.8) gives the diagonal form of the Hamiltonian

$$H = E_0 + \sum_p \epsilon(p) b_p^\dagger b_p \tag{L.17}$$

where we have introduced the ground-state energy (6.18), calculated at higher order of approximation. By observing Eq. (L.17) we conclude that the original Bose gas of interacting particles can be described by using an Hamiltonian of independent quasi-particles with energy $\epsilon(p)$ and whose annihilation and creation operators are, respectively, b_p and $b_p^\dagger$.

The ground state of the interacting particles then corresponds to the vacuum of quasi-particles $\forall p \neq 0$:

$$b_p |vac\rangle = 0 . \tag{L.18}$$

We can calculate the ground-state energy Eq. (6.18) by replacing the sum with an integral in momentum space [3]. Finally, we get the first correction to the ground-state energy per particle (6.20), where we have introduced the γ parameter, Eq. (6.2).

---

[3] In 3D the integration is performed only up the cut-off $p \sim mv_s$. For such momenta, the gas parameter na^3 is much smaller than unity. This justifies *a posteriori* the replacement of the Fourier transform of the interaction potential with its value at zero momentum.

Appendix M

Euler Mac-Laurin expansion for G(y)

In this Appendix, we show the detailed derivation of the expansion holding for $y \gg 1$ (6.48) for the series (6.47).

We use the Euler Mac–Laurin expansion which allows to approximate a series as follows [Abramowitz and Stegun, 2012]:

$$\sum_{k=0}^{+\infty} f(k) \approx \int_0^{+\infty} f(x)dx + \sum_{k=1}^{m} \frac{B_k}{k!} f^{(k-1)}(x)|_0^{+\infty} \tag{M.1}$$

where $f(x)$ is a continuous function of real numbers x in the interval $[0, +\infty]$. For $m = 2$, one considers only the first terms in the sum, whose Bernoulli's numbers are

$$\begin{cases} B_1 = -\frac{1}{2} \\ B_2 = \frac{1}{6} \end{cases} \tag{M.2}$$

and $f^{(k)}(x)$ are the k–derivatives of the function $f(x)$.

By defining the following function

$$f(x) = 2\pi x\sqrt{y + (\pi x)^2} - 2(\pi x)^2 - y \tag{M.3}$$

entering the series (6.47), one estimates the integral

$$\int_0^{+\infty} dx f(x) = -\frac{2y\sqrt{y}}{3\pi} \ , \tag{M.4}$$

which allows to calculate the thermodynamic limit of the ground-state energy per particle on a ring configuration (6.45), provided by Eq. (6.20).

By calculating the first derivative of the function (M.3), and by using Eq. (M.1) and Eq. (M.2), one finally gets the expansion (6.48) holding for large values of y parameter.

Bibliography

J. R. Abo-Shaeer, C. Raman, J. M. Vogels, and W. Ketterle. Observation of Vortex Lattices in Bose-Einstein Condensates. *Science*, **292**:476, 2001. (cited on pp. 16 and 17)

M. Abramowitz and I.A. Stegun. *Handbook of Mathematical Functions: with Formulas, Graphs, and Mathematical Tables*. Dover Publications, 2012. (cited on p. 133)

J. F. Allen and A. D. Misener. Flow of Liquid Helium II. *Nature*, **141**:75, 1938. (cited on p. 14)

A. Altmeyer, S. Riedl, C. Kohstall, M. J. Wright, R. Geursen, M. Bartenstein, C. Chin, J. Hecker Denschlag, and R. Grimm. Precision Measurements of Collective Oscillations in the BEC-BCS Crossover. *Phys. Rev. Lett.*, **98**:040401, 2007. (cited on p. 1)

M. H. Anderson, J. R. Ensher, M. R. Matthews, C. E. Wieman, and E. A. Cornell. Observation of Bose-Einstein Condensation in a Dilute Atomic Vapor. *Science*, **269**:198, 1995. (cited on pp. 1, 6, 15, and 16)

M. R. Andrews, D. M. Kurn, H.-J. Miesner, D. S. Durfee, C. G. Townsend, S. Inouye, and W. Ketterle. Propagation of Sound in a Bose-Einstein Condensate. *Phys. Rev. Lett.*, **79**:553, 1997a. (cited on pp. 17, 40, 41, and 50)

M. R. Andrews, C. G. Townsend, H.-J. Miesner, D. S. Durfee, D. M. Kurn, and W. Ketterle. Observation of Interference Between Two Bose Condensates. *Science*, **275**:637, 1997b. (cited on p. 16)

G. E. Astrakharchik. Local density approximation for a perturbative equation of state. *Phys. Rev. A*, **72**:063620, 2005. (cited on pp. 2, 62, and 97)

G. E. Astrakharchik and L. P. Pitaevskii. Motion of a heavy impurity through a Bose-Einstein condensate. *Phys. Rev. A*, **70**:013608, 2004. (cited on p. 77)

G. E. Astrakharchik, J. Boronat, J. Casulleras, and S. Giorgini. Beyond the Tonks-Girardeau Gas: Strongly Correlated Regime in Quasi-One-Dimensional Bose Gases. *Phys. Rev. Lett.*, **95**:190407, 2005a. (cited on pp. 28, 32, and 86)

G. E. Astrakharchik, R. Combescot, X. Leyronas, and S. Stringari. Equation of State and Collective Frequencies of a Trapped Fermi Gas Along the BEC-Unitarity Crossover. *Phys. Rev. Lett.*, **95**:030404, 2005b. (cited on p. 1)

M. A. Baranov and D. S. Petrov. Low-energy collective excitations in a superfluid trapped Fermi gas. *Phys. Rev. A*, **62**:041601, 2000. (cited on p. 47)

J. Bardeen and D. Pines. Electron-Phonon Interaction in Metals. *Phys. Rev.*, **99**:1140, 1955. (cited on p. 21)

J. Bardeen, L. N. Cooper, and J. R. Schrieffer. Theory of Superconductivity. *Phys. Rev.*, **108**:1175, 1957a. (cited on pp. 10, 15, and 21)

J. Bardeen, L. N. Cooper, and J. R. Schrieffer. Microscopic Theory of Superconductivity. *Phys. Rev.*, **106**:162, 1957b. (cited on pp. 10, 15, and 21)

M. Bartenstein, A. Altmeyer, S. Riedl, S. Jochim, C. Chin, J. Hecker Denschlag, and R. Grimm. Crossover from a Molecular Bose-Einstein Condensate to a Degenerate Fermi Gas. *Phys. Rev. Lett.*, **92**:120401, 2004a. (cited on pp. 21, 25, and 39)

M. Bartenstein, A. Altmeyer, S. Riedl, S. Jochim, C. Chin, J. Hecker Denschlag, and R. Grimm. Collective Excitations of a Degenerate Gas at the BEC-BCS Crossover. *Phys. Rev. Lett.*, **92**:203201, 2004b. (cited on pp. 1 and 42)

M. Barth and W. Zwerger. Tan relations in one dimension. *Annals of Physics*, **326**:2544, 2011. (cited on p. 69)

N. Bartolo. *Matter Waves in Reduced Dimensions: Dipolar-Induced Resonances and Atomic Artificial Crystals*. Phd thesis, University of Trento, Université Montpellier 2, 2014. (cited on p. 11)

S. K. Baur, E. Vogt, M. Köhl, and G. M. Bruun. Collective modes of a two-dimensional spin-1/2 Fermi gas in a harmonic trap. *Phys. Rev. A*, **87**:043612, 2013. (cited on pp. 1 and 50)

G. Baym, J.-P. Blaizot, M. Holzmann, F. Laloë, and D. Vautherin. Bose-Einstein transition in a dilute interacting gas. *The European Physical Journal B - Condensed Matter and Complex Systems*, **24**:107, 2001. (cited on p. 22)

V. L. Berezinskii. Destruction of Long-range Order in One-dimensional and Two-dimensional Systems having a Continuous Symmetry Group I. Classical Systems. *Sov. Phys. JETP*, **32**:493, 1971. (cited on p. 28)

V. L. Berezinskii. Destruction of Long-range Order in One-dimensional and Two-dimensional Systems Possessing a Continuous Symmetry Group. II. Quantum Systems. *Sov. Phys. JETP*, **34**:610, 1972. (cited on p. 28)

D. J. Bishop and J. D. Reppy. Study of the Superfluid Transition in Two-Dimensional ^{4}He Films. *Phys. Rev. Lett.*, **40**:1727, 1978. (cited on p. 28)

D. J. Bishop and J. D. Reppy. Study of the superfluid transition in two-dimensional ^{4}He films. *Phys. Rev. B*, **22**:5171, 1980. (cited on p. 28)

I. Bloch, T. W. Hänsch, and T. Esslinger. Measurement of the spatial coherence of a trapped Bose gas at the phase transition. *Nature*, **403**:166, 2000. (cited on p. 16)

I. Bloch, J. Dalibard, and W. Zwerger. Many-body physics with ultracold gases. *Rev. Mod. Phys.*, **80**:885, 2008. (cited on pp. 1 and 37)

I. Bloch, J. Dalibard, and S. Nascimbène. Quantum simulations with ultracold quantum gases. *Nat. Phys.*, **8**:267, 2012. (cited on pp. 1 and 21)

N. Bogoliubov. On the theory of superfluidity. *Journal of Physics (USSR)*, **11**:23, 1947. (cited on p. 18)

N. N. Bogoliubov. Quasimittelwerte in problemen der statistischen mechanik. *Phys. Abh. SU.*, **6**:1, 1962. (cited on p. 60)

A. Bohr and B.R. Mottelson. *Nuclear Structure: Single-particle motion*. W. A. Benjamin, 1969. (cited on p. 93)

S. Bose. Plancks Gesetz und Lichtquantenhypothese. *Z. Phys.*, **26**:178, 1924. (cited on p. 6)

I. Bouchoule, S. S. Szigeti, M. J. Davis, and K. V. Kheruntsyan. Finite-temperature hydrodynamics for one-dimensional Bose gases: Breathing-mode oscillations as a case study. *Phys. Rev. A*, **94**:051602, 2016. (cited on p. 64)

T. Bourdel, L. Khaykovich, J. Cubizolles, J. Zhang, F. Chevy, M. Teichmann, L. Tarruell, S. J. J. M. F. Kokkelmans, and C. Salomon. Experimental Study of the BEC-BCS Crossover Region in Lithium 6. *Phys. Rev. Lett.*, **93**:050401, 2004. (cited on p. 21)

C. C. Bradley, C. A. Sackett, J. J. Tollett, and R. G. Hulet. Evidence of Bose-Einstein Condensation in an Atomic Gas with Attractive Interactions. *Phys. Rev. Lett.*, **75**:1687, 1995. (cited on pp. 1 and 6)

C. C. Bradley, C. A. Sackett, and R. G. Hulet. Bose-Einstein Condensation of Lithium: Observation of Limited Condensate Number. *Phys. Rev. Lett.*, **78**:985, 1997. (cited on p. 17)

G. M. Bruun and C. W. Clark. Hydrodynamic Excitations of Trapped Fermi Gases. *Phys. Rev. Lett.*, **83**:5415, 1999. (cited on pp. 1 and 47)

S. Burger, F. S. Cataliotti, C. Fort, P. Maddaloni, F. Minardi, and M. Inguscio. Quasi-2D Bose-Einstein condensation in an optical lattice. *EPL (Europhysics Letters)*, **57**:1, 2002. (cited on p. 25)

P. Capuzzi, P. Vignolo, F. Federici, and M. P. Tosi. Sound propagation in elongated superfluid fermionic clouds. *Phys. Rev. A*, **73**:021603, 2006. (cited on p. 40)

I. Carusotto and C. Ciuti. Quantum fluids of light. *Rev. Mod. Phys.*, **85**:299, 2013. (cited on p. 98)

Y. Castin. Exact scaling transform for a unitary quantum gas in a time dependent harmonic potential. *Comptes Rendus Physique*, **5**:407, 2004. (cited on p. 48)

M. A. Cazalilla, R. Citro, T. Giamarchi, E. Orignac, and M. Rigol. One dimensional bosons: From condensed matter systems to ultracold gases. *Rev. Mod. Phys.*, **83**:1405, 2011. (cited on p. 78)

X.-L. Chen, Y. Li, and H. Hu. Collective modes of a harmonically trapped one-dimensional Bose gas: The effects of finite particle number and nonzero temperature. *Phys. Rev. A*, **91**:063631, 2015. (cited on pp. 2, 62, and 71)

F. Chevy, V. Bretin, P. Rosenbusch, K. W. Madison, and J. Dalibard. Transverse Breathing Mode of an Elongated Bose-Einstein Condensate. *Phys. Rev. Lett.*, **88**:250402, 2002. (cited on p. 37)

C. Chin, R. Grimm, P. Julienne, and E. Tiesinga. Feshbach resonances in ultracold gases. *Rev. Mod. Phys.*, **82**:1225, 2010. (cited on pp. 1, 12, 13, and 14)

A. Chiocchetta, P.-É. Larré, and I. Carusotto. Thermalization and Bose-Einstein condensation of quantum light in bulk nonlinear media. *EPL (Europhysics Letters)*, **115**:24002, 2016. (cited on p. 98)

J.-y. Choi, S. W. Seo, and Y.-i. Shin. Observation of Thermally Activated Vortex Pairs in a Quasi-2D Bose Gas. *Phys. Rev. Lett.*, **110**:175302, 2013. (cited on p. 28)

P. Cladé, C. Ryu, A. Ramanathan, K. Helmerson, and W. D. Phillips. Observation of a 2D Bose Gas: From Thermal to Quasicondensate to Superfluid. *Phys. Rev. Lett.*, **102**: 170401, 2009. (cited on p. 28)

C. Cohen-Tannoudji. *Condensation de Bose-Einstein des gaz atomiques ultra froids: effets des interactions*. Lecture notes at Collège de France, 1998-1999. (cited on p. 11)

R. Combescot, F. Alzetto, and X. Leyronas. Particle distribution tail and related energy formula. *Phys. Rev. A*, **79**:053640, 2009. (cited on p. 69)

L. N. Cooper. Bound Electron Pairs in a Degenerate Fermi Gas. *Phys. Rev.*, **104**:1189, 1956. (cited on p. 21)

M. Cozzini, S. Stringari, V. Bretin, P. Rosenbusch, and J. Dalibard. Scissors mode of a rotating Bose-Einstein condensate. *Phys. Rev. A*, **67**:021602, 2003. (cited on p. 37)

F. Dalfovo, S. Giorgini, L. P. Pitaevskii, and S. Stringari. Theory of Bose-Einstein condensation in trapped gases. *Rev. Mod. Phys.*, **71**:463, 1999. (cited on pp. 7, 39, and 49)

J. Dalibard. *Cohérence et superfluidité dans les gaz atomiques*. Lecture notes at Collège de France, 2015-2016. (cited on p. 26)

K. Damle, T. Senthil, S. N. Majumdar, and S. Sachdev. Phase transition of a Bose gas in a harmonic potential. *EPL (Europhysics Letters)*, **36**:7, 1996. (cited on p. 9)

K. B. Davis, M. O. Mewes, M. R. Andrews, N. J. van Druten, D. S. Durfee, D. M. Kurn, and W. Ketterle. Bose-Einstein Condensation in a Gas of Sodium Atoms. *Phys. Rev. Lett.*, **75**:3969, 1995. (cited on pp. 1, 6, and 15)

L. de Broglie. Recherches sur la théorie des Quanta. *Annals of Physics*, **2**:22, 1925. (cited on p. 5)

G. De Rosi and S. Stringari. Collective oscillations of a trapped quantum gas in low dimensions. *Phys. Rev. A*, **92**:053617, 2015. (cited on pp. 2, 3, 4, 38, 40, 44, 49, 61, 62, 63, 64, and 71)

G. De Rosi and S. Stringari. Hydrodynamic versus collisionless dynamics of a one-dimensional harmonically trapped Bose gas. *Phys. Rev. A*, **94**:063605, 2016. (cited on pp. 2, 3, 4, 63, 65, 72, and 74)

G. De Rosi, G. E. Astrakharchik, and S. Stringari. Thermodynamic behaviour of a one-dimensional bose gas at low temperature. *Submitted to arXiv & Phys. Rev. A*, 2017. (cited on pp. 2, 3, 4, 78, 79, 80, 81, 82, 83, 84, 88, 89, 91, 92, 93, 94, and 95)

C. De Rossi. *Gaz de Bose en dimension deux: modes collectifs, superfluidité et piège annulaire*. Phd thesis, Laboratoire de Physique des Lasers, Université Paris 13, 2016. (cited on pp. 45, 46, 47, and 48)

C. De Rossi, R. Dubessy, K. Merloti, M. de Goër de Herve, T. Badr, A. Perrin, L. Longchambon, and H. Perrin. Probing superfluidity in a quasi two-dimensional Bose gas through its local dynamics. *New Journal of Physics*, **18**:062001, 2016. (cited on p. 42)

M. Delehaye. *Mixtures of superfluids*. Phd thesis, École Normale Supérieure, 2016. (cited on pp. xii and 22)

M. Delehaye, S. Laurent, I. Ferrier-Barbut, S. Jin, F. Chevy, and C. Salomon. Critical Velocity and Dissipation of an Ultracold Bose-Fermi Counterflow. *Phys. Rev. Lett.*, **115**: 265303, 2015. (cited on p. 22)

B. DeMarco and D. S. Jin. Onset of Fermi Degeneracy in a Trapped Atomic Gas. *Science*, **285**:1703, 1999. (cited on pp. 6, 20, and 21)

R. Desbuquois, L. Chomaz, T. Yefsah, J. Leonard, J. Beugnon, C. Weitenberg, and J. Dalibard. Superfluid behaviour of a two-dimensional Bose gas. *Nat. Phys.*, **8**:645, 2012. (cited on pp. 25, 39, and 105)

S. Dettmer, D. Hellweg, P. Ryytty, J. J. Arlt, W. Ertmer, K. Sengstock, D. S. Petrov, G. V. Shlyapnikov, H. Kreutzmann, L. Santos, and M. Lewenstein. Observation of Phase Fluctuations in Elongated Bose-Einstein Condensates. *Phys. Rev. Lett.*, **87**:160406, 2001. (cited on p. 29)

E. A. Donley, N. R. Claussen, S. L. Cornish, J. L. Roberts, E. A. Cornell, and C. E. Wieman. Dynamics of collapsing and exploding Bose-Einstein condensates. *Nature*, **412**:295, 2001. (cited on pp. 10 and 17)

A. Einstein. On a Heuristic Point of View about the Creation and Conversion of Light. *Annals of Physics*, **17**:132, 1905. (cited on p. 5)

A. Einstein. *Sitzber. Kgl. Preuss. Akad. Wiss.*, 261, 1924. (cited on p. 6)

A. Einstein. *Sitzber. Kgl. Preuss. Akad. Wiss.*, 3, 1925. (cited on p. 6)

B. Fang, G. Carleo, A. Johnson, and I. Bouchoule. Quench-Induced Breathing Mode of One-Dimensional Bose Gases. *Phys. Rev. Lett.*, **113**:035301, 2014. (cited on pp. 2, 42, 52, 62, and 69)

U. Fano. Sullo spettro di assorbimento dei gas nobili presso il limite dello spettro d'arco. *Il Nuovo Cimento (1924-1942)*, **12**:154, 1935. (cited on p. 12)

U. Fano. Effects of Configuration Interaction on Intensities and Phase Shifts. *Phys. Rev.*, **124**:1866, 1961. (cited on p. 12)

P. O. Fedichev, Yu. Kagan, G. V. Shlyapnikov, and J. T. M. Walraven. Influence of Nearly Resonant Light on the Scattering Length in Low-Temperature Atomic Gases. *Phys. Rev. Lett.*, **77**:2913, 1996. (cited on p. 12)

I. Ferrier-Barbut. *Mixtures of Bose and Fermi superfluids*. Phd thesis, École Normale Supérieure, 2014. (cited on p. 14)

H. Feshbach. Unified theory of nuclear reactions. *Annals of Physics*, **5**:357, 1958. (cited on p. 12)

H. Feshbach. A unified theory of nuclear reactions. II. *Annals of Physics*, **19**:287, 1962. (cited on p. 12)

R. P. Feynman. Atomic Theory of the λ Transition in Helium. *Phys. Rev.*, **91**:1291, 1953. (cited on p. 16)

R. P. Feynman. Atomic Theory of the Two-Fluid Model of Liquid Helium. *Phys. Rev.*, **94**: 262, 1954. (cited on p. 16)

H. Frohlich. Interaction of Electrons with Lattice Vibrations. *Proceedings of the Royal Society of London A: Mathematical, Physical and Engineering Sciences*, **215**:291, 1952. (cited on p. 21)

D. M. Gangardt and G. V. Shlyapnikov. Stability and Phase Coherence of Trapped 1D Bose Gases. *Phys. Rev. Lett.*, **90**:010401, 2003. (cited on p. 69)

J. Gavoret and P. Nozières. Structure of the perturbation expansion for the bose liquid at zero temperature. *Annals of Physics*, **28**:349, 1964. (cited on p. 60)

F. Gerbier, J. H. Thywissen, S. Richard, M. Hugbart, P. Bouyer, and A. Aspect. Momentum distribution and correlation function of quasicondensates in elongated traps. *Phys. Rev. A*, **67**:051602, 2003. (cited on p. 29)

J. M. Gerton, D. Strekalov, I. Prodan, and R. G. Hulet. Direct observation of growth and collapse of a Bose-Einstein condensate with attractive interactions. *Nature*, **408**:692, 2000. (cited on p. 17)

T. K. Ghosh. Collective excitation frequencies and damping rates of a two-dimensional deformed trapped Bose gas above the critical temperature. *Phys. Rev. A*, **63**:013603, 2000. (cited on pp. 1 and 50)

T. Giamarchi. *Quantum Physics in One Dimension*. Clarendon Press, 2004. (cited on pp. 50 and 61)

T. Giamarchi. *Clean and dirty one-dimensional systems*. Proceedings of the International School of Physics "Enrico Fermi", Volume 191: Quantum Matter at Ultralow Temperatures. IOS Press, 2016. (cited on p. 50)

S. Giorgini, L. P. Pitaevskii, and S. Stringari. Theory of ultracold atomic Fermi gases. *Rev. Mod. Phys.*, **80**:1215, 2008. (cited on pp. 7 and 39)

M. Girardeau. Relationship between Systems of Impenetrable Bosons and Fermions in One Dimension. *Journal of Mathematical Physics*, **1**:516, 1960. (cited on pp. 29, 31, 51, 62, 78, 86, 94, and 105)

L. P. Gor'kov. On the Energy Spectrum of Superconductors . *Sov. Phys. JETP*, **7**:505, 1958. (cited on p. 27)

A. Görlitz, J. M. Vogels, A. E. Leanhardt, C. Raman, T. L. Gustavson, J. R. Abo-Shaeer, A. P. Chikkatur, S. Gupta, S. Inouye, T. Rosenband, and W. Ketterle. Realization of Bose-Einstein Condensates in Lower Dimensions. *Phys. Rev. Lett.*, **87**:130402, 2001. (cited on p. 25)

M. Greiner, I. Bloch, O. Mandel, T. W. Hänsch, and T. Esslinger. Exploring Phase Coherence in a 2D Lattice of Bose-Einstein Condensates. *Phys. Rev. Lett.*, **87**:160405, 2001. (cited on p. 25)

M. Greiner, C. A. Regal, and D. S. Jin. Emergence of a molecular Bose-Einstein condensate from a Fermi gas. *Nature*, **426**:537, 2003. (cited on p. 21)

A. Griffin, W.-C. Wu, and S. Stringari. Hydrodynamic Modes in a Trapped Bose Gas above the Bose-Einstein Transition. *Phys. Rev. Lett.*, **78**:1838, 1997. (cited on pp. 43, 44, and 63)

E. P. Gross. Structure of a quantized vortex in boson systems. *Il Nuovo Cimento (1955-1965)*, **20**:454, 1961. (cited on p. 19)

A. Gudyma. *Non-equilibrium dynamics of a trapped one-dimensional Bose gas*. Phd thesis, Université Paris-Saclay, 2015. (cited on pp. 2, 62, 67, 68, 85, and 86)

A. Gudyma, G. E. Astrakharchik, and M. B. Zvonarev. Reentrant behavior of the breathing-mode-oscillation frequency in a one-dimensional Bose gas. *Phys. Rev. A*, **92**: 021601, 2015. (cited on pp. 2, 62, and 67)

D. Guéry-Odelin and S. Stringari. Scissors Mode and Superfluidity of a Trapped Bose-Einstein Condensed Gas. *Phys. Rev. Lett.*, **83**:4452, 1999. (cited on pp. 46 and 73)

Z. Hadzibabic, P. Kruger, M. Cheneau, B. Battelier, and J. Dalibard. Berezinskii-Kosterlitz-Thouless crossover in a trapped atomic gas. *Nature*, **441**:1118, 2006. (cited on pp. 1 and 28)

F. D. M. Haldane. Effective Harmonic-Fluid Approach to Low-Energy Properties of One-Dimensional Quantum Fluids. *Phys. Rev. Lett.*, **47**:1840, 1981. (cited on pp. 28 and 29)

H. E. Hall and W. F. Vinen. The Rotation of Liquid Helium II. II. The Theory of Mutual Friction in Uniformly Rotating Helium II. *Proceedings of the Royal Society of London A: Mathematical, Physical and Engineering Sciences*, **238**:215, 1956. (cited on p. 16)

E. Haller, M. Gustavsson, M. J. Mark, J. G. Danzl, R. Hart, G. Pupillo, and H.-C. Nägerl. Realization of an Excited, Strongly Correlated Quantum Gas Phase. *Science*, **325**:1224, 2009. (cited on pp. 2, 32, 51, 62, and 78)

E. Haller, M. J. Mark, R. Hart, J. G. Danzl, L. Reichsöllner, V. Melezhik, P. Schmelcher, and H.-C. Nägerl. Confinement-Induced Resonances in Low-Dimensional Quantum Systems. *Phys. Rev. Lett.*, **104**:153203, 2010. (cited on p. 78)

E. Haller, M. Rabie, M. J. Mark, J. G. Danzl, R. Hart, K. Lauber, G. Pupillo, and H.-C. Nägerl. Three-Body Correlation Functions and Recombination Rates for Bosons in Three Dimensions and One Dimension. *Phys. Rev. Lett.*, **107**:230404, 2011. (cited on p. 78)

R. Haussmann, W. Rantner, S. Cerrito, and W. Zwerger. Thermodynamics of the BCS-BEC crossover. *Phys. Rev. A*, **75**:023610, 2007. (cited on p. 22)

H. Heiselberg. Collective Modes of Trapped Gases at the BEC-BCS Crossover. *Phys. Rev. Lett.*, **93**:040402, 2004. (cited on pp. 1 and 51)

D. Hellweg, S. Dettmer, P. Ryytty, J.J. Arlt, W. Ertmer, K. Sengstock, D.S. Petrov, G.V. Shlyapnikov, H. Kreutzmann, L. Santos, and M. Lewenstein. Phase fluctuations in Bose-Einstein condensates. *Applied Physics B*, **73**:781, 2001. (cited on p. 29)

D. Hellweg, L. Cacciapuoti, M. Kottke, T. Schulte, K. Sengstock, W. Ertmer, and J. J. Arlt. Measurement of the Spatial Correlation Function of Phase Fluctuating Bose-Einstein Condensates. *Phys. Rev. Lett.*, **91**:010406, 2003. (cited on p. 29)

T.-L. Ho. Universal Thermodynamics of Degenerate Quantum Gases in the Unitarity Limit. *Phys. Rev. Lett.*, **92**:090402, 2004. (cited on p. 104)

S. Hofferberth, I. Lesanovsky, B. Fischer, T. Schumm, and J. Schmiedmayer. Non-equilibrium coherence dynamics in one-dimensional Bose gases. *Nature*, **449**:324, 2007. (cited on pp. 2 and 61)

S. Hofferberth, I. Lesanovsky, T. Schumm, A. Imambekov, V. Gritsev, E. Demler, and J. Schmiedmayer. Probing quantum and thermal noise in an interacting many-body system. *Nat. Phys.*, **4**:489, 2008. (cited on pp. 34, 35, and 61)

P. C. Hohenberg. Existence of Long-Range Order in One and Two Dimensions. *Phys. Rev.*, **158**:383, 1967. (cited on pp. 27, 37, 60, 63, and 82)

M. Horikoshi, S. Nakajima, M. Ueda, and T. Mukaiyama. Measurement of Universal Thermodynamic Functions for a Unitary Fermi Gas. *Science*, **327**:442, 2010. (cited on p. 50)

Y.-H. Hou, L. P. Pitaevskii, and S. Stringari. Scaling solutions of the two-fluid hydrodynamic equations in a harmonically trapped gas at unitarity. *Phys. Rev. A*, **87**:033620, 2013a. (cited on p. 48)

Y.-H. Hou, L. P. Pitaevskii, and S. Stringari. First and second sound in a highly elongated Fermi gas at unitarity. *Phys. Rev. A*, **88**:043630, 2013b. (cited on pp. 17, 51, 64, and 104)

H. Hu, G. Xianlong, and X.-J. Liu. Collective modes of a one-dimensional trapped atomic Bose gas at finite temperatures. *Phys. Rev. A*, **90**:013622, 2014. (cited on pp. 2, 62, 64, and 71)

M. Inguscio and L. Fallani. *Atomic Physics: Precise Measurements and Ultracold Matter*. OUP Oxford, 2013. (cited on p. 6)

S. Inouye, M. R. Andrews, J. Stenger, H.-J. Miesner, D. M. Stamper-Kurn, and W. Ketterle. Observation of Feshbach resonances in a Bose-Einstein condensate. *Nature*, **392**: 151, 1998. (cited on p. 14)

IQOQI. *https://www.uibk.ac.at/exphys/ultracold/projects/cs3/index1.html*. (cited on pp. 24 and 25)

M. Ishikawa and H. Takayama. Solitons in a One-Dimensional Bose System with the Repulsive Delta-Function Interaction. *Journal of the Physical Society of Japan*, **49**: 1242, 1980. (cited on pp. 32 and 80)

D. S. Jin, J. R. Ensher, M. R. Matthews, C. E. Wieman, and E. A. Cornell. Collective Excitations of a Bose-Einstein Condensate in a Dilute Gas. *Phys. Rev. Lett.*, **77**:420, 1996. (cited on pp. 1, 25, 37, and 39)

D. S. Jin, M. R. Matthews, J. R. Ensher, C. E. Wieman, and E. A. Cornell. Temperature-Dependent Damping and Frequency Shifts in Collective Excitations of a Dilute Bose-Einstein Condensate. *Phys. Rev. Lett.*, **78**:764, 1997. (cited on pp. 1, 37, and 48)

S. Jochim, M. Bartenstein, A. Altmeyer, G. Hendl, S. Riedl, C. Chin, J. Hecker Denschlag, and R. Grimm. Bose-Einstein Condensation of Molecules. *Science*, **302**:2101, 2003. (cited on p. 21)

J. Joseph, B. Clancy, L. Luo, J. Kinast, A. Turlapov, and J. E. Thomas. Measurement of Sound Velocity in a Fermi Gas near a Feshbach Resonance. *Phys. Rev. Lett.*, **98**:170401, 2007. (cited on pp. 40, 41, and 50)

H. Kamerlingh Onnes. *Investigations into the Properties of Substances at Low Temperatures, which Have Led, amongst Other Things, to the Preparation of Liquid Helium*. Nobel Lectures, Physics 1901-1921. Elsevier Publishing Company, Amsterdam, 1967. (cited on p. 14)

T. Kaminaka and M. Wadati. Higher order solutions of Lieb–Liniger integral equation. *Physics Letters A*, **375**:2460, 2011. (cited on p. 85)

J. W. Kane and L. P. Kadanoff. Long-Range Order in Superfluid Helium. *Phys. Rev.*, **155**: 80, 1967. (cited on pp. 27 and 28)

P. Kapitza. Viscosity of Liquid Helium below the λ-Point. *Nature*, **141**:74, 1938. (cited on p. 14)

W. Ketterle and N. J. van Druten. Bose-Einstein condensation of a finite number of particles trapped in one or three dimensions. *Phys. Rev. A*, **54**:656, 1996. (cited on p. 28)

K. V. Kheruntsyan, D. M. Gangardt, P. D. Drummond, and G. V. Shlyapnikov. Finite-temperature correlations and density profiles of an inhomogeneous interacting one-dimensional Bose gas. *Phys. Rev. A*, **71**:053615, 2005. (cited on pp. 62, 81, and 110)

J. Kinast, S. L. Hemmer, M. E. Gehm, A. Turlapov, and J. E. Thomas. Evidence for Superfluidity in a Resonantly Interacting Fermi Gas. *Phys. Rev. Lett.*, **92**:150402, 2004. (cited on pp. 1, 25, and 39)

J. Kinast, A. Turlapov, and J. E. Thomas. Damping of a Unitary Fermi Gas. *Phys. Rev. Lett.*, **94**:170404, 2005. (cited on p. 1)

T. Kinoshita, T. Wenger, and D. S. Weiss. Observation of a One-Dimensional Tonks-Girardeau Gas. *Science*, **305**:1125, 2004. (cited on pp. 1, 32, 78, and 105)

T. Kinoshita, T. Wenger, and D. S. Weiss. A quantum Newton's cradle. *Nature*, **440**:900, 2006. (cited on pp. 2, 34, 35, 61, and 78)

J. M. Kosterlitz. The critical properties of the two-dimensional xy model. *Journal of Physics C: Solid State Physics*, **7**:1046, 1974. (cited on p. 28)

J. M. Kosterlitz and D. J. Thouless. Ordering, metastability and phase transitions in two-dimensional systems. *Journal of Physics C: Solid State Physics*, **6**:1181, 1973. (cited on p. 28)

H. A. Kramers. *Atti. Congr. Intern. Fisica, Como (reprinted in "Collected Scientific Papers", North-Holland, Amsterdam, 1956, p. 333)*, **2**:545, 1927. (cited on p. 55)

R. de L. Kronig. On the Theory of Dispersion of X-Rays. *J. Opt. Soc. Am.*, **12**:547, 1926. (cited on p. 55)

M. J. H. Ku, A. T. Sommer, L. W. Cheuk, and M. W. Zwierlein. Revealing the Superfluid Lambda Transition in the Universal Thermodynamics of a Unitary Fermi Gas. *Science*, **335**:563, 2012. (cited on pp. 2, 21, 22, and 77)

R. Kubo. A general expression for the conductivity tensor. *Canadian Journal of Physics*, **34**:1274, 1956. (cited on p. 54)

R. Kubo. Statistical-Mechanical Theory of Irreversible Processes. I. General Theory and Simple Applications to Magnetic and Conduction Problems. *Journal of the Physical Society of Japan*, **12**:570, 1957. (cited on p. 54)

P. P. Kulish, S. V. Manakov, and L. D. Faddeev. Comparison of the exact quantum and quasiclassical results for a nonlinear Schrödinger equation. *Theoretical and Mathematical Physics*, **28**:615, 1976. (cited on pp. 32 and 80)

H. Labuhn, D. Barredo, S. Ravets, S. de Léséleuc, T. Macrì, T. Lahaye, and A. Browaeys. Tunable two-dimensional arrays of single Rydberg atoms for realizing quantum Ising models. *Nature*, **534**:667, 2016. (cited on pp. 2 and 78)

B. Laburthe Tolra, K. M. O'Hara, J. H. Huckans, W. D. Phillips, S. L. Rolston, and J. V. Porto. Observation of Reduced Three-Body Recombination in a Correlated 1D Degenerate Bose Gas. *Phys. Rev. Lett.*, **92**:190401, 2004. (cited on pp. 2 and 61)

L. Landau. Theory of the Superfluidity of Helium II. *Phys. Rev.*, **60**:356, 1941. (cited on pp. 15 and 16)

L. D. Landau. *Quantum Mechanics*. Pergamon Press, 1958. (cited on pp. 9, 10, and 130)

L.D. Landau and E.M. Lifshitz. *Quantum Mechanics: Non-Relativistic Theory*. Elsevier Science, 1981. (cited on p. 18)

L.D. Landau and E.M. Lifshitz. *Statistical Physics*. Elsevier Science, 2013. (cited on pp. 15, 27, 28, and 50)

G. Lang, F. Hekking, and A. Minguzzi. Dynamic structure factor and drag force in a one-dimensional strongly interacting Bose gas at finite temperature. *Phys. Rev. A*, **91**: 063619, 2015. (cited on pp. 32, 81, and 85)

P.-É. Larré and I. Carusotto. Propagation of a quantum fluid of light in a cavityless nonlinear optical medium: General theory and response to quantum quenches. *Phys. Rev. A*, **92**:043802, 2015. (cited on p. 98)

T. D. Lee and C. N. Yang. Many-Body Problem in Quantum Mechanics and Quantum Statistical Mechanics. *Phys. Rev.*, **105**:1119, 1957. (cited on p. 84)

T. D. Lee, K. Huang, and C. N. Yang. Eigenvalues and Eigenfunctions of a Bose System of Hard Spheres and Its Low-Temperature Properties. *Phys. Rev.*, **106**:1135, 1957. (cited on pp. 18 and 84)

A. Leggett. Cooper pairing in spin-polarized Fermi systems. *Journal de Physique Colloques*, **41**:C7–19, 1980. (cited on p. 22)

A. J. Leggett. A theoretical description of the new phases of liquid ^{3}He. *Rev. Mod. Phys.*, **47**:331, 1975. (cited on p. 15)

J. Levinsen and M. M. Parish. Strongly interacting two-dimensional Fermi gases. *Annual Review of Cold Atoms and Molecules*, **3**:1, 2015. (cited on p. 48)

X. Leyronas and R. Combescot. Superfluid Equation of State of Dilute Composite Bosons. *Phys. Rev. Lett.*, **99**:170402, 2007. (cited on p. 21)

E. H. Lieb. Exact Analysis of an Interacting Bose Gas. II. The Excitation Spectrum. *Phys. Rev.*, **130**:1616, 1963. (cited on pp. 2, 32, 39, 61, 62, 79, 80, 84, 85, 127, and 128)

E. H. Lieb and W. Liniger. Exact Analysis of an Interacting Bose Gas. I. The General Solution and the Ground State. *Phys. Rev.*, **130**:1605, 1963. (cited on pp. 29, 30, 34, 39, 50, 61, 62, 79, 80, 84, 85, 127, and 128)

E. Lipparini and S. Stringari. Sum rules and giant resonances in nuclei. *Physics Reports*, **175**:103, 1989. (cited on p. 65)

F. London. The λ-Phenomenon of Liquid Helium and the Bose-Einstein Degeneracy. *Nature*, **141**:643, 1938. (cited on p. 15)

D. L. Luxat and A. Griffin. Dynamic correlation functions in one-dimensional quasicondensates. *Phys. Rev. A*, **67**:043603, 2003. (cited on p. 29)

K. W. Madison, F. Chevy, W. Wohlleben, and J. Dalibard. Vortex Formation in a Stirred Bose-Einstein Condensate. *Phys. Rev. Lett.*, **84**:806, 2000. (cited on pp. 16 and 17)

O. M. Maragò, S. A. Hopkins, J. Arlt, E. Hodby, G. Hechenblaikner, and C. J. Foot. Observation of the Scissors Mode and Evidence for Superfluidity of a Trapped Bose-Einstein Condensed Gas. *Phys. Rev. Lett.*, **84**:2056, 2000. (cited on pp. 1, 37, 42, 46, and 73)

M. R. Matthews, B. P. Anderson, P. C. Haljan, D. S. Hall, C. E. Wieman, and E. A. Cornell. Vortices in a Bose-Einstein Condensate. *Phys. Rev. Lett.*, **83**:2498, 1999. (cited on pp. 16 and 17)

I. E. Mazets. Integrability breakdown in longitudinaly trapped, one-dimensional bosonic gases. *The European Physical Journal D*, **65**:43, 2011. (cited on pp. 2, 23, 34, 35, and 61)

I. E. Mazets and J. Schmiedmayer. Restoring integrability in one-dimensional quantum gases by two-particle correlations. *Phys. Rev. A*, **79**:061603, 2009. (cited on pp. 2, 23, 34, 35, and 61)

I. E. Mazets and J. Schmiedmayer. Thermalization in a quasi-one-dimensional ultracold bosonic gas. *New Journal of Physics*, **12**:055023, 2010. (cited on pp. 2, 23, 34, 35, and 61)

I. E. Mazets, T. Schumm, and J. Schmiedmayer. Breakdown of Integrability in a Quasi-1D Ultracold Bosonic Gas. *Phys. Rev. Lett.*, **100**:210403, 2008. (cited on pp. 2, 23, 34, 35, and 61)

J. B. McGuire. Study of Exactly Soluble One–Dimensional N–Body Problems. *Journal of Mathematical Physics*, **5**:622, 1964. (cited on p. 32)

M.L. Mehta. *Random Matrices*. Elsevier Science, 2004. (cited on p. 28)

F. Meinert, M. Panfil, M. J. Mark, K. Lauber, J.-S. Caux, and H.-C. Nägerl. Probing the Excitations of a Lieb-Liniger Gas from Weak to Strong Coupling. *Phys. Rev. Lett.*, **115**: 085301, 2015. (cited on p. 80)

C. Menotti and S. Stringari. Collective oscillations of a one-dimensional trapped Bose-Einstein gas. *Phys. Rev. A*, **66**:043610, 2002. (cited on pp. 1, 2, 30, 51, 61, 62, and 67)

K. Merloti, R. Dubessy, L. Longchambon, M. Olshanii, and Hélène Perrin. Breakdown of scale invariance in a quasi-two-dimensional Bose gas due to the presence of the third dimension. *Phys. Rev. A*, **88**:061603, 2013. (cited on pp. 42 and 97)

N. D. Mermin and H. Wagner. Absence of Ferromagnetism or Antiferromagnetism in One- or Two-Dimensional Isotropic Heisenberg Models. *Phys. Rev. Lett.*, **17**:1133, 1966. (cited on pp. 27, 37, 60, 63, and 82)

M.-O. Mewes, M. R. Andrews, N. J. van Druten, D. M. Kurn, D. S. Durfee, C. G. Townsend, and W. Ketterle. Collective Excitations of a Bose-Einstein Condensate in a Magnetic Trap. *Phys. Rev. Lett.*, **77**:988, 1996. (cited on pp. 1, 25, 37, and 39)

D. E. Miller, J. K. Chin, C. A. Stan, Y. Liu, W. Setiawan, C. Sanner, and W. Ketterle. Critical Velocity for Superfluid Flow across the BEC-BCS Crossover. *Phys. Rev. Lett.*, **99**:070402, 2007. (cited on p. 22)

A. Minguzzi and M.P. Tosi. Collective excitations in confined Fermi gases. *Physica B: Condensed Matter*, **300**:27, 2001. (cited on pp. 43 and 47)

A. J. Moerdijk, B. J. Verhaar, and A. Axelsson. Resonances in ultracold collisions of ^{6}Li, ^{7}Li, and ^{23}Na. *Phys. Rev. A*, **51**:4852, 1995. (cited on p. 13)

C. Mora and Y. Castin. Extension of Bogoliubov theory to quasicondensates. *Phys. Rev. A*, **67**:053615, 2003. (cited on p. 29)

H. Moritz, T. Stöferle, M. Köhl, and T. Esslinger. Exciting Collective Oscillations in a Trapped 1D Gas. *Phys. Rev. Lett.*, **91**:250402, 2003. (cited on pp. 2 and 62)

S. Nascimbène, N. Navon, K. J. Jiang, L. Tarruell, M. Teichmann, J. McKeever, F. Chevy, and C. Salomon. Collective Oscillations of an Imbalanced Fermi Gas: Axial Compression Modes and Polaron Effective Mass. *Phys. Rev. Lett.*, **103**:170402, 2009. (cited on p. 42)

S. Nascimbène, N. Navon, K. J. Jiang, F. Chevy, and C. Salomon. Exploring the thermodynamics of a universal Fermi gas. *Nature*, **463**:1057, 2010. (cited on pp. 21 and 22)

N. Navon, S. Nascimbène, F. Chevy, and C. Salomon. The Equation of State of a Low-Temperature Fermi Gas with Tunable Interactions. *Science*, **328**:729, 2010. (cited on p. 21)

N. Navon, S. Piatecki, K. Günter, B. Rem, T. C. Nguyen, F. Chevy, W. Krauth, and C. Salomon. Dynamics and Thermodynamics of the Low-Temperature Strongly Interacting Bose Gas. *Phys. Rev. Lett.*, **107**:135301, 2011. (cited on p. 18)

N. Navon, S. Nascimbène, X. Leyronas, F. Chevy, and C. Salomon. Condensation energy of a spin-1/2 strongly interacting Fermi gas. *Phys. Rev. A*, **88**:063614, 2013. (cited on p. 22)

D. R. Nelson and J. M. Kosterlitz. Universal Jump in the Superfluid Density of Two-Dimensional Superfluids. *Phys. Rev. Lett.*, **39**:1201, 1977. (cited on p. 28)

P. Nozières and D. Pines. Electron Interaction in Solids. General Formulation. *Phys. Rev.*, **109**:741, 1958. (cited on p. 58)

P. Nozières and S. Schmitt-Rink. Bose condensation in an attractive fermion gas: From weak to strong coupling superconductivity. *Journal of Low Temperature Physics*, **59**: 195, 1985. (cited on p. 22)

M. Olshanii. Atomic Scattering in the Presence of an External Confinement and a Gas of Impenetrable Bosons. *Phys. Rev. Lett.*, **81**:938, 1998. (cited on pp. 30, 34, 35, and 62)

M. Olshanii and V. Dunjko. Short-Distance Correlation Properties of the Lieb-Liniger System and Momentum Distributions of Trapped One-Dimensional Atomic Gases. *Phys. Rev. Lett.*, **91**:090401, 2003. (cited on p. 69)

R. Onofrio, C. Raman, J. M. Vogels, J. R. Abo-Shaeer, A. P. Chikkatur, and W. Ketterle. Observation of Superfluid Flow in a Bose-Einstein Condensed Gas. *Phys. Rev. Lett.*, **85**: 2228, 2000. (cited on pp. 15 and 17)

L. Onsager. Statistical hydrodynamics. *Il Nuovo Cimento (1943-1954)*, **6**:279, 1949. (cited on p. 16)

D. D. Osheroff, W. J. Gully, R. C. Richardson, and D. M. Lee. New Magnetic Phenomena in Liquid He^3 below 3 mK. *Phys. Rev. Lett.*, **29**:920, 1972a. (cited on p. 15)

D. D. Osheroff, R. C. Richardson, and D. M. Lee. Evidence for a New Phase of Solid He^3. *Phys. Rev. Lett.*, **28**:885, 1972b. (cited on p. 15)

D. J. Papoular and S. Stringari. Shortcut to Adiabaticity for an Anisotropic Gas Containing Quantum Defects. *Phys. Rev. Lett.*, **115**:025302, 2015. (cited on p. 105)

D. J. Papoular, G. Ferrari, L. P. Pitaevskii, and S. Stringari. Increasing Quantum Degeneracy by Heating a Superfluid. *Phys. Rev. Lett.*, **109**:084501, 2012. (cited on pp. 2 and 77)

S. B. Papp, J. M. Pino, R. J. Wild, S. Ronen, C. E. Wieman, D. S. Jin, and E. A. Cornell. Bragg Spectroscopy of a Strongly Interacting ^{85}Rb Bose-Einstein Condensate. *Phys. Rev. Lett.*, **101**:135301, 2008. (cited on p. 18)

B. Paredes, A. Widera, V. Murg, O. Mandel, S. Folling, I. Cirac, G. V. Shlyapnikov, T. W. Hansch, and I. Bloch. Tonks-Girardeau gas of ultracold atoms in an optical lattice. *Nature*, **429**:277, 2004. (cited on pp. 1, 25, 32, and 105)

G. B. Partridge, K. E. Strecker, R. I. Kamar, M. W. Jack, and R. G. Hulet. Molecular Probe of Pairing in the BEC-BCS Crossover. *Phys. Rev. Lett.*, **95**:020404, 2005. (cited on p. 21)

O. Penrose. CXXXVI. On the quantum mechanics of helium II. *The London, Edinburgh, and Dublin Philosophical Magazine and Journal of Science*, **42**:1373, 1951. (cited on pp. 15 and 27)

O. Penrose and L. Onsager. Bose-Einstein Condensation and Liquid Helium. *Phys. Rev.*, **104**:576, 1956. (cited on pp. 15 and 27)

C.J. Pethick and H. Smith. *Bose-Einstein Condensation in Dilute Gases*. Cambridge University Press, 2002. (cited on pp. 1 and 7)

D. S. Petrov, M. Holzmann, and G. V. Shlyapnikov. Bose-Einstein Condensation in Quasi-2D Trapped Gases. *Phys. Rev. Lett.*, **84**:2551, 2000a. (cited on p. 24)

D. S. Petrov, G. V. Shlyapnikov, and J. T. M. Walraven. Regimes of Quantum Degeneracy in Trapped 1D Gases. *Phys. Rev. Lett.*, **85**:3745, 2000b. (cited on pp. 29, 30, 62, and 84)

D. S. Petrov, G. V. Shlyapnikov, and J. T. M. Walraven. Phase-Fluctuating 3D Bose-Einstein Condensates in Elongated Traps. *Phys. Rev. Lett.*, **87**:050404, 2001. (cited on p. 29)

D. S. Petrov, C. Salomon, and G. V. Shlyapnikov. Weakly Bound Dimers of Fermionic Atoms. *Phys. Rev. Lett.*, **93**:090404, 2004. (cited on p. 21)

D. Pines and P. Nozières. *The Theory of Quantum Liquids*. Westview Press, 1999. (cited on pp. 57 and 68)

L. Pitaevskii. Vortex lines in an imperfect Bose gas. *Sov. Phys. JETP.*, **13**:451, 1961. (cited on p. 19)

L. Pitaevskii. Dynamics of collapse of a confined Bose gas. *Phys. Lett. A*, **221**:14, 1996. (cited on p. 48)

L. Pitaevskii and A. Rosch. Breathing modes and hidden symmetry of trapped atoms in two dimensions. *Phys. Rev. A*, **55**:R853, 1997. (cited on p. 48)

L. Pitaevskii and S. Stringari. Uncertainty principle, quantum fluctuations, and broken symmetries. *Journal of Low Temperature Physics*, **85**:377, 1991. (cited on pp. 28, 37, and 60)

L. Pitaevskii and S. Stringari. Elementary Excitations in Trapped Bose-Einstein Condensed Gases Beyond the Mean-Field Approximation. *Phys. Rev. Lett.*, **81**:4541, 1998. (cited on p. 97)

L. Pitaevskii and S. Stringari. *Bose-Einstein Condensation and Superfluidity*. Oxford University Press, 2016. (cited on pp. 7, 8, 18, 20, 23, 26, 27, 28, 29, 32, 33, 37, 42, 43, 50, 53, 55, 57, 60, 64, 65, 66, 67, 68, 73, 7

G. Placzek. The Scattering of Neutrons by Systems of Heavy Nuclei. *Phys. Rev.*, **86**:377, 1952. (cited on p. 58)

S. E. Pollack, D. Dries, R. G. Hulet, K. M. F. Magalhães, E. A. L. Henn, E. R. F. Ramos, M. A. Caracanhas, and V. S. Bagnato. Collective excitation of a Bose-Einstein condensate by modulation of the atomic scattering length. *Phys. Rev. A*, **81**:053627, 2010. (cited on p. 37)

V. N. Popov. *Functional Integrals in Quantum Field Theory and Statistical Physics*. Springer Netherlands, 2001. (cited on pp. 27 and 61)

L. Pricoupenko, H. Perrin, and M. Olshanii. *Quantum Gases in Low Dimensions: QGLD 2003: Centre de Physique Des Houches, 15-25 Avril, 2003*. EDP Sciences, 2004. (cited on p. 37)

C. Raman, M. Köhl, R. Onofrio, D. S. Durfee, C. E. Kuklewicz, Z. Hadzibabic, and W. Ketterle. Evidence for a Critical Velocity in a Bose-Einstein Condensed Gas. *Phys. Rev. Lett.*, **83**:2502, 1999. (cited on pp. 15 and 17)

M. Randeria, J.-M. Duan, and L.-Y. Shieh. Bound states, Cooper pairing, and Bose condensation in two dimensions. *Phys. Rev. Lett.*, **62**:981, 1989. (cited on p. 21)

G. W. Rayfield and F. Reif. Quantized Vortex Rings in Superfluid Helium. *Phys. Rev.*, **136**:A1194, 1964. (cited on p. 16)

L. Reatto and G. V. Chester. Phonons and the Properties of a Bose System. *Phys. Rev.*, **155**:88, 1967. (cited on p. 28)

C. A. Regal, M. Greiner, and D. S. Jin. Observation of Resonance Condensation of Fermionic Atom Pairs. *Phys. Rev. Lett.*, **92**:040403, 2004. (cited on pp. 20 and 21)

S. Richard, F. Gerbier, J. H. Thywissen, M. Hugbart, P. Bouyer, and A. Aspect. Momentum Spectroscopy of 1D Phase Fluctuations in Bose-Einstein Condensates. *Phys. Rev. Lett.*, **91**:010405, 2003. (cited on p. 29)

S. Riedl, E. R. Sánchez Guajardo, C. Kohstall, A. Altmeyer, M. J. Wright, J. Hecker Denschlag, R. Grimm, G. M. Bruun, and H. Smith. Collective oscillations of a Fermi gas in the unitarity limit: Temperature effects and the role of pair correlations. *Phys. Rev. A*, **78**:053609, 2008. (cited on p. 1)

M. Rigol. Breakdown of Thermalization in Finite One-Dimensional Systems. *Phys. Rev. Lett.*, **103**:100403, 2009. (cited on p. 61)

M. Rigol, V. Dunjko, V. Yurovsky, and M. Olshanii. Relaxation in a Completely Integrable Many-Body Quantum System: An *Ab Initio* Study of the Dynamics of the Highly Excited States of 1D Lattice Hard-Core Bosons. *Phys. Rev. Lett.*, **98**:050405, 2007. (cited on p. 61)

J. L. Roberts, N. R. Claussen, S. L. Cornish, E. A. Donley, E. A. Cornell, and C. E. Wieman. Controlled Collapse of a Bose-Einstein Condensate. *Phys. Rev. Lett.*, **86**:4211, 2001. (cited on p. 17)

D. Rychtarik, B. Engeser, H.-C. Nägerl, and R. Grimm. Two-Dimensional Bose-Einstein Condensate in an Optical Surface Trap. *Phys. Rev. Lett.*, **92**:173003, 2004. (cited on p. 25)

C. A. R. Sá de Melo, M. Randeria, and J. R. Engelbrecht. Crossover from BCS to Bose superconductivity: Transition temperature and time-dependent Ginzburg-Landau theory. *Phys. Rev. Lett.*, **71**:3202, 1993. (cited on p. 21)

C. A. Sackett, J. M. Gerton, M. Welling, and R. G. Hulet. Measurements of Collective Collapse in a Bose-Einstein Condensate with Attractive Interactions. *Phys. Rev. Lett.*, **82**:876, 1999. (cited on p. 17)

A. I. Safonov, S. A. Vasilyev, I. S. Yasnikov, I. I. Lukashevich, and S. Jaakkola. Observation of Quasicondensate in Two-Dimensional Atomic Hydrogen. *Phys. Rev. Lett.*, **81**:4545, 1998. (cited on p. 27)

E. R. Sánchez Guajardo, M. K. Tey, L. A. Sidorenkov, and R. Grimm. Higher-nodal collective modes in a resonantly interacting Fermi gas. *Phys. Rev. A*, **87**:063601, 2013. (cited on p. 2)

F. Schreck, L. Khaykovich, K. L. Corwin, G. Ferrari, T. Bourdel, J. Cubizolles, and C. Salomon. Quasipure Bose-Einstein Condensate Immersed in a Fermi Sea. *Phys. Rev. Lett.*, **87**:080403, 2001. (cited on pp. 6, 20, and 25)

M. Schwartz. Off-diagonal long-range behavior of interacting Bose systems. *Phys. Rev. B*, **15**:1399, 1977. (cited on p. 28)

V. Schweikhard, I. Coddington, P. Engels, V. P. Mogendorff, and E. A. Cornell. Rapidly Rotating Bose-Einstein Condensates in and near the Lowest Landau Level. *Phys. Rev. Lett.*, **92**:040404, 2004. (cited on p. 25)

L. A. Sidorenkov, M. K. Tey, R. Grimm, Y.-H. Hou, L. Pitaevskii, and S. Stringari. Second sound and the superfluid fraction in a Fermi gas with resonant interactions. *Nature*, **498**:78, 2013. (cited on p. 17)

R. P. Smith, N. Tammuz, R. L. D. Campbell, M. Holzmann, and Z. Hadzibabic. Condensed Fraction of an Atomic Bose Gas Induced by Critical Correlations. *Phys. Rev. Lett.*, **107**:190403, 2011. (cited on p. 22)

D. M. Stamper-Kurn, H.-J. Miesner, S. Inouye, M. R. Andrews, and W. Ketterle. Collisionless and Hydrodynamic Excitations of a Bose-Einstein Condensate. *Phys. Rev. Lett.*, **81**:500, 1998. (cited on pp. 1, 17, 37, and 51)

S. Stringari. Collective Excitations of a Trapped Bose-Condensed Gas. *Phys. Rev. Lett.*, **77**:2360, 1996. (cited on pp. 1, 37, 43, 45, 47, 48, 51, 65, and 68)

S. Stringari. Dynamics of Bose-Einstein condensed gases in highly deformed traps. *Phys. Rev. A*, **58**:2385, 1998. (cited on pp. 1, 47, and 51)

S. Stringari. Collective oscillations of a trapped superfluid Fermi gas near a Feshbach resonance. *EPL (Europhysics Letters)*, **65**:749, 2004. (cited on pp. 1 and 51)

Collective oscillations of a trapped atomic gas in low D
& thermodynamics of 1D Bose gas
G. De Rosi

S. Tan. Energetics of a strongly correlated Fermi gas. *Annals of Physics*, **323**:2952, 2008. (cited on p. 69)

S. Tan, M. Pustilnik, and L. I. Glazman. Relaxation of a High-Energy Quasi-particle in a One-Dimensional Bose Gas. *Phys. Rev. Lett.*, **105**:090404, 2010. (cited on pp. 2, 35, and 61)

E. Taylor and A. Griffin. Two-fluid hydrodynamic modes in a trapped superfluid gas. *Phys. Rev. A*, **72**:053630, 2005. (cited on p. 64)

E. Taylor and M. Randeria. Apparent Low-Energy Scale Invariance in Two-Dimensional Fermi Gases. *Phys. Rev. Lett.*, **109**:135301, 2012. (cited on p. 48)

E. Taylor, H. Hu, X.-J. Liu, and A. Griffin. Variational theory of two-fluid hydrodynamic modes at unitarity. *Phys. Rev. A*, **77**:033608, 2008. (cited on p. 64)

E. Taylor, H. Hu, X.-J. Liu, L. P. Pitaevskii, A. Griffin, and S. Stringari. First and second sound in a strongly interacting Fermi gas. *Phys. Rev. A*, **80**:053601, 2009. (cited on pp. 63 and 64)

M. K. Tey, L. A. Sidorenkov, E. R. Guajardo Sánchez, R. Grimm, M. J. H. Ku, M. W. Zwierlein, Y.-H. Hou, L. Pitaevskii, and S. Stringari. Collective Modes in a Unitary Fermi Gas across the Superfluid Phase Transition. *Phys. Rev. Lett.*, **110**:055303, 2013. (cited on pp. 2, 51, 62, 72, and 74)

H. B. Thacker. Exact integrability in quantum field theory and statistical systems. *Rev. Mod. Phys.*, **53**:253, 1981. (cited on pp. 34 and 61)

M. Theis, G. Thalhammer, K. Winkler, M. Hellwig, G. Ruff, R. Grimm, and J. Hecker Denschlag. Tuning the Scattering Length with an Optically Induced Feshbach Resonance. *Phys. Rev. Lett.*, **93**:123001, 2004. (cited on p. 12)

L. Tisza. Transport Phenomena in Helium II. *Nature*, **141**:913, 1938. (cited on pp. 15 and 16)

L. Tisza. Sur la théorie des liquides quantiques. Application a l'hélium liquide. *J. Phys. Radium*, **1**:164, 1940. (cited on p. 15)

L. Tisza. The Theory of Liquid Helium. *Phys. Rev.*, **72**:838, 1947. (cited on p. 15)

L. Tonks. The Complete Equation of State of One, Two and Three-Dimensional Gases of Hard Elastic Spheres. *Phys. Rev.*, **50**:955, 1936. (cited on p. 62)

A. G. Truscott, K. E. Strecker, W. I. McAlexander, G. B. Partridge, and R. G. Hulet. Observation of Fermi Pressure in a Gas of Trapped Atoms. *Science*, **291**:2570, 2001. (cited on p. 6)

S. Tung, G. Lamporesi, D. Lobser, L. Xia, and E. A. Cornell. Observation of the Presuperfluid Regime in a Two-Dimensional Bose Gas. *Phys. Rev. Lett.*, **105**:230408, 2010. (cited on p. 28)

H. G. Vaidya and C. A. Tracy. One-Particle Reduced Density Matrix of Impenetrable Bosons in One Dimension at Zero Temperature. *Phys. Rev. Lett.*, **42**:3, 1979. (cited on p. 32)

M. Valiente. Exact equivalence between one-dimensional Bose gases interacting via hard-sphere and zero-range potentials. *EPL (Europhysics Letters)*, **98**:10010, 2012. (cited on p. 69)

M. Valiente and P. Öhberg. Few-body route to one-dimensional quantum liquids. *Phys. Rev. A*, **94**:051606, 2016. (cited on p. 86)

M. Valiente, N. T. Zinner, and K. Mølmer. Universal relations for the two-dimensional spin-1/2 Fermi gas with contact interactions. *Phys. Rev. A*, **84**:063626, 2011. (cited on p. 69)

A. H. van Amerongen, J. J. P. van Es, P. Wicke, K. V. Kheruntsyan, and N. J. van Druten. Yang-Yang Thermodynamics on an Atom Chip. *Phys. Rev. Lett.*, **100**:090402, 2008. (cited on p. 61)

K. Van Houcke, F. Werner, E. Kozik, N. Prokof'ev, B. Svistunov, M. J. H. Ku, A. T. Sommer, L. W. Cheuk, A. Schirotzek, and M. W. Zwierlein. Feynman diagrams versus Fermi-gas Feynman emulator. *Nat. Phys.*, **8**:366, 2012. (cited on pp. 21 and 22)

G. Veeravalli, E. Kuhnle, P. Dyke, and C. J. Vale. Bragg Spectroscopy of a Strongly Interacting Fermi Gas. *Phys. Rev. Lett.*, **101**:250403, 2008. (cited on p. 22)

E. Vogt, M. Feld, B. Fröhlich, D. Pertot, M. Koschorreck, and M. Köhl. Scale Invariance and Viscosity of a Two-Dimensional Fermi Gas. *Phys. Rev. Lett.*, **108**:070404, 2012. (cited on p. 48)

J.T.M. Walraven. *Quantum Gases - Collisions and Statistics*. Lecture course at master level, University of Vienna, 2013. (cited on p. 7)

W. Weimer, K. Morgener, V. P. Singh, J. Siegl, K. Hueck, N. Luick, L. Mathey, and H. Moritz. Critical Velocity in the BEC-BCS Crossover. *Phys. Rev. Lett.*, **114**:095301, 2015. (cited on pp. 22, 25, and 39)

F. Werner and I. Castin. Exact relations for quantum-mechanical few-body and many-body problems with short-range interactions in two and three dimensions. *arXiv*, 1001:0774, 2010. (cited on p. 69)

J. Wilks. *The Properties of Liquid and Solid Helium*. International Series of Monographs on Physics. Clarendon Press, 1967. (cited on pp. 2 and 77)

J. Wilks and D.S. Betts. *An introduction to liquid helium*. Oxford science publications. Clarendon Press, 1987. (cited on p. 15)

M. J. Wright, S. Riedl, A. Altmeyer, C. Kohstall, E. R. Sánchez Guajardo, J. Hecker Denschlag, and R. Grimm. Finite-Temperature Collective Dynamics of a Fermi Gas in the BEC-BCS Crossover. *Phys. Rev. Lett.*, **99**:150403, 2007. (cited on pp. 1 and 46)

C. N. Yang and C. P. Yang. Thermodynamics of a One–Dimensional System of Bosons with Repulsive Delta–Function Interaction. *Journal of Mathematical Physics*, **10**:1115, 1969. (cited on pp. 29, 32, 62, 80, and 81)

C. P. Yang. One-Dimensional System of Bosons with Repulsive δ-Function Interactions at a Finite Temperature T. *Phys. Rev. A*, **2**:154, 1970. (cited on pp. 32, 62, and 81)

V. A. Yurovsky, M. Olshanii, and D. S. Weiss. Collisions, correlations, and integrability in atom waveguides. volume **55** of *Advances In Atomic, Molecular, and Optical Physics*, page 61. Academic Press, 2008. (cited on pp. 34 and 61)

F. Zambelli and S. Stringari. Moment of inertia and quadrupole response function of a trapped superfluid. *Phys. Rev. A*, **63**:033602, 2001. (cited on pp. 73 and 125)

E. Zaremba. Sound propagation in a cylindrical Bose-condensed gas. *Phys. Rev. A*, **57**:518, 1998. (cited on p. 40)

W. Zwerger. *The BCS-BEC Crossover and the Unitary Fermi Gas.* Springer Berlin Heidelberg, 2011. (cited on p. 21)

M. W. Zwierlein, C. A. Stan, C. H. Schunck, S. M. F. Raupach, S. Gupta, Z. Hadzibabic, and W. Ketterle. Observation of Bose-Einstein Condensation of Molecules. *Phys. Rev. Lett.*, **91**:250401, 2003. (cited on p. 21)

M. W. Zwierlein, C. A. Stan, C. H. Schunck, S. M. F. Raupach, A. J. Kerman, and W. Ketterle. Condensation of Pairs of Fermionic Atoms near a Feshbach Resonance. *Phys. Rev. Lett.*, **92**:120403, 2004. (cited on p. 21)

M. W. Zwierlein, J. R. Abo-Shaeer, A. Schirotzek, C. H. Schunck, and W. Ketterle. Vortices and superfluidity in a strongly interacting Fermi gas. *Nature*, **435**:1047, 2005. (cited on pp. 16 and 22)

Abstract

Ultracold atoms are exceptional tools to explore the physics of quantum matter. In fact, the high degree of tunability of ultracold Bose and Fermi gases makes them ideal systems for quantum simulation and for investigating macroscopic manifestations of quantum effects, such as superfluidity.

In ultracold gas research, a central role is played by collective oscillations. They can be used to study different dynamical regimes, such as superfluid, collisional, or collisionless limits or to test the equation of state of the system. In this thesis, we present a unified description of collective oscillations in low dimensions covering both Bose and Fermi statistics, different trap geometries and zero as well as finite temperature, based on the formalism of hydrodynamics and sum rules.

We discuss the different behaviour exhibited by the second excited breathing mode in the collisional regime at low temperature and in the collisionless limit at high temperature in a 1D trapped Bose gas with repulsive contact interaction. We show how this mode exhibits a single-valued excitation spectrum in the collisional regime and two different frequencies in the collisionless limit. Our predictions could be important for future research related to the thermalization and damping phenomena in this low-dimensional system.

We show that 1D uniform Bose gases exhibit a non monotonic temperature dependence of the chemical potential characterized by an increasing-with-temperature behaviour at low temperature. This is due to the thermal excitation of phonons and reveals an interesting analogy with the behaviour of superfluids.

Finally, we investigate a gas with a finite number N of atoms in a ring geometry at $T = 0$. We discuss explicitly the deviations of the thermodynamic behaviour in the ring from the one in the large N limit.

Keywords